

LEABHARLANN CHOLÁISTE NA TRÍONÓIDE, BAILE ÁTHA CLIATH | TRINITY COLLEGE LIBRARY DUBLIN
Ollscoil Átha Cliath | The University of Dublin

Terms and Conditions of Use of Digitised Theses from Trinity College Library Dublin

Copyright statement

All material supplied by Trinity College Library is protected by copyright (under the Copyright and Related Rights Act, 2000 as amended) and other relevant Intellectual Property Rights. By accessing and using a Digitised Thesis from Trinity College Library you acknowledge that all Intellectual Property Rights in any Works supplied are the sole and exclusive property of the copyright and/or other IPR holder. Specific copyright holders may not be explicitly identified. Use of materials from other sources within a thesis should not be construed as a claim over them.

A non-exclusive, non-transferable licence is hereby granted to those using or reproducing, in whole or in part, the material for valid purposes, providing the copyright owners are acknowledged using the normal conventions. Where specific permission to use material is required, this is identified and such permission must be sought from the copyright holder or agency cited.

Liability statement

By using a Digitised Thesis, I accept that Trinity College Dublin bears no legal responsibility for the accuracy, legality or comprehensiveness of materials contained within the thesis, and that Trinity College Dublin accepts no liability for indirect, consequential, or incidental, damages or losses arising from use of the thesis for whatever reason. Information located in a thesis may be subject to specific use constraints, details of which may not be explicitly described. It is the responsibility of potential and actual users to be aware of such constraints and to abide by them. By making use of material from a digitised thesis, you accept these copyright and disclaimer provisions. Where it is brought to the attention of Trinity College Library that there may be a breach of copyright or other restraint, it is the policy to withdraw or take down access to a thesis while the issue is being resolved.

Access Agreement

By using a Digitised Thesis from Trinity College Library you are bound by the following Terms & Conditions. Please read them carefully.

I have read and I understand the following statement: All material supplied via a Digitised Thesis from Trinity College Library is protected by copyright and other intellectual property rights, and duplication or sale of all or part of any of a thesis is not permitted, except that material may be duplicated by you for your research use or for educational purposes in electronic or print form providing the copyright owners are acknowledged using the normal conventions. You must obtain permission for any other use. Electronic or print copies may not be offered, whether for sale or otherwise to anyone. This copy has been supplied on the understanding that it is copyright material and that no quotation from the thesis may be published without proper acknowledgement.

An Investigation into Novel Components and Signalling Mechanisms of Inflammasomes

Thesis submitted to the

University of Dublin

for the

Degree of Doctor of Philosophy

By

Christine Becker

School of Biochemistry and Immunology

Trinity College Dublin

Ireland

TRINITY COLLEGE
10 APR 2012
LIBRARY DUBLIN
9463

Declaration

This thesis is submitted by the undersigned to the University of Dublin for the examination of Doctorate in Philosophy. The work herein is entirely my own with the exception of the following figures:

- Figure 4.8

This work was carried out by Dr. Alex Luthi in the Department of Genetics, TCD.

- Figure 4.9 (A) and (B)

This work was carried out by Dr. Jennifer Dowling in the School of Biochemistry and Immunology, TCD.

This work has not been submitted as exercise for a degree to any other university. The library at Trinity College Dublin, has my full permission to lend or copy this thesis upon request.

Christine Becker.

Christine Becker

Acknowledgements

To my supervisor Prof. Luke O' Neill for all the enthusiastic help and guidance for the past few years and for the many enjoyable lab nights out! I would also like to thank Dr. Emma Creagh for all the advice and help given. A huge thank you to everyone in the LON lab - Andi, Anne, Becca, Cáit, Caroline, Claire, Dympna, Elaine, Emer, Eva, Fred, Gillian, Jen, Kathy, Liz, Majella, Paulina, Sarah, Seth, Sinéad and Susan for all their help and making the lab such a great place to work! To Dr. Orla Hanrahan and Dr. Barry Moran for their assistance with the confocal and FACs. To all on the HRB Molecular Medicine committee, Dr. Ross McManus and my thesis committe Prof. Orla Shiels and Dr. Derek Morris for their helpful guidance and my fellow HRB classmates – Cathy, Sinéad and Thérèse for being such great friends! To everyone in the Developmental Immunology lab in MGH especially Lynda, Adam, Anna and Mike for all the help and for being so welcoming and for all the fun nights out in Boston! A massive thank you to all my family for their support and to all my friends and housemates over the past four years!

Table of Contents

List of Figures ix

Abbreviations xiv

Abstract xx

Chapter 1 Introduction 1

1.1 Innate immunity 2

1.2 Toll-like receptors 2

1.2.1 TLR localisation 3

1.2.2 TLR ligands 3

1.2.3 TLR structure 4

1.2.4 TLR signalling 4

1.3 RIG-I like receptors 7

1.3.1 RLR structure 7

1.3.2 RLR ligands 8

1.3.3 RLR localisation 9

1.3.4 RLR signalling 10

1.4 C-type lectin receptors 11

1.5 Nod-like receptors 13

1.5.1 NLR structure 14

1.5.2 NLR localisation 14

1.5.3 NLR ligands 14

1.6 The inflammasome 15

1.6.1 NLRC4 inflammasome 15
1.6.2 NLRP1 inflammasome 16
1.6.3 NLRP3 inflammasome 17
1.6.4 AIM2 inflammasome 18
1.6.5 Inflammasome regulation 18
1.7 Caspase-1 20
1.7.1 Caspase-1 activation 20
1.7.2 Functions of caspase-1 21
1.7.3 Caspase-1 regulation 23
1.8 ASC 24
1.8.1 Regulation of ASC 25
1.8.2 Pyroptosis 25
1.9 Interleukin-1β 26
1.9.1 IL-1β secretion 27
1.9.2 IL-1β signalling 30
1.9.3 Functions of IL-1β 31
1.10 Inflammasomopathies 31
1.11 Rab GTPases 33
1.11.1 Rab GTPases and vesicle trafficking 34
1.11.2 Rab GTPases and phagocytosis 34
1.11.3 Rab GTPases and pathogenic hijacking 35
1.11.4 Rab39a 36
1.12 Aims 38

Chapter 2 Materials and Methods.....39

2.1 Materials 40

2.2 Bioinformatic Analysis 42

2.3 Cell culture 43

2.3.1 Cell lines 43

2.3.2 Human peripheral blood mononuclear cells (PBMCs) 44

2.3.3 Preparation of peritoneal macrophages 44

2.4 Cloning of Rab39a and Rab39b 45

2.4.1 Primer design 45

2.4.2 Polymerase chain reaction 45

2.4.3 Agarose gel electrophoresis 46

2.4.4 Gel extraction 47

2.4.5 Ligation into PGEM-T-Easy 47

2.4.6 Plasmid transformation 47

2.4.7 Mini-preparation of plasmid DNA 47

2.4.8 Restriction digests 48

2.4.9 Ligation into PCMV-HA and PCDNA3 48

2.5 Site directed mutagenesis of Rab39a 49

2.6 Transient transfection of plasmid DNA 52

2.7 Transient transfection of siRNA oligos 53

2.8 Western blot analysis 54

2.8.1 Preparation of whole cell lysates 54

2.8.2 Protein concentration determination 55

2.8.3 SDS polyacrylamide gel electrophoresis 55

2.8.4 Transfer of proteins to membrane 55

2.8.5 Antibody blotting 56
2.9 Rab39a processing assay 56
2.10 Co-immunoprecipitation 57
2.11 Confocal microscopy 58
2.11.1 Fixed cell imaging 58
2.11.2 Live cell imaging of phagocytosis 59
2.11.3 Live cell imaging of active caspases 59
2.11.4 Live cell imaging of ASC-FP cells 59
2.12 Analysis of phagocytosis 59
2.12.1 Bacterial uptake assay 59
2.12.2 Phagosomal acidification assay 60
2.13 RNA extraction 61
2.14 Reverse transcription PCR 61
2.15 Real Time PCR 62
2.16 Analysis of change in cytokine expression by ELISA 62
2.17 Analysis of secreted proteins 62
2.18 Immunoprecipitation and mass spectrometry of ASC 63
2.18.1 Cell free extract preparation 63
2.18.2 Immunoprecipitation from cell free extract 63
2.18.3 Isoelectric Focusing 64
2.18.4 Equilibriation for 2D gel electrophoresis 64
2.18.5 2D gel 65
2.18.6 Silver staining of gels 65
2.18.7 Trypsin digestion and peptide extraction 66
2.18.8 Analysis of tryptic digest fragments by mass spectrometry 66

2.19 ASC complex isolation 67

Chapter 3 Idenification of Rab39a as a novel binding partner of caspase-1 69

3.1 Introduction 70

3.2 Results 73

3.2.1 Cloning of Rab39a and Rab39b into PCMV-HA 73

3.2.2 Rab39a interacts with caspase-1 74

3.2.2.1 Rab39a and caspase-1 co-immunoprecipitate in 293T cells 74

3.2.2.2 GFP-Rab39a and caspase-1 co-localise in 293T cells 75

3.2.3 Bioinformatic analysis of Rab39a 76

3.2.3.1 Homology search of Rab39a 76

3.2.3.2 Conserved motifs in Rab39a 76

3.2.3.3 GTPase activity of Rab39a 77

3.2.3.4 Post-translational modifications of Rab39a 78

3.2.3.5 Rab39a contains a putative caspase-1 cleavage site 78

3.2.3.6 Rab39a structure 80

3.2.3.7 Characterisation of the promoter region of the Rab39a gene 80

3.2.3.8 Tissue and cell type distribution of Rab39a 81

3.3 Discussion 83

Chapter 4 Functional significance of the Rab39a and caspase-1 interaction 88

4.1 Introduction 90

4.2 Results 93

4.2.1 Rab39a is a substrate of caspase-1 93

4.2.1.1 Rab39a can be processed by recombinant caspase-1 93

4.2.1.2 Rab39b cannot be processed by caspase-1 93

4.2.1.3 A caspase-1 inhibitor prevents processing of Rab39a 94

4.2.1.4 The caspase-1 cleavage site on Rab39 is confirmed as D148 94

4.2.1.5 Constitutively active and dominant negative forms of Rab39a can be processed by caspase-1 96

4.2.1.6 Rab39a can be processed in macrophages by LPS and ATP 96

4.2.1.7 Rab39a cannot be processed by an ITT assay 97

4.2.1.8 Rab4a, Rab14 and Rab25 are not substrates of caspase-1 98

4.2.2 Detection of endogenous Rab39a 99

4.2.2.1 Rab39a antibody design 99

4.2.2.2 Analysis of Rab39a antibodies 100

4.2.3 Subcellular localisation of Rab39a 101

4.2.3.1 Subcellular localisation of GFP-Rab39a in 293T cells 101

4.2.3.2 GFP-Rab39a localises to endosomes in Raw 264.7 cells 103

4.2.4 Rab39a is involved in phagocytosis 104

4.2.4.1 Rab39a is found on phagosomes 104

4.2.4.2 Rab39a localises with active caspases on phagosomes 104

4.2.4.3 Rab39a is involved in bacterial uptake 105

4.2.4.4 Rab39a is not essential for phagosomal acidification 105

4.2.5 Rab39a is induced by pro-inflammatory stimuli 106

4.2.5.1 Optimisation of Rab39 primers for Real-Time PCR 106

4.2.5.2 Rab39a is inducible by LPS, Malp2 and Pam_3Cys 107

4.2.6 Knockdown of Rab39a affects IL-1β secretion 108

4.2.6.1 siRNA specifically knocks down mRNA and protein expression of Rab39a.....108
4.2.6.2 siRNA of Rab39a results in diminished levels of IL-1β secretion ..109
4.2.6.3 siRNA of Rab39a does not effect mRNA levels of IL-1β.....110
4.2.7 Over-expression of Rab39a results in increased levels of IL-1β secretion 110
4.2.8 Rab39a is secreted from the cell 111
4.3 Discussion 113

Chapter 5 Analysis of ASC in the inflammasome..... 117
5.1 Introduction 120
5.2 Results 121
5.2.1 Identification of novel binding partners of ASC 121
5.2.1.1 Immunoprecipitation of ASC from cell free extracts 121
5.2.1.2 Identification of bound proteins by mass spectrometry.....122
5.2.1.3 PSTPIP1 does not co-immunoprecipitate with ASC 123
5.2.2 Isolation of inflammasome complexes 124
5.2.3 Analysis of signalling events needed for inflammasome formation..... 125
5.2.3.1 ASC speck formation requires TLR priming.....125
5.2.3.2 Timecourse analysis of ASC speck formation.....126
5.2.3.3 ASC speck formation is upstream of caspase-1 activation.....126
5.2.3.4 ASC speck formation requires new protein synthesis 127
5.2.3.5 ASC complex formation is inhibited in the presence of MG132 127

5.2.3.5.1 ASC contains many possible sites of ubiquitination 127

5.2.3.5.2 ASC is not ubiquitinated 128

5.2.3.6 ASC speck formation is dependent on kinase signalling events 128

5.2.3.6.1 ASC contains many potential phosphorylation sites 130

5.2.3.6.2 ASC is phosphorylated 130

5.3 Discussion 133

Chapter 6 Final discussion and future perspectives 136

Chaper 7 References 143

Chapter 8 Record of publication 177

List of Figures

Chapter 1

Figure 1.1 TLR signalling

Figure 1.2 Inflammasome structure and signalling

Figure 1.3 Functions of caspase-1

Figure 1.4 Current models of IL-1β secretion

Figure 1.5 The Rab GTPase cycle

Chapter 3

Figure 3.1 Rab39a and Rab39b were cloned into PCMV-HA vectors

Figure 3.2 HA-Rab39a and HA-Rab39b expression in Hek293T cells

Figure 3.3 HA-Rab39a and caspase-1 co-immunoprecipitate in HEK293T cells

Figure 3.4 GFP-Rab39a and RFP-caspase-1 co-localise in HEK293T cells

Figure 3.5 Characterisation of Ras superfamily, Rab family and Rab subfamily motifs in Rab39a

Figure 3.6 Putative areas of GTPase activity in Rab39a

Figure 3.7 Rab39a contains many potential sites for post-translational modification

Figure 3.8 Rab39a contains a putative caspase-1 cleavage site

Figure 3.9 Predicted secondary structure of Rab39a.

Figure 3.10 Predicted tertiary structure of Rab39a.

Figure 3.11 Analysis of the promoter region of Rab39a for transcription factor binding sites

Figure 3.12 Human Rab39a is expressed at a low level in a variety of human tissues and cells

Figure 3.13 Murine Rab39a is highly expressed in cells of the immune system

Chapter 4

Figure 4.1 Rab39a can be processed by caspase-1

Figure 4.2 Rab39b cannot be processed by caspase-1

Figure 4.3 Pre-treatment with a caspase-1 inhibitor prevents processing of Rab39a

Figure 4.4. HA-Rab39aD148A cannot be cleaved by caspase-1

Figure 4.5 GFP-Rab39aC149Stop is the same size as the cleavage fragment

Figure 4.6 Constitutively active and dominant negative forms of Rab39a can still be processed by caspase-1

Figure 4.7 HA-Rab39a can be processed by LPS and ATP in RAW 264.7 cells

Figure 4.8 Rab39a is not processed by caspase-1 in an ITT assay

Figure 4.9 Rab4a, Rab14 and Rab25 cannot be processed by caspase-1 despite having caspase-1 cleavage sites

Figure 4.10 Rab39a peptide antibody

Figure 4.11 The custom made Rab39a antibody detects over-expressed Rab39a

Figure 4.12 The commercially available Rab39a antibody detects over-expressed Rab39a

Figure 4.13 GFP-Rab39a is diffuse in the cytosol of HEK293T cells

Figure 4.14 GFP-Rab39aS22N is diffuse in the cytosol of HEK293T cells

Figure 4.15 GFP-Rab39aQ72L is diffuse in the cytosol of HEK293T cells

Figure 4.16 GFP-Rab39aC149Stop is diffuse in the cytosol of HEK293T cells

Figure 4.17 GFP-Rab39aD148A is localised to vesicles in the cytosol of HEK293T cells

Figure 4.18 Rab39a localises to vesicles in cytosol of RAW 264.7 cells

Figure 4.19 Rab39a localises to phagosomes of RAW 264.7 cells induced by latex beads

Figure 4.20 Rab39a localises to phagosomes of RAW 264.7 cells induced by *S. aureus*

Figure 4.21 Rab39a co-localises with caspases on phagosomes in RAW 264.7 cells

Figure 4.22 Expression of a dominant negative version of GFP-Rab39a results in increased bacterial uptake

Figure 4.23 Caspases are required for phagosomal acidification

Figure 4.24 Rab39a is not required for phagosomal acidification

Figure 4.25 Rab39a is induced by LPS, Malp2 and Pam_3Cys

Figure 4.26 siRNA targeted to Rab39a knocks down Rab39a DNA and protein levels

Figure 4.27 siRNA of Rab39a results in diminished levels of IL-1β secretion in THP1s

Figure 4.28 siRNA of Rab39a in PBMCs results in diminished levels of IL-1β secretion

Figure 4.29 siRNA of Rab39a does not affect mRNA levels of IL-1β

Figure 4.30 Overexpression of Rab39a results in increased secretion of IL-1β

Figure 4.31 Rab39a is secreted from the cell

Chapter 5

Figure 5.1 Incubation of a CFE of THP1 cells at 37 °C results in activation of caspase-1

Figure 5.2 ASC can be immunoprecipitated from a cell free extract of THP1 cells

Figure 5.3 Silver staining of ASC immunoprecipitation from THP1 cells

Figure 5.4 PSTPIP1 is identified as a potential binding partner of ASC

Figure 5.5 ASC and PSTPIP1 do not co-immunoprecipitate

Figure 5.6 ASC complexes can be isolated from BMDM cells

Figure 5.7 ASC complex formation is Myd88 independent

Figure 5.8 ASC speck formation is induced by TLR ligands plus ATP

Figure 5.9 ASC specks begin to form after 15 mins of ATP treatment

Figure 5.10 ASC specks begin to form after 15 minutes LPS

Figure 5.11 ASC speck formation is upstream of caspase-1 activation

Figure 5.12 ASC speck formation requires de novo protein synthesis

Figure 5.13 ASC speck formation is inhibited in the presence of MG132

Figure 5.14 ASC contains numerous potential ubiquitination sites

Figure 5.15 ASC does not get ubiquitinated

Figure 5.16 ASC speck formation is dependent on kinase signalling events

Figure 5.17 Predicted phosphorylation sites of ASC

Figure 5.18 ASC is phosphorylated on a tyrosine residue

Chapter 6

Figure 6.1 Model of signalling mechanisms associated with inflammasome formation and IL-1β release

List of Tables

Chapter 1

Table 1.1 NLR nomenclature

Chapter 3

Table 3.1 Proteins with greatest homology to Rab39a

Table 3.2 Human Rab39a is highly conserved across different species

Table 3.3 The caspase-1 cleavage site in Rab39a is conserved across many species

Table 3.4 Rab proteins with potential caspase-1 cleavage sites

Chapter 5

Table 5.1 Proteins associating with ASC identified by Mass Spectrometry

List of Movies

Movie 4.1 Live cell imaging of GFP-Rab39a in RAW 264.7 cells

Movie 4.2 Live cell imaging of GFP-Rab39a and active caspases in RAW 264.7 cells

Abbreviations

AIM2	Absent in melanoma 2
AMP	Ampicillin
AP-1	Activator protein 1
APS	Ammonium persulphate
ASC	Apoptotis-associated speck-like protein containing a CARD
ATP	Adenosine triphosphate
BCL	B-cell lymphoma
BDCA	Blood dendritic cell antigen
BIR	Baculovirus IAP repeat
BMDM	Bone marrow derived macrophage
BSA	Bovine serum albumin
CARD	Caspase recruitment domain
CDD	Conserved domain database
cDNA	Complementary DNA
CLEC	C-type lectin domain family
CLR	C-type lectin receptor
CNS	Central nervous system
COP	CARD-only protein
DC	Dendritic cells
DNA	Deoxyribonuceic acid
dsRNA	Double stranded RNA
DTT	1,4-Dithiothreitol

EDTA	Ethylene diamine tetracetic acid
EEA1	Early endosome antigen 1
ELISA	Enzyme-linked immunosorbent assay
EGTA	Ethylene glycol tetracetic acid
ECL	Enhanced chemi-luminescence
ER	Endoplasmic reticulum
ERK	Extracellular signal-regulated kinase
EXOSC9	Exosome component 9
FADD	Fas-associated protein with death domain
FCS	Fetal calf serum
FCU	Familial cold urticaria
FMF	Familial meditteranean fever
GAP	Guanine triphosphate activating protein
GAPDH	Glyceraldehyde-3-phosphate dehydrogenase
GDI	Guanine dissociation inhibitor
GDP	Guanine diphosphate
GEF	Guanine exchange factor
GTP	Guanine triphosphate
HEK	Human embryonic kidney
HIN-200	Hematopoietic interferon-inducible nuclear proteins with a 200-amino-acid repeat
IAP	Inhibitor of apoptosis
IC	Intermediate compartment
ICE	Interleukin-1β converting enzyme
IEF	Iso-electric focussing

IFN	Interferon
IL	Interleukin
IL-1R	Interleukin 1 receptor
INCA	Inhibitory caspase recruitment domain
IP	Immunoprecipitation
IPG	Immobilised pH Gradient
IPTG	Isopropyl β-D-1-thiogalactopyranoside
IRAK	Interleukin-1 receptor-associated kinase
IRF	Interferon regulatory factor
ITAM	Immunoreceptor tyrosine-based activation motif
iTRAQ	Isobaric tag for relative and absolute quantitation
ITT	*In vitro* transcription and translation
JNK	Jun N-terminal kinase
Kbp	Kilo base pairs
kDa	Kilodalton
LB	Lysogeny broth
LPS	Lipopolysaccharide
LRR	Leucine rich repeat
Mal	MyD88-adaptor-like
MALDI-TOF	Matrix-assisted laser desorption/ionisation-time of flight
Malp2	Macrophage-activating lipoprotein 2kDa
MAP	Mitogen activated protein
MAPK	Mitogen activated protein kinase
MDP	Muramyl dipeptide
MHC	Major histocompatability complex

MOI	Multiplicity of infection
MSU	Monosodium urate
mRNA	Messenger RNA
MVB	Multivesicular body
MWS	Muckle-wells syndrome
MyD88	Myeloid differentiation factor 88
NF-κB	Nuclear factor κB
NO	Nitric oxide
NOD	Nucleotide oligomerisation domain
NOMID	Neonatal onset multisystem inflammatory disease
NLR	NOD-like receptor
NLRA	NLR family acidic domain containing
NLRB	NLR family BIR domain containing
NLRC	NLR family CARD domain containing
NLRP	NLR family PYD containing
NLRX	NLR family with no strong homology to the N-terminal of any other subfamily member
NP-40	Nonyl phenoxylpolyethoxylethanol 40
PAGE	Polyacrylimide gel electrophoresis
PAMP	Pathogen associated molecular pattern
PAPA	Pyogenic arthritis, pyoderma gangrenosum and acne
PBS	Phosphate buffered saline
PCR	Polymerase chain reaction
PI	Isoelectric point
PKC	Protein kinase C

PMA	Phorbol 12-myristate 13-acetate
PMSF	Phenylmethanesulphonylfluoride
POP	Pyrin-only protein
PRR	Pattern recognition receptor
PS	Penicillan streptomycin
PSTPIP1	Proline serine threonine phosphatase interacting protein 1
PVDF	Polyvinylidine fluoride
PYD	Pyrin domain
P_2X_7	Purinergic receptor P2X, ligand-gated ion channel, 7
RD	Repressor domain
RIG-I	Retinoic acid inducible gene I
RIP	Receptor interacting protein
RHIM	RIP homotypic interaction motif
RNA	Ribonucleic acid
RNAi	Ribonucleic acid interference
RLR	Retinoic acid inducible gene I like receptor
ROS	Reactive oxygen species
RT-PCR	Reverse transcription PCR
SARM	Sterile alpha and HEAT-Armadillo motifs
SDS	Sodium dodecyl sulfate
SeV	Sendai virus
SNP	Single nucleotide polymorphism
SREBP	Sterol regulatory element binding protein
ssRNA	Single stranded RNA
T2DM	Type 2 Diabetes Mellitus

TAB	Tak1 binding protein
TAE	Tris-acetate ethylene diamine tetracetic acid
TAK	Transforming growth-factor-activated β kinase
TBS	Tris-buffered saline
TEMED	Tetramethylethylenediamine
TFA	Trifluoroacetic acid
TGF	Transforming growth factor
TH	T-helper
TIR	Toll/Interleukin-1 receptor
TIRAP	Toll-interleukin 1 receptor domain containing adaptor protein
TLR	Toll-like receptor
TNF	Tumour necrosis factor
TRADD	Tumour necrosis factor receptor-associated death domain
TRAM	Trif-related adaptor molecule
TRAF	Tumour necrosis factor receptor-associated factor
TRIF	TIR -domain-containing adapter-inducing interferon-β
TRIM	Tripartite motif

Abstract

This thesis concerns an analysis of caspase-1 and ASC, key components of the inflammasome. At the outset Rab39a had been found in a complex with caspase-1. Rab39a is a member of the Rab GTPase family, a group of proteins which have important roles in protein trafficking and secretion. Rab39a was successfully cloned and its binding to caspase-1 was confirmed by co-immunoprecipitation and confocal microscopy experiments. Biological assays were carried out to try and determine the functional relevance of this interaction. Bioinformatic analysis showed that Rab39a contains a highly conserved caspase-1 cleavage site and can be cleaved in the presence of recombinant caspase-1 or in cells treated with LPS and ATP. Rab39a was found to localise with active caspases on phagosomes formed in response to *S. aureus* and was shown to have a role in bacterial uptake. The Rab39a promoter contains many putative transcription factor binding sites and Real Time PCR analysis showed that Rab39a mRNA levels are significantly increased in response to LPS, Malp2 and Pam_3Cys.

Knock-down of Rab39a with siRNA resulted in diminished levels of secreted IL-1β but had no effect on induction of pro-IL-1β mRNA by LPS. Furthermore, over-expression of Rab39a results in an increase in IL-1β secretion and over-expression of a Rab39a construct lacking the caspase-1 cleavage site leads to an additional increase in IL-1β secretion. Results show that Rab39a exists in exosome-like vesicles in the cell and that these vesicles along with active caspase exit the cell together. Altogether, these findings

show that Rab39a interacts with caspase-1 and suggests that Rab39a functions as a trafficking adaptor linking caspase-1 to IL-1β secretion.

The regulation of ASC in the inflammasome was also analysed. Using a one-step immunoprecipitation approach to isolate endogenous ASC from the monocytic THP1 cell line, previously undescribed binding partners of ASC were identified using mass spectrometry. Novel signalling pathways involving ASC necessary for inflammasome formation were also investigated. It was established that tyrosine kinase signalling events were essential for inflammasome formation and that ASC itself is tyrosine phosphorylated.

Overall, this study provides insight into a key aspect of inflammation: the molecular regulation of IL-1β production. I have found that Rab39a is a novel interactor for caspase-1 and is required for IL-1β secretion and also found a possible mechanism for ASC activation involving tyrosine phosphorylation.

Chapter 1

Introduction

1.1 Innate immunity

The immune system is composed of two major subdivisions, the innate system and the adaptive system. The innate immune system is our first line of defence against invading organisms while the adaptive immune system acts as a second line of defence and also affords protection against re-exposure to the same pathogen. A key function of the innate immune system is to recognise invading microbes and mount a quick and effective response. This is done through a variety of receptors, referred to as pattern recognition receptors (PRRs), which recognise molecular patterns on pathogens called pathogen-associated molecular patterns (PAMPs) (Janeway, 1992). PRRs include Toll-like receptors (TLRs), Retinoic acid inducible gene (RIG)-I like receptors (RLRs) C-type lectin receptors (CLRs) and nucleotide oligomerisation domain (Nod) - like receptors (NLRs). These PRRs are described below. This thesis focuses mainly on the NLR proteins and their role in a molecular platform called the inflammasome, however all of these PRRs engage in a certain amount of cross-talk with each other so it is important that they are all considered.

1.2 Toll-like receptors

TLRs are arguably the most studied of the PRRs. They are transmembrane receptors that recognise individual PAMPs on invading microbes. Recognition of PAMPs by the TLRs triggers a series of events that leads to the expression of many immune and inflammatory genes. TLRs also induce dendritic cell maturation, which is essential for the induction of pathogen-specific adaptive immune responses. To date, 10 TLRs (TLR1–10) in human and 12 TLRs (TLR1–9 and TLR11–13) in mice have been described (O'Neill, 2006).

1.2.1 TLR localisation

TLRs are expressed on a range of immune cells, which include macrophages, dendritic cells (DC), B cells and certain types of T cells. TLRs are also expressed on certain non-immune cells, such as epithelial cells, which lie at potential sites of entry, including the skin, respiratory, intestinal and genitourinary tracts, endothelial cells and smooth muscle cells. Their pattern of expression is modulated by activation, maturation or differentiation of the different cell types. TLRs 3, 7, 8 and 9 are expressed intracellularly on endosomes, whilst TLRs 1, 2, 4, 5, 6 and 10 are expressed on the cell surface.

1.2.2 TLR ligands

TLRs form heterodimers such as TLR1-TLR2 and TLR2-TLR6, or homodimers such as TLR3-TLR3. TLR4 requires co-receptors MD2 and CD14 to signal. TLRs recognise a diverse range of PAMPs. Briefly, the heterodimer TLR1/2 can recognise bacterial triacyl lipopeptide, while TLR2/6 recognises bacterial diacyl lipopeptide. TLR3 recognises double-stranded RNA (dsRNA) from viruses. TLR4 recognises lipopolysaccharide (LPS) of gram-negative bacteria, TLR5 recognises bacterial flagellin, TLR7 recognises synthetic imidazoquinioline-like molecules, guanosine analogs such as loxoribrine, and single stranded RNA (ssRNA) from HIV-1, vesicular stomatitis virus and influenza virus, TLR8 recognises imidazoquinolines and ssRNA, TLR9 recognises bacterial and viral CpG DNA motifs (Hemmi *et al.*, 2000) and malaria pigment hemozoin (Coban *et al.,* 2005). The ligand for TLR10 remains unknown at present. TLR11 is only found in mice and recognises a profilin-like protein from *Toxoplasma gondii* (Kawai *et al.*, 2007).

1.2.3 TLR structure

All TLRs are type-1 transmembrane glycoprotein receptors. The extracellular domain contains 16-28 consecutive leucine rich repeat (LRR) motifs, each of which is 20-30 amino acids in length, and are involved in ligand binding. The intracellular tail contains a highly conserved region, called the Toll-interleukin-1 receptor (TIR) domain, which mediates interactions between TLRs and downstream signalling molecules. The crystal structures of several TLRs and the complexes they form with their ligands have recently been solved. The crystal structures of TLR3 binding dsRNA (Liu *et al.*, 2008), TLR1-TLR2 binding Pam_3Csk_4 (Jin *et al.*, 2007), and TLR4-MD2 binding LPS (Park *et al.*, 2009), are all now known. Each of the structures reported shows that the extracellular domains converge into an 'M' shape, bringing the intracellular TIR-domains into close proximity with each other which results in their interaction and propagates downstream signalling.

1.2.4 TLR signalling

The recognition of PAMPs by TLRs triggers the activation of a signalling cascade which culminates in the induction of genes involved in the inflammatory response (Figure 1.1). After ligand binding, TLRs dimerise and undergo conformational changes which are required for the recruitment of adaptor molecules, via their TIR domains. These adaptor molecules, namely Myeloid differentiation factor 88 (MyD88), MyD88 adapter-like (Mal), Toll-receptor-associated activator of interferon (TRIF), TRIF-related adaptor molecule (TRAM) and Sterile α and HEAT-Armadillo motifs (SARM), contribute to the specificity of individual responses to pathogens. Each TLR can mediate a tailored response in association with different combinations of these adaptors. Two major pathways can be activated by TLRs; the MyD88 dependent pathway results

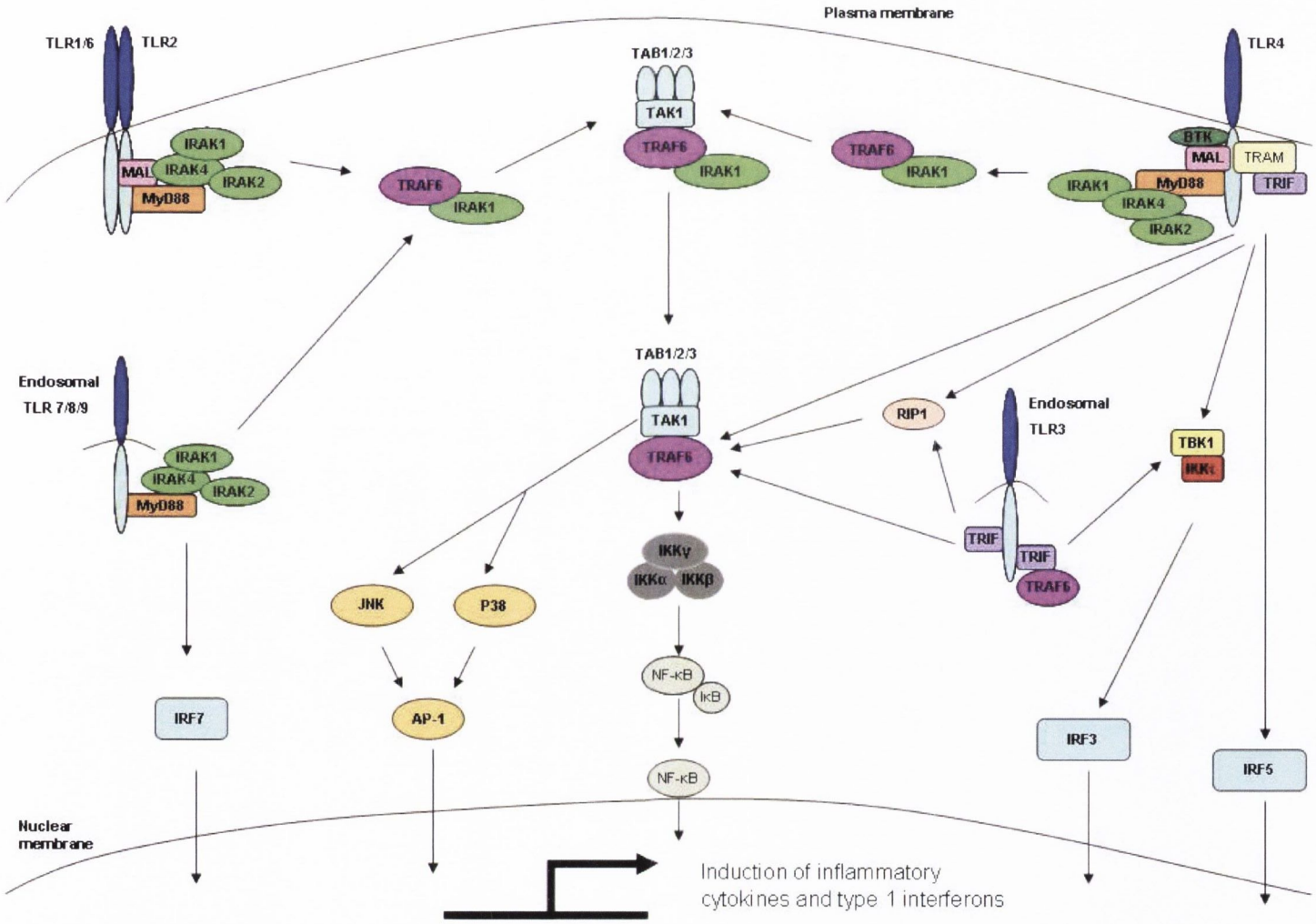

Plasma membrane
TLR1/6
TLR2
IRAK1
IRAK4
IRAK2
MAL
MyD88
TRAF6
IRAK1
TAB1/2/3
TAK1
TRAF6
IRAK1
TRAF6
IRAK1
TLR4
BTK
MAL
TRAM
TRIF
IRAK1
MyD88
IRAK4
IRAK2
Endosomal
TLR 7/8/9
IRAK1
IRAK4
IRAK2
MyD88
TAB1/2/3
TAK1
TRAF6
RIP1
Endosomal
TLR3
TRIF
TRIF
TRAF6
TBK1
IKKε
IKKγ
IKKα
IKKβ
JNK
P38
NF-κB
IκB
NF-κB
AP-1
IRF7
IRF3
IRF5
Nuclear
membrane
Induction of inflammatory
cytokines and type 1 interferons

Figure 1.1 TLR signalling. TLRs respond to a variety of ligands from various bacteria, fungi and viruses. Signalling occurs via different combinations of the adaptors MyD88, Mal, Tram and Trif. All TLRs, except TLR3, use the MyD88-dependent pathway. TLR3 uses the TRIF-dependent pathway. TLR signaling results in the induction of inflammatory cytokines and type I interferons.

in the activation of Nuclear factor κB (NF-κB) and activating protein-1 (AP-1), while the TRIF-dependent pathway results in the activation of type I interferons (IFNs) (O'Neill, 2006).

The MyD88 - dependent pathway is used by all TLRs, except TLR3, and is also used by the Type I IL-1 receptor (IL-1R1). Signalling is initiated by recruitment of MyD88 to TLRs, via TIR-TIR interactions. MyD88 recruits IL-1 receptor kinase-4 (IRAK4), allowing association and phosphorylation of IRAK1. IRAK1 catalyses the phosphorylation and activation of Pellino proteins, which then causes Lys^{63}- linked polyubiquitination of IRAK1 (Butler *et al.*, 2007). IRAK1 is then thought to recruit and activate tumour necrosis factor receptor-associated factor 6 (TRAF6) (Ye *et al.,* 2002). However, recent research has proposed that another member of the IRAK family, IRAK2, rather than IRAK1, is the key IRAK in the TRAF6 pathway. IRAK2 interacts with TRAF6, triggering the Lys^{63}- linked polyubiquitination of TRAF6 (Keating *et al.* 2007). TAB2 and TAB3 recognise the Lys^{63}- linked polyubiquitin chains on TRAF6. TGF-β activated kinase 1 (TAK1) is recruited to TRAF6 via TAB2 and TAB3. TAK1 then activates the IKK complex, which phosphorylates the IκB family and leads ultimately to activation of NF-κB. TAK1 also activates members of the MAP kinase family, which activate Jun N-terminal kinase (JNK), p38 and extracellular signal-related kinases (ERKs), leading to the activation of AP-1. The transcription factor IRF7 forms a complex with MyD88, IRAK1 and TRAF6. Another transcription factor, IRF5, also associates in a trimeric complex with TRAF6 and MyD88. The IRF family of transcription factors are structurally related to NF-κB family members and have important roles in the regulation of type I IFN production. The translocation of these transcription factors, AP-1, NF-κB and IRFs, to the nucleus regulates the transcription,

mRNA stability and translation of numerous pro-inflammatory cytokine genes, such as tumour necrosis factor (TNF)-α, Interleukin (IL)-1β, IL-6, IL-12 and IFNs (Akira, 2006).

The TRIF-dependent pathway culminates in the induction of type I IFNs, as well as other proinflammatory signals. TLR3 and TLR4 make use of this pathway, and the adaptor molecule TRIF is essential for this pathway. The adaptor molecule TRAM is essential for the TLR4 mediated TRIF-dependent pathway and appears to act as a bridging adaptor between TLR4 and TRIF. TRIF interacts with TBK and IKKε, which phosphorylate IRF3 and IRF7. Phosphorylated IRF3 and IRF7 form homodimers and translocate into the nucleus to induce IFN-α and IFN-β. TRIF can also activate the NF-κB pathway in two possible ways; firstly, by recruiting TRAF6 via its TRAF6 binding domains in the N-terminal region, and secondly, the C-terminal region of TRIF contains a receptor interacting protein (RIP) homotypic interaction motif (RHIM), which mediates interaction with members of the RIP family, which also results in NF-κB activation. Both of these pathways may converge at the IKK complex, resulting in maximum activation of NF-κB (Yamamoto *et al.*, 2003).

In the case of the other adaptors, Mal interacts with TLR1, TLR2 and TLR4 as a bridging adaptor for MyD88. Mal is essential for TLR4 signalling but only needed for TLR2 signalling when lower doses of ligands are used. Mal also has an inhibitory role in TLR3 signalling (Kenny *et al.*, 2009). TRAM, as mentioned already, is used by TLR4 for recruitment of TRIF and subsequent downstream signaling. TRAM Adaptor with GOLD domain (TAG), is a splice variant of TRAM, and has been shown to inhibit IRF3 activation by LPS (Palsson-McDermott *et al.*, 2009). The final adaptor molecule,

SARM, has been described as a specific inhibitor of TRIF-dependent signalling (Carty *et al.*, 2006).

TLR signalling needs to be tightly controlled and various negative regulatory mechanisms exist, ranging from extracellular decoy receptors, intracellular inhibitors and membrane bound suppressors, to degradation of TLRs and TLR-induced apoptosis. Since many TLRs are implicated in autoinflammatory and infectious diseases, it is possible that some of these disease processes could involve over-activation of TLRs or dysregulated TLR signalling.

1.3 RIG-I like receptors

The RIG-I like receptors (RLRs) are important intracellular sensors for the detection of RNA derived from viruses. Infected host cells can sense and activate anti-viral signaling pathways mainly through the induction of type I IFNs and inflammatory cytokines. The RLR family has three members - RIG-I, melanoma differentiation associated gene 5 (MDA5) and laboratory of genetics and physiology 2 (LGP2) (Akira *et al.*, 2006, Yoneyama *et al.*, 2008).

1.3.1 RLR structure

RIG-I contains two tandem repeats of the caspase recruitment domain (CARD) at their N-terminus, which functions as an interaction domain with other CARD-containing proteins. This is followed by the helicase domain, which is similar to other members of the DExD/H-box RNA helicase family. This domain contains an adenosine triphophate (ATP) - binding region, which is essential for RIG-I function. The C-terminal contains a repressor domain (RD), which binds to RNA (Cui *et al.*, 2008, Takahasi *et al.*, 2008). In

resting cells, RIG-I is inactive as a monomer, but virus infection and RNA binding trigger conformational changes to facilitate self-association, which promotes CARD interaction with downstream signalling molecules (Takahasi *et al.*, 2008).

MDA5 also contains tandem CARD-like regions and the DExD/H helicase domain, however, an ATP-binding region in this domain was not found. It is also unclear whether the C-terminal region of MDA5 functions as an RD.

LGP2 contains a DExD/H helicase domain and an RD, but lacks a CARD domain. LGP2 was suggested to serve as a negative regulator of RNA virus-induced responses, because the LGP2 RD binds to that of RIG-I and suppresses signaling by interfering with the self-association of RIG-I (Yoneyama *et al.*, 2008).

1.3.2 RLR ligands

RIG-I is essential for the recognition of various viruses, which include paramyxoviruses, influenza A virus, vesicular stomatitis virus and Japanese encephalitis virus, Newcastle-disease virus, Sendai virus and Hepatisis C Virus (Kato *et al.*, 2005, Loo *et al.*, 2008, Saito *et al.*, 2008, Kato *et al.*, 2006). In a recent development, RIG-I has also been implicated in antibacterial responses. RIG-I is inducible by LPS and depletion of RIG-I by RNAi or gene targeting inhibited the LPS-induced phagocytosis of bacteria. Moreover, RIG-I deficient mice were found to be more susceptible to infection with *E. coli* as compared to wild-type mice (Kong *et al.*, 2009).

MDA5 is required for the recognition of other RNA viruses, including picornaviruses such as Encephalomyocarditis virus (EMCV), Mengo virus and Theiler's virus. MDA5 is also involved in the recognition of poly I:C (Kato *et al.*, 2006).

The length of dsRNA appears to be important for differential recognition by RIG-I and MDA5 and previous reports revealed that RIG-I and MDA5 preferentially recognize short and long dsRNA, respectively (Kato *et al.*, 2008). Two other reports showed that viral RNA with 5' triphosphate is also a crucial determinant for RNA recognition by RIG-I (Hornung *et al.,* 2006; Pichlmair *et al.*, 2006). Most recently, Schlee *et al.* (2009) and Schmidt *et al.* (2009) uncovered that 5' tri-phosphate along with panhandle structures of viral RNA are crucial for RIG-I activation to initiate an antiviral response program. In contrast, agonists for MDA5 remain less well characterised. However, a recent report has shown that MDA5 activation requires a RNA 'web' rather than simply long molecules of dsRNA. This web consists of highly ordered branched structures containing both ssRNA and dsRNA (Pichlmair *et al.* 2009)

1.3.3 RLR localisation

RLRs are cytosolic and found in a variety of different cell types. RIG-I localises to membrane ruffles in non-polarized epithelial cells where it associates with the F-actin cytoskeleton. Interaction of RIG-I with F-actin is important as actin de-polymerisation results in RIG-I redistribution and activation of downstream signalling events. MDA-5 localises to the cytoplasm but does not co-localise with F-actin (Mukherjee *et al.*, 2009).

1.3.4 RLR signalling

RLR signalling results in activation of NF-κB, MAPK and IRFs for induction of type I IFN and inflammatory cytokines. IFNβ promoter stimulator 1 [IPS-1, also known as mitochondrial anti-viral signalling (MAVS), CARD adapter inducing IFNβ (Cardif) or virus-induced signalling adapter (VISA)] serves as an adapter for RIG-I and MDA5 (Kawai *et al.*, 2005, Seth *et al.*, 2006, Meylan *et al.*, 2005, Xu *et al.*, 2005). IPS-1 recruits TNF-receptor-associated death domain (TRADD), which in turn assembles Fas-associated death domain protein (FADD) and RIP-1 (Kawai *et al.*, 2005, Michallet *et al.*, 2008). Caspase-8 and caspase-10 are then recruited to FADD, where they are processed and activate NF-κB (Takahashi *et al.*, 2006). TRADD simultaneously forms a complex with TRAF3, which induces TBK1–IKKi-dependent IRF3 activation. TBK1–IKKi also interacts with an RNA helicase, DEAD box polypeptide 3 X linked (DDX3) (Schröder *et al.*, 2008). Functions for DDX3 had previously been described in processes regulating gene expression, including transcription, splicing, mRNA export and translation, and has also been suggested to be involved in cell cycle control and the regulation of apoptosis (Schröder 2009). Binding of TBK1-IKKi to DDX3 enhances cytosolic RNA- and DNA-mediated IFNβ induction, (Schröder *et al.*, 2008, Soulat *et al.*, 2008).

Stimulator of IFN genes (STING) is involved in RIG-I signalling (Ishikawa *et al.*, 2008). STING interacts with RIG-I but not MDA5. Mediator of IRF3 activation (MITA) was also found to activate an IFN promoter and was found to be identical to STING (Zhong *et al.*, 2008). Unlike STING, which was initially shown to reside in the endoplasmic reticulum (ER), MITA was shown to be localized at the outer membrane of mitochondria, where it interacts with IPS-1 and recruits IRF3. The mechanistic basis for

differences regarding cellular localization of STING and MITA is unclear but may be due to cell type specific differences.

Signalling through RIG-I is further regulated by ubiquitination. TRIM25, an E3 ubiquitin ligase, directly binds to RIG-I and promotes Lys^{63}-linked ubiquitination of the CARD of RIG-I, which facilitates the recruitment of IPS-1 to activate signalling (Gack *et al.*, 2008). TRAF3, an E3 ubiquitin ligase that polyubiquitinates through its C-terminal TRAF domain, was shown to interact with IPS-1 and activates TBK1 and IKKi (Oganesyan *et al.*, 2006, Hacker *et al.*, 2006, Saha *et al.*, 2006). By contrast, RIG-I is targetted by another ubiquitin ligase, RNF125, which induces ubiquitination and proteasomal degradation of RIG-I (Arimoto *et al.*, 2007). Recently, a de-ubiquitinase enzymatic protein called de-ubiquitinating enzyme A (DUBA) was reported to deubiquitinate TRAF3 and inhibit the RLR-mediated signalling pathway (Kayagaki *et al.*, 2007). These observations suggest that ubiquitination is an additional regulatory mechanism for the RIG-I-mediated signalling pathway.

Interestingly, in a recent study it was demonstrated that stimulating cells with LPS and ATP also induced secretion of endogenous RIG-I in macrophages and that caspase-1 interacts with RIG-I and promotes RIG-I secretion into the cytosol (Kim *et al.*, 2008).

1.4 C-type lectin receptors

C-type lectin receptors (CLRs) are another group of pathogen recognition receptors identified. CLRs share at least one carbohydrate recognition domain, which is a compact structural module that contains conserved residue motifs and determines the carbohydrate specificity of the CLRs. The CLR family includes proteins that have one or more domains that are homologous to carbohydrate recognition domains but do not

always bind a carbohydrate structures (Zelensky *et al.*, 2005). The majority of CLRs mediate endocytosis and/or phagocytosis, play a role in antigen presentation and keep endogenous glycoprotein levels constant (Palsson-McDermott *et al.*, 2007). CLRs can be divided into two groups: group I CLRs belong to the mannose receptor family and group II CLRs belong to the asialoglycoprotein receptor family (Geijtenbeek *et al.*, 2009).

CLRs interact with pathogens primarily through the recognition of mannose, fucose and glucan carbohydrate structures. Together, these CLRs recognize most classes of human pathogens; mannose specificity allows the recognition of viruses, fungi and mycobacteria, fucose structures are more specifically expressed by certain bacteria and helminths and glucan structures are present on mycobacteria and fungi (Geijtenbeek *et al.*, 2009, Rothfuchs *et al.*, 2007, van Kooyk *et al.*, 2008).

CLR triggering by different pathogens can induce diverse immune responses. Recent studies suggest that there are two general ways by which CLRs induce signalling pathways. CLRs, such as macrophage-inducible C-type lectin (mincle; also known as C-type lectin domain family (CLeC) - 4e), Dectin 2 (also known as CLeC6A), blood DC antigen 2 protein (BDCA2; also known as CLeC4C) and CLeC5A, are associated with and induce signalling pathways through immunoreceptor tyrosine-based activation motif (ITAM)-containing adaptor molecules, such as Fc receptor γ-chain (FcRγ) or DAP12 (Sato *et al.*, 2006, Cao *et al.*, 2007, Yamasaki *et al.*, 2008).

Other CLRs, such as Dectin 1, DC-specific ICAM3-grabbing non-integrin (DC-SIGN; also known as CD209), DC-immunoreceptor (DCIR) and myeloid C-type lectin-like receptor (MICL; also known as CLeC12A) induce signalling pathways through the activation of protein kinases or phosphatases that either directly or indirectly interact with their cytoplasmic domains (Gringhuis *et al.*, 2007, Rogers *et al.*, 2005, Marshall *et al.*, 2004).

Dectin-1 is the most studied member of this subgroup and contains an intracellular ITAM. Dectin-1 recognizes the fungal component zymosan through its C-type lectin-like domain (CTLD). Upon ligand recognition, the ITAM of Dectin-1 recruits the tyrosine kinase Syk, and a scaffold complex consisting of CARD9, BCL-10 and MALT, resulting in the activation of NF-κB and an increased expression of pro-inflammatory cytokines (Gross *et al.*, 2006).

1.5 Nod-like receptors

The NLR family is a group of cytoplasmic PRRs that contains more than 20 members in humans. Although the ligands and functions of many of these receptors are still being identified it is clear that their major role is to recognise cytoplasmic microbial PAMPs and/or endogenous danger signals, and initiate immunological responses. NLRs contain a variable C-terminus, a middle nucleotide binding domain (NACHT-NAD) and an LRR domain. There are four possible N-terminal domains - an acid transactivation domain (AD); baculovirus 'inhibitor of apoptosis' repeat domain (BIR), a CARD domain or a pyrin domain (PYD). NLRs are classified into subfamilies based on these domains - NLR family AD containing proteins (NLRA), NLR family BIR domain

containing proteins (NLRB), NLR family CARD containing proteins (NLRC), NLR family PYD containing proteins (NLRP) and NLR family with no strong homology to the N-terminal of any other subfamily member (NLRX proteins) (Ting *et al.*, 2008). These NLR family members are shown in Table 1.1. Four members of the NLR family namely NLRA, NLRB1, NLRC1 and NLRC2, are more commonly referred to as CIITA, NAIP, NOD1 and NOD2 respectively.

1.5.1 NLR localisation

Most NLRs are thought to be localised to the cytosol. Recent evidence however, shows that in epithelial cells NOD2 contains molecular sequences that allow association with the plasma membrane. Another recent study showed that NLRP1 is located mainly in the nucleus whereas NLRP3 is predominantly cytoplasmic.

1.5.2 NLR ligands

Several NLRs are capable of detecting bacterial components, although the mechanisms for this are not clearly understood. NOD1 and NOD2 were the first NLRs reported to have a direct function as PRRs, in the recognition of peptides that are derived from the degradation of peptidoglycan (PGN), a bacterial cell wall component. NOD1 senses γ-D-glutamyl-*meso*-diaminopimelic acid (iE-DAP), while NOD2 - senses muramyl dipeptide (MDP). NOD2 functions more as a general sensor of bacteria, since PGN from both gram-negative and gram-positive bacteria contain MDP, while NOD1 mainly senses products from gram-negative bacteria, as this is where iE-DAP is found.

When NODs detect PGN they rapidly form oligomers, which lead to the recruitment of RIP2 kinase, through CARD-CARD interactions. This complex of NOD1-RIP2 or

NLR family nomenclature			
Subfamily	Symbol	Other names and aliases	Domain organization
NLRA	CIITA	NLRA; MHC2TA; C2TA	(CARD)-AD-NACHT-NAD-LRR
NLRB	NAIP	NLRB1; BIRC1; CLR5.1	BIR3x-NACHT-NAD?-LRR
NLRC	NOD1	NLRC1; CARD4; CLR7.1	CARD-NACHT-NAD-LRR
	NOD2	NLRC2; CARD15; CD; BLAU; IBD1; PSORAS1; CLR16.3	CARD2x-NACHT-NAD-LRR
	NLRC3	NOD3; CLR16.2	CARD-NACHT-NAD-LRR
	NLRC4	CARD12; CLAN; CLR2.1; IPAF	CARD-NACHT-NAD-LRR
	NLRC5	NOD27; CLR16.1	CARD-NACHT-NAD-LRR
NLRP	NLRP1	NALP1; DEFCAP; NAC; CARD7; CLR17.1	PYD-NACHT-NAD-LRR-FIIND-CARD
	NLRP2	NALP2; PYPAF2; NBS1; PAN1; CLR19.9	PYD-NACHT-NAD-LRR
	NLRP3	CIAS1; PYPAF1; Cryopyrin; CLR1.1; NALP3	PYD-NACHT-NAD-LRR
	NLRP4	NALP4; PYPAF4;PAN2; RNH2; CLR19.5	PYD-NACHT-NAD-LRR
	NLRP5	NALP5; PYPAF8; MATER; PAN11; CLR19.8	PYD-NACHT-NAD-LRR
	NLRP6	NALP6; PYPAF5; PAN3; CLR11.4	PYD-NACHT-NAD-LRR
	NLRP7	NALP7; PYPAF3; NOD12; PAN7; CLR19.4	PYD-NACHT-NAD-LRR
	NLRP8	NALP8; PAN4; NOD16; CLR19.2	PYD-NACHT-NAD-LRR
	NLRP9	NALP9; NOD6; PAN12; CLR19.1	PYD-NACHT-NAD-LRR
	NLRP10	NALP10; PAN5; NOD8; Pynod; CLR11.1	PYD-NACHT-NAD
	NLRP11	NALP11; PYPAF6; NOD17; PAN10; CLR19.6	PYD-NACHT-NAD-LRR
	NLRP12	NALP12; PYPAF7; Monarch1; RNO2; PAN6; CLR19.3	PYD-NACHT-NAD-LRR
	NLRP13	NALP13; NOD14; PAN13; CLR19.7	PYD-NACHT-NAD-LRR
	NLRP14	NALP14; NOD5; PAN8; ; CLR11.2	PYD-NACHT-NAD-LRR
NLRX	NLRX1	NOD9; CLR11.3	X-NACHT-NAD-LRR

Table 1.1 NLR family nomenclature. The domain structure of each NLR family member is listed. AD – acid transactivation domain; BIR – baculoviral inhibitory repeat; PYD – pyrin domain; NACHT – NAIP, CIITA, HET-E and TP1; CARD – caspase recruitment domain; NAD – NACHT associated domain; LRR – leucine rich repeats. Adapted from HUGO recommended nomenclature (www.genenames.org/genefamily/nacht.html)

NOD2-RIP2 then recruits IKK, leading to activation of NF-κB. The RIP2 interacting protein TRIP6, and CARD6 positively regulate NOD1 and NOD2 dependent signalling of NF-κB. NOD2 activation is also regulated by GRIM19, TAK1 and erbin. Another outcome resulting from NOD1 and NOD2 activation is the MAPK pathway that leads to activation of p38 and ERK. NOD1 signaling also results in activation of JNK.

Several NLRs, namely NLRP1, NLRP3, and NLRC4, are involved in the assembly of cytosolic protein complexes, called inflammasomes which are described in more detail below.

1.6 The inflammasome

Various levels of crosstalk between the TLR and NLR pathways have been described, most notably the description of a multi-protein complex termed the inflammasome which requires input from both pathways, and leads to the activation of the pro-inflammatory cytokines interleukin (IL)-1β and IL-18. TLR activation by a variety a stimulants is needed for the induction of pro-IL-1β and NLRP3. The inflammasome consists of an NLR protein (such as NLRP3, NLRP1 or NLRC4) or the hematopoietic interferon-inducible nuclear proteins with a 200-amino-acid repeat (HIN-200) family member absent in melanoma 2 (AIM2), and an adaptor protein called apoptosis-associated speck-like protein containing a CARD (ASC). The complex recruits and activates caspase-1. Once activated, caspase-1 then cleaves the IL-1β precursor, and mature IL-β is released (Figure 1.2).

1.6.1 NLRC4 inflammasome

Various intracellular bacteria have the ability to activate caspase-1 in an NLRC4-dependent manner: *Salmonella typhimurium, Pseudomonas aeruginosa, Shigella flexneri* and *Legionella pneumophila. S. typhimurium, P. aeruginosa* and *S. flexneri* make use of a type-III secretion system to inject NLRC4-activating virulence factors (mainly flagellin) into the host cell, whilst *L. pneumophila* makes use of a type-IV secretion system. It is thought that flagellin and/or other bacterial products might leak into the cytosol through pores generated by these bacterial secretion systems.

1.6.2 NLRP1 inflammasome

The human NLRP1 inflammasome was the first caspase-1-activating platform to be identified and consists of pro-caspase-1, pro-caspase-5, ASC, and NLRP1. (Martinon *et al.*, 2002). Studies using purified NLRP1, ASC and caspase-1 have shown that NLRP1 forms oligomers with caspase-1 in the presence of MDP (Faustin *et al.,* 2007). Their study suggests that caspase-1 is activated by a two-step mechanism whereby microbial MDP induces a conformational change in NLRP1, which in turn allows it to bind nucleotides and to form oligomers, thus creating a platform for caspase-1 activation. Notably, caspase-1 activation by NLRP1 does not require but is enhanced by ASC (Faustin *et al.*, 2007).

NLRP1b (a murine variant) senses *Bacillus anthracis* lethal toxin, which is delivered into the cytoplasm by receptor-mediated endocytosis. NLRP1b does not contain a PYD and hence ASC is not required for the caspase-1 activation in mouse macrophages. The mechanism by which lethal factor, a metalloprotease, triggers activation of the NLRP1 inflammasome remains to be determined (Boyden *et al.*, 2006).

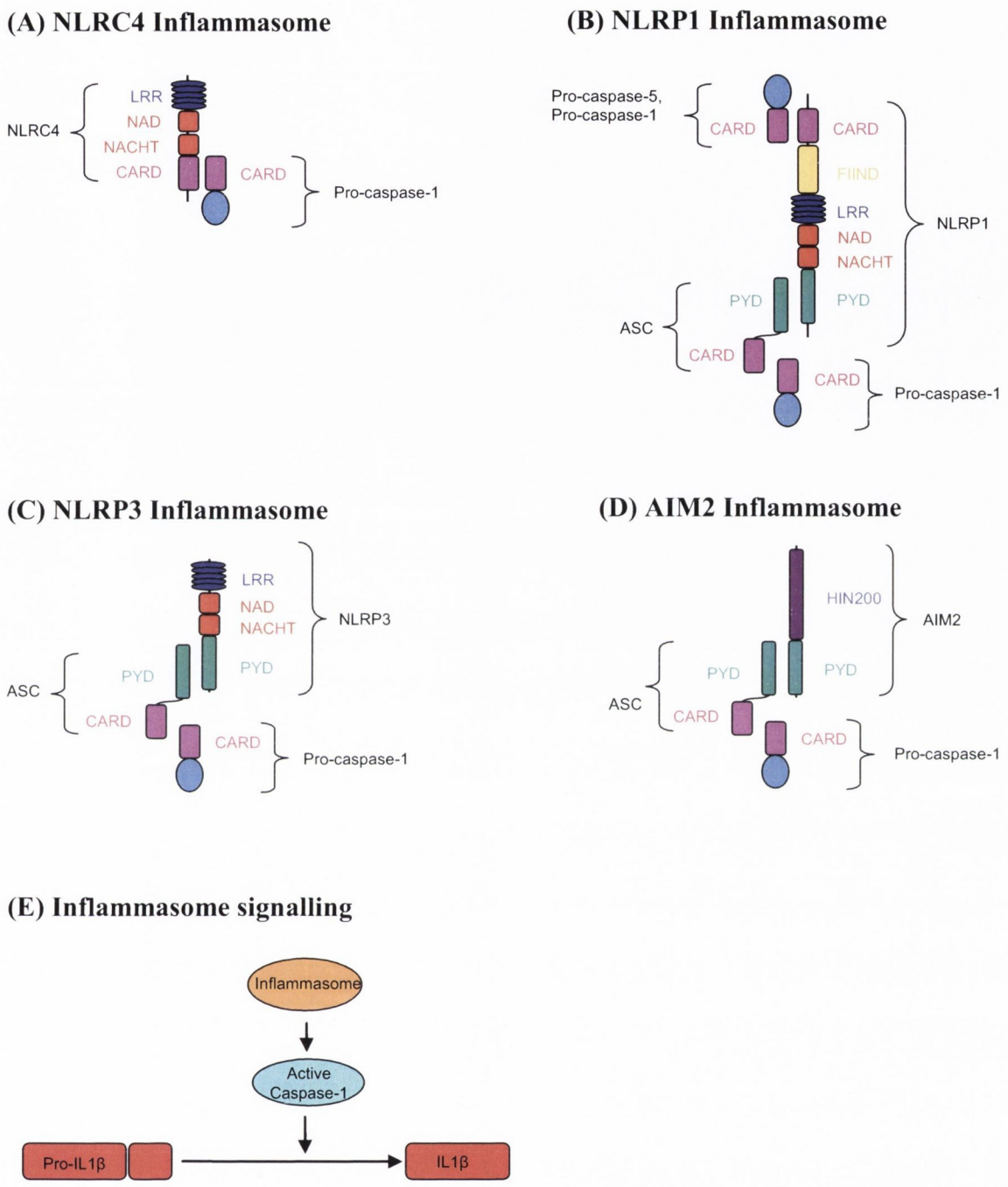


Figure 1.2 Inflammasome structure and signalling. (**A**) NLRC4 contains, in addition to the NLR-typical LRR, NAD and NACHT domains, a CARD that can directly recruit pro–caspase-1. **(B)** NLRP1 contains a PYD, a FIIND, and a CARD. NLRP1 can recruit pro–caspase-1 and -5. Recruitment of ASC enhances activation of pro–caspase-1. (**C**) NLRP3 activates pro–caspase-1 via recruitment of ASC. (**D**) AIM2 contains a PYD and a HIN200 domain and assembles an inflammasome with ASC and pro–caspase-1. **(E)** Pro-caspase-1 is activated within the inflammasome. Once activated, caspase-1 then cleaves the IL-1β precursor, and mature IL-1β is released.

1.6.3 NLRP3 inflammasome

NLRP3 mediates activation of caspase-1 in response to a variety of stimuli. These include nucleic acids such as bacterial DNA and RNA, MDP, ATP, monosodium urate (MSU) crystals, calcium pyrophosphate dehydrate crystals, UV irradiation, the dsRNA analog Poly:IC, R837, R848 and changes in ion concentrations, particularly potassium, following exposure to bacterial pore-forming toxins such as nigericin and maitotoxin (Feldmeyer *et al.,* 2007, Kanneganti *et al.*, 2006, Mariathasan *et al.,* 2006). Recently, exposure to environmental factors such as silica crystals, aluminium crystals and asbestos have been shown to activate the NLRP3 inflammasome (Dostert *et al.*, 2008, Eisenbarth *et al.*, 2008, Hornung *et al.*, 2008, Cassel *et al.*, 2008). Amyloid-β which plays a chief function in the role of Alzheimer's disease, was also shown to activate the NLRP3 inflammasome (Halle *et al.*, 2008). Pore-froming toxins from *Staphylococcus aureus* and *Listeria monocytogenes* can also activate the NLRP3 inflammasome. NLRP3 has also been linked to the activation of caspase-1 induced by viruses such as Sendai virus, Influenza virus and certain adenovirus strains used as vectors for gene therapy (Kanneganti *et al.*, 2006, Ichinohe *et al.*, 2009, Allen *et al.*, 2009, Thomas *et al.*, 2009, Delaloye *et al.*, 2009).

This list of NLRP3 activators is extensive and contains microbial pathogen associated molecules and toxins, host derived molecules, and environmental and neurodegenerative stimuli. It is therefore likely that a common pathway is triggered 'downstream' of these diverse stimuli. One possibility is that reactive oxygen species (ROS) induced by stimuli is the common trigger (Cassel *et al.*, 2008, Dostert *et al.*, 2008). However, the most recent evidence suggests that phagocytic uptake of particulates leads to swelling and

rupture of the phagasomes, releasing proteolytic enzymes such as cathepsin B which may be sensed by NLRP3 (Hornung *et al.*, 2008).

1.6.4 AIM2 inflammasome

Four new reports describe the HIN-200 family member AIM2 as the elusive sensor of cytoplasmic dsDNA for IL-1β release, providing new insight into innate viral defense systems (Burckstummer *et al.*, 2009, Fernandes-Alnemri *et al.*, 2009, Hornung *et al.*, 2009, Roberts *et al.*, 2009). The results suggest that AIM2 binds directly to cytoplasmic DNA and triggers the assembly of an AIM2 inflammasome resulting in caspase-1 activation and maturation of IL-1β. The only necessity is that DNA must be double-stranded and it was found that immunogenicity increases with DNA length. The source and sequence of cytoplasmic dsDNA appear to be unimportant for inflammasome activation, as viral, bacterial, mammalian and synthetic dsDNA could all activate caspase-1 (Schroder *et al.*, 2009).

1.6.5 Inflammasome regulation

The two major types of regulators of the inflammasome are CARD-only proteins (COPs) and PYD-only proteins (POPs). COPs include the proteins Iceberg, COP1/Pseudo-ICE, inhibitory caspase recruitment domain (INCA), caspase-12s and Nod2-S, whilst POPs include the proteins ASC2, ASCI, ASCL, PYDC1 (Stehlik *et al.*, 2007). COPs are further described in section 1.7.3 and POPs in section 1.8.1.

COPs and POPs essentially function as endogenous dominant-negative proteins that modulate the activity of the inflammasome. However COPs and POPs lack mouse orthologs. It is presumed that various other levels of regulation occur such as feedback loops and checkpoints, which ultimately ensure that inflammasome activation is tightly controlled.

An ASC-binding protein called pyrin has also been suggested to function as a negative regulator of inflammasomes, because targeted disruption of pyrin in mice resulted in enhanced secretion of IL-1β (Chae *et al.*, 2003). Pyrin disrupts PYD interactions between NLRP3 and ASC and is capable of interacting directly with other inflammasome components, resulting in caspase-1 inhibition (Chae *et al.*, 2006, Papin *et al.*, 2007, Dowds *et al.*, 2003). However, this is contentious as other groups have reported that pyrin can activate the inflammasome (Yu *et al.*, 2006, Seshadri *et al.*, 2007). Therefore, the precise role of pyrin in the regulation of inflammasomes is still controversial, but could be influenced by the type of activation of inflammasomes (Stehlik *et al.*, 2007).

Other NLRP family members have been shown to have negative roles in inflammasome activation. NLRP10 can inhibit ASC and caspase-1-mediated IL-1β maturation (Wang *et al.*, 2004) and therefore may play a role in inflammasome regulation. NLRP7 can also inhibit IL-1β secretion and NLRP2 inhibits the NF-κB activation that is induced by the combined expression of NLRP3 and ASC (Kinoshita *et al.*, 2005). Thus, NLRP2, 7 and 10 constitute an anti-inflammatory subgroup of NLRPs. As many of the NLRPs are still uncharacterised, it remains to be seen whether more of them may have similar roles in the negative regulation of the inflammasome.

Other proteins which have been implicated in inflammasome regulation are the anti-apoptotic proteins Bcl-2 and Bcl-X_L, which bind and suppress NLRP1, reducing caspase-1 activation and therefore IL-1β secretion (Bruey *et al.*, 2007).

1.7 Caspase-1

Much of this thesis focuses on caspase-1 and it will therefore now be described in more detail. Caspase-1 is the central effector of the inflammasome and activation of the inflammasome results in the cleavage and activation of caspase-1 which in turn cleaves and activates the pro-inflammatory cytokines IL-1β and IL-18 (Thornberry *et al.*, 1992, Akita *et al.*, 1997). Caspase-1 is a member of a family of intracellular cysteine proteases which can be subgrouped into different subfamilies depending on their function. In humans, 13 caspases have been identified to date, and caspase-1 belongs to the inflammatory caspase subfamily, which also includes caspases-4, -5 and -12. The remaining caspases form a subfamily with essential roles in cell death.

1.7.1 Caspase-1 activation

Caspase-1 consists of an N-terminal CARD, a large P20 domain and a small P10 domain. Caspase-1 is synthesized as an inactive zymogen and active caspase-1 is produced by proteolytic cleavage of the pro-domain, which contains the CARD. Activation of caspase-1 occurs in the inflammasome by an induced dimerisation method. It is still unclear whether caspase-1 is activated by homo-dimerisation of caspase-1 monomers or by hetero-dimerisation with other components of the inflammasome such as caspase-5 (Boatright *et al.*, 2004, Pop *et al.*, 2009).

1.7.2 Functions of caspase-1

The functions of caspase-1 are varied and are depicted in Figure 1.3. The best described function of caspase-1 is cytokine processing. Pro-IL-1β is the most documented substrate of caspase-1 and is described in more detail in section 1.9. Other cytokines that are substrates are pro-IL-1F7b and pro-IL-18. IL-18 induces IFN-γ production and promotes the differentiation of type-1 helper T cells (Th1). IL-33 is a ligand of the ST2 receptor and plays a role in allergic type disease via mediation of type 2 helper T cell (Th2) responses. IL-33 was widely assumed to be a caspase-1 substrate (Lamkanfi *et al.*, 2009), however recent evidence has emerged that IL-33 does not require caspase-1 processing for activation (Luthi *et al.*, 2009, Talabot-Ayer *et al.*, 2009, Cayrol *et al.*, 2009).

As well as cytokine processing, caspase-1 has also been shown to process *in vitro* other proteins, including the kinase PITSLRE (Beyaert *et al.*, 1997), the exosome subuit EXOSC9 (Schilders *et al.*, 2007), cytosolic phospholipase A2 ($cPLA_2$) (Luschen *et al.*, 1998) and parkin (Kahns *et al.*, 2003). Caspase-1 cleaves the TLR adaptor Mal (Miggin *et al.*, 2007), and recently caspase-1 has been shown to cleave pyrin (Chae *et al.*, 2008). Several recent reports have used approaches that have identified large numbers of potential substrates. Using a diagonal gel proteomic approach, Shao and colleagues identified 41 cellular proteins, collectively called the digestesome, which were processed *in vitro* by caspase-1 (Shao *et al.*, 2007). Among these were chaperones, cytoskeletal and translation machinery proteins, and proteins involved in immunity. A series of proteins along the glycolysis pathway were also identified, including aldolase, triose-phosphate isomerase, glyceraldehyde-3-phosphate dehydrogenase (GAPDH), α-

enolase, and pyruvate kinase. They showed that *Salmonella* infection, which fully activates caspase-1 and induces a caspase-1 form of cell death called pyroptosis, caused a pronounced degradation of these glycolysis enzymes and lowered the glycolytic rate of wild-type macrophages, but not caspase-1-deficient cells. Because glycolysis is essential for macrophage survival and activation, the cleavage of the glycolysis substrates, which results in reduction of cellular glycolysis, is therefore predicted to be an essential step toward cell death. Lamkanfi *et al.* used a proteome-wide gel free differential peptide sorting methodology to identify new substrates. They identified 20 new substrates and notably, caspase-7 was shown to be a substrate (Lamkanfi *et al.*, 2008).

A role for caspase-1 in unconventional protein secretion has recently been described. Using an Isobaric tag for relative and absolute quantitation (iTRAQ) proteomic approach Keller *et al.* identified multiple proteins that are secreted upon activation of caspase-1 including IL-1α, IL-1β, thioredoxin-1 and fibroblast growth factor-2 (FGF2). Caspase-1 binds to these leaderless proteins that lack a signal peptide and mediates their unconventional secretion (Keller *et al.*, 2008).

A role for caspase-1 has also been described in activating sterol regulatory element binding proteins (SREBPs) to promote lipid biogenesis in response to microbial pore forming toxins (Gurcel *et al.*, 2006).

Caspase-1 is also involved in pro-inflammatory form of cell death called pyroptosis (Fernandes-Alnemri *et al.*, 2007) which is described further in section 1.8.2.

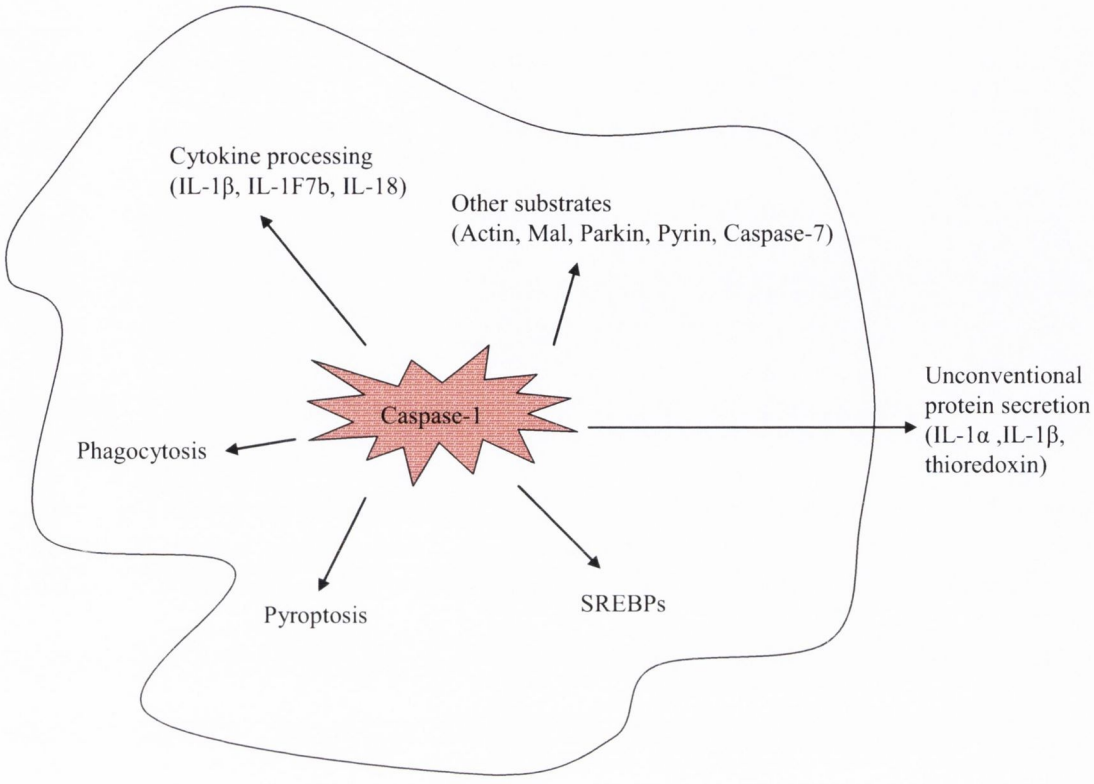


Figure 1.3 Functions of caspase-1. The functions of caspase-1 include cytokine processing, processing of other substrates, unconventional protein secretion, activating sterol regulatory element binding proteins (SREBPs), a form of pro-inflammatory form of cell death called pyroptosis and phagocytosis.

Caspase-1 also plays an important role in phagocytosis as it has been recently shown that caspase-1 activation in response to *S. aureus* infection can regulate phagosome maturation and acidification (Lynda Stuart, personal communincation).

1.7.3 Caspase-1 regulation

Because of the wide variety of important functions of caspase-1 it is essential that caspase-1 activity is tightly controlled. Caspase-1 is regulated at many different levels. Alternative splicing, tissue-specific distribution and gene induction by inflammatory mediators add to the complexity of its regulation. Alternative splicing of human caspase-1 yields four different transcripts. The expression patterns of caspase-1 have been studied extensively. Caspase-1 is expressed at low levels in most tissues, but is constitutively expressed at high levels in monocytes, macrophages, and to a lesser extent in neutrophils.

As mentioned previously, COPs have emerged as important modulators of caspase-1. The COP family comprises of 6 members each containing a CARD domain that is highly similar to that of caspase-1. The members of the COP family are Iceberg, COP1/Pseudo-ICE, INCA, caspase-12s, NOD2-s and CARD8 (Stehlik *et al.*, 2007). Iceberg is 53% similar to the CARD of caspase-1 and functions as a decoy protein by sequestering caspase-1 via CARD interaction, which prevents binding to activating adaptors. Expression of Iceberg in monocytes abrogates the secretion of IL-1β in response to LPS challenge. Because expression of Iceberg is elevated during inflammation, it might function as a negative feedback regulator to prevent systemic inflammation (Humke *et al.*, 2000). COP1/Pseudo-ICE is 92 % identical with the CARD of caspase-1. Similar to Iceberg, COP1/Pseudo-ICE interacts with the CARD of caspase-1 to prevent its

activation (Lee *et al.*, 2001). INCA shares 81% protein identity with the CARD of caspase-1 and also blocks caspase-1 activation by similar means (Lamkanfi *et al.*, 2004). Caspase-12 was recently identified as a negative regulator of the inflammatory cytokine response by binding to and inhibiting caspase-1. The pro-domain contains a CARD and is sufficient for causing reduced cytokine secretion (Saleh *et al.*, 2006, Saleh *et al.*, 2004). Significantly, in the majority of the human population a single nucleotide polymorphism (SNP) causes a premature stop codon that results in the expression of only the CARD, comprising essentially a COP (Saleh *et al.*, 2004). A short variant of Nod2, Nod2-S, was identified, which encodes only the first CARD and functions similar to other COPs. Nod2-S does not interact with caspase-1 but with its adaptor RIP2 and competes with Nod2 for RIP2 binding, resulting in impaired caspase-1 activation (Rosenstiel *et al.*, 2006). CARD-8 interacts with caspase-1, Iceberg and COP1/pseudo-ICE and negatively regulates caspase-1-dependent signalling (Razmara *et al.*, 2002).

1.8 ASC

ASC is another essential component of the inflammasome and much of the work in chapter 5 is focused on ASC. As one of the critical factors in the formation of inflammasomes, the adaptor protein ASC functions as a mediator to recruit NLRs and pro-caspase-1. ASC has a C-terminal CARD and an N-terminal PYD. ASC was originally found and identified as a molecule which formed a speck near the nucleus in HL-60 cells (Masumoto *et al.*, 1999).

ASC has also been reported to act as a tumour suppressor gene downregulated by methylation (Conway *et al.*, 2000) and this has been confirmed in many types of cancer (Guan *et al.*, 2003, Machida *et al.*, 2006).

Martinon *et al.* reported that ASC is indispensable for the activation of pro-caspase-1. By using a cell-free system they showed that pro-inflammatory caspase-1 activation and pro-IL-1β processing is lost upon prior immunodepletion of ASC. Moreover, expression of a dominant negative form of ASC in THP1 cells blocks pro-IL-1β maturation and activation of inflammatory caspases induced by LPS *in vitro*. In ASC deficient mice no activation of caspase-1 occurs and thereby no activation of pro-IL-1β. Thus, these mice were resistant to LPS induced endotoxin shock (Martinon *et al.*, 2002).

1.8.1 Regulation of ASC

As previously mentioned ASC can be regulated by a group of proteins called POPs. POPs are characterised by the presence of a PYD and are thought to interfere with PYD-PYD interactions between ASC and NLRP proteins (Fairbrother *et al.*, 2001). Members of this group are POP1 and POP2. They have PYD domains which are highly similar to those in ASC and NLRPs, and have been shown to regulate inflammasome assembly and IL-1β secretion (Stehlik *et al.*, 2003, Dorfleutner *et al.*, 2007, Bedoya *et al.*, 2007).

1.8.2 Pyroptosis

As well as having a role in the inflammasome, ASC has a role in a caspase-1 dependent-form of programmed cell death called pyroptosis. *S. flexneri,* the etiological agent of bacterial dysentery, was the first invasive bacterial pathogen reported to induce caspase-1-dependent programmed cell death (Zychlinsky *et al.*, 1992, Chen *et al.*, 1996, Hilbi *et al.*, 1998). Caspase-1-dependent programmed cell death has also been extensively reported in *S. typhimurium* infected macrophages (Hersh *et al.*, 1999, Brennan *et al.*, 2000, Lara-Tejero *et al.*, 2006, Mariathasan *et al.*, 2004), and DCs (van der Velden *et*

al., 2003). Further reports of caspase-1-dependent cell death have also been described in macrophages infected with *L. monocytogenes* (Cervantes *et al.*, 2008), *P. aeruginosa* (Sutterwala *et al.*, 2007), *F. tularensis* (Mariathasan *et al.*, 2005), *L. Pneumophila* (Zamboni *et al.*, 2006, Molofsky *et al.*, 2006), *Y. pseudotuberculosis* (Bergsbaken *et al.*, 2007), and *B. pseudommalel* (Sun *et al.*, 2005).

Recently, it was shown in THP1 cells, a human monocytic cell line, that upon stimulation with inflammatory agonists and K^+ efflux that ASC in the cell oligomerised into a single cytoplasmic speck termed a 'pyroptosome'. This platform then recuits and activates caspase-1 necessary for the caspase-1 dependent cell death (Fernandes-Alnemri *et al.*, 2007). The same lab subsequently showed that proline- serine-threonine phosphatase interacting protein 1 (PSTPIP1) is crucial for the formation of the pyroptosome. PSTPIP1 requires pyrin to assemble the ASC pyroptosome. Pyrin is a cytosolic receptor for PSTPIP1. Pyrin exists as a homotrimer in an autoinhibited state due to intramolecular interactions between its pyrin domain and B-box. Ligation by PSTPIP1, which is also a homotrimer, activates pyrin by unmasking its PYD, thereby allowing it to interact with ASC and facilitate ASC oligomerization into an active ASC pyroptosome (Yu *et al.*, 2007).

1.9 Interleukin-1β

Ultimately activation of the inflammasome results in the processing and release of IL-1β. It forms an important part of the inflammatory response of the body against infection. IL-1β is produced as a precursor peptide. It is made as a 31 kDa protein (pro-IL-1β) that is then processed to release a shorter (17 kDa), active molecule termed mature IL-1β. Mature IL-1β is released from pro-IL-1β following cleavage by caspase-1.

It is currently hypothesized that two signals are required for IL-1β processing in normal human monocytes. TLR ligands bind to TLRs and the downstream signalling cascade results in the induction of NF-κB and the subsequent transcription of pro-IL-1β. Pro-IL-1β is then stored in the cell. The second signal is NLRP-induced IL-1β processing and release through a caspase-1-dependent mechanism. Thus, stimulation through both TLRs and NLRs are required for processing and release of IL-1β.

1.9.1 IL-1β secretion

Most proteins have signal peptides or leader sequences and can be exported from the cell by the endoplasmic reticulum/Golgi-dependent pathway. However, during the initial characterisation of IL-1, the lack of a signal sequence at the N-terminal or elsewhere was noted (Auron *et al.*, 1984, March *et al.*, 1985). Supporting this, immunoelectron microscopy and subcellular fractionation studies failed to demonstrate IL-1 molecules in the ER and in the Golgi apparatus (Singer *et al.*, 1988, Matsushima *et al.*, 1986, Bakouche *et al.*, 1987). Release was initially thought to be due to cell lysis (Hogquist *et al.*, 1991) or passage through a plasma membrane pore (Singer *et al.*, 1995). In 1990 Rubartelli *et al.* showed that Brefeldin A, which blocks protein release from the ER, did not affect the release of IL-1β. They also showed that Monensin, which blocks protein transport to the Golgi, had no effect on IL-1β release. They discovered that IL-1β is contained within intracellular vesicles and released from monocytes upon LPS activation (Rubartelli *et al.*, 1990). From the same lab, Andrei *et al.* suggested that activated monocytes secrete IL-1β by exocytosis in endolysosomal related organelles. These organelles were shown to contain the endolysosomal hydrolase cathepsin D and the lysosomal marker Lamp-1 (Andrei *et al.*, 1999). A further paper in 2004, showed

that pro-caspase-1 was also in these secretory vesicles and that their release is facilitated by extracellular ATP which triggers the efflux of K^+ from the cell, followed by Ca^{2+} influx and activation of three phospholipases: phosphatidylcholine-specific phospholipase C and calcium-independent and -dependent phospholipase A_2 (Andrei *et al.*, 2004). Carta *et al.* showed that a functional microtubule network is required for IL-1β secretion (Carta *et al.*, 2006).

MacKensie *et al.* have shown that IL-1β is present in microvesicles shed from PMA/LPS/ATP activated THP-1 monocytes by isolating microvesicles released into the supernatant with annexin-coated beads and then assaying for the presence of IL-1β in both vesicular and vesicle-free supernatant fractions (MacKenzie *et al.*, 2001). They proposed a model whereby following priming with LPS, activation of the purinergic receptor P_2X, ligand-gated ion channel, 7 (P_2X_7) receptors by extracellular ATP causes phosphatidylserine (PS) flip and loss of plasma membrane asymmetry within a few seconds. Some seconds later, PS-exposed microvesicles containing bioactive IL-1β pinch off from the cell, and this IL-1β is able to activate IL-1 receptors on other cells.

Studies by Brough and Rothwell revealed that in murine peritoneal macrophages, IL-1β does not colocalize with the early endosome marker early endosomal antigen 1 (EEA1) or with the late endosome/early lysosome marker cathepsin D, suggesting that IL-1β is released neither via lysosomes nor via exosomes. The lack of a contribution of lysosomes in IL-1β release was further demonstrated in experiments using Digitonin, which selectively permeabilizes the plasma membrane, while leaving lysosomes intact. In digitonin-treated cells, both intracellular pro-IL-1β and mature IL-1β were lost, while

intracellular signals of the lysosomal marker cathepsin D remained unaffected. They saw that IL-1β processing occurred intracellularly, and therefore excluded that microvesicle shedding contributes significantly to the release of IL- 1β from peritoneal macrophages. It was, therefore suggested that mature IL-1β is released from ATP-stimulated peritoneal macrophages by direct passage through the plasma membrane via a plasma membrane transporter (Brough *et al.*, 2007).

The latest evidence suggests that IL-1β is released in exosomes. Qu *et al.* suggest a mechanism whereby a P_2X_7 receptor-induced concentration of caspase-1 inflammasomes and pro-IL-1β occurs in the cytosol within the region of recycling endosomes. This is followed by the formation of multivesicular bodies containing entrapped IL-1β with eventual exocytosis of IL-1β, caspase-1, other inflammasome components, and membrane marker proteins such as Major Histocompatability Complex II (MHC-II) (Qu *et al.*, 2007). This was followed up by a further paper from this group describing how the secreted vesicles could be divided into groups. One group comprises 100- to 600-nm microvesicles derived from direct budding of the plasma membrane, while the second group is composed of 50- to 80-nm exosomes released from multivesicular bodies. ASC and NLRP3 were required for the P_2X_7-regulated release of the exosome but not the microvesicle MHC-II pool. Treatment of bone marrow derived macrophages (BMDMs) with YVAD-cmk, a peptide inhibitor of caspase-1, also prevented P_2X_7R-dependent MHC-II secretion. However, MHC-II release in response to ATP was intact in caspase-1 deficient macrophages (Qu *et al.*, 2009).

Therefore, we can see that a variety of methods for IL-1β secretion have been proposed (Figure 1.4). It will remain to be seen whether there is one unifying model of IL-1β

release. It is possible however, that IL-1β secretion mechanisms may vary with the cell type examined, the stimulus used and the degree of activation.

1.9.2 IL-1β signalling

IL-1β exerts its function through the IL-1 receptor IL-1RI. There are two forms of IL-1R. IL-1RI possesses a long cytoplasmic domain and is capable of activating cells. IL-1RII has only a short intracellular domain and is biologically inert. However, IL-1RII may negatively regulate cell activation by acting in the membrane to compete for ligand binding with IL-1RI. In addition, IL-1RII is readily released from cells where it may bind IL-1 in the cell micro-environment, preventing interaction with cell surface IL-1RI (Arend *et al.*, 2008).

After IL-1β binds to IL-1RI, a second chain called the IL-1R accessory protein (IL-1RAcP) joins with IL-1/IL-RI to form a complex, leading to cell activation mediated by the cytoplasmic domains of both receptor chains. This complex recruits a number of intracellular adapter molecules, including MyD88 and TRAF6, to activate signal transduction pathways such as NF-κB, AP-1, JNK, and p38 MAPK (Arend *et al.*, 2008).

Signalling via the IL-1RI receptor can be blocked by the binding of the receptor antagonist IL-1Ra. The IL-1Ra molecule is closely related structurally to IL-1β but has undergone mutations rendering it incapable of interacting with IL-1RAcP. As already mentioned a second receptor, IL-1RII, binds IL-1β as a decoy receptor and does not recruit the necessary proteins for signal transduction.

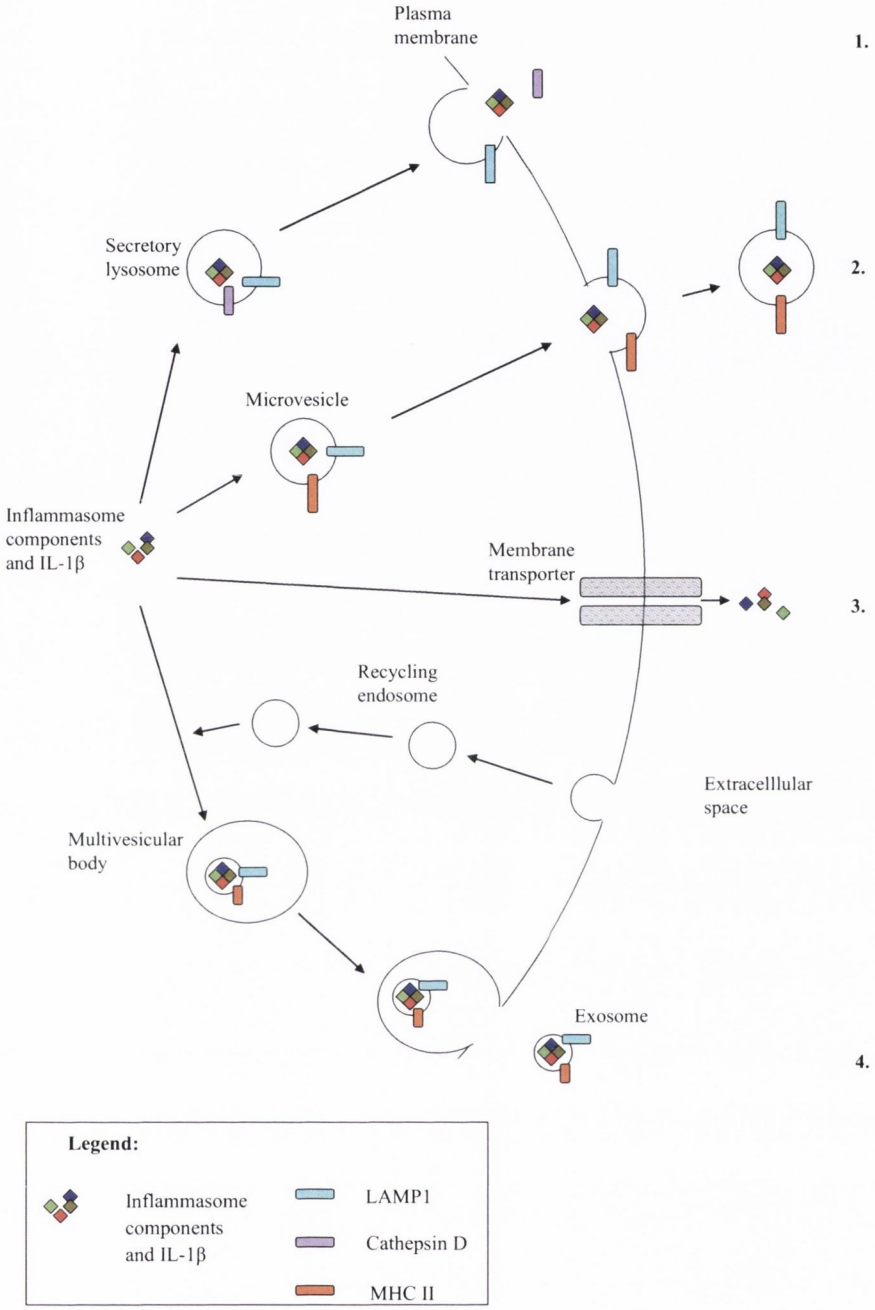


Figure 1.4 Current models of IL-1β secretion. Pathway 1 suggests the release of IL-1β via exocytosis of secretory lysosomes. Pathway 2 proposes microvesicle shedding and release of IL-1β from shed microvesicles. Pathway 3 suggests the transport of IL-1β from the cytosol to the extracellular space via specific membrane transporters. Pathway 4 shows the formation of multivesicular bodies followed by the release of IL-1β-containing exosomes.

1.9.3 Functions of IL-1β

IL-1β is an important mediator of the inflammatory response, and is involved in a variety of cellular activities, including cell proliferation, differentiation, and apoptosis. It increases the expression of adhesion factors on cells, such as intracellular adhesion molecule-1 (ICAM-1) on mesenchymal cells and vascular cell adhesion molecule-1 (VCAM-1) on endothelial cells. This enables transmigration of leukocytes to sites of infection. The induction of cyclooxygenase-2 (COX2) by this cytokine in the central nervous system (CNS) is found to contribute to inflammatory pain hypersensitivity. IL-1β signalling also results in platelet activation, induction of Prostaglandin (PG) E2 which causes non-specific suppression of T cell responses, increases Type 2 phospholipases, inducible nitric oxide synthase (iNOS) and nitric oxide (NO) production. This results in the infiltration of inflammatory and immunocompetent cells from the circulation into the extra vascular space and then into tissues. The end result is tissue re-modelling. These IL-1β functions manifest themselves as fever, a lowered pain threshold, vasodilation and hypertension. IL-1β is also an angiogenic factor and has a role in tumour metastasis and blood vessel formation (Dinarello, 2009) (Voronov *et al.*, 2003).

1.10 Inflammasomopathies

Several chronic and often debilitating inflammatory diseases are due to an increase in inflammasome activity, and this represents a failure of the caspase-1 inflammasome to control the processing of the IL-1β precursor. The symptoms of these auto-inflammatory syndromes and diseases, termed inflammasomopathies (Masters *et al.*, 2009), constitute a portfolio of destructive inflammation events and are accompanied by fever, painful joints and muscles, fatigue associated with high white blood cell counts, elevated acute phase proteins, anemia, and high platelet counts.

Firstly, there are the intrinsic inflammasomopathies which represent molecular lesions in the constituent proteins of the complex. For example mutations in the cold-induced autoinflammatory syndrome 1 (CIAS1) gene can result in muckle-wells syndrome (MWS), familial cold urticaria (FCU), or neonatal-onset multisystem inflammatory disease (NOMID), also known as chronic infantile neurologic, cutaneous, articular syndrome (CINCA). These disorders are characterised by recurrent episodes of fever with inflammatory responses in multiple organs including the joints, skin, eyes, ears and central nervous system. All of these disorders are characterised by over-production of IL-1β and are linked to mutations in the CIAS1 gene which encodes NLRP3 leading to enhanced caspase-1 activity.

The extrinsic inflammasomopathies are caused by mutations in proteins that regulate the production of IL-1β but are not constituents of the inflammasome complex. Pyogenic sterile arthritis, pyoderma gangrenosum, and acne (PAPA) syndrome is due to a single amino acid mutation in the pyrin-binding protein PSTPIP1. It has been shown that these PAPA-associated PSTPIP1 mutants have higher binding affinity to pyrin and were found to be more effective than wild type PSTPIP1 in inducing ASC oligomerisation and subsequently more caspase-1 activation. Mutations in pyrin itself result in familial Mediterranean fever (FMF). DIRA is a very newly described auto-inflammatory disease and is due to mutations in IL1-Receptor antagonist (Aksentijevich *et al.*, 2009).

Complex or acquired inflammasomopathies are multigenic or environmentally predisposed. For example gout is due to deposition of MSU crystals in the joint which activate the inflammasome leading to inflammation. Type 2 diabetes mellitus (T2DM) is

due to a combination of insulin resistance and impaired islet cell insulin secretion. Recent evidence suggests that the innate immune system plays an important role in the pathogenesis of T2DM (Masters *et al.*, 2009). T2DM is associated with persistent elevation of certain proinflammatory cytokines, particularly IL-1β and IL-6. IL-1β can damage the insulin producing pancreatic β-cells. A 13 week trial of IL-1Ra therapy improved glycaemic control and function of the insulin producing cells (Larsen *et al.*, 2007).

1.11 Rab GTPases

This thesis deals with caspase-1 and its novel association with the previously uncharacterised Rab39a. Rab proteins are monomeric small guanosine triphosphate (GTPases). They regulate many steps of membrane traffic, including vesicle formation, vesicle movement along actin and tubulin networks, and membrane fusion.

Rab GTPases were first identified in 1987 as evolutionarily conserved, essential regulators of membrane trafficking (Touchot *et al.*, 1987). To date, over 70 members of this family have been identified in humans (Schwartz *et al.*, 2007).

Rab proteins are present on all compartments of the endomembrane system (endoplasmic reticulum, Golgi, endosomes, lysosome), the nucleus, the plasma membrane (including cell junctions and focal adhesions), mitochondria and centrioles (Schwartz *et al.*, 2007). Rabs are thought to act as molecular switches, being active in their GTP-bound state and inactive in their guanosine diphosphate (GDP) - bound state. Rabs are regulated by other proteins, guanine nucleotide exchange factors (GEFs) and GTPase-activating proteins (GAPs). In their GDP-bound state, Rabs are typically

soluble and bound to a guanine nucleotide dissociation inhibitor (GDI). At the acceptor membrane, the Rab-GDI complex is thought to interact with GDI displacement factor, which removes GDI and allows membrane insertion. Next, a GEF converts Rab to its GTP-bound, active conformation, allowing it to interact with its downstream effectors. (Figure 1.5)

1.11.1 Rab GTPases and vesicle trafficking

Rab GTPases are key regulators of protein transport in all eukaryotic cells. They are involved in all aspects of vesicle trafficking: vesicle formation, motility, and docking, and membrane remodelling and fusion. Eukaryotic cells transport proteins between different compartments. Contents are sorted and packaged into vesicles, which then bud and detach from one compartment (donor membrane), and move to its target membrane where they can fuse and release their contents into the lumen of the organelle (Zerial *et al.*, 2001, Goud *et al.*, 1988, Kamal *et al.*, 2000, Hawes *et al.*, 1999). Rab proteins were first implicated in vesicular trafficking with the identification of SEC4 as the gene mutated in a yeast mutant which displays blocked transport to the plasma membrane (Goud *et al.*, 1988, Salminen *et al.*, 1987).

1.11.2 Rab GTPases and phagocytosis

After their formation, phagosomes undergo a maturation process by interacting with the endosomal pathway (Vieira *et al.*, 2002). Recruitment of Rab5 to early phagosomes is one of the earliest known events during phagosomal maturation (Gorvel *et al.*, 1991). Progression through to late phagosomes involves the recruitment of Rab5 effectors and the recruitment of Rab7. It is not known how Rab7 is recruited to the phagosome, or how recruitment is related to the release of Rab5. However, recent studies suggest that Rab5 is

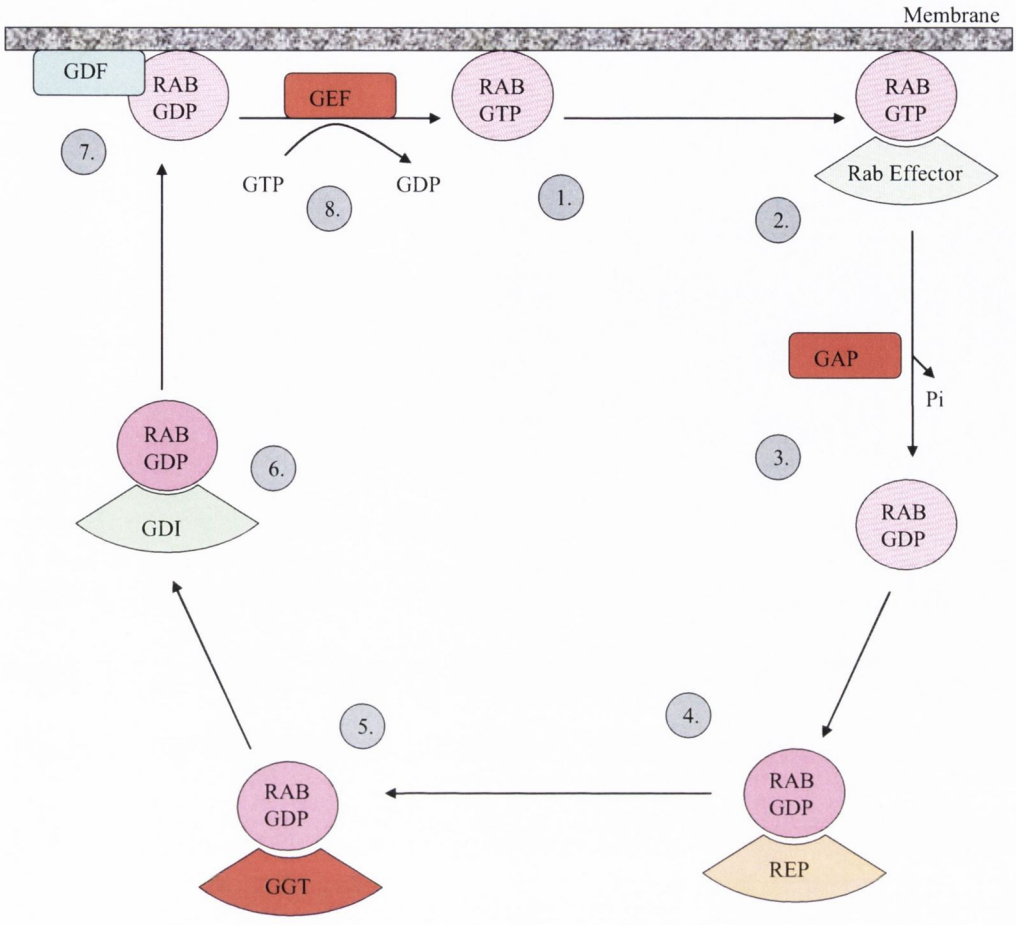


Figure 1.5 The Rab GTPase cycle. **1**. GTP-bound 'active' Rab is attached to a specific membrane **2**. The GTP-bound Rab is recognised by effector proteins **3**. GTP-Rab is converted back to the GDP-bound 'inactive' form through hydrolysis of GTP, which is stimulated by a GTPase-activating protein (GAP) and an inorganic phosphate (Pi) is released **4.** GDP-Rab is recognized by a Rab escort protein (REP) **5.** The REP presents the Rab to a geranylgeranyl transferase (GGT), which geranylgeranylates the Rab **6**. The geranylgeranylated, GDP-bound Rab is recognized by Rab GDP dissociation inhibitor (GDI) **7.** The Rab–GDI complex is targeted to specific membranes by interaction with a membrane-bound GDI displacement factor (GDF). GDF displaces the GDI and allows the prenyl Rab to bind to the membrane **8.** The GDP-Rab can then be activated by a specific guanine nucleotide exchange factor (GEF), converting the Rab back into its GTP-bound form.

simultaneously exchanged for Rab7 during endocytosis by a process called Rab conversion (Rink *et al.*, 2005). After Rab7 removal, the phagosome fuses with the lysosome to become a phagolysosome where lysosomal degradation occurs. Rab5 and Rab7 are the best characterised phagosomal Rabs however recent proteomics approaches have identified a number of other different Rab GTPases that are localized to the phagosome at different times. These include Rab1, Rab2, Rab3, Rab6, Rab8, Rab9, Rab10, Rab11, Rab14, Rab20, Rab22, Rab23, Rab32, Rab33, Rab35 (Kinchen *et al.*, 2008, Brumell *et al.*, 2007). These Rabs may be involved in the delivery of cargo (for example, from the Golgi and ER to the phagosome), potentially delivering lysosomal proteases and other degradatory components. Another possibility is that one (or more) of these Rabs mediates transport from the phagosome to the ER, carrying processed antigens that will be presented on the cell surface by MHC class I proteins (Kinchen *et al.*, 2008).

1.11.3 Rab GTPases and pathogenic hijacking

Whilst the immune system is incredibly efficient at seeking out and destroying potential pathogens, certain pathogens have developed mechanisms for interfering with the recruitment and functions of Rabs (Brumell *et al.*, 2007, Kinchen *et al.*, 2008). There are many examples of pathogenic hijacking of GTPases, two of which are given here.

M. tuberculosis has the ability to colonise a nondegradative phagosome in macrophages, avoiding lysosomal degradation (Armstrong *et al.*, 1971, Crowle *et al.*, 1991). Several Rab GTPases have been implicated in this phagosomal maturation arrest. The maturation of mycobacterium-containing phagosomes is blocked at the Rab5-positive stage. Rab22a also accumulates on mycobacterial phagosomes. Live mycobacteria

retained increasing amounts of Rab22a, while dead mycobacteria and latex bead phagosomes did not. Reduced expression of Rab22a enhanced the maturation of phagosomes containing live mycobacteria, whilst the overexpression of a constitutively active mutant of Rab22a, Rab22aQ64L, prevented the maturation of phagosomes containing heat-killed mycobacteria (Roberts *et al.*, 2006). Rab14 also appears to be involved in phagosomal maturation arrest. The reduced expression of Rab14 or overexpression of dominant negative Rab14S25N promoted the fusion of lysosomes with phagosomes containing live mycobacteria. The expression of constitutively active Rab14Q70L prevented the fusion of phagosomes containing dead mycobacteria with lysosomes (Kyei *et al.*, 2006). Together, those studies suggest that *M. tuberculosis* can modulate the phagosome-associated Rab network at various levels.

L. pneumophila, is able to recruit membranes from the ER or the pre-Golgi intermediate compartment (IC). This effectively changes the composition of the phagosomal membrane so that it contains many features of the ER allowing it to persist and replicate within the cell. *L. pneumophila* secretes two proteins to do this. The first is SidM which acts as a GEF and GDF for Rab1, whilst the second secreted protein LepB is a Rab1 GAP. The expression of these proteins means that *L. pneumophila* – containing vacuoles can recruit Rab1 and behave as ER or IC membranes and avoid lysosomal destruction (Ingmundson *et al.*, 2007, Machner *et al.*, 2007).

1.11.4 Rab39a

Rab39a (previously called RabK28) was first described in 1997 by Stankovich *et al.* whilst assembling a transcription map of the ataxia telangieactasia gene region. They found that the gene is widely expressed in a variety of tissues including spleen, thymus,

prostate, testis, ovary, small intestine, colon and peripheral blood leukocytes (Stankovic *et al.*, 1997). Rab39b was described as a novel Rab protein in 2002 and is 76 % similar to Rab39a (Cheng *et al.*, 2002). The functions of Rab39a and Rab39b are previously undescribed.

1.12 Aims

This project concerns an analysis of the regulation of caspase-1 and ASC. At the outset Rab39a was found in a complex with caspase-1. Thus, the initial aim of the project was to determine the role of Rab39a in caspase-1 regulation. The second aim of this project was to characterise the molecular regulation of ASC in the inflammasome.

The specific aims were as follows:

- To confirm the interaction between caspase-1 and Rab39a
- To use bioinformatic analyses to characterise Rab39a
- To analyse if Rab39a is a substrate for caspase-1
- To address the function of the interaction between Rab39a and caspase-1 by examining if Rab39a has a role in phagocytosis and if Rab39a has a role in IL-1β secretion
- To identify other novel binding partners of the inflammasome by mass spectrometry
- To investigate novel signalling pathways involving ASC necessary for inflammasome formation

Overall, I have found a novel interactor for caspase-1 (Rab39a) required for IL-1β secretion and found a possible mechanism for ASC activation involving tyrosine phosphorylation. This thesis therefore provides insight into a key aspect of inflammation: the molecular regulation of IL-1β production.

Chapter 2

Materials and Methods

2.1 Materials

Ultrapure Lipopolysaccharide (LPS) and macrophage-activating lipopeptide 2 kDa (Malp2) were purchased from Alexis (Dorset, UK). Pam_3Cys_4 was obtained from Calbiochem (San Diego, California, USA). PolyI:C was purchased from Amersham (GE Healthcare, Buckinghamshire, UK). ATP was purchased from Sigma (Dorset, UK)

The empty vector pcDNA3.1 was purchased from Invitrogen (California, USA). PCMV-SPORT6-Rab39a and PCMV-SPORT6-Rab39b were purchased from ATCC (Middlesex, UK). PGEM-T-Easy was purchased from Promega. PCMV-HA was from Clontech (Saint-Germain-en-Laye, France). AU-1-Caspase-1 was a gift from Prof. Seamus Martin, Dept. Genetics, Trinity College Dublin, Ireland. The expression vector encoding ASC was a gift from Prof. Jurg Tschopp, Institute of Biochemistry, University of Lausanne, Switzerland. The plasmid encoding PCDNA3-HA-Rab25 was a gift from Dr. Mary McCaffrey, Dept. Biochemistry, University College Cork, Ireland. PCDNA3-MYC-PSTPIPI was a gift from Prof. Dan Kastner, National Institute of Arthritis and Musculoskeletal and Skin Diseases, Bethesda, Maryland, USA. GFP-Rab39a was a gift from Prof. Mitsunori Fukuda, Department of Developmental Biology and Neurosciences Tohoku University, Japan. GFP-Rab14 and Myc-Rab4 were gifts from Dr. Richard Scheller, Genentech, San Francisco, USA. RFP-caspase-1 was a gift from Prof. Christian Stehlik, Division of Rheumatology, NorthWestern University, USA.

HA antibody was purchased from Cambridge Biosciences (Cambridge, UK). The ASC antibody was from Alexis (Exeter, UK). Caspase-1 and MYC antibodies were obtained from Santa Cruz (Santa Cruz, USA). Anti-β-actin antibody was obtained from Sigma. IL-1β antibodies were from Cell Signaling (Massachusettes, USA) or Upstate

(Massachusettes, USA). Rab5 and Rab7 antibodies were also from Cell Signaling. The anti-rabbit IgG and anti-mouse IgG antibodies were obtained from Sigma. Secondary horse-radish conjugated anti-mouse and anti-rabbit were from Jackson ImmunoResearch Inc (Suffolk, UK). Rab39a antibody was designed and purchased from Eurogentech (Searaing, Belgium) or purchased from Abnova (Heidelberg, Germany).

The human embryonic kidney cell line 293T (HEK293T) were a gift from Dr. Kate Fitzgerald, University of Massachusetts, USA. TLR4-MD2-CD14 transfected HEK293 Cell Line were purchased from Invivogen (San Diego, USA). The human macrophage THP1 cell line was obtained from the European collection of Animal Cell Cultures (Salisbury, UK). The immortalised (I) wild-type BMDM and MyD88 knockout BMDMs were a kind gift from Prof. Douglas Golenbock, University of Massachusetts, USA. Stably transfected ASC-FP macrophages were a kind gift from Dr. Eicke Latz, University of Massachusetts, USA. The mouse leukaemic monocyte macrophage cell line RAW 264.7 was from ATCC. RPMI 1640 and DMEM cell culture media were obtained from GIBCO (Biosciences, Dublin, Ireland). Fetal calf serum (FCS) was obtained from Biosera (East Sussex, UK). Penicillin, streptomycin (PS) and trypsin were obtained from Sigma.

General laboratory chemicals were purchased from Sigma with the exception of: broad range pre-stained protein marker and DNA markers which were from New England BioLabs Ltd. (Massachusetts, USA), 20X LumiGLO® Reagent and 20X Peroxide Supersignal® were from Cell Signaling. GeneJuice® was purchased from Novagen (Nottingham, UK). The general caspase inhibitor (Z-VAD-FMK), the specific caspase-1

inhibitor (Y-VAD-CMK), recombinant caspase-1, cyclohexamide, kinase inhibitors and MG132 were all purchased from Calbiochem (California, USA). TNF-α, IL-1β and IL-6 ELISA Duosets were purchased from RnD Systems (Abingdon, UK). Maxiprep and Miniprep kits were purchased from Promega (Southhampton, UK) or Qiagen (Sussex, UK). Protein A/G beads were from Santa Cruz. Trypsin Gold was from Promega. Gel extraction kits and RNA extraction kits were purchased from Qiagen. Primers were ordered from MWG (Eberbsberg, Germany) and siRNA oligos were ordered from Ambion (Texas, USA) and Qiagen. The Site Directed Mutagensis Kit was from Stratagene (Californai, USA). SuperScript® III First-Strand Synthesis System for RT-PCR and SYBR Green were purchased from Invitrogen (Dun Laoghaire, Ireland). IPG strips and electrode wicks were purchased from Biorad (Blessington, Ireland). Ultrafee-CL centrifugal filters were from Millipore (Cork, Ireland).

2.2 Bioinformatic analysis

Homology searches were carried out using NCBI BLAST program and NCBI Taxonomy BLAST reports (http://blast.ncbi.nlm.nih.gov). Conserved domains were found using NCBI conserved domains database (www.ncbi.nlm.nih.gov/structure/cdd/cdd/shtml). Sequence alignments were carried out using ClustalW2 (www.ebi.ac.uk/clustalw). Peptide cutter (www.expasy.ch/tools/peptidecutter/) was used to predict potential cleavage sites cleaved by caspase-1 in a given protein sequence. Secondary structure prediction was done using PSIPRED predictive software (www.bioinf.cs.ucl.ac.uk/psipred/). Tertiary structure prediction was done using 3D-Jigsaw software (www.bmm.cancerresearchuk.org/~3djigsaw/). Promoter analysis was carried out using the Genomatix website (www.genomatix.de). Predicted sites of ubiquitination were

found using BDM-PUB (http://bdmpub.biocuckoo.org/). Phosphorylation sites were predicted using NetPhos 2.0 (www.cbs.dtu.dk/services/NetPhos). Tissue expression arrays were analysed using data from the Bio GPS database (http://biogps.gnf.org).

2.3 Cell culture

2.3.1 Cell lines

HEK293T, TLR4-MD2-CD14 HEK293, RAW 264.7, ASC-FP macrophages, I-WT-BMDMS and I-MyD88 knockout BMDM cell lines were cultured in DMEM medium containing 10 % FCS (v/v), and 1 % PS (v/v). THP1 cells were cultured in RPMI 1640 medium containing 10 % FCS (v/v) and 1 % PS (v/v).

Cells were maintained at 37 °C in a humidified atmosphere of 5 % CO_2. Cells were generally seeded at 2-5 x 10^5 per ml and sub-cultured two or three times a week. HEK293T's, ASC-FP macrophages, RAW 264.7 cells, and I-BMDMs were removed from the surface of the flask by incubation with 5 ml of trypsin-EDTA (0.05 mg/ml). 5 ml of media was then added to the cells and they were centrifuged at 120 rcf for 5 minutes before resuspending the pellet in fresh media. THP1 cells were poured directly into sterile falcon tubes and centrifuged at 120 rcf for 5 minutes before re-suspending the pellet in fresh media. THP1 cells were differentiated using 0.5 μM PMA where indicated. Cell viability was determined using the dye Trypan blue, which is excluded from healthy cells but taken up by non-viable cells. Cells were counted using a haemocytometer and a bright light microscope. For cryo-preservation, cells were grown to confluency and centrifuged. The pellet was resuspended in FCS and dimethyl sulphoxide (DMSO) (9:1) such that each 1 ml aliquot contained 2 x 10^6 cells and were placed in 1.5 ml cryotubes. For THP1 cells DMSO was replaced with glycerol. These

aliquots were placed in a cryo freezing container at -80 °C overnight before being transferred to liquid nitrogen.

2.3.2 Human peripheral blood mononuclear cells (PBMCs)

Blood was taken directly from a healthy donor or obtained from the Irish Blood Transfusion Service at St. James Hospital, Dublin. Blood was transferred into 50 ml falcon tubes and diluted 1:2 with phosphate buffered saline (PBS). 10 ml of Ficoll Plague Plus was added to the bottom of 50 ml falcon tubes and the diluted blood was slowly added to the Ficoll Plaque Plus at a ratio of 1:1. Tubes were centrifuged at 500 rcf for 30 minutes. This separates the blood into its various components – red blood cells, white blood cells and serum. The white blood cells were transferred into a new 50 ml falcon tube and an equal volume of PBS was added. The tubes were centrifuged at 500 rcf for 10 minutes. If red blood cell contamination occurred, then 3 ml of Red Blood Cell Lysis Buffer was added for 2 minutes. The volume was made up to 10 ml with PBS and tubes were centrifuged at 500 rcf for 3 minutes. This step was repeated as necessary until no red blood cell contamination was present. The pellet was resuspended in RPM1 media (with 10 % FCS (v/v) and 1 % PS (v/v)). Cells were counted and plated as required.

2.3.3 Preparation of peritoneal macrophages

Mice were injected intraperitoneally with 1 ml of 3 % thioglycollate (v/v). After 3 days, mice were euthanized in a CO_2 chamber and injected intraperitoneally with 10 ml of PBS. After 10 minutes the injected PBS was collected and transferred to a 50 ml tube. Tubes were centrifuged at 200 rcf for 5 minutes. Cells were counted and plated as required.

2.4 Cloning of Rab39a and Rab39b

Clones of Rab39a and Rab39b (in PCMV SPORT6 vectors) were obtained from ATCC and were subcloned into PCMV-HA and PCDNA3 vectors.

2.4.1 Primer design

Primers were designed such that they contained the restriction sites for *EcoR1* and *Xho1* and were in frame with the plasmids they were being put into. GC content was kept between 50-60 % and melting temperatures were between 55-80 ^{o}C. Primers designed were as follows, the underlined nucleotides denote the sequence of restriction enzymes *EcoR1* (forward primers) and *Xho1* (reverse primers):

Rab39a forward primer: 5' CGAATTCGGATGGAGACCATCTGGATC 3'

Rab39a reverse primer: 5' CCTCGAGTCAGCAGAAGCATTCTTTCC 3'

Rab39b forward primer: 5' CGAATTCGGATGGAGGCCATCTGGCTG 3'

Rab39b reverse primer: 5' CCTCGAGCTAGCACAAACATCTCCTCTC 3'

2.4.2 Polymerase chain reaction

Polymerase chain reaction (PCR) was carried out using the primers specific for Rab39a and Rab39b. The following PCR reaction was used:

Thermopol reaction buffer 5 µl

DNA template 10 ng

Forward Primer 2 µl

Reverse Primer 2 µl

10mM dNTPs 2.5 µl

Taq 0.2 µl

Made up to 50 µl with nuclease free (NF) H_20

The following PCR parameters were used:

95 °C 3 minutes

95 °C 15 seconds
60 °C 30 seconds
72 °C 1 minute
} x 30 cycles

72 °C 5 minutes

4 °C Hold

2.4.3 Agarose gel electrophoresis

In order to visualise DNA preparations a 1 % (w/v) agarose gel was prepared as follows:

100 mls Tris-Acetate-EDTA (TAE)

1 g agarose

This mixture was heated to dissolve the agarose and allowed to cool before adding 0.5 µg/ml Ethidium Bromide (EtBr). The mixture was added to the gel rack and allowed to set with the combs in place. When the gel had set, the combs were removed and the gel was placed in the gel box and filled with TAE. DNA loading buffer (50 % (v/v) sterile glycerol in sterile H_2O and 10 mg bromophenol blue) was added to each sample and samples were loaded onto the gel. Molecular weight markers (1 kb or 100 bp) were

added. The gel was connected to a power supply and maintained at 100 V for 1-2 hours. The gel was then visualised using a UV gel docking system.

2.4.4 Gel extraction

Resulting PCR products were excised using a scalpel and DNA was extracted using the QIAquick Gel Extraction Kit (Qiagen) according to the manufacturers' protocol.

2.4.5 Ligation into PGEM-T-Easy

DNA was ligated into the intermediate vector PGEM-T-Easy with T4 DNA ligase according to the manufacturers' protocol.

2.4.6 Plasmid transformation

DNA was transformed into DH5α cells. 50 ng of plasmid DNA was placed in eppendorfs and 50 µl of cells were added. The cells were incubated on ice for 30 minutes. Cells were then placed at 42 °C for 45 seconds and then on ice for 2 minutes. All of the cells were then plated on lysogeny broth (LB) ampicillin (Amp) agar plates containing isopropyl-beta-D-thiogalactopyranoside (IPTG) (100 mM) and xGal (50 mg/ml). Agar plates were incubated at 37 °C for 18 hours.

2.4.7 Mini-preparation of plasmid DNA

White colonies (which contain the insert) were grown up in 4 mls LB Amp^+ overnight and DNA was prepared using Wizard Plus SV Miniprep DNA Purification System according to the manufacturers protocol.

2.4.8 Restriction digests

Double restriction digests of Rab39a or Rab39b in PGEM-T-Easy were carried out using *EcoR1* and *Xho1* restriction enzymes. The empty vectors PCMV-HA and PCDNA3 were also digested. The following reaction was used:

5 µg DNA

10 µl *EcoR1* buffer

10 µl BSA

2 µl *EcoR1* (40 units)

2 µl *Xho1* (40 units)

Made up to 80µl with nuclease free H_2O

Digestions were left for 3-4 hours at 37 °C, 16 µl of 6X sample buffer was added and products were run on 1 % agarose gels. Bands of interest were extracted as outlined previously.

2.4.9 Ligation into PCMV-HA and PCDNA3

Ligation reactions were carried out using T4 ligase and a vector to insert ratio of either 1:1 or 1:3. The following reaction was used:

1 µl T4 Ligase

2 µl 10x buffer

1 µl vector (PCDNA3 or PCMV-HA)

DNA inserts (Rab39a or Rab39b)

Made up to 20 µl with H_2O

Reactions were left on the bench for 1 hour to ligate and transformed into DH5α cells. 2 µl of ligation reaction was added to 50 µl DH5α cells and left on ice for 20 minutes. Samples were heated to 42 °C for 45 seconds and replaced on ice for 2 minutes. 950 µl of LB Amp^+ was added and allowed to shake at 150 rpm for 90 minutes at 37 °C. Samples were spun at 220 rcf for 10 minutes; the resulting pellet was resuspended in 200 µl of LB Amp^+ and plated out on LB Amp^+ plates. Agar plates were incubated at 37 °C for 18 hours. Resulting colonies were grown up in 4 mls LB Amp^+ overnight and DNA was prepared using Wizard Plus SV Miniprep DNA Purification System. Samples were sent for sequencing at MWG to confirm the results. Samples with the correct sequence were then re-transformed, grown in 4 mls LB Amp^+ overnight, transferred to a 100 ml LB Amp^+ and prepared by maxiprep according to the manufacturers' instruction.

2.5 Site directed mutagenesis of Rab39a

The following constructs were prepared using site directed mutagenesis:

- HA-Rab39a-D148A (lacks the caspase-1 cleavage site)
- HA-Rab39a-Q72L (constitutively active)
- HA-Rab39a-S22N (dominant negative)
- GFP-Rab39a-D148A (lacks the caspase-1 cleavage site)
- GFP-Rab39a-Q72L (constitutively active)
- GFP-Rab39a-S22N (dominant negative)
- GFP-Rab39a-C149Stop (cleaved version)

The mutant oligonucleotide primers used were as follows:

HA-Rab39a-D148A Forward:

5' CTG AAA AAC TGT CAG CAG CCT GTG GAA TGA AGT ATA TAG 3'

HA-Rab39a-D148A Reverse:

5' CTA TAT ACT TCA TTC CAC AGG CTG CTG ACA GTT TTT CAG 3'

HA-Rab39a Q72L Forward:

5' GCTCTGGGACACGGCGGGACTGGAGCGGTTCAGATCAATAACC 3'

HA-Rab39a-Q72L Reverse:

5' GGTTATTGATCTGAACCGCTCCAGTCCCGCCGTGTCCCAGAGC 3'

HA-Rab39a-S22N Forward:

5' GACTCCACCGTGGGCAAGAACTGCCTCCTGCACCGCTTC 3'

HA-Rab39a-S22N Reverse:

5' GAAGCGGTGCAGGAGGCAGTTCTTGCCCACGGTGGAGTC 3'

GFP-Rab39a-D148A Forward:

5' GCTGAAAGACTGTCAACAGCCTGTGGAATGAAGTACATA 3'

GFP-Rab39a-D148A Reverse:

5' TATGTACTTCATTCCACAGGCTGTTGACAGTCTTTCAGC 3'

GFP-Rab39a-Q72L Forward:

5' GCTCTGGGACACGGCGGGGCTGGAGCGCTTCAGATCAATAAC 3'

GFP-Rab39a-Q72L Reverse:

5' GTTATTGATCTGAAGCGCTCCAGCCCCGCCGTGTCCCAGAGC 3'

GFP-Rab39a-S22N Forward:

5' GGACTCCACGGTGGGCAAGAACTGCCTTCTGCACCGCTTC 3'

GFP-Rab39a-S22N Reverse:

5' GAAGCGGTGCAGAAGGCAGTTCTTGCCCACCGTGGAGTCC 3'

GFP-Rab39a-C149Stop Forward:

5' GAAAGACTGTCAACAGACTGAGGAATGAAGTACATAGAGAC 3'

GFP-Rab39a-C149Stop Reverse:

5' GTCTCTATGTACTTCATTCCTCAGTCTGTTGACAGTCTTTC 3'

Mutant strand synthesis reaction was conducted using the QuikChange XL Site-Directed Mutagenesis Kit. Sample reactions were prepared as indicated below:

5 µl 10 X reaction buffer

5-50 ng of parental DNA

125 ng of forward primer

125 ng of reverse primer

1 µl of dNTP mix

3 µl of Quiksolution

ddH_2O to a final volume of 50 µl

Lastly, 1 µl of *PfuTurbo* DNA polymerase (2.5 U/µl) was added.

The cycling parameters for the site-directed mutagenesis were as follows:

95 °C for 30 seconds

95 °C for 30 seconds
55 °C for 60 seconds
68 °C for 6 minutes
} x 18 cycles

68 °C for 5 minutes

The reaction was then placed on ice for 2 minutes to cool the reaction to approximately 37 °C and 1 µl of the *Dpn I* restriction enzyme (10 U/µl) was added directly to the amplification reaction and mixed thoroughly. The reaction mixture was centrifuged in a microcentrifuge for 1 minute and incubated immediately at 37 °C for 1 hour to digest the parental supercoiled dsDNA. Samples were transformed into DH5α cells or XL1 Blue supercompetent cells

2.6 Transient transfection of plasmid DNA

HEK293T cells were seeded at 4 x 10^5 per ml in 10 cm dishes 24 hours prior to transfection. Cells were transfected with 4-8 µg DNA per transfection. In all cases, the amount of DNA used per transfection was normalised using the appropriate amount of

relevant empty vector control. For 10 cm dishes, 15 µl GeneJuice® was mixed with 785 µl serum-free DMEM per transfection and incubated at room temperature for 5 minutes. 800 µl of this mixture was added to the DNA and incubated for 15 minutes at room temperature. This mixture was then added dropwise to the cells, which were then left to recover for 24-48 hours at 37 °C prior to harvesting.

RAW 246.7 cells were transfected by nucleofection using the Amaxa system. 2 x 10^6 cells per ml were used for each transfection and were combined with 100 µl of nucleofector solution V. 2 µg of DNA was added to the cell, the solution was transferred to an Amaxa cuvette and electroporated using Amaxa Program D-032. An Amaxa pipette was used to transfer the sample into 1 ml of pre-warmed DMEM containing 10 % FCS (v/v) and 1 % PS (v/v).

THP1s were transfected as above using 1 x 10^6 cells per ml for each transfection and programs S019 or V001.

2.7 Transient transfection of siRNA oligos

siRNA oligos specific to Rab39a were obtained from Ambion and Qiagen. The following oligos were used:

Oligo 1: Ambion, CCGACGAUCUUUUGAACAUtt

Oligo 2: Ambion, GGAGCGGUUCAGAUCAAUAtt

Oligo 3: Ambion, GGAAUUACAUUCUCUUGAGtt

Oligo 4: Qiagen, UCAGUUCAGGAUAAATACCAA

Oligo 5: Qiagen, AAGGTTACAAACCCACACCAA

Oligo 6: Qiagen, CAGGAGCGGUUCAGAUCAAUA

Oligo 7: Qiagen, UAGCTTCACAACGTCAAGTTA

THP1s were transfected with siRNA by electroporation with the Amaxa system. 1 x 10^6 cells per ml were used for each transfection and were combined with 100 µl of nucleofector solution V. 1.5 µg of siRNA was added to the cells, the solution was transferred to an Amaxa cuvette and electroporated using Amaxa Program V001. An Amaxa pipette was used to transfer the sample into 1 ml of pre-warmed RPMI containing 10 % FCS (v/v) and 1 % PS (v/v). Cells were incubated at 37 °C for 48 hours. Additional media was added after 24 hours and cells were stimulated with LPS or Malp2 24 hours prior to harvesting. After 48 hours, the supernatants were removed and kept at -80 °C for analysis by ELISA. The cells from each sample were divided in two, half for RNA extraction and half for lysis in 50 µl lysis buffer and analysis by Western blotting. PBMCs were transfected with siRNA in a similar manner but using program Y001 instead.

2.8 Western blot analysis

2.8.1 Preparation of whole cell lysates

Cells were washed with phosphate buffered saline (PBS) and lysed in 150-300 µl of lysis buffer (1 % (v/v) Nonidet P40 (NP40), 0.5 % (w/v) sodium deoxycholate and 0.1 % (w/v) Sodium Dodecyl Sulfate (SDS) containing 10 µg/ml phenylmethylsulphonyl fluoride (PMSF), 30 µg/ml aprotinin, and 1 µg/ml sodium orthovanadate). The cells were then incubated on ice for 30 minutes. Following this incubation period samples were centrifuged at top speed for 15 minutes at 4 °C.

2.8.2 Protein concentration determination

Protein determination was carried out using the Coomassie (Bradford) Protein Assay Kit. 4 µl of water was added to each required well in a 96 well plate. 1 µl of cell lysate and 250 µl of Bradford reagent was added. Each sample was analysed in triplicate. The OD values were read at 595 nm. Protein concentrations were calculated using a standard curve of known protein concentrations.

2.8.3 SDS polyacrylamide gel electrophoresis

Lysates were mixed with 5 X SDS sample buffer (5 ml glycerol, 10 ml 10 % SDS, 10 mg bromophenol blue, 6.25 ml 1 M Tris pH 6.25, 28.75 ml H_2O). 50 µl of β-mercaptoethanol was added per ml of sample buffer immediately prior to use. Samples were then boiled at 100 °C for 5 minutes.

Samples were resolved on SDS - polyacrylimide gel electrophoresis (PAGE) using a constant current of 25 mA per gel. Samples were first run through a stacking gel (30 % (w/v) bisacrylamide mix, 0.75 ml 1 M Tris pH 6.8, 60 µl 10 % ammonium persulphate (APS) and 6 µl Tetramethylethylenediamine (TEMED) made up to 6 ml with H_2O) to condense protein and then resolved according to size using 10-15 % polyacrylamide gels (30 % bisacrylamide mix, 3.75 ml 1.5 M Tris pH 8.8, 150 µl 10 % (w/v) APS, 6 µl TEMED made up to 15 ml with H_2O). Samples were run with pre-stained protein markers as molecular weight standards.

2.8.4 Transfer of proteins to membrane

The resolved proteins were transferred to Immobilon™ polyvinylidene diflouride (PVDF) membrane using a wet transfer system. All components were soaked

beforehand in transfer buffer (25 mM Tris-HCl pH 8.0, 0.2 M glycine, 20 % (v/v) methanol). The gel was placed on two sheets of filter paper and sponge overlaid with the membrane. Two more sheets of filter paper were placed on top followed by a second sponge. The entire assembly was placed in a cassette, the chamber filled with transfer buffer and a constant current of 150 mA was applied for 2 hours.

2.8.5 Antibody blotting

Membranes were blocked for non-specific binding by incubation in blocking buffer made of either 5 % (w/v) non-fat dried milk in 1 % (v/v) Tris Buffered Saline (TBS)-Tween or 5 % (w/v) bovine serum albumin (BSA) in 1 % (v/v) TBS-Tween at 4 °C overnight or at room temperature for 1 hour The membrane was then incubated for two hours at room temperature or at 4 °C overnight with the primary antibody of interest at 1:100 to 1:1000 dilutions depending on the particular antibody. Next, the membrane was washed for 5 minutes five times in 1 % v/v TBS-Tween and incubated with the appropriate secondary horseradish peroxidase (HRP) linked enzyme for forty minutes at room temperature. The blots were then washed for 5 minutes three times in 1 % (v/v) TBS-Tween. Blots were developed by enhanced chemiluminescence (ECL) according to manufacturers instructions.

2.9 Rab39a processing assay

HEK293T cells were set up in 10 cm dishes at 2 x 10^5 cells per ml and transfected with plasmids encoding Rab39a or Rab39b. Cells were lysed in 800 µl of low-stringency buffer for 15 minutes at 4 °C followed by centrifugation at top speed for 5 minutes. Lysates were incubated with 2 µl (150 units) of recombinant caspase-1 in assay buffer

(100 mM Hepes, 10 % sucrose, 0.1 % Chaps, 10 mM DTT, pH 7.5) for 90 minutes at 30 °C. Lysates were subjected to SDS/PAGE and followed by immunoblot analysis.

RAW 246.7 cells were set up in 6-well plates and transfected using the Amaxa system as previously described. Cells were stimulated with 100 ng/ml LPS for 3 hours, treated with 50 μM YVAD where necessary for 1 hour, and further stimulated with 5 mM ATP for 1 hour. Cells were lysed in 150 μl low astringency lysis buffer. Lysates were subjected to SDS/PAGE and followed by immunoblot analysis.

Alternatively, proteins were generated by *in vitro* transcription and translation (ITT) with the TnT T7-coupled rabbit reticulocyte lysate system. For detection of the translation products, [^{35}S] was added to the translation reactions. Proteins translated *in vitro* were incubated with recombinant caspase-1, -4 or -5 for 2 hours at 37 °C. The resulting cleavage products were analyzed by SDS-PAGE and Western blotting followed by autoradiography.

2.10 Co-immunoprecipitation

HEK293T cells were transfected with 8 μg of DNA where the total amount of DNA was kept constant. 36-48 hours later, cells were lysed in immunoprecipitation (IP) lysis buffer (150 mM NaCl, 50 mM Tris-HCl pH8, 1 % NP40, 1 mM PMSF, 10 μg/ml leupeptin and 1 μg/ml aprotinin). Lysates were pre-cleared twice for 30 minutes with Protein A/G Plus Agarose Beads. Lysates were then incubated with the required antibodies and Protein A/G Plus Agarose Beads for 4 hours. The immune complexes were precipitated, washed 3 times in 1 ml of lysis buffer, eluted by the addition of 30 μl sample buffer, and followed by SDS-PAGE and immunoblotting.

2.11 Confocal microscopy

2.11.1 Fixed cell imaging

Sterile coverslips were coated with 1 mg/ml poly-L-lysine. Excess poly-L-lysine was aspirated off after 3 minutes. The coverslips were left to dry for 1 hour in a laminar flow hood. Coverslips were placed in 6-well plates and cells were seeded on the plates at a concentration of 1×10^5 cells per ml for 24 hours. Cells were then rinsed gently in 1 X PBS twice. Cells were fixed by incubating them in 2 % para-formaldehyde for 15 minutes at room temperature. The formaldehyde was removed and slides were washed three times in 1 X PBS. In order to permeabilise the cells 0.2 % (v/v) Triton X 100 in PBS was added and the cells were left on ice for 10 minutes. This was then removed and the cells were washed three times in 1 X PBS. At this point the coverslips were placed in new wells of a 6-well plate. Cells were rinsed once in blocking buffer (2 % BSA-PBS). Primary antibody was diluted 1:100 in 2 % BSA-PBS and 100 µl was placed on the coverslips for 1 hour. The antibody was removed and cells were washed in blocking buffer three times with gentle shaking. The secondary antibody was diluted 1:250 in blocking buffer and 100 µl was added to each coverslip in the dark and left to incubate for 45 minutes. The secondary antibody was removed and washed 3 times in blocking buffer with gentle shaking. In the dark the coverslips were removed and rinsed in distilled water. Approximately 10 µl of mounting solution (50 % (v/v) glycerol, 0.5 X PBS, 2 mg/ml para-p-phenylendiamine, 1 µl/ml 4',6-diamidino-2-phenylindole (DAPI) stain) was dropped onto a slide. The coverslip was placed cell-side down onto the mounting solution and sealed with nail polish to prevent drying and movement under the microscope. Alternatively cells were mounted using Mowiol. The cells were observed with an Olympus FluoViewTM FV1000 Microscope.

2.11.2 Live cell imaging of phagocytosis

HEK293T cells or RAW 264.7 cells were seeded in 96-well plates or 8-well chamber slides and transfected with GFP-Rab39a for 24 hours. Fresh media containing 1 % FCS (v/v) and 1 % PS (v/v) was added. 1 μm – 3 μm Latex beads or *S. aureus* at a multiplicity of infection (MOI) of 10 was added and cells were spun at 120 rcf for 5 minutes. MOI is a ratio of beads (or bacteria) to cells. Cells were placed at 37 °C for 1 hour and live cell images were taken.

2.11.3 Live cell imaging of active caspases

RAW 264.7 cells were transfected and phagocytosis was induced as previously described. 1X FLICA reagent (SR-VAD-FMK) was added to the cells for 1 hour and live cell images were taken.

2.11.4 Live cell imaging of ASC-FP cells

ASC-FP cells were set up at 2 x 10^5 per ml the day before usage on 35mm glass bottom culture dishes. Cells were pre-treated for 1 hour with inhibitors where indicated and then stimulated with TLR and NLR ligands as required. Imaging was performed on an Olympus FluoViewTM FV1000 Microscope equipped with a temperature and CO_2 controlled chamber.

2.12 Analysis of phagocytosis

2.12.1 Bacterial uptake assay

HEK293T cells were set up in 12 well plates at 2 x 10^5 cells per ml. The following day cells were transfected with GFP-Rab39 constructs. After 48 hours the media was removed and fresh media containing 1 % FCS and 1 % PS was added. Cells were placed

on ice for 15 minutes. Alexa-Fluor 647 - labelled *S. aureus* was added at a MOI of 50 and cells were spun at 120 rcf for 5 minutes. Cells were placed on ice for a further 30 minutes to ensure phagocytosis was synchronised and then placed at 37 °C or left on ice as a control. After 1 hour, the media was removed and cells were washed 3 times in ice-cold PBS-EDTA. Cells were resuspended in 500 µl PBS and analysed by FACS for GFP expression and Alexa Fluor 647 - labelled *S. aureus*.

2.12.2 Phagosomal acidification assay

Peritoneal macrophages were set up at 2 x 10^5 per ml in 12 well plates. Cells were pre-treated with 100 µM zVAD or 100 µM Bafilomycin A for 1 hour. Cells were placed on ice for 30 minutes and then *S. aureus* doubly labelled with FITC and Alexa-flour was added to the cells at a MOI of 2. Cells were kept on ice for a further 30 minutes and then placed at 37 °C for 1 hour or kept on ice as a control. The media was then removed and cells were washed 3 times in ice-cold PBS-EDTA. Cells were resuspended in 500 µl PBS and analysed by FACS.

RAW 264.7 cells were set up at 1 x 10^6 cells per 500 µl in 12 well plates and transfected as previously described with GFP-Rab39 constructs. Cells were placed on ice for 30 minutes and then infected with *S. aureus* labelled with pH Rodo Dye at a MOI of 2. Cells were kept on ice for a further 30 minutes and then placed at 37 °C for 1 hour or kept on ice as a control. The media was then removed and cells were washed 3 times in ice-cold PBS-EDTA. Cells were resuspended in 500 µl PBS and analysed by FACS.

2.13 RNA extraction

RNA extractions were carried out using RNeasy minikit from Qiagen according to the manufacturers' instructions. RNA was normalised and separated on a 1 % agarose gel to check RNA integrity and to ensure RNA was normalised correctly.

2.14 Reverse transcription PCR

Reverse transcription (RT) - PCR was carried out on the RNA to create cDNA using Applied Biosystems cDNA Archive Kit. The following protocol was used:

2 µl 10 X RT Buffer

0.8 µl 100 mM dNTP

2 µl 10 X Random Primers

1 µl RTase

1 µl RNase inhibitor

3.2 µl nuclease free H_2O

10 µl RNA

The following parameters were used:

25 °C	10 minutes
37 °C	2 hours
85 °C	15 minutes
4 °C	Hold

2.15 Real Time PCR

SYBR-Green Real Time PCR was carried out on the cDNA using primers specific for Rab39a, Rab39b, IL-1β or GAPDH. The following primers were used:

Rab39a forward - TCTACCAGTTCCGCCTCATC

Rab39a reverse – ATTGATCTGAACCGCTCCTG

Rab39b forward – TTTTTCCCCATTCTCTGGAA

Rab39a reverse – AGCGGTCCTCCGTTTTTAAT

IL-1β forward - GGGCCTCAAGGAAAAGAATC

IL-1β reverse – TTCTGCTTGAGAGGTGCTGA

GAPDH forward – GAACGGGAAGCTTGTCATCAA

GAPDH reverse - CTA AGC AGT TGG TGG TGC AG

2.16 Analysis of change in cytokine expression by ELISA

Supernatants were analysed for IL-1β, IL-1α, or TNF-α using Duoset ELISA kits according to the manufacturers' instructions. The absorbance measurements were read at 450 nm and concentrations were calculated using the known standards. Each experiment was done in triplicate, and data are expressed as picograms per ml (mean ± S.D.) for a representative of at least three independent experiments.

2.17 Analysis of secreted proteins

Supernatants were collected and 500 µl methanol and 125 µl chloroform was added. Samples were vortexed and centrifuged for 5 minutes at 9500 rcf. The upper phase was removed. 500 µl methanol was added and samples were centrifuged for 5 minutes at 9500 rcf. The supernatant was removed and the pellet was dried for 5

minutes at 50 °C. Sample buffer was added and samples were separated on 12 % SDS-PAGE gels and immuno-blotted as required.

2.18 Immunoprecipitation and mass spectrometry of ASC

2.18.1 Cell free extract preparation

THP1 cells were pelleted at 200 rcf for 10 minutes and washed twice in PBS. Cells were resuspended in 2 mls of PBS, transferred to a tissue grind pestle and centrifuged at 600 rcf for 10 minutes. PBS was removed and resuspended in 2 volumes of WCEB (20 mM Hepes, 10 mM KCL, 1.5 mM MgCl2, 1 mM EDTA, 1 mM EGTA, 1 mM DTT and protease inhibitors). Cells were left on ice for 10 minutes and dounced 30 times to break open cells. Cells were transferred to eppendorfs and spun at top speed for 10 minutes at 4 °C.

2.18.2 Immunoprecipitation from cell free extract

Cell free extract samples were diluted in IP buffer (20 mM HEPES-KOH (pH 7.5), 50 mM NaCl, 0.3 % (w/v) CHAPS, 10 mM KCl, 1.5 mM $MgCl_2$, 1 mM EDTA, 1 mM EGTA, I mM DTT, 2 µg/ml aprotinin, 1 µg/ml leupeptin and 250 µM PMSF) and pre-cleared with protein A/G agarose beads at 4 °C for 1 hour. Pre-cleared cell-free extracts were incubated with fresh protein A/G agarose beads and anti-ASC antibody overnight at 4 °C. Captured complexes were washed 3 times in IP buffer and eluted into 2D gel sample buffer (8 M Urea, 4 % CHAPS, 0.05 % (w/v) SDS, 100 mM DTT, 0.03 % (w/v) bromophenol blue, 0.2 % (v/v) ampholytes). Samples were either separated on large 1D or 2D 12 % SDS polyacrylamide gels.

2.18.3 Isoelectric Focusing

After solubilising samples in sample buffer, samples were carefully pipetted against the back of the rehydration tray without introducing air bubbles. The exposed gel face of a 7 cm (small gel) or a 17 cm (large gel) Immobilised pH Gradient (IPG) strip was placed face down on the sample, ensuring that no bubbles became trapped. The strips were overlayed with 1 ml (7 cm strips) or 2 ml (17 cm strips) of mineral oil to prevent dehydration/crystallisation of the urea. Strips were allowed to rehydrate for 12-16 hours. 2 electrode wicks per IPG were moistened in dH_2O, and excess moisture was absorbed by placing them briefly on 3M paper. A moistened wick was placed on top of each electrode in the focus tray. The rehydrated IPGs were removed from the rehydration tray and residual oil was allowed to drain off. Excess oil was removed by blotting with 3M paper. The IPGs were mounted face down on the focusing tray, ensuring that the edges of the strip come in contact with the electrodes. IPG strips were overlaid with mineral oil (as above) to prevent dehydration during the isoelectric focussing (IEF). IPG strips were focused using the following conditions:

Step 1:	Linear Slope to 500 V	1 hour
Step 2:	Constant 500 V	5 hours
Step 3:	Linear slope to 3,500 V	5 hours
Step 4:	Constant 3500 V	12 hours
Step 5:	50 V	Hold

2.18.4 Equilibriation for 2D gel electrophoresis

IPG strips were incubated (face upwards) for 5 minutes in reducing buffer (6 M Urea, 375 mM Tris, pH 8.8, 2 % (w/v) SDS, 20 % (v/v) glycerol and 2 % (w/v) DTT)

followed by 5 minutes in alkylating buffer (6 M Urea, 375 mM Tris, pH 8.8, 2 % SDS, 20 % glycerol and 2.5 % (w/v) iodacetamide). 2 ml of buffers for 17 cm IPG strips and 1 ml for 7 cm IPG strips was used.

2.18.5 2D gel

12 % 2D gels was prepared as follows: Resolving gel: 13.2 ml H_2O, 16 ml Acrylimide Mix, 10 ml 1.5 M Tris, pH 8.8, 400 µl 10 % SDS, 400 µl 10 % APS and 16 µl TEMED. Stacking gel: 12.3 ml H_2O, 3 ml Acrylimide Mix, 2.25 ml 1.5 M Tris, pH 6.8, 180 µl 10% SDS, 180 µl 10 % APS and 18 µl TEMED. Sealing plug: 5 ml of resolving gel mix, 10 µl TEMED. 800 µl of sealing plug was added to the base of large format gels and allowed to set prior to the addition of the resolving gel and the stacking gel. Following the alkylation step, the IPGs were dipped briefly into 1 X SDS-PAGE running buffer to wash off excess urea. IPG strips were mounted on the gel and secured in place by overlaying them with 0.5 % molten agarose in 1 X SDS-PAGE running buffer. The overlay agarose was allowed to solidify and gels were electrophoresed at 75 mA per 2 gels for 4-5 hours.

2.18.6 Silver staining of gels

The gel was placed in fixer solution (50 % methanol, 10 % acetic acid) for 30 minutes and then washed with 50 % methanol for 10 minutes. This was followed by 3 washes in dH_2O. The gel was sensitised in 0.02 % $Na_2S_2O_3$ for 1 minute and rinsed twice in dH_20. The gels were then incubated in chilled 0.1 % $AgNO_3$ for 20 minutes and rinsed in dH_2O. Developer solution (0.04 % Formalin, 2 % Na_2CO_3) was then added to the gel until the bands were clearly visible. The gel was then rinsed in 5 % acetic acid and stored in 1 % acetic acid.

2.18.7 Trypsin digestion and peptide extraction

Bands or spots of interest were extracted from the gel using a pipette tip. Gel pieces were destained by shaking in 500 µl oxidation buffer (15 mM $K_3Fe(CN)_6$/50 mM $Na_2S_2O_3$) for 2 X 5 minutes at 1000 rpm. Gel pieces were washed 5 times in 500 µl wash buffer (50 % MeOH, 40 % H_2O, 10 % AcOH) for 5 minutes at 1000 rpm. Gel pieces were equilibriated by shaking for 5 minutes in 500 µl of 50 mM NH_4HCO_3. Gel pieces were dehydrated by shaking for 5 minutes in 500 µl of 100 % CH_3CN at 1000 rpm. Liquid was aspirated and samples were desiccated in a speedivac for 5 minutes at a low heat setting. 15 µg of Trypsin Gold was diluted with 45 µl of digestion buffer (25 mM NH_4HCO_3, 0.1 % n-octylglucoside). 1-3 µl of dilute trypsin was added directly onto the dried gel piece and allowed to rehydrate. A further 10 µl of digestion buffer was added to each sample and samples were left at 37 °C overnight to ensure complete digestion. After overnight digestion, samples were pulsed briefly at low speed to collect the supernatant. Supernatant was transferred into a clean eppindorf and peptides were extracted by adding 40 µl of CH_3CN/H_2O/trifluoracetic acid (TFA) (66:33:0.1 v/v/v). Samples were sonicated for 10 minutes at 25 °C and supernatant was added to the original supernatant. The extraction was repeated and the combined supernatants were desiccated in a speedivac for 45 minutes at a low heat setting or until dried.

2.18.8 Analysis of tryptic digest fragments by mass spectrometry

Peptides were solubilised in 5-10 µl of 5 % formic acid. A matrix mix was prepared by adding α-cyano-4-hydroxycinnamic acid (CHCA) matrix to 1 ml matrix diluent (60 % CH_3CN, 0.1 % TFA). 0.5 µl of peptide samples followed by 0.5 µl of matrix mix were added to each well on the Matrix-assisted laser desorption/ionization (MALDI) target plate. Calibration samples were prepared by adding 2 µl of calibration mix to 24 µl of

matrix mix. 0.5 µl of calibration samples were added to the MALDI target plate. The plate was allowed to dry for a few minutes until matrix crystals had formed.

Tryptic digested fragments were analysed by MALDI - Time of flight (TOF) using a Voyager DE-PRO mass spectrometer. Firsty, calibration data was acquired and then spectra were collected from each of the samples based on the calibration data. For protein identification, peak lists were submitted to databases MASCOT and MS-FIT.

2.19 ASC complex isolation

40 mls I-BMDM cells were prepared (per point) at a density of 1 x 10^6 cells per ml in 10 cm plates. The following day, cells were pre-treated with zVAD (50 µM) for 30 minutes to prevent cell death, and treated with 100 ng/ml LPS or 5 nM Malp2 for 3 hours and 5 mM ATP for 1 hour. Cells were centrifuged at 125 rcf for 5 minutes, medium removed, and resuspended in 1 ml PBS. Cells were pelleted at 125 rcf. Cells were resuspended in 0.5 ml of Buffer A (20 mM Hepes-KOH, pH7.5, 10 mM KCl, 1.5 mM MgCl2, 1 mM EDTA, 1 mM EGTA, 320 mM sucrose, 0.1 mM PMSF, 10 µg/ml leupeptin and 1 µg/ml aprotinin). Cells were lysed on ice by syringing 30 times with a 1 ml syringe with 21-gauge needle. Lysates were centrifuge at 180 rcf for 8 minutes. Supernatants were transferred to a fresh eppendorf, taking care not to disturb the nuclear pellet. A 30 µl sample was removed and saved for Western blot analysis. The remaining supernatants were diluted with two volumes of buffer A and then filtered with 5 µm Ultrafree-CL Centrifugal Filters at 2000 rcf. This filtration step removes any contaminating nuclei and un-lysed cells. Filtered lysates were collected and diluted with one volume of CHAPS buffer (20 mM Hepes-KOH, pH 7.5, 5 mM MgCl2, 0.5 mM EGTA, 0.1 % CHAPS, 0.1 mM PMSF, aprotinin and leupeptin) to lyse organelles such

as mitochondria and then centrifuged at 1400 rcf for 8 minutes. Pellets were resuspended in 1 ml CHAPS buffer, by gentle pipeting and then centrifuged at 1400 rcf for 8 minutes. This was repeated twice to wash the ASC complexes. Pellets were resuspended in 30-40 µl CHAPS buffer. For Western blot analysis, equal amounts of the resuspended pellets and 2X SDS sample buffer, were mixed, boiled and then fractionated on 12 % SDS-polyacrylamide gel. Fractionated proteins were immunoblotted with an anti-ASC antibody.

Chapter 3

Identification of Rab39a as a Novel Binding Partner of Caspase-1

3.1 Introduction

Previous work in the laboratory focused on finding novel binding partners of caspase-1. A variety of potential novel binding partners of caspase-1 were uncovered by a mass spectrometry screen. One of the proteins was Rab39a, a newly identified member of the GTPase family. Given the role for caspase-1 in unconventional protein secretion and phagocytosis processes, Rab39a appeared to be an exciting interacting protein, thus this project aimed to further elucidate the role, if any, for Rab39a in caspase-1 functions.

The human Rab GTPase family is part of the Ras superfamily of small GTPases. All Ras proteins contain GDP/GTP-binding motif elements which make up a ~20 kDa G domain that is essential for GTPase activity. There are at least 60 Rab proteins in the human genome. Sequence-analysis studies have shown that the Rab GTPase family members contain five distinct amino-acid stretches. These so-called RabF motifs are regions of high homology within the Rab family (Pereira-Leal *et al.*, 2000, Moore *et al.*, 1995). Based on sequence similarity, Rab proteins have been further grouped into fourteen different subfamilies. Rab39a has been grouped in a subfamily that also contains Rab2, Rab4, Rab11, Rab14, Rab25 and Rab42 (Schwartz *et al.*, 2007). Each subfamily contains subfamily-specific sequence motifs called RabSF motifs.

Rab proteins are highly evolutionarily conserved with several Rab GTPases conserved from yeast to humans. Rab proteins are present on all compartments of the endomembrane system (endoplasmic reticulum, Golgi, endosomes, lysosomes), the nucleus, the plasma membrane (including cell junctions and focal adhesions), mitochondria and centrioles (Schwartz *et al.*, 2007).

The different Rab GTPases are localized to the cytosolic face of specific intracellular membranes, where they function as regulators of distinct steps in membrane trafficking pathways. At present over half of all known Rab GTPases are characterised highlighting a vast array of functions in trafficking circuits.

Rab GTPases function as molecular switches that alternate between two conformational states: The GTP-bound 'on' form and the GDP-bound 'off' form (Stenmark, 2009). The conversion between GDP- and GTP-bound forms of Rab GTPases involves conformational changes in two regions, termed switch I and switch II. It is through the conformational changes in these two switches that regulatory proteins and effectors 'sense' the nucleotide status of the small GTPases. Rab effectors, proteins with which Rab interacts and through which it functions, only bind the GTP-bound form of Rab. GDP/GTP cycling is controlled by regulatory proteins. Guanine-nucleotide-exchange factors (GEFs) catalyse the conversion of GDP-bound to GTP-bound form (Schmidt *et al.*, 2002), whereas GTPase-activating proteins (GAPs) accelerate the intrinsic GTPase activity to promote formation of the inactive GDP-bound form (Bernards *et al* 2004). The Rab GDP dissociation inhibitor (GDI) prevents the release of GDP from Rab, thereby stabilising the inactive form.

The vast majority of Rab GTPases undergo posttranslational lipid modifications, which act as hydrophobic membrane anchors, interacting with the cytoplasmic leaflet of cellular membranes and/or participating in protein-protein interactions. The most common lipid modification affecting Rab GTPases is protein prenylation, which involves the covalent addition of either farnesyl (15 carbon) or geranylgeranyl (20 carbon) pyrophosphate to proteins via thioether linkages catalyzed by protein prenyl

transferases (Higgins *et al.*, 1996). The majority of Rab proteins contain two cysteine residues, such as CC or CXC at the C terminus, and undergo two geranylgeranylation reactions.

Rab39a is a relatively uncharacterised member of the Rab GTPase family. It was initially described as a novel Rab protein that is widely expressed in a variety of tissues including spleen and small intestine and in peripheral leukocytes (Stankovic *et al.*, 1997). Rab39a shows 76 % identity at the amino acid level to another recently described Rab protein Rab39b (Cheng *et al.*, 2002).

The first aim of this chapter was to confirm the interaction between caspase-1 and Rab39a. As Rab39a is a relatively uncharacterised protein, the second aim of this chapter was to use a bioinformatic approach to characterise Rab39a.

3.2 Results

Previous work in the laboratory identified potential novel binding partners of caspase-1. This was done by immunoprecipitating active caspase-1 from THP1 cells. Associated proteins were separated using 2D gel electrophoresis and were identified using mass spectrometry. One of the proteins identified was a relatively uncharacterised GTPase protein called Rab39a.

The first aim was to confirm the interaction between caspase-1 and Rab39a. It was decided to use co-immunoprecipitation experiments and co-localisation experiments as methods to confirm this interaction. As no antibody was available for detecting Rab39a, it was first necessary to clone Rab39a into a tagged vector so that it could be transfected into cells and detected by Western blotting. It was also decided to clone Rab39b into a tagged vector and determine if it could also associate with caspase-1.

3.2.1 Cloning of Rab39a and Rab39b into PCMV-HA

Rab39a and Rab39b were cloned into a tagged vector (pCMV-HA) so that they could be detected by Western blotting for the HA-tag. Rab39a and Rab39b expressed in pCMV-SPORT6 vectors were purchased from ATCC. Forward and reverse primers for each product were designed such that they contained the relevant restriction sites and would ensure that the sequences would be in frame. Rab39a and Rab39b were amplified out of pCMV-SPORT6 by PCR. Figure 3.1 (A) shows the results of the Rab39a PCR reaction. Different concentrations of pCMV-SPORT6-Rab39a template were used 1.0 ng/ml (lane 1), 0.5 ng/ml (lane 2), 0.1 ng/ml (lane 3) and 10 ng/ml (lane 4). Water was used as a template in lane 5. The band from lane 4 was extracted and ligated into PGEM T-Easy. Figure 3.1 (B) shows the results of the Rab39b PCR reaction. Again, different

concentrations of pCMV-SPORT6-Rab39b were used. This time the reaction worked much better as bands were visible in all of the reactions. The band from lane 1 was extracted and ligated into PGEM-T-Easy. Once the sequences were confirmed to be correct they were subcloned into PCMV-HA vectors. Figure 3.1 (C) shows the vector map of pcMV-HA. Once the HA-Rab39a and HA-Rab39b had been cloned these sequences were sent for sequencing and were confirmed to be correct.

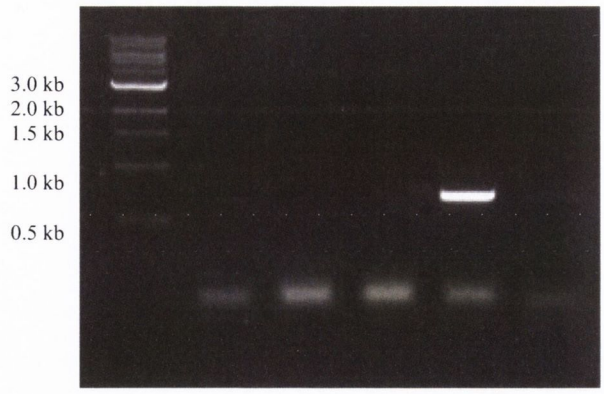
The expression of the newly constructed HA-Rab39a and HA-Rab39b was next examined by transiently transfecting the plasmids into the HEK293T cell line. Cells were lysed after 24 hours and lysates were separated by SDS-PAGE and products were detected with the anti-HA antibody. An empty PCMV-HA vector was used as a control to ensure no non-specific bands were being detected. Figure 3.2 shows the expression of HA-Rab39a (lane 3) and HA-Rab39b (lane 4).

3.2.2 Rab39a interacts with caspase-1

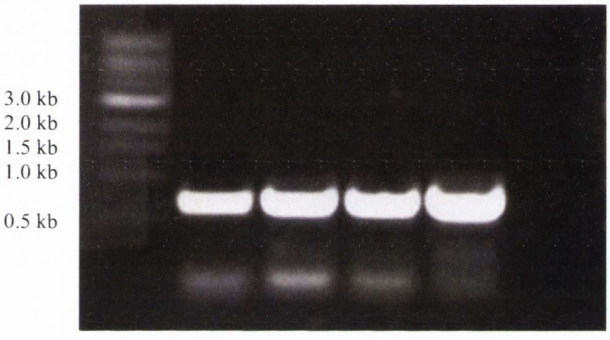
3.2.2.1 Rab39a and caspase-1 co-immunoprecipitate in HEK293T cells

It was now possible to investigate whether caspase-1 and HA-Rab39a could co-immunoprecipitate. This was done by transiently transfecting HA-Rab39a and caspase-1 into HEK293T cells. After 48 hours, cells were lysed. After pre-clearing the lysates, caspase-1 was immunoprecipitated from cells using a specific caspase-1 antibody. Samples were analysed by Western blotting and probed with the anti-HA antibody. Rab39b is 76 % similar to Rab39a, and it was therefore also analysed whether Rab39b could bind caspase-1.

(A)



(B)



(C)

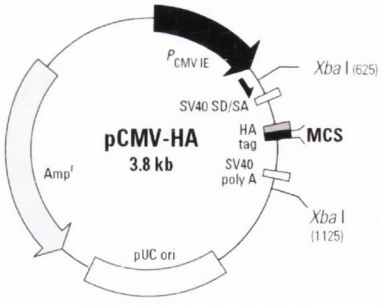


Figure 3.1 Rab39a and Rab39b were cloned into PCMV-HA vectors. Primers for Rab39a and Rab39b were designed and used to PCR Rab39a **(A)** and Rab39b **(B)** from PCMV-SPORT6. Different concentrations of DNA template were used in the PCR reactions - 1.0 ng/ml (lane 1), 0.5 ng/ml (lane 2), 0.1 ng/ml (lane 3) and 10 ng/ml (lane 4). Water was used as a template in lane 5. **(C)** Plasmid map of PCMV-HA vector into which Rab39a and Rab39b were ligated.

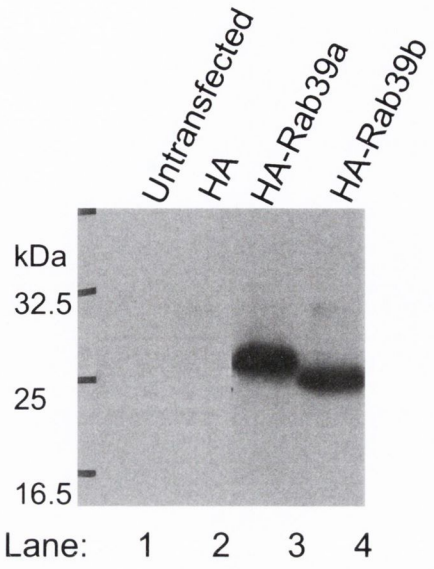


Figure 3.2 HA-Rab39a and HA-Rab39b expression in Hek293T cells. HEK293T cells were set up at 2 x 10^5 per ml in 10 cm dishes. 24 hours later, cells were transfected with 5 µg of HA-control, HA-Rab39a or HA-Rab39b. After 24 hours cells were lysed in 300 µl low astringency lysis buffer. Lysates were mixed with 5X sample buffer, separated on 12 % SDS-PAGE gels, transferred onto PVDF membrane and immunoblotted using the anti-HA antibody.

Figure 3.3 shows the results of the co-immunoprecipitation. An interaction between caspase-1 and HA-Rab39a can be seen in lane 3 of the upper blot. There is no band in the IgG control (lane 1) confirming that the immunoprecipitaion was specific. There is a faint band in lane 2, this may be due to the immunoprecipitation of a small amount of endogenous caspase-1. There is no band in lane 5, indicating that HA-Rab39b and caspase-1 do not co-immunoprecipitate. The middle blot (anti-HA) confirms that equal amounts of HA-Rab39a or HA-Rab39b were transfected into the samples. The lower blot (anti-caspase-1) confirms that equal amounts of caspase-1 were transfected into the samples. These results therefore show that using an over-expression system, HA-Rab39a and caspase-1 co-immunoprecipitate but HA-Rab39b and caspase-1 do not.

3.2.2.2 GFP-Rab39a and caspase-1 co-localise in HEK293T cells

At a later date a mouse GFP-Rab39a construct became available. This was made by Mitsonuri Fukada, Tohoku University, Japan. The sequence of murine Rab39a is 97 % identical to human Rab39a. This construct was used in fluorescent microscopy experiments to examine if GFP-Rab39a could co-localise with a RFP-caspase-1 plasmid.

GFP-Rab39a and RFP-caspase-1 were transiently transfected into HEK293T cells. 48 hours later cells were viewed using a confocal microscope. As shown in Figure 3.4, GFP-Rab39a (green) and RFP-caspase-1 (red) co-localise (yellow).

3.2.3 Bioinformatic analysis of Rab39a

As the interaction between Rab39a and caspase-1 had now been confirmed, a bioinformatics analysis of Rab39a was next carried in order to characterise this previously undescribed protein.

3.2.3.1 Homology search of Rab39a

The protein sequence of human Rab39a was obtained from the NCBI website and inserted into the BLAST 2 program (http://blast.ncbi.nlm.nih.gov) to obtain a list of proteins that showed the greatest similarity to Rab39a. The results are shown in Table 3.1. Within the human genome, Rab39a is most similar to Rab39b (76 % identity), Rab42 (48 % identity) and Rab2 (48 % identity).

In order to determine which species contain a homolog of Rab39a, the sequence of human Rab39a was inserted into NCBI HomoloGene (http://www.ncbi.nlm.nih.gov/homologene). The results are shown in Table 3.2. It can be seen that it is highly evolutionarily conserved as it is present in a variety of species including *M. musculus, D. rerio, D. melanogaster* and *C. elegans.*

3.2.3.2 Conserved motifs in Rab39a

Rab39a belongs to the Rab GTPase family, the largest family of the Ras GTPases. As mentioned in the introduction, all Ras proteins share a set of conserved G box GDP/GTP-binding motif elements. These are the G1 box motif (GXXXXGKS/T), the G2 box motif (T), the G3 box motif (DXXGQ/H/T), the G4 box motif (T/NKXD) and the G5 box motif (C/SAK/L/T) (Bourne *et al.*, 1991). The NCBI Conserved Domains Database (CDD) was used to reveal these GDP/GTP-binding motif elements

HA-Rab39a	+	+	+	-	-	-
HA-Rab39b	-	-	-	+	+	+
Caspase-1	+	-	+	+	-	+
IP: Caspase-1	-	+	+	-	+	+
IP: IgG	+	-	-	-	+	-



Whole-cell lysates:

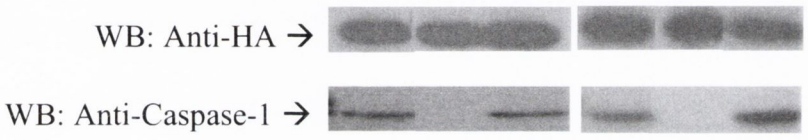


Figure 3.3 HA-Rab39a and caspase-1 co-immunoprecipitate in HEK293T cells. HEK293T cells were set up at 2 x 10^5 cells per ml in 10 cm dishes. 24 hours later cells were transiently transfected with caspase-1 and HA-Rab39a or HA-Rab39b as indicated, such that the total amount of DNA was kept constant at 8 µg. 36 hours later cells were lysed in 800 µl IP lysis buffer. 50 µl of lysate was kept for whole cell lysate analysis. Lysates were pre-cleared twice for 30 minutes with 15 µl of Protein A/G beads. Lysates were mixed with 20 µl of Protein A/G beads and mixed with either 5 µg of caspase-1 or 5 µg rabbit IgG antibody for 3-4 hours at 4 °C with gentle rolling. Samples were washed three times in 1 ml of IP lysis buffer and resuspended in 35 µl sample buffer. IP samples and whole cell lysate samples were separated on 12 % SDS-PAGE, transferred onto PVDF membrane and immunoblotted with anti-HA and anti-caspase-1 antibodies. Results are representative of 3 independent experiments.

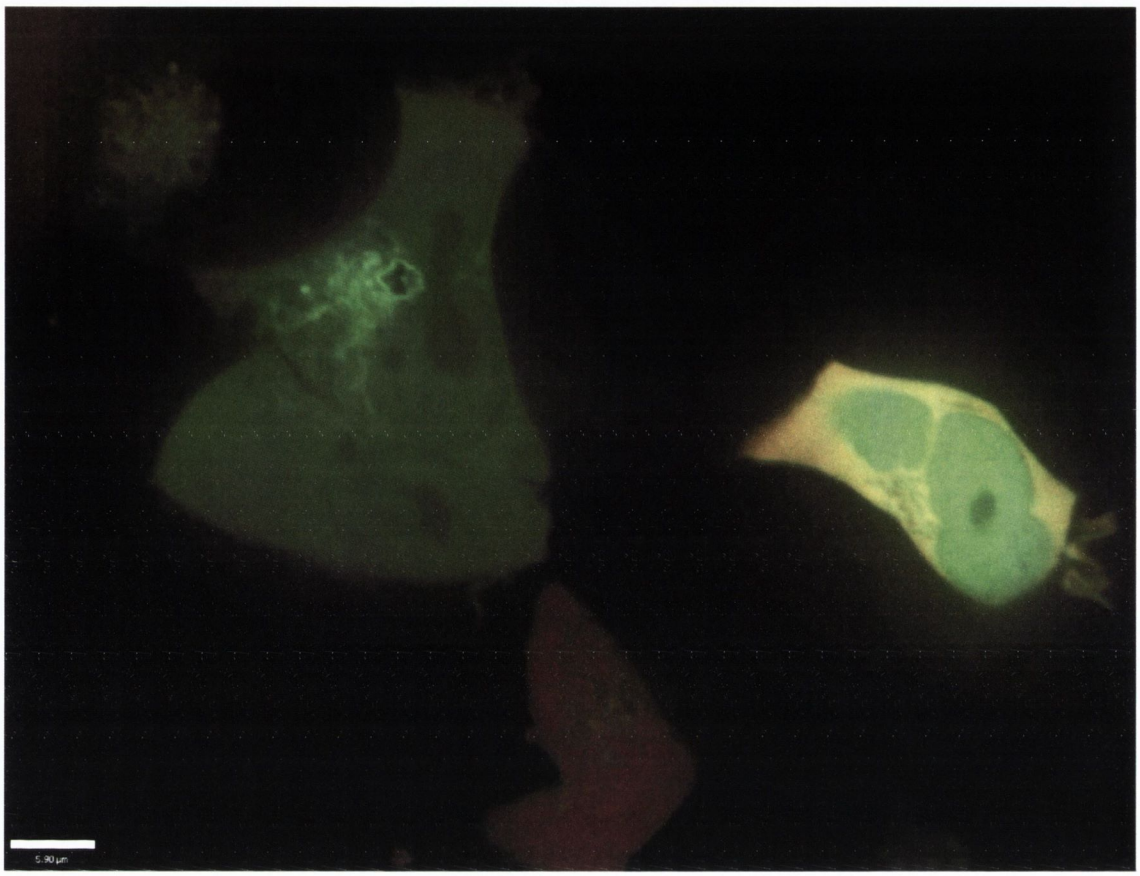


Figure 3.4 GFP-Rab39a and RFP-caspase-1 co-localise in HEK293T cells

HEK293T cells were seeded at 2 x 10^5 cells per ml in 12 well plates. GFP-Rab39a and RFP-caspase-1 were transfected into cells using Genejuice. Cells were viewed 48 hours later by confocal microscopy. Co-localisation of GFP-Rab39a and RFP-caspase-1 is shown in yellow. Results are representative of two independent experiments.

Name	Protein ID	Length	% Identity	% Positives
Rab39b	NP_741995.1	213	76	88
Rab42	EAW_81413.1	216	48	69
Rab2a	AAA_60241.1	212	48	69
Rab2b	CAI_46103.1	209	48	68
Rab14	NP_057406.2	215	41	63
Rab8b	NP_057614.1	207	47	72
Rab8a	NP_0005361.2	207	46	70
Rab13	NP_002861.1	203	45	71
Rab4a	NP_004569.2	218	39	60
Rab1a	NP_004152.1	205	45	66
Rab11a	BAG_59943.1	261	40	63
Rab11b	ABQ_59034.1	218	40	62

Table 3.1 Proteins with greatest homology to Rab39a. Proteins displaying greatest sequence similarity to Rab39a as generated by the NCBI BLAST program (http://blast.ncbi.nlm.nih.gov/). The protein sequence of human Rab39a (Q14964) was inserted into the program and the results above are the proteins which show the highest percentage identity and positive residues to Rab39a.

Name	Protein ID	Length	% Identity	% Positives
M. mulatta	XP_001103335	217	100	100
E. caballus	XP_001501057	217	99	100
B. taurus	XP_614612	217	98	100
M. musculus	NP_780771	217	97	99
D. rerio	NP_998207	213	59	78
P. troglodytes	XP_001136512	160	99	100
D. melanogaster	NP_572405	218	54	71
S. purpuratus	XP_782114	227	54	72
C. elegans	NP_495984	229	53	72

Table 3.2 Human Rab39a is highly conserved across different species. Human Rab39a is conserved across different species as generated by the NCBI BLAST program and NCBI Taxonomy BLAST reports (http://blast.ncbi.nlm.nih.gov/). The protein sequence of human Rab39a (Q14964) was inserted into the programs and the results above show the species which have Rab39a. The percentage identity and positive residues of Rab39a in each of the species is listed as compared to human Rab39a.

(www.ncbi.nlm.nih.gov/structure/cdd/cdd.shtml). These conserved motifs in Rab39a are highlighted in boxes in Figure 3.5 (A). The G4 box motif of Rab39a differs slightly from expected as it has a histindine (H) residue in place of the expected threonine (T) or asparagine (N).

As mentioned in the introduction, all members of the Rab GTPase family contain five regions of high homology called RabF motifs. The sequence of human Rab39a was inserted into NCBI CDD and the RabF motifs were identified. These motifs are highlighted in boxes in Figure 3.5 (B).

Each subfamily of Rab proteins also contains subfamily-specific sequence motifs called RabSF motifs. The sequence of human Rab39a was inserted into NCBI CDD and the RabSF motifs were identified. These motifs are highlighted in boxes in Figure 3.5 (C).

3.2.3.3 GTPase activity of Rab39a

The switch I and switch II regions of Rab proteins are important for their GTPase activity. The sequence of human Rab39a was inserted into NCBI CDD and these switch regions were identified. These regions are highlighted in boxes in Figure 3.6 (A).

Effector interaction sites, GEF interaction sites, and GDI interaction sites can also be predicted based on sequence comparison with other Rab proteins. The sequence of human Rab39a was inserted into NCBI CDD and sites were identified. Potential effector interaction sites are shown in Figure 3.6 (B), GEF interaction sites in Figure 3.6 (C), and GDI interaction sites in Figure 3.6 (D).

3.2.3.4 Post-translational modifications of Rab39a

Bioinformatic analysis can reveal potential details of post-translational modifications of a protein. The protein sequence of human Rab39a was inserted into NCBI CDD and ExPASy ProSite (http://www.expasy.ch/prosite/) to determine if Rab39a contained any lipid modification sites. As shown in Figure 3.7 (A), Rab39a contains a potential myristolyation site and a potential prenylation site at the C-terminus.

NetPhos 2.0 predicts phosphorylation sites in a given sequence and assigns a score to each site (Blom *et al.*, 1999). The protein sequence of human Rab39a was inserted into NetPhos 2.0. Figure 3.7 (B) shows that Rab39a contains ten potential phosphorylation sites which are greater than the required threshold of 0.5. Among these sites are eight serine sites, one tyrosine site and one threonine site.

3.2.3.5 Rab39a contains a putative caspase-1 cleavage site

Because Rab39a was found by mass spectrometry to associate with caspase-1, the question of whether Rab39a is a substrate of caspase-1 was next addressed. ExPASy Peptide Cutter (www.expasy.ch/tools/peptidecutter/) is a bioinformatic tool that predicts potential cleavage sites in a given protein sequence. Figure 3.8 (A) displays a schematic representation of a caspase-1-substrate complex with eight binding sites. Positions Pn to Pm' are counted from the bond between P1 and P1', where caspase-1 cleavage occurs. Figure 3.8 (B) displays the amino acids which must be present at each site in order for caspase-1 cleavage to occur. The sequence of Rab39a contains this pattern of amino acids that therefore implicate Rab39a as a putative substrate of caspase-1. The sequence of Rab39b is also shown and, despite their similarity (76 %), Rab39b does not contain a putative caspase-1 cleavage as it contains an alanine residue in place of the required



Figure 3.5 Characterisation of Ras superfamily, Rab family and Rab subfamily motifs in Rab39a. (A) Ras superfamily motifs (G1 – G5) are highlighted in boxes **(B)** Rab family motif regions RabF1-F5 are shown in boxes. **(C)** Rab subfamily motif regions RabSF1-SF4 are shown in boxes. Adapted from NCBI – conserved domains database (www.ncbi.nlm.nih.gov/Structure/cdd/cdd.shtml).

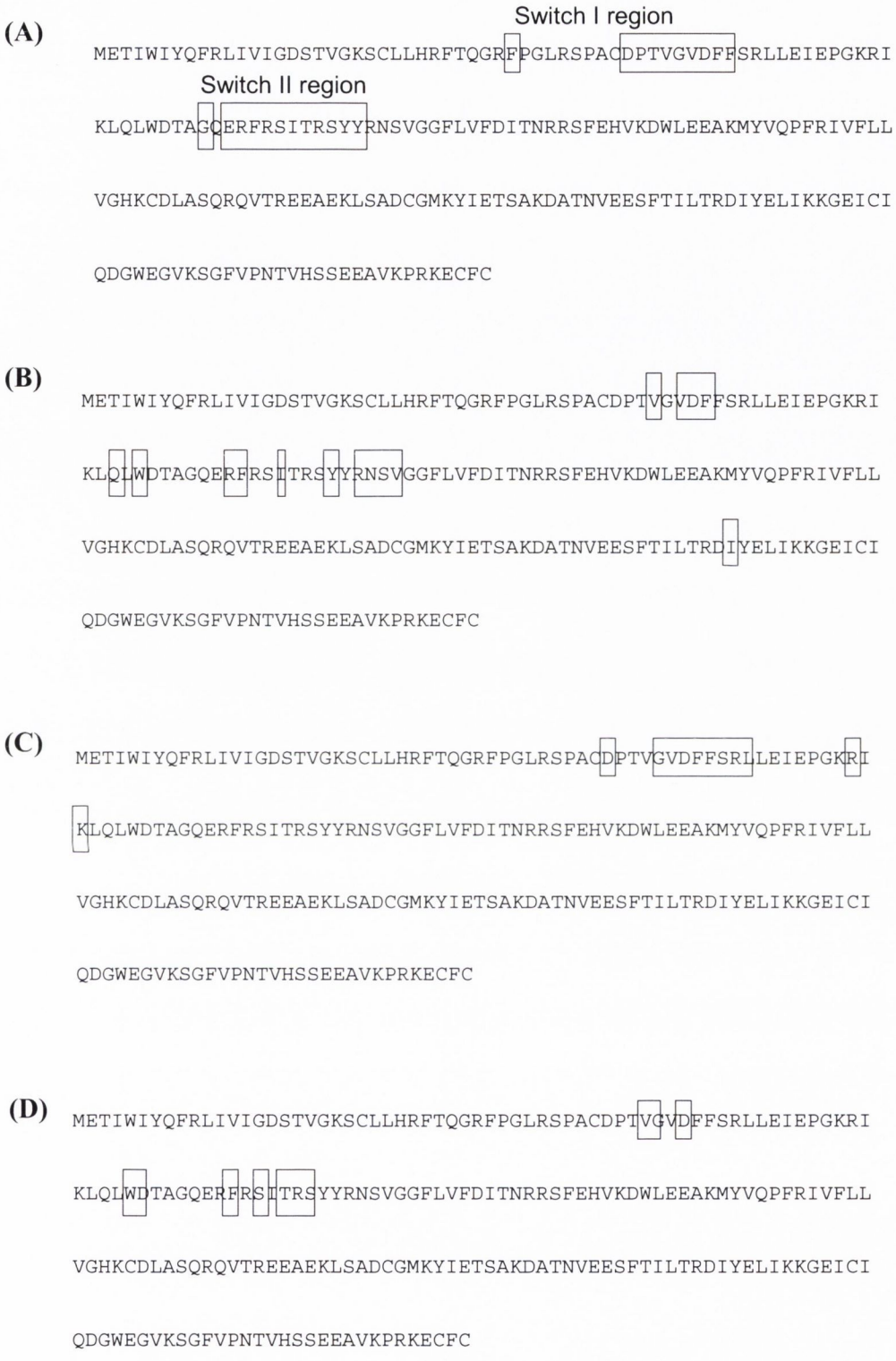


Figure 3.6 Putative areas of GTPase activity in Rab39a. (A) Switch regions **(B)** Effector interaction site **(C)** GEF interaction site and **(D)** GDI interaction sites of Rab39a are highlighted in boxes. Adapted from NCBI – conserved domains database (www.ncbi.nlm.nih.gov/Structure/cdd/cdd.shtml).

(A) METIWIYQFRLIVIGDSTVGKSCLLHRFTQGRFPGLRSPACDPTVGVDFFSRLLEIEPGKRI

KLQLWDTAGQERFRSITRSYYRNSVGGFLVFDITNRRSFEHVKDWLEEAKMYVQPFRIVFLL

VGHKCDLASQRQVTREEAEKLSADCGMKYIETSAKDATNVEESFTILTRDIYELIKKGEICI

Myristoylation site Prenylation site

QDGWEGVKSGFVPNTVHSSEEAVKPRKECFC

(B) METIWIYQFRLIVIGDSTVGKSCLLHRFTQGRFPGLRSPACDPTVGVDFFSRLLEIEPGKRI

KLQLWDTAGQERFRSITRSYYRNSVGGFLVFDITNRRSFEHVKDWLEEAKMYVQPFRIVFLL

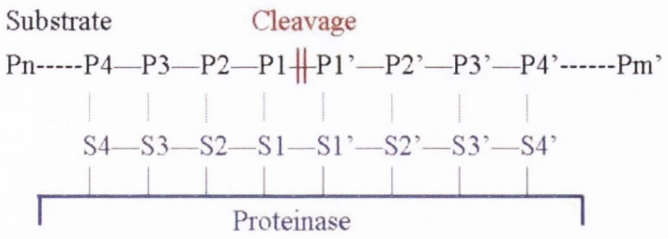
VGHKCDLASQRQVTREEAEKLSADCGMKYIETSAKDATNVEESFTILTRDIYELIKKGEICI

QDGWEGVKSGFVPNTVHSSEEAVKPRKECFC

Pos	Context	Score	Pred
38	PGLRSPACD	0.575	*S*
77	ERFRSITRS	0.944	*S*
81	SITRSYYRN	0.982	*S*
86	YYRNSVGGF	0.810	*S*
100	TNRRSFEHV	0.990	*S*
138	QRQVTREEA	0.890	*T*
157	YIETSAKDA	0.997	*S*
176	TRDIYELIK	0.772	*Y*
204	NTVHSSEEA	0.997	*S*
205	TVHSSEEAV	0.671	*S*

Figure 3.7 Rab39a contains many potential sites for post-translational modification. (A) Two potential lipid modification sites - a myristoylation site and a prenylation site - of Rab39a are indicated by the boxed areas. Adapted from NCBI – conserved domains database (www.ncbi.nlm.nih.gov/Structure/cdd/cdd.shtml) and ProSite from ExPASy (http://www.expasy.ch/prosite/). **(B)** Potential sites of phosphorylation are highlighted in boxes (upper panel). Each site is given a score (lower panel). Scores greater than 0.5 are considered significant. Adapted from NetPhos 2.0 (www.cbs.dtu.dk/services/NetPhos).

(A)



(B)

Enzyme	P4	P3	P2	P1	P1'	P2'	P3'	P4'
Substrate	F,W,Y or L	-	H, A or T	D	Not P,E,D, Q,K,R	-	-	-
Rab39a	L	S	A	D	C	G	M	K
Rab39b	L	A	A	A	Y	G	M	K

(C)

```
Rab39a          METIWIYQFRLIVIGDSTVGKSCLLHRFTQGRFPGLRSPACDPTVGVDFFSRLLEIEPGK
Rab39b          MEAIWLYQFRLIVIGDSTVGKSCLIRRFTEGRFAQVS----DPTVGVDFFSRLVEIEPGK
                **:**:********************:***:***. :      ************:******

Rab39a          RIKLQLWDTAGQERFRSITRSYYRNSVGGFLVFDITNRRSFEHVKDWLEEAKMYVQPFRI
Rab39b          RIKLQIWDTAGQERFRSITRAYYRNSVGGLLLFDITNRRSFQNVHEWLEETKVHVQPYQI
                *****:***************:*******:*:**********:::*::****:*::***::*

Rab39a          VFLLVGHKCDLASQRQVTREEAEKLSADCGMKYIETSAKDATNVEESFTILTRDIYELIK
Rab39b          VFVLVGHKCDLDTQRQVTRHEAEKLAAAYGMKYIETSARDAINVEKAFTDLTRDIYELVK
                **:********* :******.******:*  **********:** ***::** ********:*

Rab39a          KGEICIQDGWEGVKSGFVPNTVHSSEEAVKPRKECFC 217
Rab39b          RGEITIQEGWEGVKSGFVPNVVHSSEEVVKSERRCLC 213
                :*** **:************.******.**.::.*:*
```

Figure 3.8 Rab39a contains a putative caspase-1 cleavage site. (A) Schematic representation of an enzyme-substrate complex with eight binding sites. Positions Pn to Pm' are counted from the bond between P1 and P1', where caspase-1 cleavage occurs. **(B)** Amino acids of Rab39a and Rab39b at each binding site are listed. **(C)** The sequence of human Rab39a was inserted into ExPASy peptide cutter. Caspase-1 is predicted to cleave Rab39a at aspartate 148. This would separate the 25 kDa protein into two sections of 17 kDa and 7 kDa. (www.expasy.ch/tools/peptidecutter)

aspartate at position P1. This putative caspase-1 cleavage site of Rab39a occurs at position 148 as shown in Figure 3.8 (C). Rab39a is expected to be approximately 25 kDa and cleavage at this site would therefore result in fragments of 17 kDa and 7 kDa. Interestingly, this processed 17 kDa form still contains the switch regions, GDI interaction sites, GEF interaction sites and the majority of effector interaction sites.

The evolutionary conservation of this caspase-1 cleavage site was next assessed. Rab39a proteins in a variety of species were analysed for potential caspase-1 cleavage sites. Sequences were obtained from NCBI BLAST (http://blast.ncbi.nlm.nih.gov/Blast.cgi), and inserted into ExPASy Peptide Cutter (www.expasy.ch/tools/peptidecutter) to identify potential caspase-1 cleavage sites. As shown in Table 3.3 this caspase-1 cleavage site is highly conserved as it is present in many other species such as *P. troglodytes*, *E. caballus*, *B. taurus*, *M. musculus*, and *D. rerio*. It was also investigated whether the presence of a potential caspase-1 cleavage site correlated with the presence of caspase-1 in that species. NCBI Homologene (www.ncbi.nlm.nih.gov/homologene) was used to find caspase-1 homologs. The presence or absence of a caspase-1 homolog in each species is also listed in Table 3.3. It can be seen that the presence of a caspase-1 cleavage site is closely linked to the presence of a caspase-1 homolog in that species.

As proteolytic processing of Rab GTPases by caspase-1 is an unreported phenomenon it was therefore investigated whether other Rab GTP proteins contained caspase-1 cleavage sites. Protein sequences of all known human Rabs were obtained from NCBI and inserted into ExPASy Peptide Cutter to determine if they contained caspase-1 cleavage sites. Of the 63 Rab proteins analysed it was found that 9 have caspase-1 cleavage sites. The other

Rab proteins which have caspase-1 cleavage sites are Rab3c, Rab4a, Rab4b, Rab9a, Rab9b, Rab14, Rab25 and Rab34. These are shown in Table 3.4.

3.2.3.6 Rab39a structure

Unlike many other Rab proteins, details of the structure of Rab39a are unknown. Understanding the structure of a protein may provide clues as how the protein functions and the other proteins it may interact with. Prediction programs can be used to predict the secondary and tertiary structures of proteins. PSIPRED prediction software (http://bioinf.cs.ucl.ac.uk/psipred/) was used to determine the secondary structure of human Rab39a. This predicted structure is shown in Figure 3.9 and it can be seen that Rab39a is predicted to contain six α-helices and six β-strands.

3D-JIGSAW (version 2.0) builds three-dimensional models for proteins based on homologues of known structures (http://bmm.cancerresearchuk.org/~3djigsaw/). This program was used to predict the tertiary structure of Rab39a and the result is shown in Figure 3.10. From the predicted tertiary structure it can be seen that the putative caspase-1 cleavage site, D148, is predicted to be exposed, making it accessible for proteolytic processing.

3.2.3.7 Characterisation of the promoter region of the Rab39a gene

The promoter region of Rab39a was analysed for transcription factor binding sites using the genomatix database (www.genomatix.de). The database revealed many putative transcription factor binding sites. Each site is given a score which measures how close the nucleotides within the promoter correspond to nucleotides in the transcription factor.

Name	Protein ID	Length	Caspase-1 cleavage site	Caspase-1 Homolog
M. mulatta	XP_001103335	217	D148	Yes
E. caballus	XP_001501057	217	D148	Yes
B. taurus	XP_614612	217	D148	Yes
M. musculus	NP_780771	217	D148	Yes
D. rerio	NP_998207	213	D144	Yes
P. troglodytes	XP_001136512	160	D91	Yes
D. melanogaster	NP_572405	218	D31	No
S. purpuratus	XP_782114	227	-	No
C. elegans	NP_495984	229	-	No

Table 3.3 The caspase-1 cleavage site in Rab39a is conserved across many species. Sequences were obtained from NCBI BLAST (http://blast.ncbi.nlm.nih.gov/Blast.cgi), and inserted into ExPASy Peptide Cutter (www.expasy.ch/tools/peptidecutter) to identify potential caspase-1 cleavage sites. NCBI Homologene (www.ncbi.nlm.nih.gov/homologene) was used to find caspase-1 homologs.

Name	Accession no.	Length (aa)	Cleavage site(s)
Rab 3c	AAK08968	227	D202
Rab 4a	NP_004569	218	D110
Rab 4b	AAP97171	213	D105
Rab 9a	AAM21092	201	D110
Rab 9b	CAB76967	201	D110
Rab 14	CAG33675	215	D39, D108
Rab 25	NP_065120	213	D40
Rab 34	AAH91510	259	D149
Rab 39a	Q14964	217	D148

Table 3.4 Rab proteins with potential caspase-1 cleavage sites. All human Rab GTPases were analysed for the presence of a caspase-1 cleavage site. Sequences were obtained from NCBI BLAST (http://blast.ncbi.nlm.nih.gov/Blast.cgi), and inserted into ExPASy Peptide Cutter (www.expasy.ch/tools/peptidecutter) to identify potential caspase-1 cleavage sites. Rab proteins which contain the site are shown.

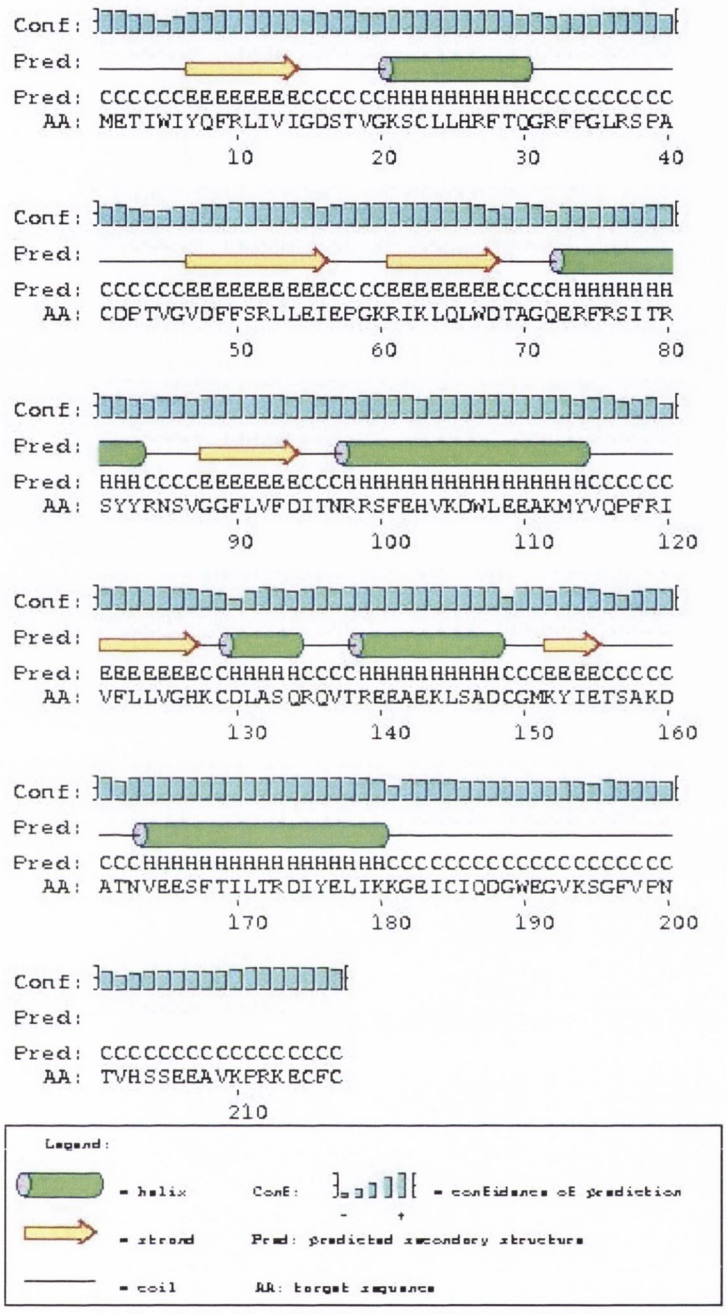


Figure 3.9 Predicted secondary structure of Rab39a. The predicted secondary structure model of Rab39a was constructed using PSIPRED prediction software (http://bioinf.cs.ucl.ac.uk/psipred/).

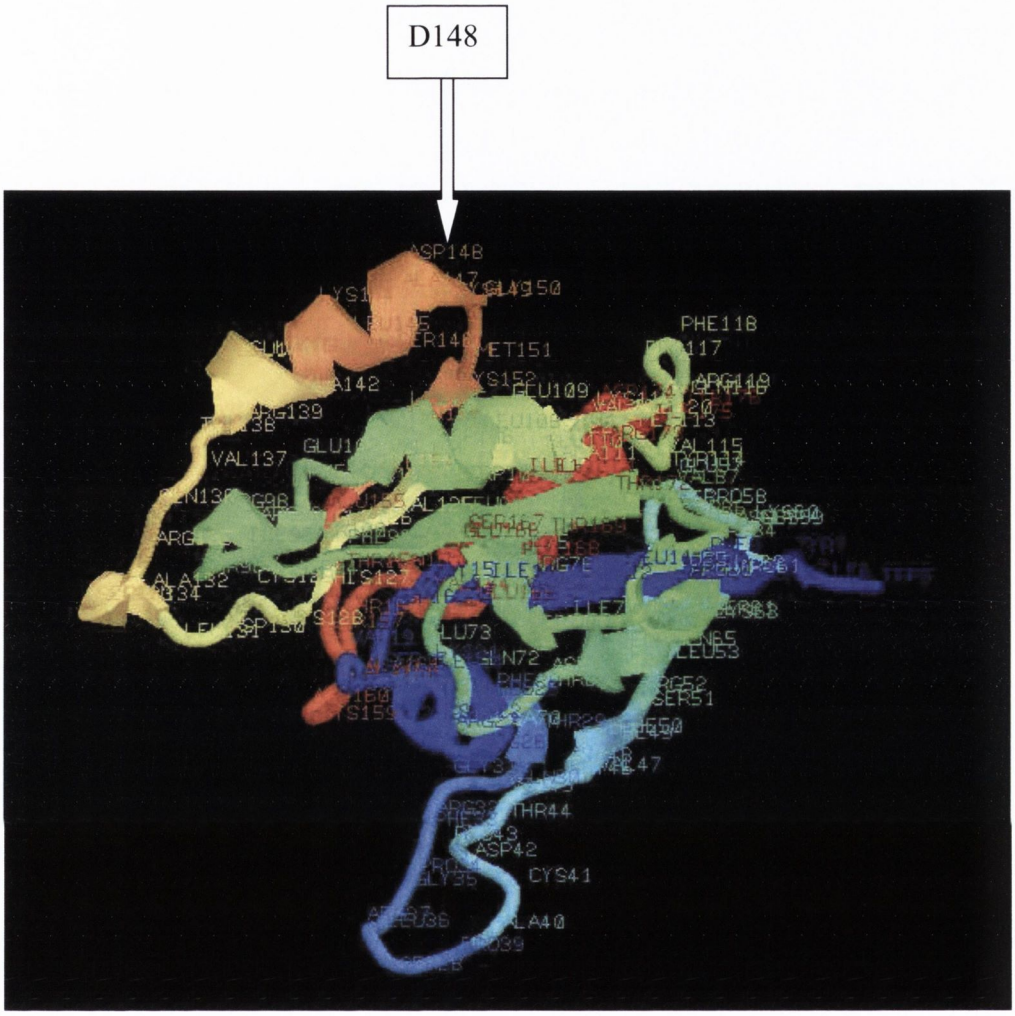


Figure 3.10 Predicted tertiary structure of Rab39a. A model of the predicted tertiary structure of Rab39a was constructed using 3D-JIGSAW (version 2.0) (http://bmm.cancerresearchuk.org/~3djigsaw/). The exposed D148 residue which is the predicted site of caspase-1 cleavage is indicated by the arrow.

Those sites of interest which are above the required threshold score, such as NF-κB, p53 and SP-1, are shown in Figure 3.11.

3.2.3.8 Tissue and cell type distribution of Rab39a

In order to determine the expression of Rab39a within various tissues and cell types, data from the BioGPS database was used (http://biogps.gnf.org/). This shows expression levels of Rab39a in a variety of tissues samples and cell lines. The results in Figure 3.12 show that within human samples Rab39a is expressed ubiquitously at a low level. The expression of Rab39a was also examined in the murine database. The results are shown in Figure 3.13. In the murine dataset, Rab39a seems to display higher levels of expression in cells of the immune system. For example, it is highly expressed in B-cells and dendritic cells. It is also expressed in macrophages and expression is increased when cells are treated with LPS.



Figure 3.11 Analysis of the promoter region of Rab39a for transcription factor binding sites. The promoter region of human Rab39a was identified using Promoter Inspector (www.genomatix.de). Potential transcription factor binding sites of interest are indicated in the shaded areas. Sites are all significant as they have a matrix score greater than 0.8.

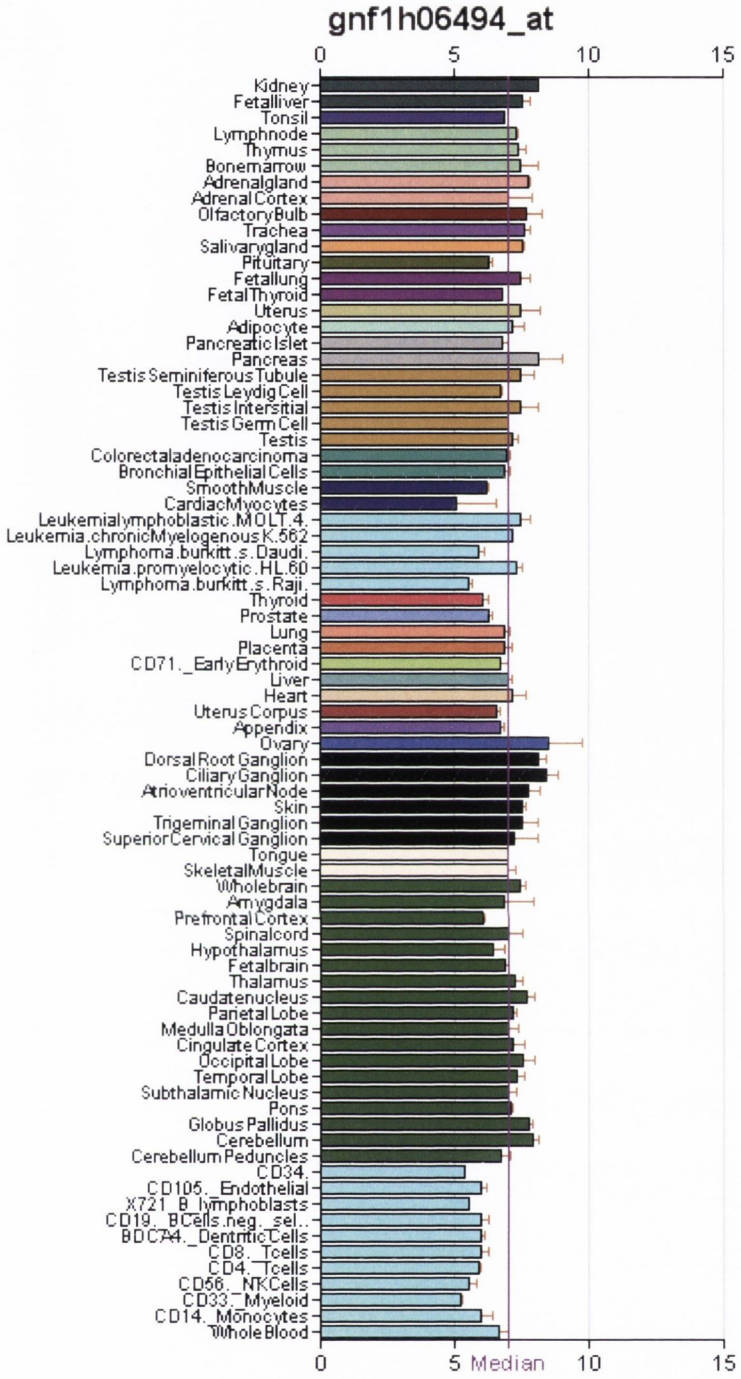


Figure 3.12 Human Rab39a is expressed at a low level in a variety of human tissues and cells. Expression levels of human Rab39 in a variety of tissues and cells were obtained from the BioGPS database (http://biogps.gnf.org).

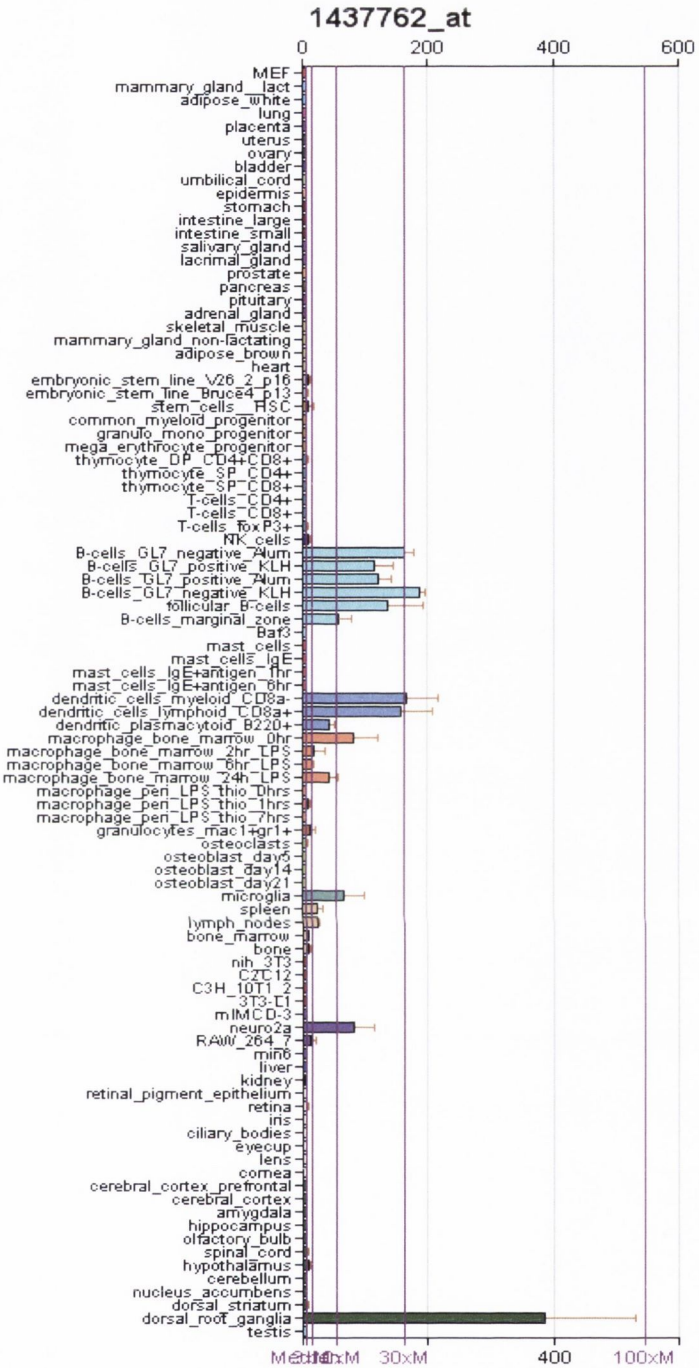


Figure 3.13 Murine Rab39a is highly expressed in cells of the immune system

Expression levels of murine Rab39a in a variety of tissues and cells were obtained from the BioGPS database (http://biogps.gnf.org).

3.3 Discussion

Previous work in the laboratory identified Rab39a as a potential novel binding partner of caspase-1. This was done by immunoprecipitating caspase-1 from THP1 cells and identifying bound proteins by mass spectrometry. The first aim of this chapter was to confirm this interaction. Firstly, it was shown that Rab39a and caspase-1 can co-immunoprecipitate in HEK293T cells. Interestingly, although Rab39b is 76 % similar to Rab39a, it was unable to co-immunoprecipitate with caspase-1. Secondly, confocal microscopy was used to show that GFP-Rab39a and RFP-caspase-1 can co-localise in HEK293T cells.

The second part of this chapter focused on the characterisation of Rab39a by bioinformatics. Analysis of Rab39a was carried out in order to reveal more about the family grouping, evolutionary conservation, GTPase activity, possible post-translational modifications, secondary and tertiary structure, promoter characteristics and tissue and cellular expression of the protein.

A homology search of Rab39a shows that within the human genome, Rab39a is most similar to Rab39b, Rab42, Rab2, Rab14, Rab8, Rab13 and Rab4. The homology searches are based on amino acid alignments between the various proteins. However, the alignments do not differentiate whether the sequence similarity underlies a common basic structure, effector binding, regulatory protein interactions, subcellular localisation or another aspect of the protein. Hence, caution must be exercised in making predictions about the functions of Rab39a on the basis of these homology searches. Indeed, within the Rabs listed above there is a wide range of functions evident, and also many Rabs have been implicated in multiple roles. The functions of Rab39b and Rab42 which are

the closest homologs of Rab39a are unfortunately unknown. However, of the other Rabs similar to Rab39a, Rab2a and Rab2b are localised to the endoplasmic reticulum (ER) and are involved in ER to Golgi transport (Tisdale *et al.*, 1992). Rab14 has been shown to be localised to rough ER, Golgi/trans-Golgi and early endosomes and plays a role in phagosome and early endosome fusion and trafficking between early endosomes and Golgi (Junutula *et al.*, 2004, Kyei *et al.*, 2006, Proikas-Cezanne *et al.*, 2006). Rab8 has been reported to be localised in the Golgi region, on endosomes, dendrites, and on the basolateral plasma membrane. Its reported functions include trafficking between Golgi, endosomes and the plasma membrane; cholesterol degradation; extension of the primary ciliary membrane, basolateral transport in epithelia and dendritic transport in neurons; and adherens junction assembly (Nachury *et al.*, 2007, Chen *et al.*, 2001, Hattula *et al.*, 2006, Linder *et al.*, 2007). Rab13 is localised to tight junctions and endosomes and has a role in tight junction biogenesis (Marzesco *et al.*, 2002). Rab4a, Rab4b and Rab4c are localised in early and recycling endosomes and are implicated in rapid endocytic recycling to the plasma membrane (van der Sluijs *et al.*, 1992), Rab4a is also involved in adherens junction disassembly, α-granule secretion from platelets, amylase release from pancreatic acinar cells and Glut4 transport from 3T3-L1 adipocytes (Bottger *et al.*, 1996). Because of this diverse range of functions found within these similar Rabs, other factors besides homology must be considered when predicting Rab39a functions.

By examining the presence of Rab39a in other species it can be seen that it is highly evolutionarily conserved as it is present in a variety of species including *M. musculus, D. rerio, D. melanogaster* and *C. elegans*. The number of Rab GTPases varies from species to species, ranging from 11 in budding yeasts to 29 in *C. elegans* and *D. melanogaster*, and to more than 60 in humans and mice. Only five Rab GTPases,

Rab1/Ypt1, Rab5/Ypt5, Rab6/Ypt6, Rab7/Ypt7, and Rab11/Ypt31 are conserved from yeasts to humans, and only 17 Rab GTPases, including Rab39a, are shared by *C. elegans*, *D. melanogaster* and humans (Fukuda, 2008). Therefore, Rab39a is highly evolutionarily conserved, indicating that its functions are potentially very important.

The post-translational modification of a protein extends the range of functions of that protein. Modifications include the attachment of other biochemical functional groups such as acetate, phosphate, lipids and carbohydrates; changing the chemical nature of an amino acid; or by making structural changes, like the formation of disulfide bridges. Other modifications, like phosphorylation, are part of common mechanisms for controlling the behaviour of a protein.

Rab GTPases undergo cotranslational or posttranslational lipid modifications, which act as hydrophobic membrane anchors, interacting with the cytoplasmic leaflet of cellular membranes and/or participating in protein-protein interactions. Bioinformatic analysis suggests that Rab39a contains a prenylation motif at the C - terminal. Prenylation of Rab proteins is important for their targeting and functioning (Leung *et al.*, 2006). Myristoylation is a lipid modification that can help direct proteins to membranes. The importance of the myristoylation site for Rab protein functioning is not known but myristoylation sites have been proposed as specific protein-protein interaction sites (Taniguchi, 1999).

The amino acid sequence of Rab39a contains 10 possible sites of phosphorylation which are above the required threshold. The significance of this is unclear, however many Rab proteins undergo phosphorylation, which results in a variety of

consequences. For example, Rab1, Rab3, Rab4, Rab5, Rab6, Rab8, Rab14, Rab17 and Rab24 all undergo phosphorylation (Bailly *et al.*, 1991, Fitzgerald *et al.*, 1999, Uno *et al.*, 2004).

Since Rab39a was found to interact with caspase-1, the next step was to investigate if Rab39a could be a substrate of caspase-1 and therefore it was analysed to see if it contained the consensus caspase-1 cleavage site sequence. Bioinformatic analysis indicated that Rab39a contained a conserved caspase-1 cleavage site at D148. Interestingly, Rab39b which is 76 % similar to Rab39a does not contain this site. Rab39a is 25 kDa and cleavage at this site would result in fragments of 17 kDa and 7 kDa. From the characterisation of the functional domains and motifs within Rab39a this suggests that cleavage would dissociate Rab39a from the membrane as the lipid modification motif, anchoring Rab39a to the membrane, would be contained in the smaller C-terminal section. Therefore, this could result in inactivation of Rab39a as it is thought that Rab proteins need to be associated with membranes for proper functioning. Most of the motifs important for GTPase activity are also contained within the larger 17 kDa section again suggesting that caspase-1 cleavage at D148 would result in the inactivation of Rab39a, unless the Rab protein can still function without membrane attachment.

The D148 caspase-1 cleavage site appears to be a more recent feature of the Rab39a protein as it is only evident in *H. sapiens, M. mulatta, E. caballus, B. taurus, M. musculus. D. rerio* contains the same site at D144. *P. troglodytes* has a much shorter version of Rab39a (it is missing the first 53 amino acids) but the cleavage site remains intact. *D. melanogaster* does not contain the D148 site but instead has a different site

closer to the N-terminus at D31. Interestingly, the addition of this caspase-1 cleavage site at D148 appears to correlate with the emergence of caspase-1.

Furthermore, several other Rab proteins contain the putative caspase-1 cleavage site. Proteolysis is a key regulatory process that promotes the (in)activation, translocation, and/or degradation of proteins. Rab10, Rab11b and Rab-like protein 2A are also all reported to undergo caspase-dependant proteolysis (Dix *et al.*, 2008). Therefore, cleavage of Rab proteins may represent a general mechanism by which caspases modulate protein trafficking within the cell.

Next, the predicted secondary and tertiary structures of Rab39a were analysed. Often the function of a protein can be inferred by knowing the secondary and tertiary structure. However, without further analysis this can only be used as a guide as some proteins require stabilisation by additional domains or binding partners to adopt their native structure. The tertiary structure of a native protein may also not be readily formed without the aid of additional post-translational modifications. However, one notable point of interest from the tertiary structure prediction is that the potential caspase-1 cleavage site is located on the surface of the protein, making it easily accessible for caspase-1. This supports the idea that Rab39a contains a functional caspase-1 cleavage site.

The promoter region of Rab39a was analysed. Numerous transcription factor binding sites were found. Notably, there were several sites of interest including NF-κB sites, P53 sites and SP1 sites. Since these transcription factors are regulated by pro-inflammatory stimuli, this suggests that Rab39a itself may be inducible.

Finally, the expression of Rab39a in a variety of tissues and cell types was analysed. Human Rab39a appears to have a low basal expression in most tissues and cell types that were available in the dataset. If Rab39a is inducible by pro-inflammatory stimuli as predicted then this may explain the low basal levels. The mouse Rab39a is also expressed at a low basal level in most tissues and cell types. However, unlike the human dataset, the mouse dataset includes many more cells of the immune system such as B cells, dendritic cells, and BMDMs, and Rab39a is highly expressed in these cells indicating a role for Rab39a in cells of the immune system. Interestingly, the dataset suggests that Rab39a may be inducible, as LPS treatment led to increased expression of Rab39a.

To summarise, this chapter of work has firstly confirmed that Rab39a interacts with caspase-1. This was shown through co-immunoprecipitation experiments and confocal microscopy. Secondly, Rab39a was characterised by bioinformatics. Rab39a is a highly evolutionary conserved protein displaying typical domains and motifs necessary for GTPase function. Rab39a contains two lipid modification motifs at the C-terminal. A conserved caspase-1 cleavage site is located at D148 and cleavage at this site suggests inactivation of the protein. Tertiary structure analysis predicts that this D148 site is exposed. Analysis of the promoter region of Rab39a shows a variety of transcription factor binding motifs indicating that Rab39a may be inducible. Finally, analysis of cellular expression suggests that Rab39a can be found in cells of the immune system and may be inducible by LPS.

Chapter 4

Functional Significance of the Rab39a and Caspase-1 Interaction

4.1 Introduction

The previous chapter confirmed that caspase-1 binds Rab39a. It also characterised Rab39a using bioinformatics and this computer based research found that Rab39a contains many interesting features making it worthy of future research. The aim of this chapter therefore, was to investigate the nature of the interaction between caspase-1 and Rab39a.

Caspase-1 is an important regulatory molecule in the innate immune response that has a variety of functions. The best described role for caspase-1 is its involvement in the inflammasome. The inflammasome is a multi-protein complex, which along with caspase-1, also contains NLRP1, NLRP3, NLRC4 or AIM2 and the adaptor protein ASC. A diverse range of stimuli can activate inflammasomes such as bacteria, viruses, and in the case of the NLRP3 inflammasome, danger signals such as uric acid and ATP and aggregated materials such as silica and asbestos. Activation of the inflammasome in response to pro-inflammatory stimuli results in the activation of caspase-1 and the subsequent processing of the pro-inflammatory cytokine pro-IL-1β into its active form. IL-1β is then released from the cell into the extracellular milieu where it plays a crucial role in host defence.

Besides its well documented role in IL-1β processing and in the inflammasome, other roles for caspase-1 are emerging. Caspase-1 has been shown to have an important role in phagocytosis. In caspase-1 deficient mice it has been shown that phagolysosomal fusion does not occur (Amer *et al.,* 2006). Recently, it has also been shown that caspase-1, although not necessary for bacterial uptake, it is needed for phagosomal acidification (Lynda Stuart, personal communication).

Another recent study describes how caspase-1 is important for the secretion of IL-1β as well as many other unconventionally secreted proteins such as FGF-2 and IL-1α. Using iTRAQ proteomics 77 leaderless proteins with extracellular functions whose secretion is mediated by caspase-1 were identified. Many of these proteins are involved in inflammation, cytoprotection, or tissue repair (Keller *et al.*, 2008).

Results in the previous chapter showed that Rab39a binds caspase-1. It was decided to follow up on the nature of this interaction because there were several intriguing possibilities as to why they might be interacting.

Firstly, caspase-1 is a cysteine protease, and until recently many of its substrates were unknown. In recent years a number of large scale screening efforts have resulted in the emergence of a host of caspase-1 substrates. Initial bioinformatics analysis showed that Rab39a contained a putative caspase-1 cleavage site and therefore it was decided to investigate if Rab39a was a substrate a caspase-1.

Secondly, many Rab GTPase proteins have roles in phagocytosis such as Rab2, Rab5, Rab7, Rab11 and Rab14. It has previously been proposed that a Rab protein could be a substrate for caspase-1 and play a role in regulating phagosomal maturation. An RNAi screen of components thought to be involved in phagocytosis in Drosophila showed that the absence of Rab39a resulted in a significant reduction in bacterial uptake in response to *S. aureus* and *E. coli* (Stuart *et al.*, 2007). Therefore, it was decided to investigate if Rab39a associated with caspase-1 in order to fulfil a phagocytic role.

Thirdly, it was hypothesised that Rab39a could be playing a role in IL-1β secretion. Most proteins that are secreted from the cell contain signal peptides that direct their transport to the plasma membrane through the ER-Golgi pathway. However, certain proteins including IL-1β do not contain signal peptides, and are secreted by unconventional means, the mechanism of which is not entirely understood. Several models for IL-1β secretion have been described, including the lysosome-dependent pathway (Andrei *et al.*, 1999, Andrei *et al.*, 2004), micro-vesicle shedding (MacKenzie *et al.*, 2001, Pelegrin *et al.*, 2008) and exosome release (Qu *et al.*, 2007). Since, caspase-1 has been shown to have a role in the unconventional secretion of IL-1β and Rab proteins are important in protein trafficking and secretion; it was decided to investigate if Rab39a could have a role in this secretion process too.

This chapter explores the nature of the interaction between Rab39a and caspase-1 using techniques such as siRNA, over-expression studies and confocal microscopy. Overall, results suggest that Rab39a is a substrate of caspase-1, which plays a role in phagocytosis and also acts a novel trafficking protein in the IL-1β secretion pathway.

4.2 Results

4.2.1 Rab39a is a substrate of caspase-1

4.2.1.1 Rab39a can be processed by recombinant caspase-1

In the previous chapter it was shown that Rab39a and caspase-1 can interact. Therefore, the next goal was to examine if Rab39a was a substrate for caspase-1. Bioinformatic analysis predicted that Rab39a contains a caspase-1 cleavage site at amino acid position 148. Cleavage in this manner would result in processing of the 25 kDa full length protein into two portions of 17 kDa and 7 kDa. The effect of caspase-1 on Rab39a was tested by incubating lysates from HEK293T cells transfected with a plasmid containing HA-Rab39a (or with a control plasmid containing the HA-tag only) with 2 µl of active recombinant caspase-1 at 30 °C for 90 minutes. The results are shown in Figure 4.1. Lane 1 and 2 contain the control plasmid and no bands are present as expected. Lanes 3 – 8 contain increasing amounts of lysate containing HA-Rab39a. Full length Rab39a is 25 kDa as indicated. Caspase-1 treatment (lanes 4, 6 and 8) led to the appearance of an additional form of Rab39a at 17 kDa as indicated. This is consistent with processing of Rab39a by caspase-1 at the putative caspase-1 cleavage site. It appears that some endogenous processing of Rab39a takes place as there is a weaker band at 17 kDa in the lanes where recombinant caspase-1 has not been added (lanes 3, 5 and 7).

4.2.1.2 Rab39b cannot be processed by caspase-1

Bioinformatic analysis suggests that Rab39b does not contain a putative caspase-1 cleavage site. Therefore, no additional forms of Rab39b should be evident when it is incubated with recombinant caspase-1 using the method described above. The results are shown in Figure 4.2. Full length Rab39b is 25 kDa as indicated. Caspase-1 treatment

(lanes 2, 4 and 6) did not lead to the appearance of any additional forms of Rab39b, indicating that Rab39b cannot be processed by the addition of recombinant caspase-1.

4.2.1.3 A caspase-1 inhibitor prevents processing of Rab39a

The next step was to confirm that it is caspase-1 that is processing Rab39a. The effect of caspase-1 was blocked by pre-treatment of cells with the inhibitor YVAD-cmk. YVAD-cmk is a synthetic tetrapeptide (Tyr-Val-Ala-Asp) which is a competitive inhibitor of caspase-1. The chloromethyl (cmk) conjugate forms a covalent bond with caspase-1 creating irreversible linkage. The results are shown in Figure 4.3. As before, the addition of recombinant caspase-1 led to an increase in the size of the 17 kDa fragment (lane 2). When cells were pre-treated with YVAD-cmk (lanes 3 and 4) this fragment was not visible. This indicates that YVAD-cmk was blocking both the cleavage caused by any endogenous caspase-1 (lane 3) and the added recombinant caspase-1 (lane 4).

4.2.1.4 The caspase-1 cleavage site on Rab39 is confirmed as D148

The next goal was to determine if the predicted caspase-1 cleavage site was correct. Bioinformatic predictions suggested that Rab39a may be cleaved by caspase-1 after the aspartate at position 148. A construct HA-Rab39aD148A, was made using the QuikChange XL Site-Directed Mutagenesis Kit (Stratagene). The construct has an aspartate to alanine change and can no longer be cleaved by caspase-1 according to the ExPASy predictive software.

The effect of caspase-1 on this construct was tested by incubating lysates from HEK293T cells transfected with the plasmid containing HA-Rab39aD148 (or with HA-

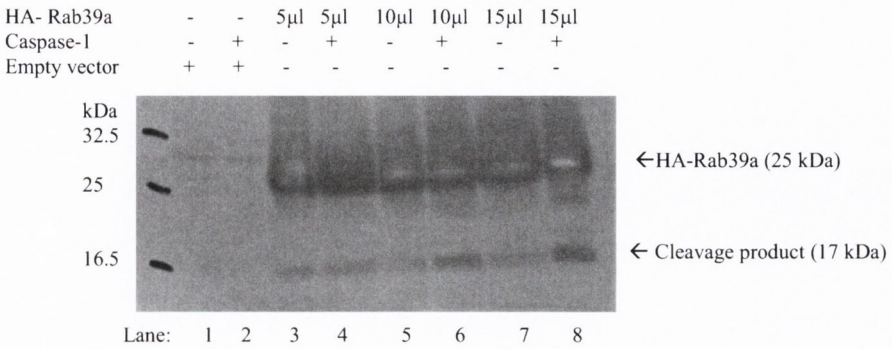


Figure 4.1 Rab39a can be processed by caspase-1. HEK293T cells were set up at 4 x 10^5 cells per ml in 10 cm dishes. The following day cells were transfected with 5 µg of a plasmid containing HA-Rab39a or a plasmid containing the HA tag only. 24 hours later cells were lysed in 300 µl of low astringency lysis buffer. The indicated amounts of lysate (5 µl, 10 µl or 15 µl) were mixed with assay buffer such that the total volume of the sample was 20 µl. Samples were incubated with 2 µl of recombinant caspase-1 at 30 °C for 90 minutes. 5X sample buffer was added and samples were separated on 12 % SDS-PAGE gels and analysed by Western blotting. The HA antibody was used to detect products. Data shown is representative of at least three independent experiments.

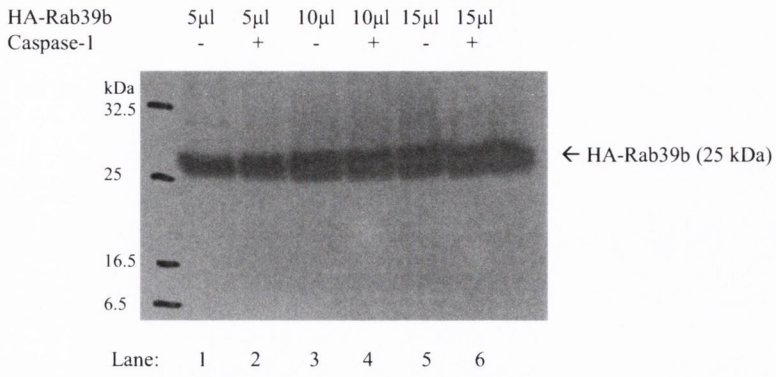


Figure 4.2 Rab39b cannot be processed by caspase-1. HEK293T cells were set up at 4 x 10^5 cells per ml in 10 cm dishes. The following day cells were transfected with 5 µg of a plasmid containing HA-Rab39b. 24 hours later cells were lysed in 300 µl of low astringency lysis buffer. The indicated amounts of lysate (5 µl, 10 µl or 15 µl) were mixed with assay buffer such that the total volume of the sample was 20 µl. Samples were incubated with 2 µl of recombinant caspase-1 at 30 °C for 90 minutes. 5X sample buffer was added and samples were separated on 12 % SDS-PAGE gels and analysed by Western blotting. HA antibody was used to detect products. Data shown is representative of at least three independent experiments.

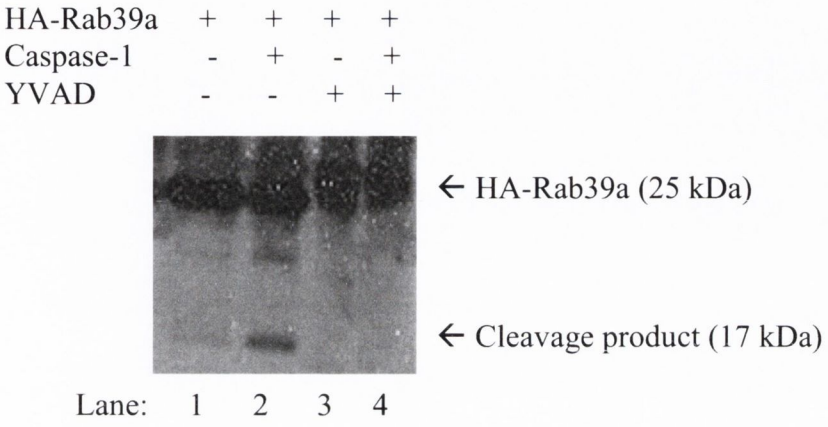


Figure 4.3 Pre-treatment with a caspase-1 inhibitor prevents processing of Rab39a. HEK293T cells were set up at 4 x 10^5 cells per ml in 10 cm dishes. The following day cells were transfected with 5 μg of a plasmid containing HA-Rab39a. 100 μM of caspase-1 inhibitor (YVAD-cmk) was added 1 hour prior to lysing. 24 hours after cells were set up they were lysed in 300 μl of low astringency lysis buffer. 10 μl of lysate and 10 μl of assay buffer was mixed and incubated with 2 μl of recombinant caspase-1 at 30 °C for 90 minutes. 5X sample buffer was added and samples were separated on 12 % SDS-PAGE gels and analysed by Western blotting. HA antibody was used to detect products. Data shown is representative of three independent experiments.

Rab39a as a control) with increasing amounts of active recombinant caspase-1 at 30 °C for 90 minutes. The results are shown in Figure 4.4. Lanes 1-6 contain HA-Rab39a and it can be seen that the addition of recombinant caspase-1 leads to the processing of Rab39a as before. The intensity of the 17 kDa fragment increases as more recombinant caspase-1 is added. Lanes 7-12 contain HA-Rab39aD148A and it can be seen that the addition of recombinant caspase-1 does not lead to any processing. This indicates that the predicted D148 site is the site of caspase-1 cleavage.

As an additional way to confirm that the cleavage site was D148, a construct was made which would mimic the predicted cleaved version of Rab39a. This was done by inserting a stop codon at position 149 after the cleavage site. In this case, GFP-Rab39a was used and site directed mutagenesis was carried out to mutate the cysteine residue at amino acid position 149 to a stop codon thereby creating GFP-Rab39aC149Stop. {GFP-Rab39aC149Stop was made with the technical assistance of Ashish Sarraju, Developmental Immunology Lab, Massachusetts General Hospital, USA}. The effect of caspase-1 on this mutant was tested by incubating lysates from HEK293T cells transfected with the plasmid containing GFP-Rab39aC149Stop (or with GFP-Rab39a as a control) with recombinant caspase-1 at 30 °C for 90 minutes. The results are shown in Figure 4.5. GFP-Rab39a is expressed in lane 1 and 2 and it can be seen that the addition of recombinant caspase-1 (lane 2) leads to the appearance of an additional band. GFP-Rab39aC149 is expressed in lanes 3 and 4 and it can be seen that the size of these bands are identical to that of processed Rab39a (lane 2). This therefore confirms that the predicted cleavage site D148 is correct.

4.2.1.5 Constitutively active and dominant negative forms of Rab39a can be processed by caspase-1

It was next decided to examine if the GTPase activity of Rab39a affects its processing. Dominant negative and constitutively active versions of HA-Rab39a were made by site directed mutagenesis. The S22N mutation (in the G1 motif) locks the protein in its GDP state (dominant negative) while the Q72L mutation (in switch 2) locks the protein in a GTP state (constitutively active).

The effect of caspase-1 on these mutants were tested by incubating lysates from HEK293T cells transfected with plasmids containing HA-Rab39a, HA-Rab39aQ72L, HA-Rab39S22N (or with HA-Rab39a as a control) with recombinant caspase-1 at 30 °C for 90 minutes. The results are shown in Figure 4.6. Lanes 1 and 2 contain Rab39a-HA, and addition of recombinant caspase-1 (lane 2) leads to the appearance of the 17 kDa fragment as before. Lanes 3 and 4 contain the constitutively active version (HA-Rab39Q72L) and addition of recombinant caspase-1 (lane 3) leads to the appearance of the 17 kDa fragment similar to the wild type version. Lanes 5 and 6 contain the dominant negative version (HA-Rab39aS22N) and addition of recombinant caspase-1 (lane 6) leads to the appearance of the 17 kDa fragment which is again similar to the wild type version. Therefore, this shows that both a constitutively active version and a dominant negative version of Rab39a can be processed by caspase-1. This result indicates that the activation state of Rab39a does not affect the cleavage of Rab39a.

4.2.1.6 Rab39a can be processed in macrophages by LPS and ATP

It was next decided to examine whether Rab39a could be processed by endogenous caspase-1 in macrophages. RAW 264.7 cells were used as they can be transfected

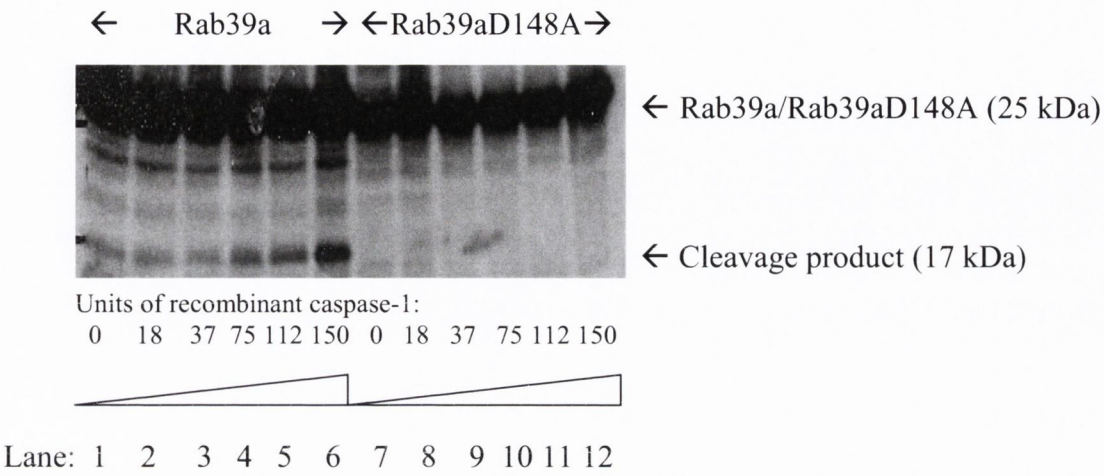


Figure 4.4. HA-Rab39aD148A cannot be cleaved by caspase-1. HEK293T cells were set up at 4 x 10^5 cells per ml in 10 cm dishes. The following day cells were transfected with 5 µg of a plasmid containing HA-Rab39a or HA-Rab39aD148A. 24 hours later cells were lysed in 300 µl of low astringency lysis buffer. 10 µl of lysate and 10 µl of assay buffer was mixed and incubated with 2 µl of recombinant caspase-1 at 30 °C for 90 minutes. 5X sample buffer was added and samples were separated on 12 % SDS-PAGE gels and analysed by Western blotting. HA antibody was used to detect products. Data shown is representative of three independent experiments.

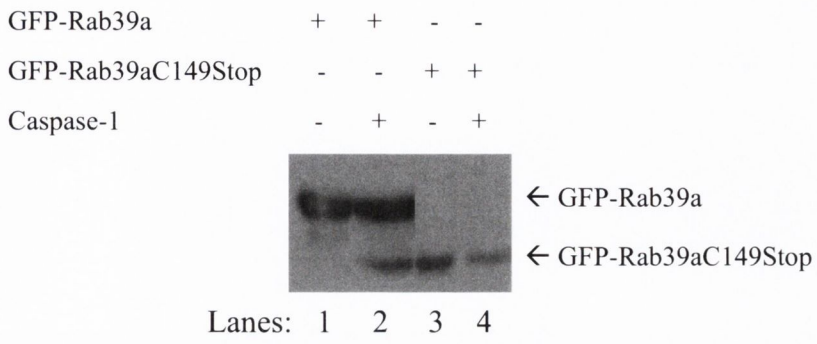


Figure 4.5 GFP-Rab39aC149Stop is the same size as the cleavage fragment. HEK293T cells were set up at 4 x 10^5 cells per ml in 10 cm dishes. The following day cells were transfected with 5 µg of a plasmid containing GFP-Rab39a or GFP-Rab39aC148Stop. 24 hours later cells were lysed in 300 µl of low astringency lysis buffer. 10 µl of lysate and 10 µl of assay buffer was mixed and incubated with 2 µl of recombinant caspase-1 at 30 °C for 90 minutes. 5X sample buffer was added and samples were separated on 12 % SDS-PAGE gels and analysed by Western blotting. GFP antibody was used to detect products.

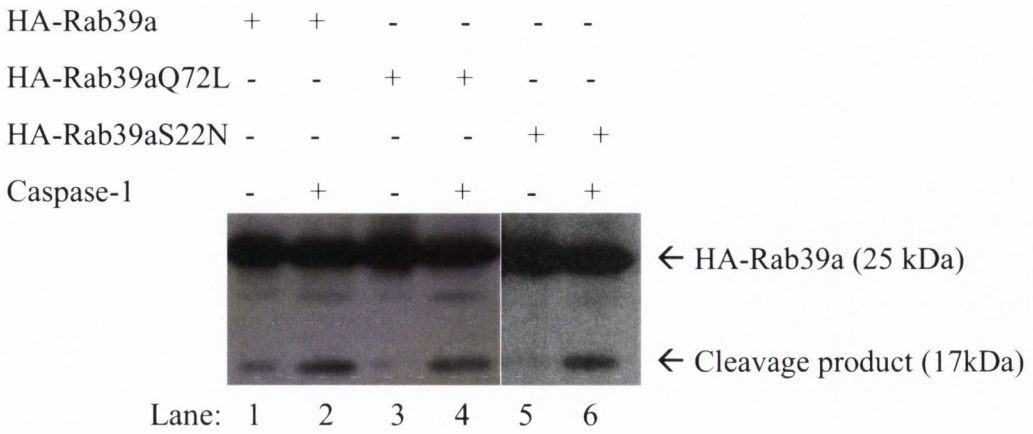


Figure 4.6 Constitutively active and dominant negative forms of Rab39a can still be processed by caspase-1. HEK293T cells were set up at 4 x 10^5 cells per ml in 10 cm dishes. The following day cells were transfected with 5 µg of a plasmid containing HA-Rab39a, HA-Rab39aQ72L or HA-Rab39aS22N. 24 hours later cells were lysed in 300 µl of low astringency lysis buffer. 10 µl of lysate and 10 µl of assay buffer was mixed and incubated with 2 µl of recombinant caspase-1 at 30 °C for 90 minutes. 5X sample buffer was added and samples were separated on 12 % SDS-PAGE gels and analysed by Western blotting. HA antibody was used to detect products. This result represents two independent experiments.

easily. Cells were transfected with plasmids containing HA-Rab39a or HA-Rab39aD148A using the Amaxa transfection system. Caspase-1 was activated by stimulating the cells for 3 hours with 100 ng/ml LPS followed by 1 hour with 5 mM ATP. The results are shown in Figure 4.7. Western blot analysis revealed the appearance of an additional band at 17 kDa when cells were treated with LPS and ATP (lane 2). This band is not present when cells were treated with the caspase-1 inhibitor YVAD (lane 3). Significantly, no processing took place of the HA-Rab39aD148A construct when treated with LPS and ATP (lane 5).

4.2.1.7 Rab39a cannot be processed by an ITT assay

Although the previous assays demonstrated that Rab39a could be processed by caspase-1, a further assay was carried out in conjunction with Dr. Alex Luthi in the Department Genetics, TCD, to assess this.

For this assay it was necessary for Rab39a and Rab39b to be in pcDNA3 vectors. Rab39a and Rab39b were sub-cloned from the pGEM-T-Easy vectors into pcDNA3. Constructs were sequenced to ensure that the sequence was correct.

Proteins were generated by i*n vitro* transcription and translation (ITT). For detection of the translation products, [^{35}S] methionine was added to the translation reactions. Proteins translated *in vitro* were incubated with recombinant caspase-1, -4 or -5 for 2 hours at 37 °C. The resulting cleavage products were analyzed by SDS-PAGE and Western blotting followed by autoradiography. In this experiment IL-1β was used as a positive control as it is a known substrate of caspase-1. The results are shown in Figure 4.8. The upper blot shows full length Rab39a when incubated with different doses of

recombinant caspase-1, caspase-4 or caspase-5. There is no evidence of any processing as no other bands can be seen. The middle blot shows full length Rab39b when incubated with different doses of recombinant caspase-1, caspase-4 or caspase-5. Again, there is no evidence of any processing as no other bands can be seen. The lower blot shows pro-IL-1β at 32.5 kDa. When incubated with different doses of recombinant caspase-1 there is additional bands present at 16.5 kDa which represent processed IL-1β. There is no evidence of any processing of IL-1β when incubated with caspase-4 or caspase-5 as no other bands can be seen.

4.2.1.8 Rab4a, Rab14 and Rab25 are not substrates of caspase-1

A screen of Rab family members revealed that nine other Rab proteins have caspase-1 cleavage sites. These sites are predicted by sequence analysis and although a protein may have a site it does not imply that it is a substrate. Some of these Rab proteins, namely Rab4, Rab14 and Rab25, were tested to see if they were substrates of caspase-1.

The effect of caspase-1 on these Rab proteins were tested by incubating lysates from HEK293T cells transfected with plasmids containing HA-Rab25, Myc-Rab4, GFP-Rab14 (or with HA-Rab39a as a control) with recombinant caspase-1 at 30 °C for 90 minutes. The results are shown in Figure 4.9.

Figure 4.9 (A) shows full length MYC-Rab4a at 25 kDa as indicated (lanes 1 and 2). Cleavage by caspase-1 at the predicted D110 site would give a MYC-tagged fragment of 12.5 kDa. Incubation with recombinant caspase-1 (lane 2) does not result in any additional bands. HA-Rab39a was used as a positive control (lanes 3 and 4) and as

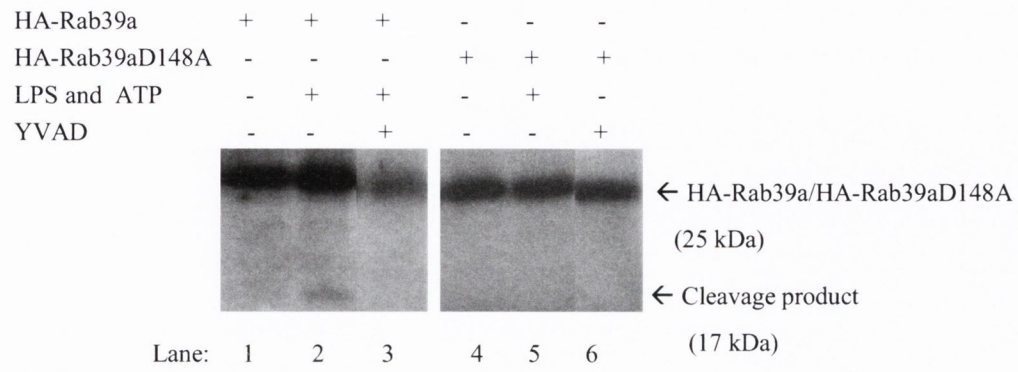


Figure 4.7 HA-Rab39a can be processed by LPS and ATP in RAW 264.7 cells. RAW 264.7 cells were set up at 2 x 10^6 cells per ml and transfected with HA-Rab39a or HA-Rab39aD148A using the Amaxa system. 24 hours later cells were treated with 100 ng/ml LPS for 3 hours, 100 μM YVAD for 1 hour and 5 mM ATP for 1 hour as indicated. Cells were lysed in 150 μl lysis buffer, 5X sample buffer was added and samples were separated on 12 % SDS-PAGE and analysed by Western blotting. Anti-HA antibody was used to detect products. This result represents two independent experiments

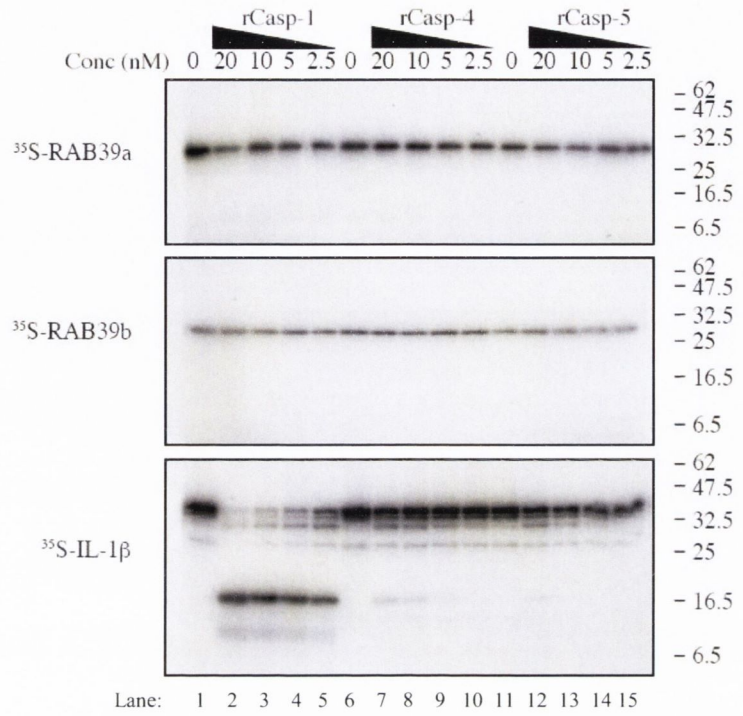


Figure 4.8 Rab39a is not processed by caspase-1 in an ITT assay. Rab39a, Rab39b and IL-1β were prepared by in vitro transcription and translation. For detection of the translation products, [^{35}S] methionine was added to the translation reactions. Proteins translated in vitro were incubated with recombinant caspase-1, -4 or -5 for 2 hours at 37 °C. The resulting cleavage products were analyzed by SDS-PAGE and Western blotting followed by autoradiography. Data shown is representative of two independent experiments. (**Alex Luthi, Dept. Genetics, TCD)**

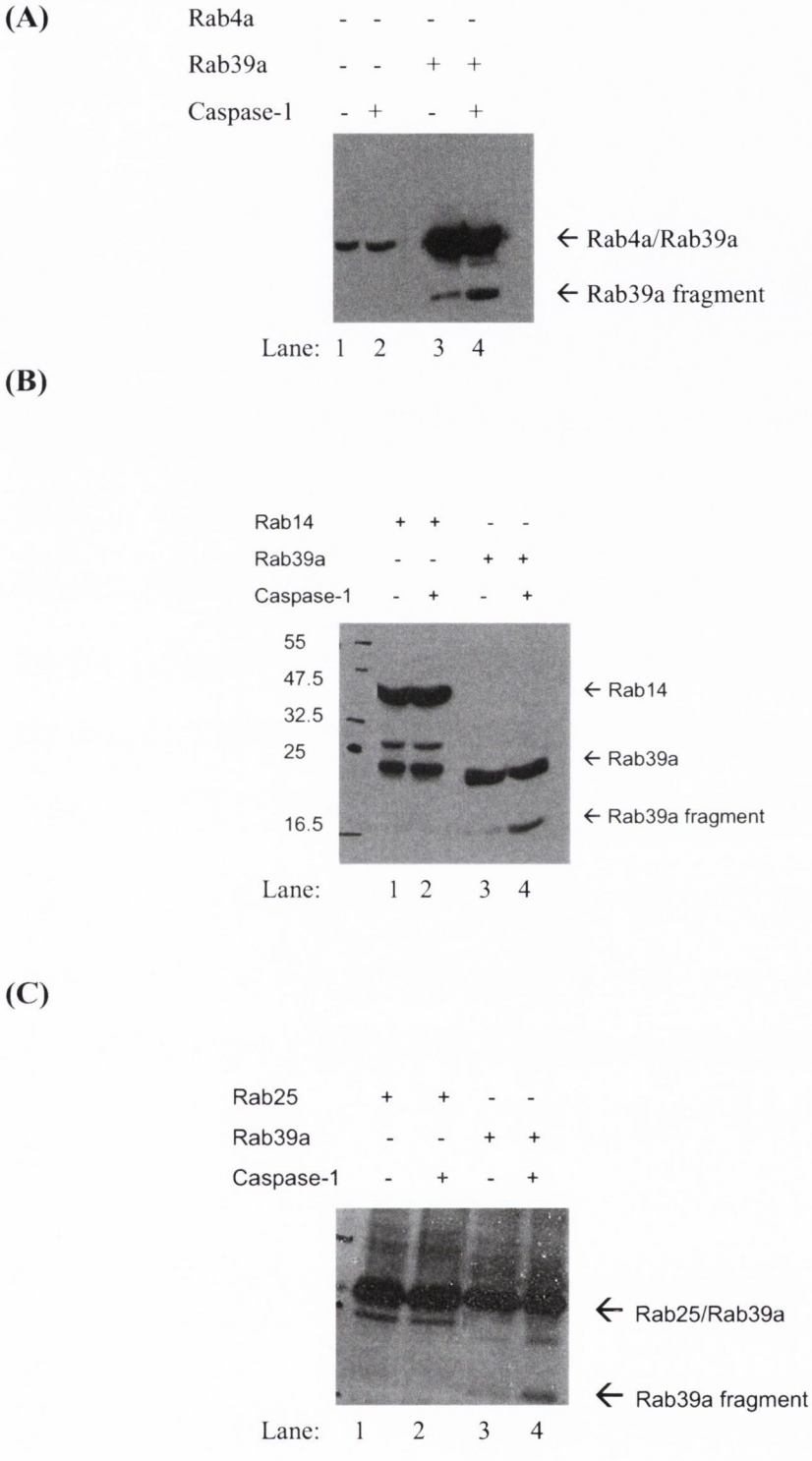


Figure 4.9 Rab4a, Rab14 and Rab25 cannot be processed by caspase-1 despite having caspase-1 cleavage sites. HEK293T cells were set up at 4 x 10^5 cells per ml in 10 cm dishes. The following day cells were transfected with 5 µg of a plasmid containing **(A)** Myc-Rab4a or HA-Rab39a **(B)** GFP-Rab14 or HA-Rab39a **(C)** HA-Rab25 or HA-Rab39a. 24 hours later cells were lysed in 300 µl of low astringency

lysis buffer. 10 µl of lysate and 10 µl of assay buffer was mixed and incubated with 2 µl of recombinant caspase-1 at 30 °C for 90 minutes. 5X sample buffer was added and samples were separated on 12 % SDS-PAGE gels and analysed by Western blotting. HA, Myc or GFP antibodies were used to detect products. Data shown is representative of two independent experiments.

expected, incubation with recombinant caspase-1 (lane 4) results in the processing of HA-Rab39a.

Figure 4.9 (B) shows full length GFP-Rab14 at 52 kDa as indicated (lanes 1 and 2). There are also non-specific bands at 30 kDa and 25 kDa. Cleavage by caspase-1 at the predicted D39 or D108 sites would give GFP-tagged fragments of 32.5 kDa or 40 kDa. Incubation with recombinant caspase-1 (lane 2) does not result in any additional bands. HA-Rab39a was used as a positive control (lanes 3 and 4) and again incubation with recombinant caspase-1 (lane 4) results in the processing of Rab39a.

Figure 4.9 (C) shows full length HA-Rab25 at 25 kDa (lanes 1 and 2). Cleavage by caspase-1 at the predicted D40 site would give a HA-tagged fragment of 19 kDa. Incubation with recombinant caspase-1 (lane 2) does not result in any additional bands. HA-Rab39a was used as a positive control (lanes 3 and 4) and again incubation with recombinant caspase-1 (lane 4) results in the processing of Rab39a.

4.2.2 Detection of endogenous Rab39a

4.2.2.1 Rab39a antibody design

In an attempt to examine endogenous Rab39a a peptide antibody was designed since no commercial antibody was available. Rab39a is 217 aa in length and a 12 aa peptide antibody sequence was chosen. The peptide sequence is - QGRFPGLRSPAC - which corresponds to amino acids 30 to 41 of Rab39a. This sequence was chosen because it is the only area of the Rab39a sequence which is significantly different from Rab39b. It also has positive antigenic index and hydrophilicity. However surface probability of the chosen peptide was lower than optimal but since this was the only area of Rab39a

significantly different from Rab39b it had to be chosen. The antibody was produced by Eurogentec. An alignment of Rab39a and Rab39b is shown in Figure 4.10 and the chosen peptide is indicated.

4.2.2.2 Analysis of Rab39a antibodies

The antibody was produced in a rabbit. Three boosts where given after the initial immunisation shot meaning that pre-immune sera and three test bleeds were provided. Experiments were carried out on each test bleed at a range of concentrations (1:500, 1:1000, 1:10000) to try to detect endogenous Rab39a. This was carried out in HEK293T cells and in THP1 cells. Unfortunately, no bands of the correct size were evident. Affinity purification of the final test bleed was carried out and this was again tested at a variety of concentrations. Again no bands of the correct size were seen. In an attempt to concentrate any Rab39a in the cell, an immunoprecipitation experiment was carried out. Firstly, Rab39a was immunoprecipitated with the antibody and Rab39a was blotted for. Secondly, as caspase-1 and Rab39a had been found in a complex, caspase-1 was immunoprecipitated and Rab39a was probed for. As Rab39a may be inducible, cells were treated with various stimuli in an attempt to upregulate Rab39a. None of these approaches resulted in bands of the correct size. When HA-Rab39a was overexpressed in HEK293T cells it could be detected by the Rab39a antibody. This result is shown in Figure 4.11.

At a later date a commercial antibody became available from Abnova. This was tested; however similarly to the designed antibody it was also unable to detect endogenous levels of Rab39a. Like the designed antibody it was able to detect over-expressed HA-Rab39a in HEK293T cell. This is shown in Figure 4.12.

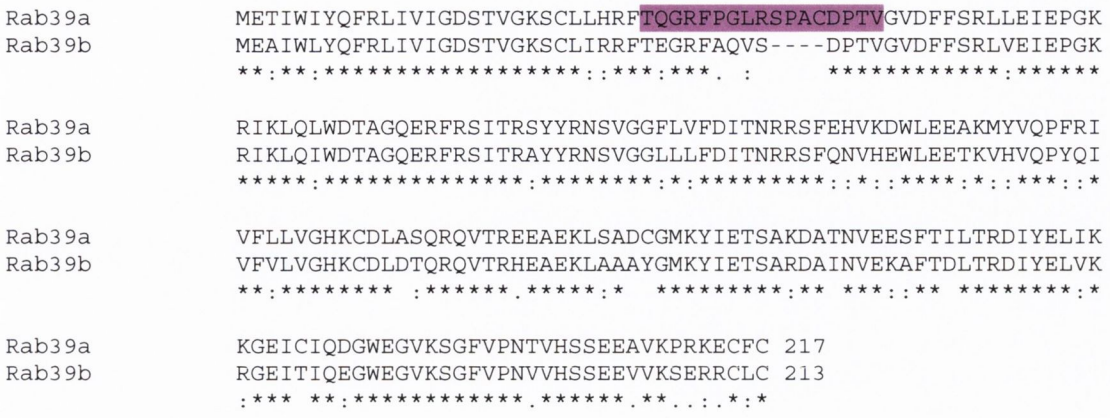


Figure 4.10 Rab39a peptide antibody. The amino acid sequences of hRab39a and hRab39b are aligned. The highlighted area displays a 12 amino acid region of Rab39a which displays the greatest dissimilarity to Rab39b. This sequence was used to design the peptide antibody.

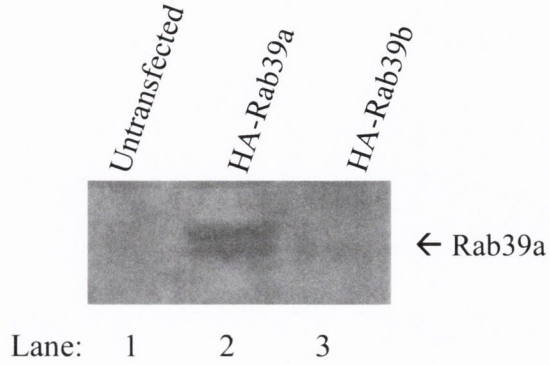


Figure 4.11 The custom made Rab39a antibody detects over-expressed Rab39a. HEK293T cells were set up at 2 x 10^5 cells per ml. 24 hours later cells were untransfected (lane 1), transfected with 5 µg of HA-Rab39a (lane 2) or transfected with 5 µg of HA-Rab39b (lane 3). After 24 hours, cells were lysed in 300 µl of low astringency lysis buffer, sample buffer was added and analysed by Western blotting. The custom made antibody from Eurogentech was used for immunoblotting. Data is representative of at least 3 independent experiments.

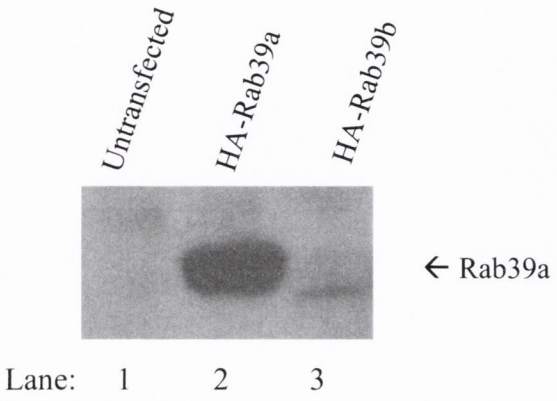


Figure 4.12 The commercially available Rab39a antibody detects over-expressed Rab39a. HEK293T cells were set up at 2 x 10^5 cells per ml. 24 hours later cells were untransfected (lane 1), transfected with 5 µg of HA-Rab39a (lane 2) or transfected with 5 µg of HA-Rab39b (lane 3). After 24 hours, cells were lysed in 300 µl of low astringency lysis buffer, sample buffer was added and analysed by Western blotting. The commercially available antibody from Abnova was used for immunoblotting. Data is representative of at least 3 independent experiments.

As it was not possible to detect Rab39a using either a custom made antibody or a commercial antibody, this meant that overexpression studies continued to be used.

4.2.3 Subcellular localisation of Rab39a

4.2.3.1 Subcellular localisation of GFP-Rab39a in HEK293T cells

The subcellular localisation of the Rab39a was next analysed. Initially this was done by transfecting HA-Rab39a into HEK293T cells, fixing the cells and staining them with the HA specific antibody (results not shown). However, when GFP-Rab39a became available this construct was used instead as this meant the cells did not need to be fixed and live-cell imaging could be performed instead. GFP-Rab39a was transfected into HEK293T cells and cells were analysed by live-cell imaging 24 hours later. Results are shown in Figure 4.13. It can be seen that GFP-Rab39a is diffusely localised in the cytosol of HEK293T cells.

It was next examined whether the GTPase activity of Rab39a effected its subcellular localisation. Site directed mutagenesis was carried out on GFP-Rab39a to create dominant negative (GFP-Rab39aS22N) and constitutively active (GFP-Rab39aQ72L) versions of GFP-Rab39a. As before, the S22N mutation (in the G1 motif) locks the protein in its GDP state (dominant negative) while the Q72L mutation (in switch 2) locks the protein in a GTP state (constitutively active). The subcellular localisation of the dominant negative version of Rab39a (GFP-Rab39aS22N) is shown in Figure 4.14. GFP-Rab39aS22N is also diffusely localised in the cytosol of HEK293T cells. The subcellular localisation of the constitutively active version of Rab39a (GFP-Rab39aQ72L) is shown in Figure 4.15. GFP-Rab39aQ72L is also diffusely localised in

the cytosol of HEK293T cells. Therefore, it appears that the GTPase activity of Rab39a does not effect its subcellular localisation.

It was next examined whether the caspase-1 cleavage site could affect Rab39a localisation. The subcellular localisation of GFP-Rab39aC149stop was next examined. This construct mimics the cleaved 17 kDa fragment of Rab39a. As shown in Figure 4.16 GFP-Rab39aD148Stop is diffusely localised in the cytosol.

Next, the subcellular localisation of a construct lacking the caspase-1 cleavage site was examined. Site directed mutagenesis was carried out on GFP-Rab39a to mutate the cleavage site, which is an aspartate residue at amino acid position 148, to an alanine creating GFP-Rab39aD148A. {GFP-Rab39aD148A was made with the technical assistance of Ashish Sarraju, Developmental Immunology Lab, Massachusetts General Hospital, USA}. The results of GFP-Rab39aD148A expression in HEK293T cells are shown in Figure 4.17. The localisation of GFP-Rab39aD148A is strikingly different from the other constructs. This construct lacks the D148 site and therefore cannot be cleaved by caspase-1, indicating that caspase-1 is important for the localisation of Rab39a. In this image it can be seen that GFP-Rab39aD148A is localised to specific circular structures which resemble endosomes.

In order to try and further define the localisation of Rab39a, it was attempted to see if Rab39a could co-localise with endosomal markers. Rab5 is a marker of early endosomes whilst Rab7 is a marker of late endosomes. HEK293T cells were transfected with GFP-Rab39a. 24 hours later cells were fixed and stained for endogenous Rab5 or

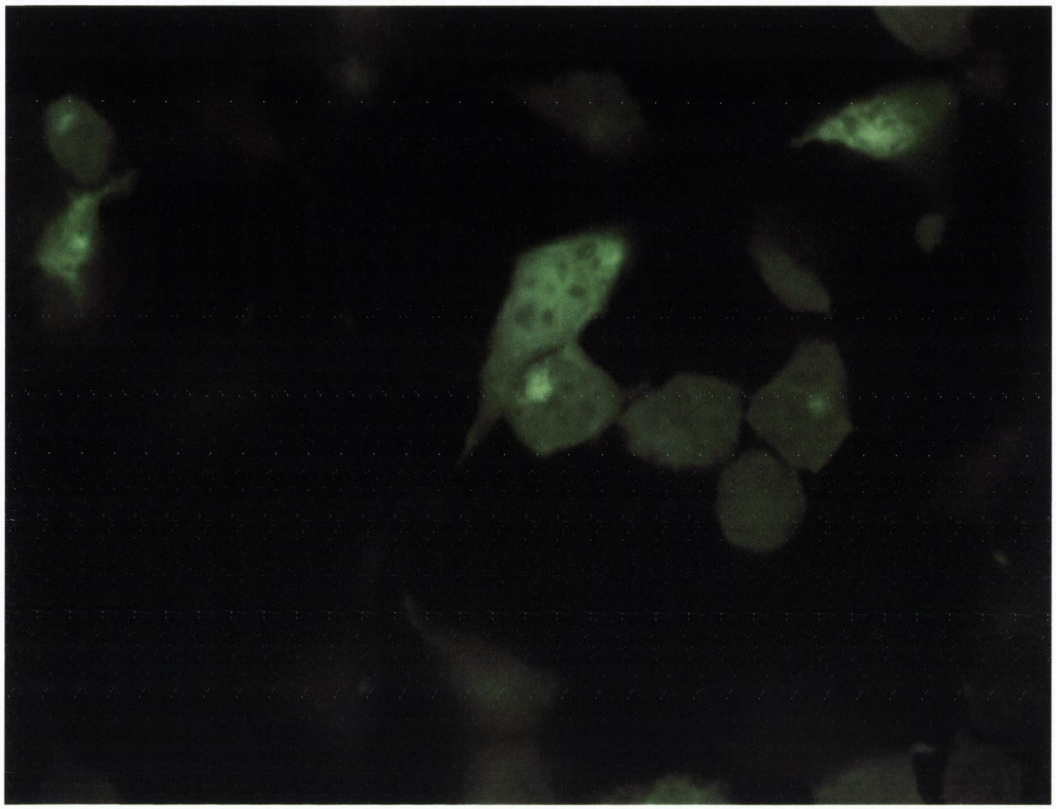


Figure 4.13 GFP-Rab39a is diffuse in the cytosol of HEK293T cells. HEK293T cells were set up at 1 x 10^5 cells per well in 8-well chamber slides. 24 hours later, cells were transfected with 0.1 μg GFP-Rab39a. After 24 hours, cells were viewed by live-cell imaging. Data shown is representative of two independent experiments.

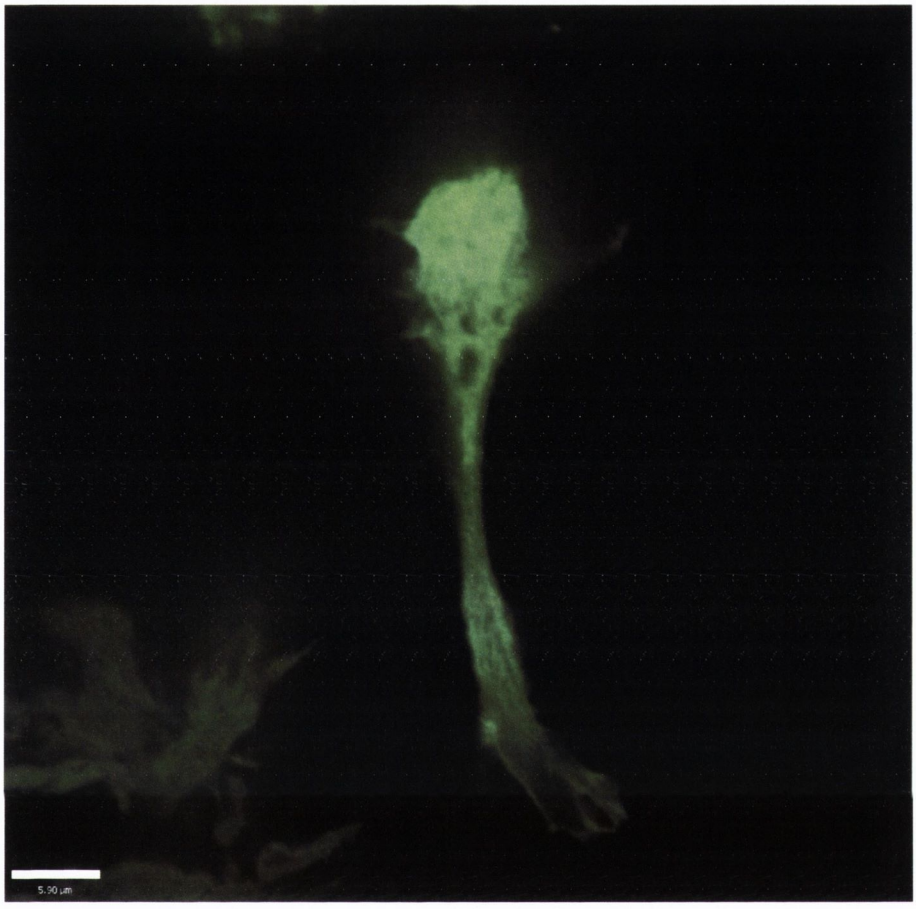


Figure 4.14 GFP-Rab39aS22N is diffuse in the cytosol of HEK293T cells. HEK293T cells were set up at 1 x 10^5 cells per well in 8-well chamber slides. 24 hours later, cells were transfected with 0.1 µg GFP-Rab39aS22N. After 24 hours, cells were viewed by live-cell imaging. Data shown is representative of two independent experiments.

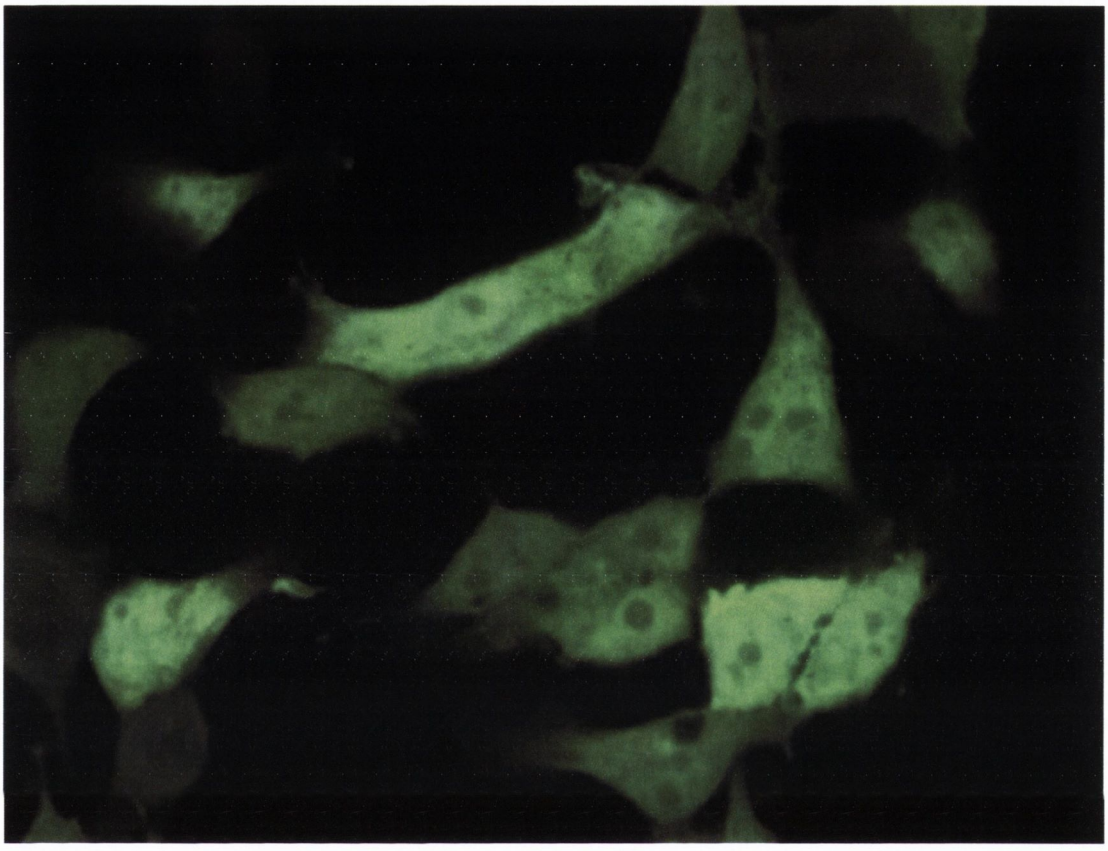


Figure 4.15 GFP-Rab39aQ72L is diffuse in the cytosol of HEK293T cells. HEK293T cells were set up at 1 x 10^5 cells per well in 8-well chamber slides. 24 hours later, cells were transfected with 0.1 μg GFP-Rab39aQ72L. After 24 hours, cells were viewed by live-cell imaging. Data shown is representative of two independent experiments.

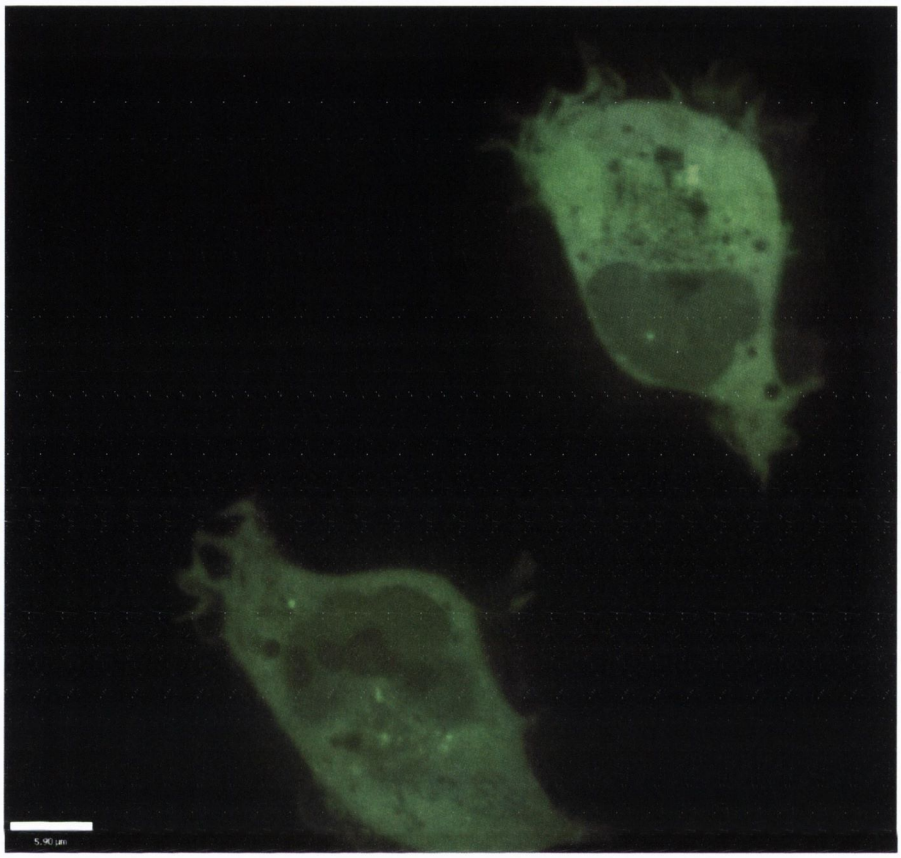


Figure 4.16 GFP-Rab39aC149Stop is diffuse in the cytosol of HEK293T cells. HEK293T cells were set up at 1 x 10^5 cells per well in 8-well chamber slides. 24 hours later, cells were transfected with 0.1 μg GFP-Rab39aC149Stop. After 24 hours, cells were viewed by live-cell imaging.

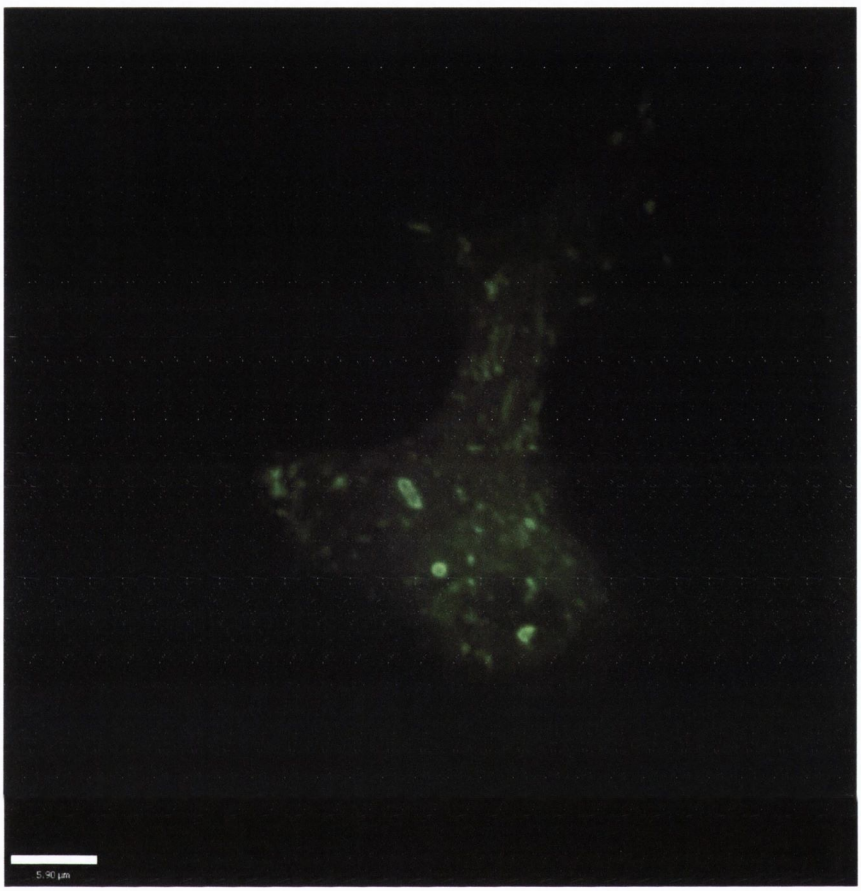


Figure 4.17 GFP-Rab39aD148A is localised to vesicles in the cytosol of HEK293T cells. HEK293T cells were set up at 1 x 10^5 cells per well in 8-well chamber slides. 24 hours later, cells were transfected with 0.1 μg GFP-Rab39aD148A. After 24 hours, cells were viewed by live-cell imaging.

Rab7 using antibodies. However, the Rab5 and Rab7 antibodies showed non-specific staining (results not shown) so could not be further used.

4.2.3.2 GFP-Rab39a localises to endosomes in RAW 264.7 cells

It was also decided to examine the subcellular localisation of GFP-Rab39a in RAW 264.7 cells. Cells were transfected by electroporation using the Amaxa system and analysed by live-cell imaging 24 hours later. In Figure 4.18, it can be seen that GFP-Rab39a displays a much more defined expression pattern in the RAW 264.7 cells than in the HEK293T cells. GFP-Rab39a appears to be in many endosomal-like vesicles.

It was next examined whether adding latex beads or *S. aureus* to cells could affect the localisation of Rab39a. When beads or *S. aureus* was added to the cells, Rab39a was present on an increased number of endosomes. (Rab39a was also seen on phagosomes and this topic will be dealt with in the following section).

Live-cell images of the cells over time were taken and these can be seen in the attached DVD. Movie 4.1 shows Rab39a trafficking around the cell in exosome-like structures within larger structures that resemble multi-vesicular bodies (MVBs). *S. aureus* induces caspase-1 activation and active caspase was stained using FLICA. Movie 4.2 shows GFP-Rab39a and active caspase (red) co-localising (yellow) in small vesicles and trafficking throughout the cell. It appears that Rab39a and caspase are being secreted from the cell together. This topic of Rab39a and caspase-1 and their role in secretion will be re-addressed later in this chapter.

4.2.4 Rab39a is involved in phagocytosis

4.2.4.1 Rab39a is found on phagosomes

It has recently been shown that caspase-1 is involved in phagocytosis (Amer *et al.*, 2006, Lynda Stuart, personal communication). Several Rab proteins have been implicated in the phagosomal pathway such as Rab4 and Rab14. Therefore it was decided to investigate if Rab39a could potentially play a role in phagocytosis. This work was carried out in the Developmental Immunology Lab at Massachusetts General Hospital under the supervision of Dr. Lynda Stuart and Dr. Anna Sokolovska. RAW 264.7 cells were used since they are professional phagocytes. GFP-Rab39a was transfected by electroporation using the Amaxa system and latex beads were added to induce phagocytosis. GFP-Rab39a was clearly seen on phagosomes around the beads (Figure 4.19). As an alternative to using latex beads to induce phagocytosis, *S. aureus* was added to cells and again GFP-Rab39a could clearly be seen on phagosomes (Figure 4.20).

4.2.4.2 Rab39a localises with active caspases on phagosomes

It has recently been shown that active caspase-1 can localise to phagosomes (Lynda Stuart, personal communication). It was therefore investigated whether Rab39a co-localised with active caspases during phagocytosis. RAW 264.7 cells were transfected with GFP-Rab39a and after 24 hours cells were infected with *S. aureus*. Figure 4.21 shows Rab39a in green localising around phagosomes, caspase activity was shown by FLICA staining and can be seen in red. Co-localisation between GFP-Rab39a and active caspases is shown in yellow. The nucleus of the cell was stained with Hoechst and is shown in blue.

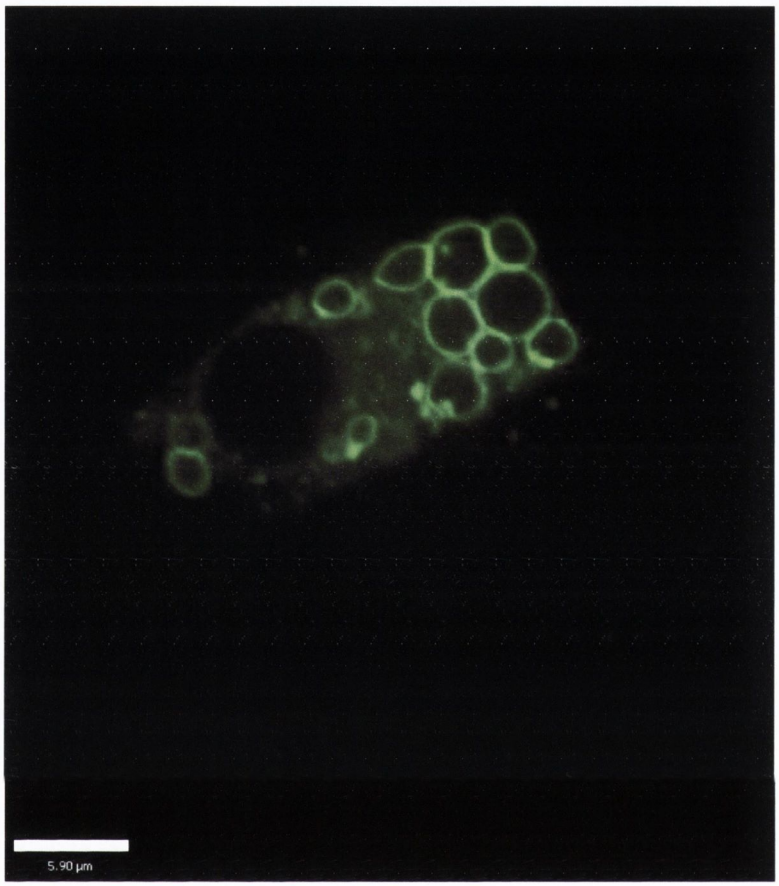


Figure 4.18 Rab39a localises to vesicles in cytosol of Raw 264.7 cells. Raw 264.7 cells were set up at 1 x 10^5 cells per well in 8-well chamber slides and transfected with 0.2 µg GFP-Rab39a using the Amaxa electroporation system. After 24 hours, cells were viewed by live-cell imaging. Data shown is representative of two independent experiments.

Movies are attached on the accompanying DVD

Movie 4.1 Live cell imaging of GFP-Rab39a in RAW 264.7 cells. Raw 264.7 cells were set up at 2 x 10^6 and transfected with GFP-Rab39a. 24 hours later latex beads were added and cells were observed by live cell imaging.

Movie 4.2 Live cell imaging of GFP-Rab39a and active caspases in RAW 264.7 cells. Raw 264.7 cells were set up at 2 x 10^6 and transfected with GFP-Rab39a. 24 hours later *S. aureus* was added. Active caspases were stained using FLICA reagent (red) and cells were observed by live cell imaging. Co-localisation between GFP-Rab39a and active caspases is shown in red.

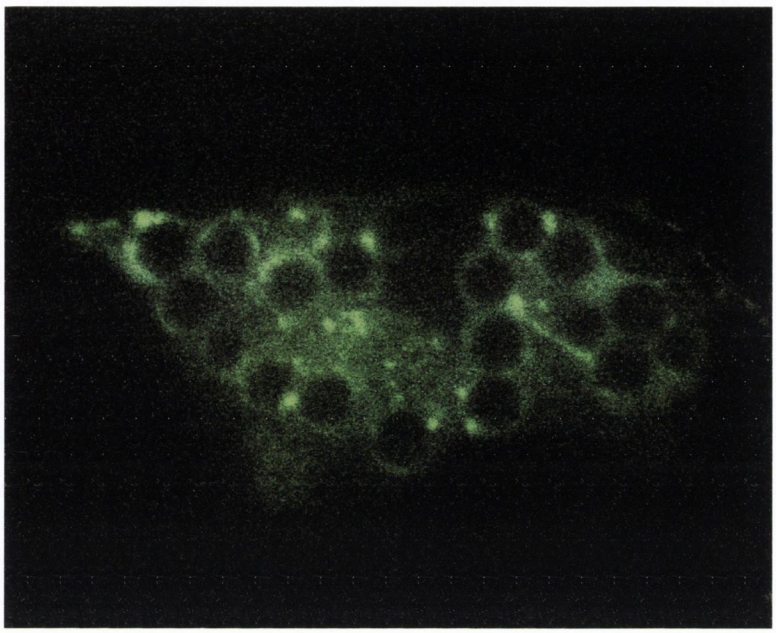


Figure 4.19 Rab39a localises to phagosomes of Raw 264.7 cells induced by latex beads. Raw 264.7 cells were set up at 1 x 10^5 cells per well in 8-well chamber slides and transfected with 0.2 μg GFP-Rab39a using the Amaxa electroporation system. After 24 hours latex beads were added to cells and allowed to phagocytose for 30 minutes before being viewed by live cell imaging. Data shown is representative of two independent experiments.

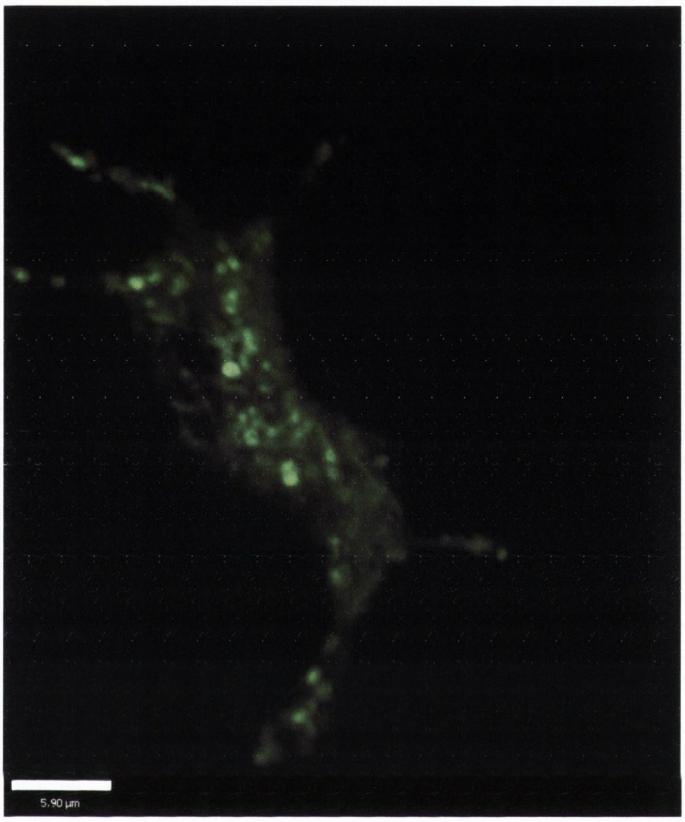


Figure 4.20 Rab39a localises to phagosomes of Raw 264.7 cells induced by *S. aureus*. Raw 264.7 cells were set up at 1 x 10^5 cells per well in 8-well chamber slides and transfected with 0.2 µg GFP-Rab39a using the Amaxa electroporation system. After 24 hours *S. aureus* was added to cells (at a MOI of 10) and allowed to phagocytose for 30 minutes before being viewed by live cell imaging. Data shown is representative of two independent experiments.

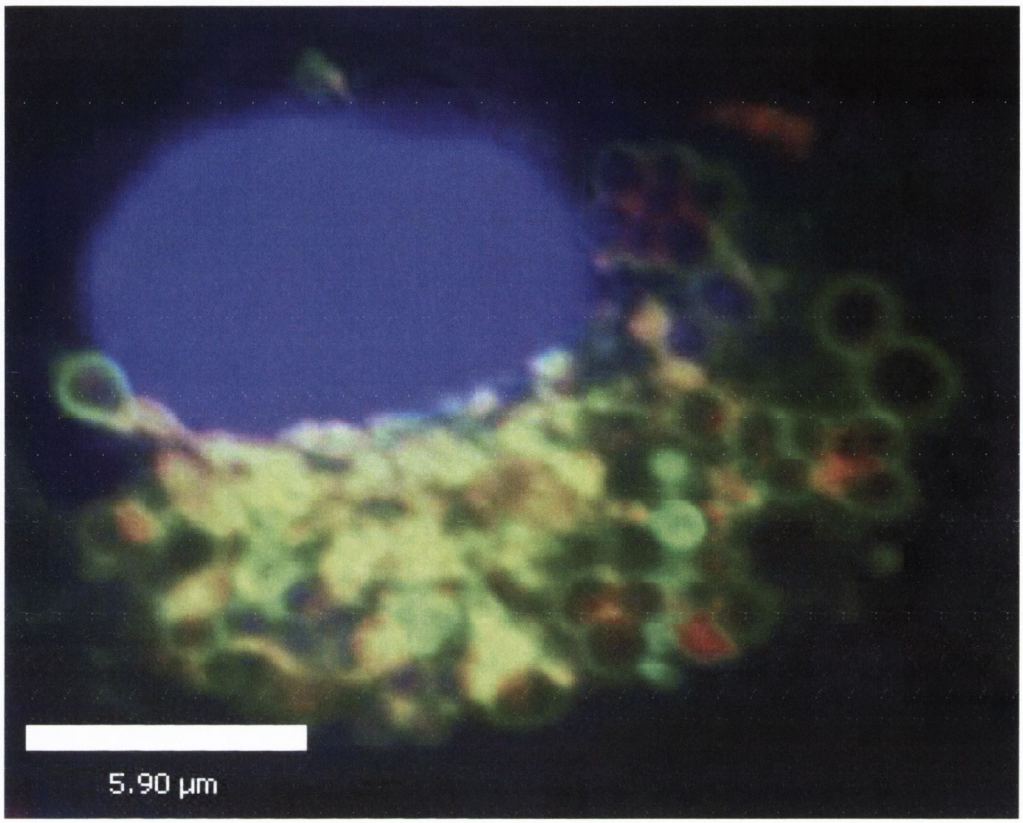


Figure 4.21 Rab39a co-localises with caspases on phagosomes in Raw 264.7 cells. Raw 264.7 cells were set up at 1 x 10^5 cells per well in 8-well chamber slides and transfected with 0.2 µg GFP-Rab39a using the Amaxa electroporation system. After 24 hours *S. aureus* was added to cells (at a MOI of 10) and allowed to phagocytose for 30 minutes. Active caspases were stained using FLICA SR-VASD-FMK reagent (red). Cells were viewed by live cell imaging. Data shown is representative of two independent experiments.

4.2.4.3 Rab39a is involved in bacterial uptake

To determine if Rab39a has a role in bacterial uptake, HEK293T cells were transfected with GFP-Rab39a, GFP-Rab39aS22N or GFP-Rab39aQ72L. Cells were infected with fluorescently labelled *S. aureus* and bacterial uptake was measured by FACs. Results were normalised to account for differences in expression levels of the plasmids. As can be seen in Figure 4.22, uptake of *S. aureus* was increased in those cells that had been transfected with the dominant negative version of Rab39a (GFP-Rab39aS22N). This indicates that Rab39a may play a role in bacterial uptake.

4.2.4.4 Rab39a is not essential for phagosomal acidification

It has recently emerged that caspase-1 is necessary for phagosomal acidification (Lynda Stuart, personal communication). It was briefly attempted to replicate these results. Peritoneal macrophages were pre-treated with the pan-caspase inhibitor zVAD, the v-ATPase inhibitor Bafilomycin or DMSO as a control. To induce phagocytosis, *S. aureus* were added to the cells for 90 minutes. The *S. aureus* was fluorescently labelled so that it could be detected by FACs. FACs analysis was carried out and phagocytosis of *S. aureus* was measured and plotted against a standard curve of pH values. The results are shown in Figure 4.23. Results showed that phagosomal acidification occurred as normal in the DMSO treated samples (1st set of bars), zVAD somewhat inhibited phagosomal acidification (2nd set of bars), and Bafilomycin completely prevented phagosomal acidification as expected (3rd set of bars).

To investigate if Rab39a could be involved in phagosomal acidification, RAW 264.7 cells were transfected with a GFP control plasmid, GFP-Rab39a, GFP-Rab39aQ72L or GFP-Rab39aS22N. After 24 hours cells were infected with *S. aureus* which was

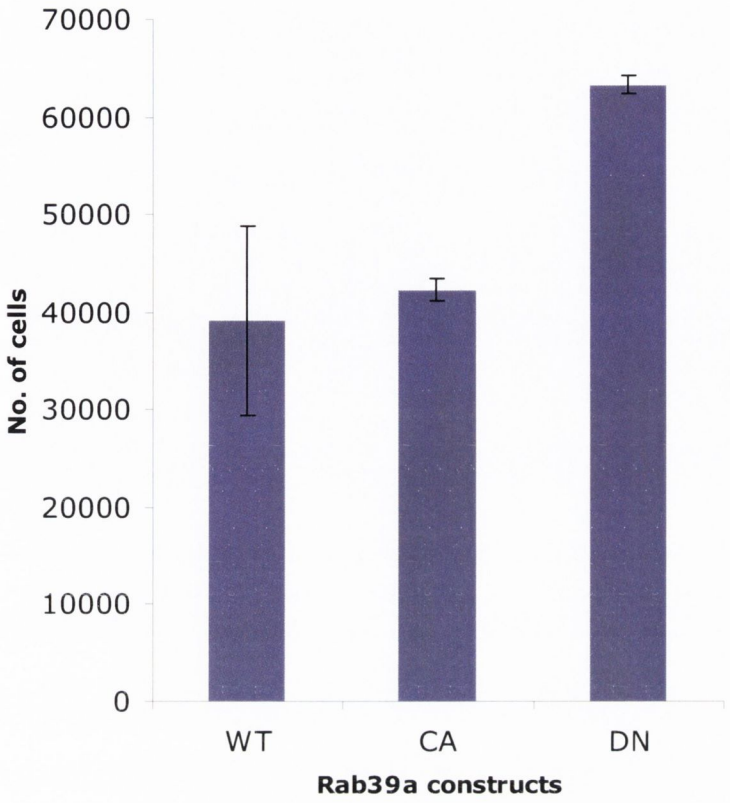
labelled with pH-Rodo Dye. The pH-Rodo Dye is not fluorescent at neutral pH and fluoresces in acidic environments i.e. during phagosomal acidification. Fluorescence of the dye was measured by FACs. Data was normalised to account for any differences in expression levels of the plasmids. Figure 4.24 shows that there was no difference in fluorescence between the various different constructs indicating that Rab39a was not involved in phagosomal acidification.

4.2.5 Rab39a is induced by pro-inflammatory stimuli

It was next examined whether Rab39a, like pro-IL-1β was inducible by pro-inflammatory stimuli. Analysis of the Rab39a promoter region in the previous chapter showed that it contained many putative transcription factor binding sites including NF-κB sites, p53 sites and SP1 sites. Other bioinformatic results also suggested that Rab39a could be induced by LPS. In order to investigate this further the expression patterns of Rab39a mRNA were analysed by quantitative Real Time PCR in THP1 cells and it was tested whether expression was altered by treatment with pro-inflammatory stimuli.

4.2.5.1 Optimisation of Rab39 primers for Real-Time PCR

The Primer3 design program (http://frodo.wi.mit.edu/primer3/) was used to design primers for the mRNA sequence of Rab39a and Rab39b. To ensure that the primers spanned over exons, the Blat database was used (http://genome.brc.cw.edu/cgi-bin/hgBlat). The designed primers were diluted to various concentrations (1 μM, 3 μM and 6 μM) and dissociation curves were analysed to ensure that only one product was being detected and that primer dimers were kept to a minimum. A concentration of



4.22 Expression of a dominant negative version of GFP-Rab39a results in increased bacterial uptake. HEK293T cells were set up in 12 well plates at 2 x 10^5 cells per ml. 24 hours later cells were transfected with 0.2 µg GFP-Rab39a, GFP-Rab39aQ72L or GFP-Rab39aS22N. After 48 hours the media was removed and fresh media containing 1 % FCS and 1 % PS was added to facilitate phagocytosis. Cells were placed on ice for 15 minutes. Alexa-Fluor 647-labelled *S. aureus* was added at a MOI of 50 and cells were spun at 1000 rpm for 5 minutes. Cells were placed on ice for a further 30 minutes to ensure phagocytosis was synchronised and then placed at 37 ˚C or left on ice as a control. After 1 hour, the media was removed and cells were washed 3 times in ice-cold PBS-EDTA. Cells were resuspended in 500 µl PBS and analysed by FACS for GFP expression and Alexa Fluor-labelled *S. aureus*.

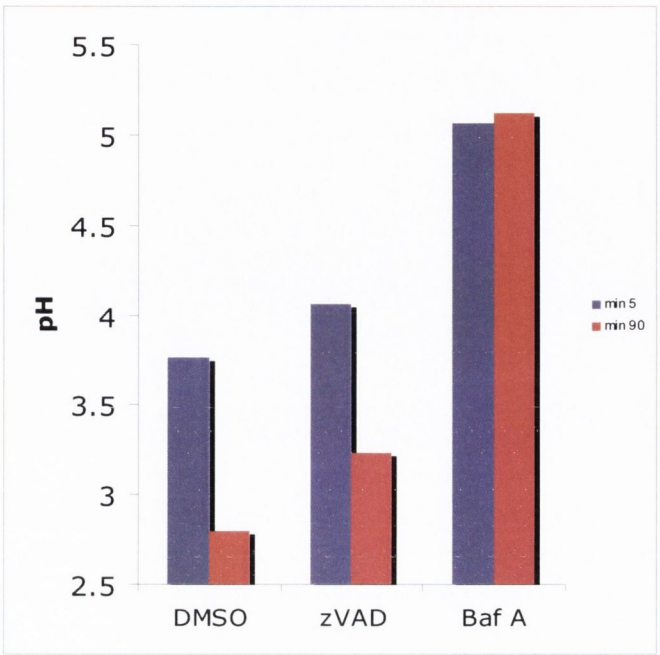


Figure 4.23 Caspases are required for phagosomal acidification. Peritoneal macrophages were set up at 2 x 10^5 per ml in 12 well plates. Cells were pre-treated with 100 µM zVAD or 100 µM Bafilomycin A (or DMSO as a control) for 1 hour. Cells were placed on ice for 30 minutes and then *S. aureus* doubly labelled with FITC and Alexa-Flour 647 was added to the cells at a MOI of 2. Cells were kept on ice for a further 30 minutes and then placed at 37 °C for 90 minutes or 5 minutes. The media was then removed and cells were washed 3 times in ice-cold PBS-EDTA. Cells were resuspended in 500 µl PBS and analysed by FACS. Results are from one experiment.

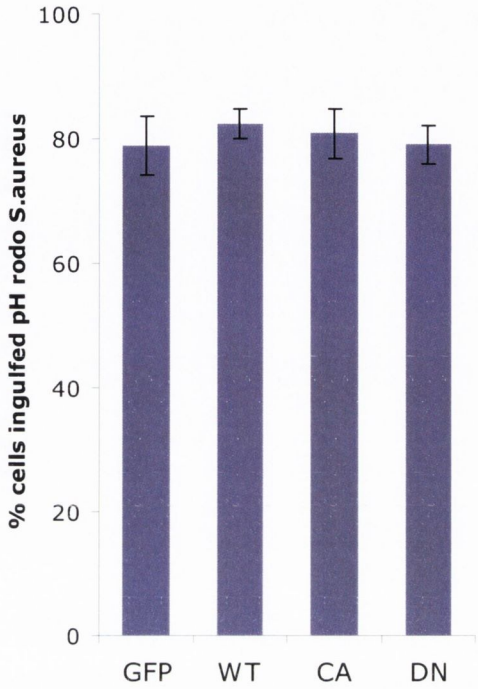


Figure 4.24 Rab39a is not required for phagosomal acidification. Raw 264.7 cells were set up at 1 x 10^6 cells per 500 µl in 12 well plates and transfected using the Amaxa system with 0.2 µg GFP-control plasmid, GFP-Rab39a, GFP-Rab39aQ72L (CA) or GFPRab39aS22N (DN). Cells were placed on ice for 30 minutes and then infected with *S. aureus* labelled with pH Rodo Dye at a MOI of 2. Cells were kept on ice for a further 30 minutes and then placed at 37 ˚C for 1 hour or kept on ice as a control. The media was then removed and cells were washed 3 times in ice-cold PBS-EDTA. Cells were resuspended in 500 µl PBS and analysed by FACS. Results were normalised for equal GFP-expression and percentage of cells containing pH Rodo *S. aureus* was calculated.

3 μM was found to be the most specific for both Rab39a and Rab39b primers and was used for all future experiments.

4.2.5.2 Rab39a is inducible by LPS, Malp2 and Pam_3Cys

THP1 cells were treated over a 24 hour time course with 100 ng/ml LPS, 5 nM Malp2 or 1 μg/ml Pam_3Cys. RNA was extracted and converted to cDNA. Real-Time PCR was carried out on the cDNA using the optimised primers specific for Rab39a or Rab39b. GAPDH was used as a control. Results are shown in Figure 4.25. Expression is normalized to that of GAPDH and is presented relative to that of untreated controls. Figure (A) shows that in response to LPS, Rab39a mRNA increases over time and is highest at 21 hours. Rab39b mRNA increases slightly at 6 hours. Figure (B) shows that in response to MALP2, mRNA levels of Rab39a increase steadily and are highest at 21 hours. mRNA levels of Rab39b increase very slightly and then level off again. Figure (C) shows that in response to Pam_3Cys, mRNA levels of Rab39a increase dramatically and are highest at 21 hours. mRNA levels of Rab39b are increased slightly at 6 and 21 hours.

The results shown are a representative of 3 separate experiments. Whilst the levels of fold changes were different between different experiments the overall trend was the same. In all cases mRNA levels of Rab39a significantly increased in response to LPS, MALP2 and Pam_3Cys treatment whereas mRNA levels of Rab39b were not as significantly altered.

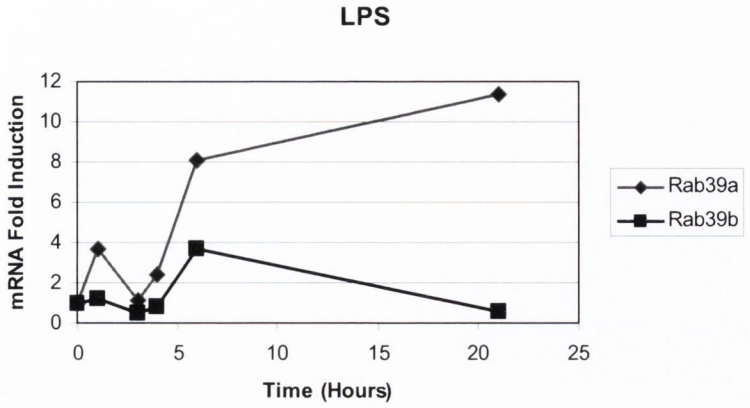
4.2.6 Knockdown of Rab39a affects IL-1β secretion

It was hypothesized that Rab39a may play a role in the secretion of IL-1β as many Rab protein family members are involved in trafficking and secretion of proteins. To determine if Rab39a was necessary for IL-1β secretion, siRNA nucleotides targeting Rab39a were transfected into THP1 cells and secreted IL-1β was measured by ELISA.

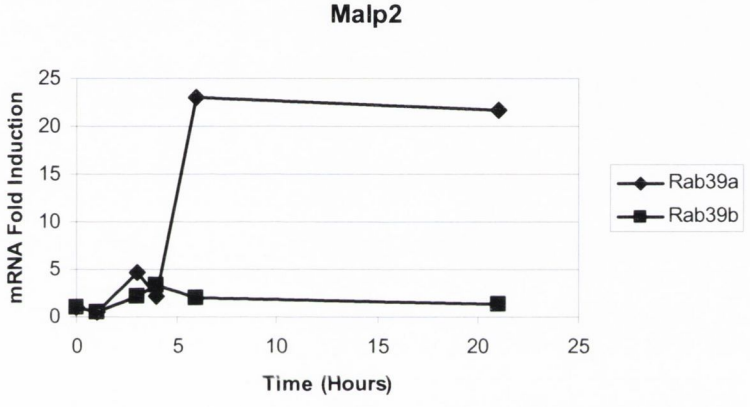
4.2.6.1 siRNA specifically knocks down mRNA and protein expression of Rab39a

Initially, a range of pre-designed siRNA oligos were obtained from Ambion and Qiagen and were tested to optimise the knockdown of Rab39a in THP1 cells. siRNA oligos were transfected into THP1 cells using the Amaxa system. 48 hours later, the cells were centrifuged to obtain a cell pellet and RNA was extracted. Reverse transcription was carried out to create cDNA. Primers specific to Rab39a were designed and endpoint PCR was carried out to determine which of the oligos resulted in the greatest knockdown of Rab39a. Non-targeting siRNA was used as a negative control to ensure that the knockdown is specific. Oligo #2 {GGAGCGGUUCAGAUCAAUAtt} from Ambion had the greatest knockdown efficiency and was used for all future experiments. GAPDH was used as a control. This is shown in Figure 4.26 (A). In the upper blot, either control siRNA or Rab39a siRNA is used and knockdown is detected by PCR using primers specific for Rab39a. It can be seen that Rab39a is specifically knocked down (lane 2), and no decrease in Rab39a expression is seen with the control siRNA (lane 1). The lower blot shows GAPDH expression, confirming that each sample contained a similar amount of DNA

(A)



(B)



(C)

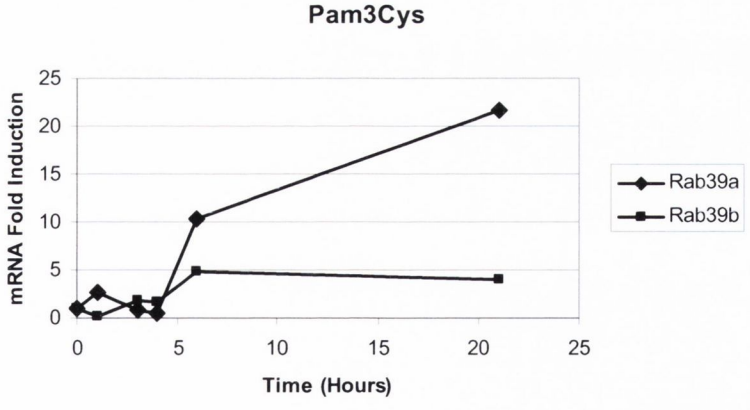


Figure 4.25 Rab39a is induced by LPS, Malp2 and Pam_3Cys. THP1 cells were set up at 1 x 10^6 in 6-well plates. 24 hours later, cells were treated with either **(A)** 100 ng/ml uLPs **(B)** 5 nM Malp2 **(C)** 1 μg/ml Pam_3Cys for the indicated times. RNA was extracted using RNeasy Mini Kit and normalised using nuclease free H_2O. Reverse

transcription was carried out and was followed by Real Time PCR with primers specific to Rab39a or Rab39b and GAPDH as a control. Expression of Rab39a mRNA or Rab39b mRNA was normalized to that of GAPDH mRNA. Data was calculated as fold change and is presented relative to that of untreated controls. Results are a representative of 3 different experiments.

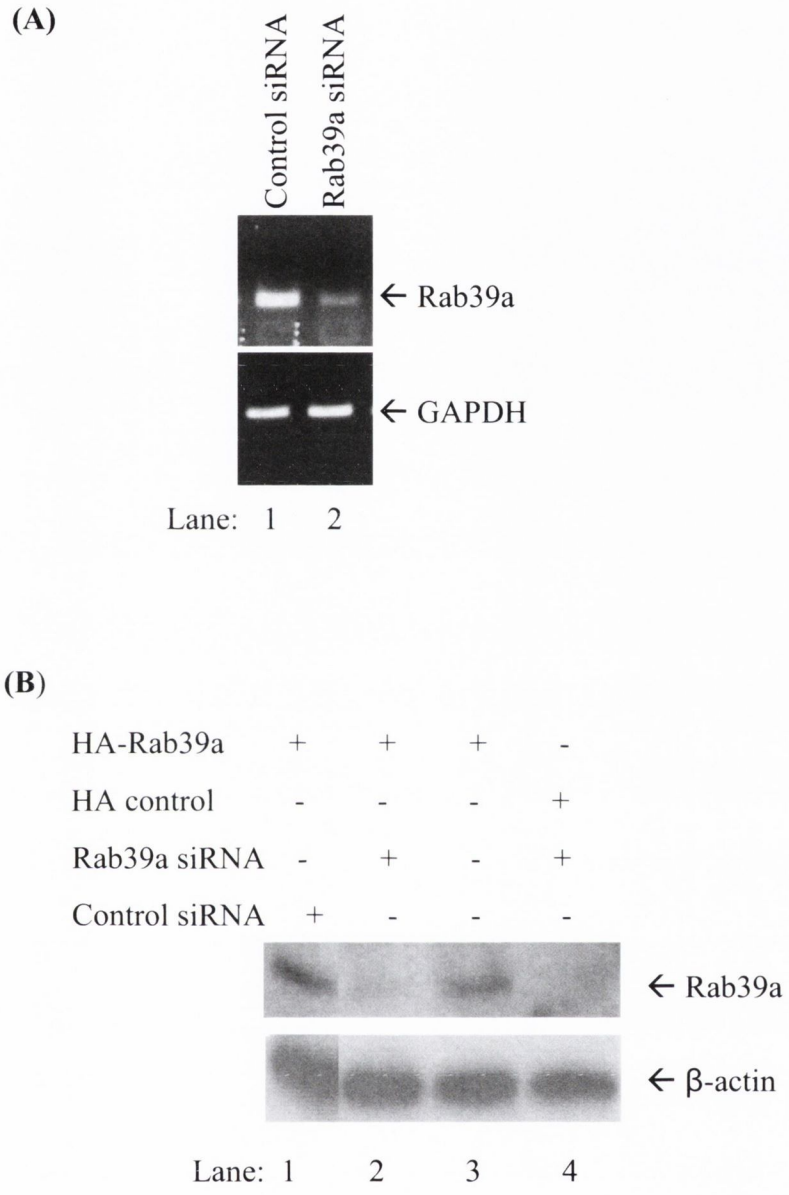


Figure 4.26 siRNA targeted to Rab39a knocks down Rab39a DNA and protein levels. (A) THP1s were transfected with siRNA by electroporation with the Amaxa system. 1 x 10^6 cells per ml were used for each transfection and were combined with 100 µl of nucleofector solution V. 1.5 µg of either control siRNA or Rab39a siRNA was added to the cells, the solution was transferred to an Amaxa cuvette and electroporated using Amaxa Program V001. Cells were incubated at 37 ˚C for 48 hours. Cells from each sample were centrifuged to obtain a pellet and RNA was extracted using an RNeasy Mini Kit. Reverse transcription was carried out followed

by PCR using primers specific for Rab39a and GAPDH. **(B)** THP1 cells were set up at 1 x 10^6 per ml and transfected with 1 μg of HA-Rab39a or HA control plasmid using the Amaxa system. After 24 hours, cells were transfected with 1.5 μg of either control siRNA or Rab39a siRNA and incubated for a further 48 hours. Cells were centrifuged and lysed in 50 μl low astringency lysis buffer. Sample buffer was added and samples were analysed by Western blotting. Samples were immunoblotted with HA antibody and β-actin antibody. Results are representative of three independent experiments.

Subsequently, it was necessary to show that Rab39a could be knocked down at the protein level. However as discussed earlier, no antibody was available to detect Rab39a. Therefore, in order to show that the protein was being knocked down, HA-Rab39a (lanes 1-3) or HA-control (lane 4) was transfected into THP1 cells and after 24 hours cells were transfected with control siRNA (lane 1), Rab39a siRNA (lane 2) or no siRNA (lanes 3 and 4). After a further 48 hours, cells were lysed and Rab39a expression was determined by Western blotting for HA. The siRNA successfully knocked down protein expression levels of Rab39a as shown in Figure 4.26 (B). In lane 2, it can be seen that the siRNA reduces the level of Rab39a, whilst there is no reduction in Rab39a when control siRNA is added (lane 1).

4.2.6.2 siRNA of Rab39a results in diminished levels of IL-1β secretion

To determine if Rab39a was affecting IL-1β secretion, siRNA to Rab39a (or control siRNA) was transfected into THP1 cells for 48 hours. Cells were treated overnight with 100 ng/ml LPS. Supernatants were removed and IL-1β and TNF-α secretion was measured by ELISA. LPS stimulation results in IL-1β secretion, however compared to the control siRNA, knock-down of Rab39a resulted in less IL-1β being secreted as shown in Figure 4.27 (A). Levels of TNF-α, which is externalised by the classical secretory pathway, were also measured. TNF-α levels remained constant despite Rab39a knock-down indicating that it is specific for IL-1β secretion as shown in Figure 4.27 (B).

This experiment was repeated in human peripheral blood mononuclear cells (PBMC). Knock-down of Rab39a by siRNA in PBMCs again resulted in a dramatic decrease in IL-1β secretion (Figure 4.28 (A)) but not TNF-α (Figure 4.28 (B)).

4.2.6.3 siRNA of Rab39a does not effect mRNA levels of IL-1β

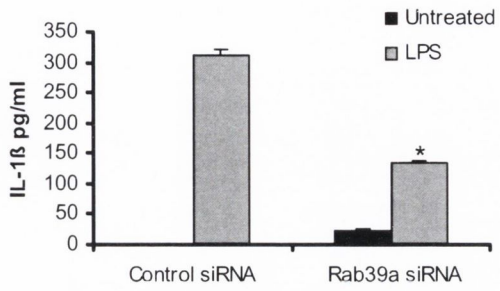
To examine if Rab39a was affecting mRNA levels of IL-1β, primers specific for IL-1β mRNA were designed as described previously (4.2.5.1.). Optimisation of the primers was carried out as before to ensure that the primers were only detecting one product and that no primer dimers were forming.

To determine if Rab39a was affecting levels of IL-1β mRNA, siRNA to Rab39a (or control siRNA) was transfected into THP1 cells for 48 hours. Cells were treated overnight with 100 ng/ml LPS. RNA was extracted from the cells, converted to cDNA by reverse transcription and analysed by Real-Time PCR with specific primers to IL-1β to determine mRNA levels. GAPDH was used as a control. The results are shown in Figure 4.29. Expression is normalized to that of GAPDH and is presented as fold change relative to that of untreated controls. mRNA levels of IL-1β, induced by LPS, remained constant even when Rab39a was knocked down. This indicates that the decrease in IL-1β might be due to a decrease in secretion and not in induction of the mature form of IL-1β.

4.2.7 Over-expression of Rab39a results in increased levels of IL-1β secretion

As it was now apparent that knockdown of Rab39a resulted in diminished levels of IL-1β secretion, it was next examined whether over-expression of Rab39a could affect IL-1β secretion. To test this, HA-Rab39a or HA-Rab39aD148A was over-expressed in THP1 cells. 24 hours later, cells were treated with 100 ng/ml LPS overnight and IL-1β in the supernatant was measured by ELISA. Figure 4.30 shows that over-expression of Rab39a results in increased levels of IL-1β secretion. Interestingly, when HA-Rab39aD148 (which lacks the caspase-1 cleavage site) was over-expressed this strongly

(A)



(B)

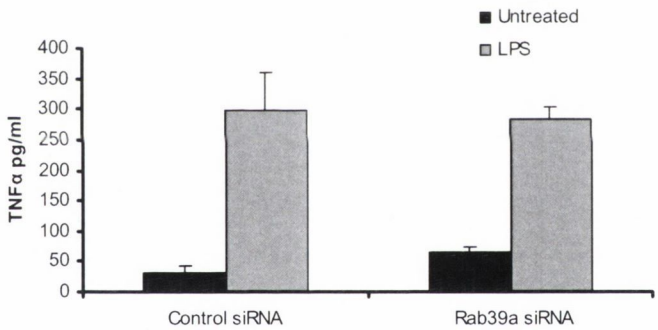
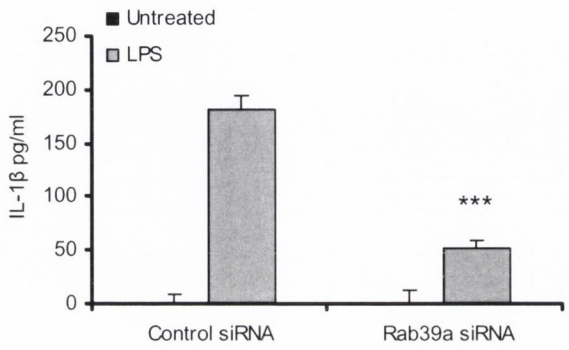


Figure 4.27 siRNA of Rab39a results in diminished levels of IL-1β secretion in THP1s. THP1s were transfected with siRNA by electroporation with the Amaxa system. 1 x 10^6 cells per ml were used for each transfection and were combined with 100 µl of nucleofector solution V. 1.5 µg of either control siRNA or Rab39a siRNA was added to the cells, the solution was transferred to an Amaxa cuvette and electroporated using Amaxa Program V001. Cells were incubated at 37 °C for 48 hours. Cells were stimulated with 100 ng/ml LPS overnight before harvesting. Supernatants were removed and **(A)** IL-1β and **(B)** TNF-α levels were measured by ELISA. Results are presented as pg/ml of cytokine and data is representative of at least 3 independent experiments. Results are expressed as mean +/- SD, * $p < 0.05$.

(A)



(B)

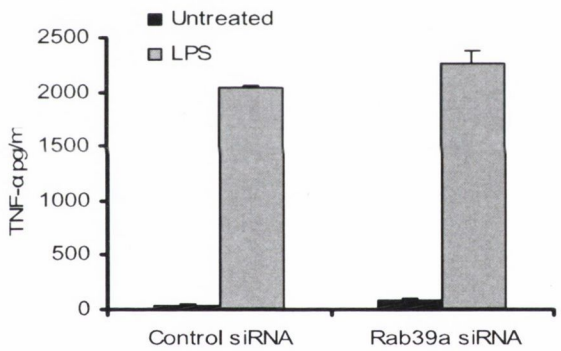


Figure 4.28 siRNA of Rab39a in PBMCs results in diminished levels of IL-1β secretion

PBMCs were transfected with siRNA by electroporation with the Amaxa system. 1 x 10^6 cells per ml were used for each transfection and were combined with 100 µl of nucleofector solution V. 1.5 µg of either control siRNA or Rab39a siRNA was added to the cells, the solution was transferred to an Amaxa cuvette and electroporated using Amaxa Program Y001. Cells were incubated at 37 °C for 48 hours. Cells were stimulated with 100 ng/ml LPS overnight before harvesting. Supernatants were removed and **(A)** IL-1β and **(B)** TNF-α levels were measured by ELISA. Results are presented as pg/ml of cytokine and data is representative of 3 independent experiments. Results are expressed as mean +/- SD, *** $p < 0.005$

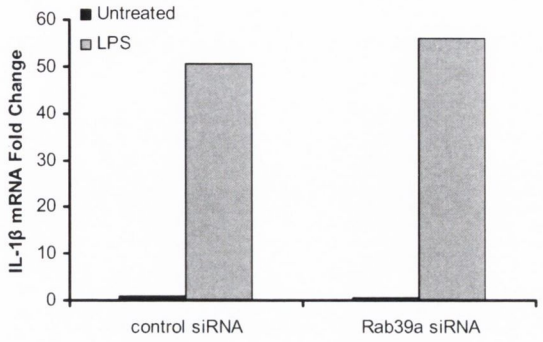


Figure 4.29 siRNA of Rab39a does not affect mRNA levels of IL-1β. THP1s were transfected with siRNA by electroporation with the Amaxa system. 1 x 10^6 cells per ml were used for each transfection and were combined with 100 µl of nucleofector solution V. 1.5 µg of either control siRNA or Rab39a siRNA was added to the cells, the solution was transferred to an Amaxa cuvette and electroporated using Amaxa Program V001. Cells were incubated at 37 °C for 48 hours. Cells were stimulated with 100 ng/ml uLPS overnight before harvesting. Cells were centrifuged at 1000 rpm for 5 minutes and RNA was extracted using RNeasy mini kit and normalised using nuclease free H_2O. Reverse transcription was carried was carried followed by Real Time PCR with primers specific to IL-1β and GAPDH as a control. Expression of IL-1β mRNA was normalized to that of GAPDH mRNA. Data was calculated as fold change and is presented relative to that of untreated controls. Results shown are a representative of 3 different experiments.

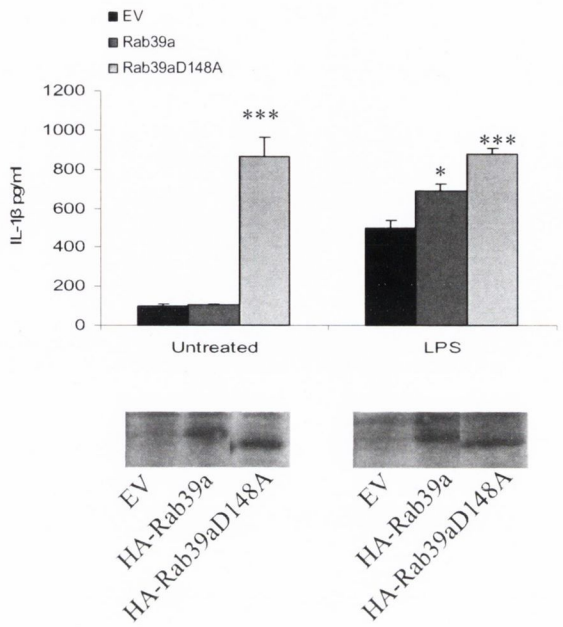


Figure 4.30 Overexpression of Rab39a results in increased secretion of IL-1β. THP1 cells were set up at 1 x 10^6 cells per point. A plasmid expressing HA-Rab39a was transfected into THP1 cells using the Amaxa electroporation program V-001. Following electroporation, cells were added to RPMI media in 12 well plates and incubated at 37 °C for 48 hours. Cells were stimulated with 100 ng/ml μLPS for 18 hours. Supernatants were collected and IL-1β levels were measured by ELISA. Cells were lysed in 50 μl of low astringency lysis buffer, sample buffer was added and samples were separated on 12 % SDS-PAGE gels. The anti-HA antibody was used to detect products. Data is a representative of 3 independent experiments. Results are expressed as mean +/- SD, * $p < 0.05$, *** $p < 0.005$

increased IL-1β secretion on its own. This was not further enhanced by LPS treatment. The caspase-1 resistant form of Rab39a therefore appears to be able to drive IL-1β production. As a control, protein was extracted from the cells and analysed by Western blotting for HA-Rab39a expression. This is also shown in Figure 4.30 and it can be seen that there is equal amounts of Rab39a present in each sample.

4.2.8 Rab39a is secreted from the cell

Because Rab39a had now been shown to be involved in IL-1β secretion it was next tested whether Rab39a itself was being secreted from the cell. In order to test this, THP1 cells were transfected with HA-Rab39a and treated with LPS to cause IL-1β secretion. Secreted proteins were extracted from the supernatant. Cells were lysed and lysates were also prepared. Secreted proteins and cell lysates were separated on gels, transferred onto PVDF and immuno-blotted with antibodies specific for HA, caspase-1, ASC, pro-IL-1β, IL-1β and β-actin. The results are shown in Figure 4.31. Figure (A) shows the proteins that have been secreted. Rab39a, caspase-1, ASC and β-actin are present in the supernatant in untreated samples and in LPS treated samples, meaning that they are constitutively released from the cell. The p35 subunit, which is indicative of caspase-1 processing, is only present in LPS treated samples as expected. A shorter variant of ASC is also present in the supernatant of LPS treated cells. Both pro-IL-1β and mature IL-1β can be found in the supernatant in LPS treated samples. This implies that IL-1β processing may occur outside the cell to a certain extent. Figure 4.31 (B) shows the proteins which are present in the cell lysates. Rab39a, caspase-1, ASC, pro-IL-1β and β-actin are all in the cell lysate as expected. There is no mature IL-1β as expected, as this is all released from the cell (or processing of IL-1β may only take

place outside the cell). These results therefore suggest that Rab39a can be secreted from the cell.

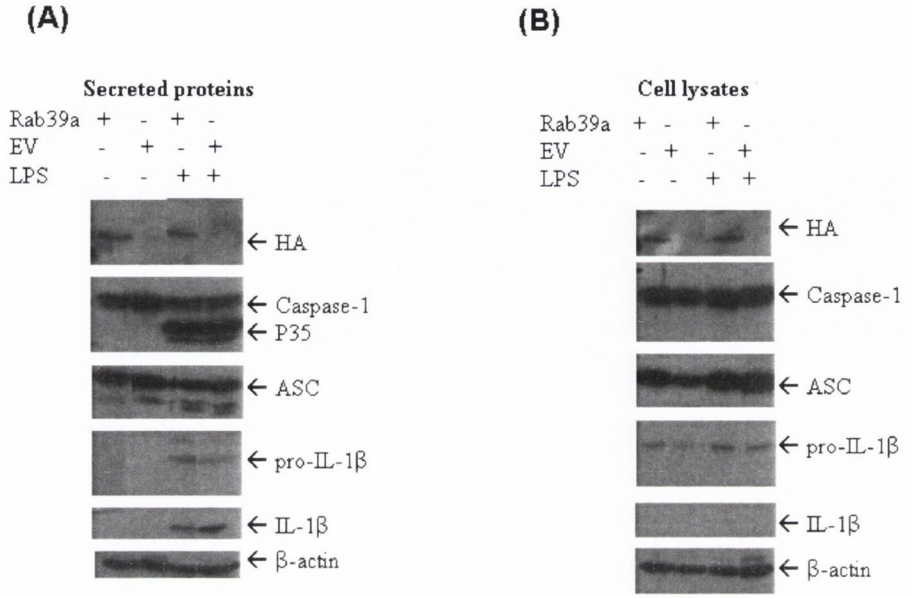


Figure 4.31 Rab39a is secreted from the cell. THP1 cells were set up at 1 x 10^6 cells per point. A plasmid expressing HA-Rab39a (or just the HA tag as a control) was transfected into THP1 cells using the Amaxa electroporation program V-001. Following electroporation, cells were added to RPMI media in 12 well plates and 0.5 μM PMA was added. Cells were incubated at 37 °C for 48 hours. Cells were stimulated with 100 ng/ml LPS for 18 hours. Supernatants were collected and 500 μl methanol and 125 μl chloroform was added. Samples were vortexed and centrifuged for 5 minutes at 13000 rpm. The upper phase was removed. 500 μl methanol was added and samples were centrifuged for 5 minutes at 13000 rpm. The supernatant was removed and the pellet was dried for 5 minutes at 50 °C and sample buffer was added. Cell lysates were also prepared by adding 50 μl of low astringency lysis buffer to the cells. Both secreted samples **(A)** and cell lysates **(B)** were separated on 12 % SDS-PAGE gels and immuno-blotted for HA, caspase-1, ASC, pro-IL-1β, IL-1β and β-actin. Data is a representative of 3 independent experiments.

4.3 Discussion

This chapter focused on Rab39a, a previously uncharacterised Rab GTPase, and its association with caspase-1. Since the interaction between caspase-1 and Rab39a was confirmed in the previous chapter, it was now necessary to investigate the nature of this interaction. The question of whether Rab39a is a substrate of caspase-1 was firstly addressed. Results demonstrated that Rab39a was cleaved using an *in vitro* assay in HEK293T cells. Importantly, Rab39a could also be cleaved in macrophages treated with LPS and ATP. This processing was inhibited by YVAD-cmk, a caspase-1 inhibitor confirming the specificity for caspase-1 cleavage.

To confirm the predicted cleavage site, a mutant of Rab39a was made which lacks the caspase-1 cleavage site. When this construct was used in the assay no cleavage occurred indicating that the predicted site D148 was correct. Furthermore, a construct with a stop codon inserted after the predicted cleavage site is identical in size to the cleavage fragment again confirming that the predicted cleavage site is correct.

It is a possibility that high levels of recombinant caspases can non-specifically cleave proteins at aspartate sites. In this regard, it would be beneficial to try this cleavage assay using other recombinant caspases (e.g. caspase-3) as a control to show that cleavage is specific for caspase-1. However, the fact that Rab4, Rab14 and Rab25 contain caspase-1 cleavage sites and cannot be cleaved when incubated with recombinant caspase-1 suggests that cleavage of Rab39a is specific and not merely due to the presence of an aspartate residue.

Nevertheless, this type of cleavage assay should still be interpreted with caution since a further assay failed to show that Rab39a was a substrate for caspase-1. In this assay, [^{35}S] methionine-labeled Rab39a was expressed using an *in vitro* transcription/translation system, which was then added to cell-free reactions for subsequent visualization by direct autoradiography. One major disadvantage of this assay however is that proteins synthesized by coupled transcription/translation lack post-translational modifications and may not be folded properly (Shao *et al.*, 2007). This is important as bioinformatic analysis highlighted that Rab39a may undergo post-translational modifications.

If Rab39a is a genuine substrate of caspase-1, the question of why it is being cleaved needs to be addressed. Rab GTPases are active when membrane bound. Cleavage of Rab39a at position D148 could remove a 17 kDa section from the membrane, as the prenylation motif needed for membrane attachment is located on the 7 kDa fragment. This is likely to result in an inactive version of Rab39a, as Rab proteins are thought to only function correctly when attached to a membrane. However, Rab39a may have roles that do not require it to be attached to a membrane, and perhaps if Rab39a is bound to caspase-1 or other proteins it may not need to be bound to a membrane. How this cleavage may affect the functions that Rab39a has been implicated in will be discussed shortly.

The role of Rab39a in phagocytosis was addressed. Latex beads or *S. aureus* were used to induce phagocytosis. Rab39a localises to phagosomes in both HEK293T cells and in RAW 264.7 cells. Rab39a also co-localises with active caspases during phagocytosis. It was shown that Rab39a is implicated in bacterial uptake but does not affect phagosomal

acidification. A dominant negative version of Rab39a resulted in an increase in bacterial uptake. This may mean that Rab39a is involved in blocking phagosomal maturation. For example, Rab39a could be found on early phagosomes and needs to be removed, perhaps by caspase-1 cleavage, to allow phagosome matutation to progress. Due to the non-specific binding properties of the early and late phagosome markers tested, it was not possible to detect whether Rab39a was localised to early phagosomes or late phagosomes. Other Rab proteins, such as Rab5 and Rab14 block phagosome maturation and must be removed in order for phagocytosis to progress.

Next, the role of Rab39a in IL-1β secretion was addressed. Results unveiled insight into the mechanism of caspase-1-dependent IL-1β secretion. IL-1β is a multifunctional cytokine and plays a major role in host defence. Unlike other pro-inflammatory cytokines, IL-1β lacks a signal peptide and is secreted via unconventional methods. The process by which it is secreted from the cell has always been contentious. The role of caspase-1 in inflammasome functions and IL-1β processing has been widely described. However, a role for caspase-1 in unconventional protein secretion is emerging. A recent paper describes how IL-1β secretion is mediated by caspase-1 (Keller *et al.,* 2008). This in turn may be mediated by factors that are substrates of caspase-1, the cleavage products of which might have a direct role in IL-1β secretion. These results provide evidence that Rab39a is necessary for the secretion of IL-1β but not induction of pro-IL-1β as siRNA targeted to Rab39a results in diminished secretion of IL-1β but does not affect mRNA levels of IL-1β.

Interestingly, over-expression of a Rab39a construct lacking the caspase-1 cleavage site, results in a boosting of IL-1β secretion. This suggests that cleavage of Rab39a by

caspase-1 would serve as a mechanism of inactivating Rab39a, and therefore act as a mechanism to control levels of IL-1β secretion. Hence, over-expression of a construct that cannot be cleaved results in an excess of IL-1β secretion.

The precise mechanism of IL-1β secretion remains elusive as many models exist as to how this event may occur. Three of the best described models include the lysosome-dependent pathway, micro-vesicle shedding and exosome release. In the lysosome dependent pathway pro-IL-1β is translocated into secretory lysosomes together with caspase-1. The mature form of IL-1β is produced within the lysosome by caspase-1 cleavage, after which the lysosomes fuse with the plasma membrane and the contents are released into the extracellular space. In microvesicle shedding caspase-1 activates IL-1β in the cytoplasm and is exported along with the mature cytokine into the extracellular space. The third mechanism, exosome release, is where caspase-1 and IL-1β are contained in the cytoplasm within endosomal internal vesicles which are released as exosomes.

These models involve many unknown trafficking requirements and interestingly the last two models require the formation of specific vesicles which exit from the cell. Rab proteins have roles in trafficking and secretion and Rab39a, although largely uncharacterised is likely to function in this manner. The most recent and convincing data published suggests that IL-1β is released in exosomes (Qu *et al.*, 2007)(Qu 2007). Exosomes are 30-100 nm in diameter and found within multivesicular bodies (MVB) within the cell. When the MVB fuses with the plasma membrane, the exosomes within the MVB are released into the extracellular milieu. The data presented here also suggests that IL-1β is secreted by a Rab39a dependent process. Live cell imaging of

Rab39a in RAW 264.7 cells displayed an expression pattern consistent with that of exosomes. Results also suggest that Rab39a is secreted from the cell along with IL-1β, caspase-1 and ASC. Altogether, this provides compelling evidence that Rab39a is involved in caspase-1 dependent IL-1β secretion through exosome release.

Other papers published recently also support this idea. A proteomic analysis of exosomes revealed a peptide matching Rab39a (Pisitkun *et al.*, 2004). It is also worth noting that Rab4 and Rab11 have been shown to be key Rab proteins involved in exosome release. Interestingly, Rab4, Rab11 and Rab39a all belong to the same subfamily and exosome trafficking maybe a common role for this subfamily of Rab GTPases.

Little is known about the involvement of caspase-1 in the exosome. However, a 2007 study revealed that exosome component 9 (EXOSC9), also known as PM/Scl-75, is a substrate of caspase-1. Furthermore, another recent study revealed 41 previously unknown substrates of caspase-1 and through literature searching it is clear that many of these substrates are also components of exosomes. For example, pyruvate kinase, GAPDH, α-enolase, EEF1A1, β-tubulin, β-actin and Hsp90 are all substrates of caspase-1 that are key components of exosomes (Thery *et al.*, 2009).

This raises an interesting concept about the role of caspase-1 in exosome trafficking. Perhaps caspase-1 cleavage of exosomal proteins, such as Rab39a, is required for exosome secretion. The cleavage of Rab39a may be a way of controlling exosome secretion, and if Rab39a cannot be cleaved this results in excessive exosome secretion and therefore IL-1β secretion.

Results also showed that Rab39a contains many transcription factor binding sites and is inducible by pro-inflammatory stimuli. The following mechanism of action is proposed by which Rab39a associates with caspase-1 and together are required for efficient IL-1β secretion. During an inflammatory response Rab39a is induced and binds to caspase-1. As IL-1β is secreted in a caspase-1 dependent manner, it is proposed that Rab39a is needed to help traffic IL-1β from the cell in a vesicle dependent manner. Indeed, caspase-1 itself and other components of the inflammasome which also lack signal peptides are also released from activated macrophages and Rab39a may be necessary in helping to secrete the entire inflammasome complex from the cell.

Interestingly, the association between Rab39a and caspase-1 is highly specific. Rab39a is 76 % similar to another Rab protein, Rab39b, but they have very different profiles with regard to caspase-1. Unlike Rab39a, Rab39b was not found to associate with caspase-1 in the mass spectrometry screen and it does not co-immunoprecipitate with caspase-1. It lacks a caspase-1 cleavage site and cannot be cleaved *in vitro*, and it is not induced by pro-inflammatory stimuli to the same extent as Rab39a. The role of Rab39a in IL-1β secretion is therefore specific.

To summarise, this section of work shows that caspase-1 binds Rab39a. Investigation into the nature of this interaction suggested that Rab39a is a substrate of caspase-1. Results suggest that Rab39a can be localised to phagosomes and is involved in bacterial uptake. Results also suggest that Rab39a functions as a trafficking adaptor linking caspase-1 to IL-1β secretion.

Chapter 5

Analysis of ASC in the Inflammasome

5.1 Introduction

ASC is a central component of inflammasomes. The inflammasome was first described in 2002 (Martinon *et al.*, 2002) and since then tremendous advances have been made in unravelling the role of the inflammasome in the innate defence system. A variety of ligands have been identified which activate the inflammasomes, particularly ligands for NLRP3, the number of which has soared in recent months. The signalling pathways surrounding the inflammasome are beginning to unfold and the relevance of the inflammasome in auto-inflammatory diseases is emerging.

ASC also exists in another supramolecular assembly called the pyroptosome (Fernandes-Alnemri *et al.*, 2007). This is described as an NLRP-independent complex that forms prior to a caspase-1 dependent form of cell death called pyroptosis.

Although a lot of information is known about inflammasomes, many questions remain unanswered. There is much to discover about many aspects of inflammasomes, for instance the significance of TLR priming, the regulation of how the inflammasome is activated and the intricacies of the signalling pathways involved in inflammasome formation.

Since ASC is a crucial player in inflammasomes, it was decided to investigate different aspects of ASC and its involvement in inflammasome formation and regulation. This was done firstly by looking for novel binding partners of ASC and secondly by visualising ASC during inflammasome formation. This chapter aims to address some of the unsolved issues of ASC complex formation in cells during an immune response.

5.2 Results

5.2.1 Identification of novel binding partners of ASC

5.2.1.1 Immunoprecipitation of ASC from cell free extracts

Through mass spectrometry Rab39a was discovered as a novel binding partner of caspase-1. It was decided to take a similar approach in order to find novel binding partners of ASC, with the view that discovery of novel binding partners would help in further understanding the intricacies of the signalling events needed for inflammasome formation. Briefly, this approach requires the preparation of cell free extracts (CFE's) from THP1 cells and incubation of the CFE at 37 °C which results in activation of caspase-1 and therefore the inflammasome caused by the induced proximity model (Martinon *et al.*, 2002). This was followed by immunoprecipitation of ASC from the CFE and identification of bound proteins by mass spectrometry.

Firstly, it was necessary to ensure that the conditions being used were suitable. Cell free extracts (CFE's) from THP1 cells were prepared and incubated at 37 °C for 90 minutes. The CFE was then analysed by Western blotting for caspase-1 and ASC. Figure 5.1 (upper blot) shows that the inflammasome was activated by this procedure as indicated by the processing of caspase-1. p45 is the full-length inactive form of caspase-1 and it decreases over time as it is processed. The p35 and p10 subunits are the activated forms of caspase-1 and increase over time which is indicative of caspase-1 processing. The p45, p35 and p10 subunits are indicated with arrows. Figure 5.1 (lower blot) demonstrates that ASC is highly expressed in this preparation and that expression levels remain constant during inflammasome activation. This confirmed that the CFE was a good model for inflammasome activation and a suitable source of ASC.

The next step was to confirm that ASC could be specifically isolated from the CFE. The ASC antibody from Alexis was found to be the best antibody for immuno-precipitating ASC. As shown in Figure 5.2, ASC can be immunoprecipitated from the CFE (upper blot lane 1). Rabbit IgG was used as a control (upper blot lane 2) and no ASC is present. Cell lysates (lower blot lanes 1 and 2) confirm that the samples contained equal amounts of ASC.

5.2.1.2 Identification of bound proteins by mass spectrometry

As it was now established that ASC could be successfully immunoprecipitated from a CFE of THP1 cells, the next step was to use mass spectrometry to identify any bound proteins. CFE was prepared and incubated at 37 °C to activate the inflammasome or left at 4 °C as a control. As all cellular ASC is known to redistribute to the inflammasome upon stimulation (Bauernfeind *et al.*, 2009, Bryan *et al.*, 2009), it is speculated that any novel binding partners of ASC in the 37 °C sample may themselves be part of the inflammasome or have roles in the inflammasome, whereas proteins in the 4 °C sample may not. Samples were also immunoprecipitated with a rabbit IgG as a control to determine non-specific binding.

Initially, samples were run on large 2D gels. This involves separating the samples firstly by isoelectric point (PI), using isoelectric focusing and secondly by molecular weight. However, it was difficult to obtain sufficient amounts of protein for detection by mass spectrometry, so it was decided to run the samples on large 1D gels instead. Silver staining was used to visualise the proteins on the gels. Figure 5.3 shows results obtained using a large 1D gel. Bands that immunoprecipitated with ASC (lanes 1 and 3) and not with the IgG control (lanes 2 and 4) were extracted from the gel and digested with

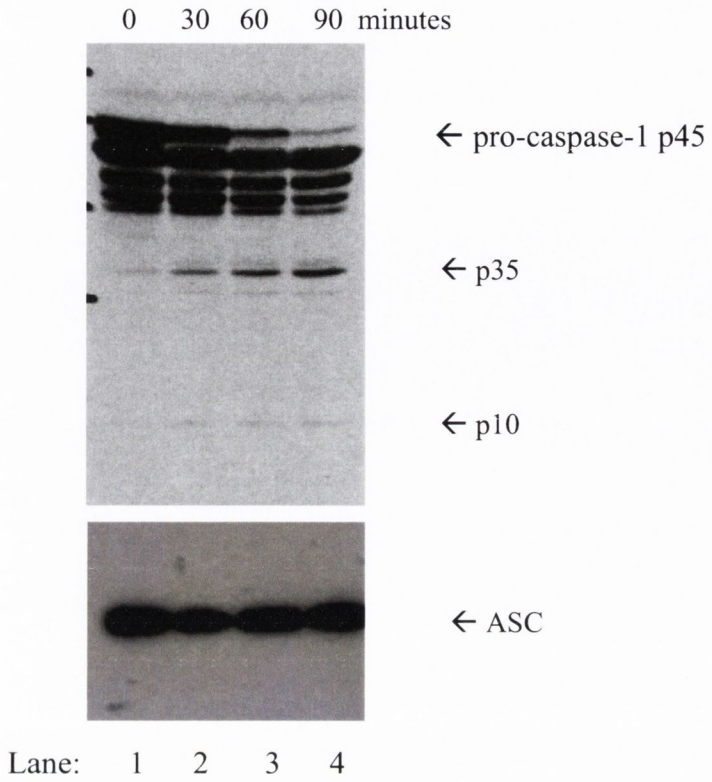


Figure 5.1 Incubation of a CFE of THP1 cells at 37 ˚C results in activation of caspase-1. A CFE was prepared from THP1 Cells. Cells were pelleted at 200 rcf for 10 minutes and washed twice in PBS. Cells were resuspended in 2 mls of PBS, transferred to a tissue grind pestle and centrifuged at 600 rcf for 10 minutes. PBS was removed and resuspended in 2 volumes of WCEB. Cells were left on ice for 10 minutes and dounced 30 times to break open cells. Cells were transferred to eppendorfs and spun at top speed for 10 minutes at 4 ˚C. Samples were incubated at 37 ˚ for 0 - 90 minutes as indicated to induce inflammasome formation and then separated on 12 % gels and immunoblotted for caspase-1 and ASC. This result represents three independent experiments

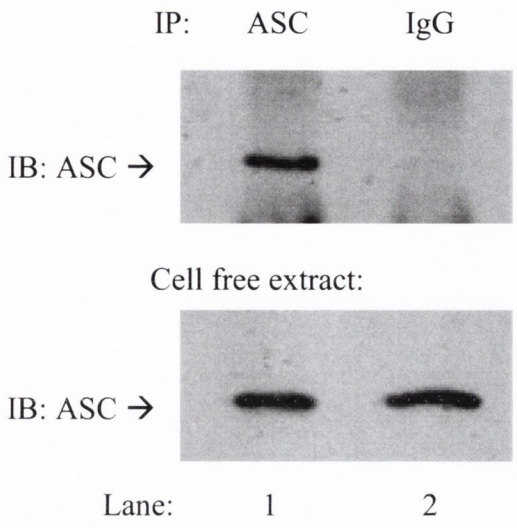


Figure 5.2 ASC can be immunoprecipitated from a cell free extract of THP1 cells. THP1 cells were pelleted at 200 rcf for 10 minutes and washed twice in PBS. Cells were resuspended in 2 mls of PBS, transferred to a tissue grind pestle and centrifuged at 600 rcf for 10 minutes. PBS was removed and resuspended in 2 volumes of WCEB. Cells were left on ice for 10 minutes and dounced 30 times to break open cells. Cells were transferred to eppendorfs and spun at top speed for 10 minutes at 4 ˚C. 50 µl of extract was removed for analysis by Western blotting. This CFE was diluted with IP lysis buffer. 2 µg of ASC antibody (or rabbit IgG as a control) and 40 µl of protein A/G beads were added and samples were incubated at 4 ˚C with gentle rolling overnight. Beads were washed three times with IP lysis buffer and then mixed with 35 µl of sample buffer. Sample buffer was added, samples were separated on a 12 % SDS gel, transferred onto PVDF membrane and immunoblotted with anti-ASC antibody. This result represents two independent experiments.

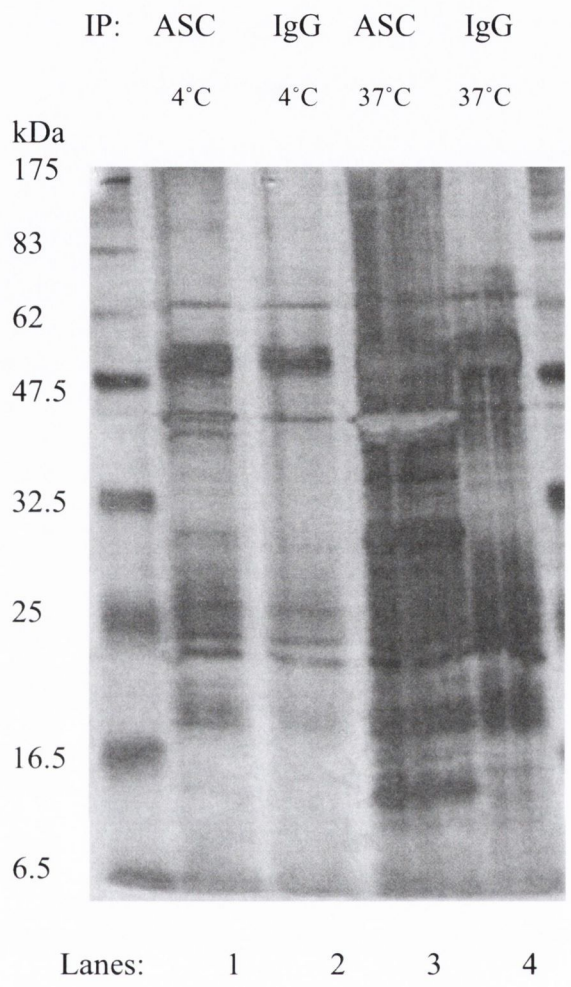


Figure 5.3 Silver staining of ASC immunoprecipitation from THP1 cells. THP1 cells were pelleted at 200 rcf for 10 minutes and washed twice in PBS. Cells were resuspended in 2 mls of PBS, transferred to a tissue grind pestle and centrifuged at 600 rcf for 10 minutes. PBS was removed and resuspended in 2 volumes of WCEB. Cells were left on ice for 10 minutes and dounced 30 times to break open cells. Cells were transferred to eppendorfs and spun at top speed for 10 minutes at 4 °C. 50 µl of extract was removed for analysis by Western blotting. This CFE was diluted with IP lysis buffer and incubated at 37 °C for 2 hours or left at 4 °C . 2 µg of ASC antibody (or rabbit IgG as a control) and 40 µl of protein A/G beads were added and samples were incubated at 4 °C with gentle rolling overnight. Beads were washed three times with IP lysis buffer and then mixed with 150 µl of sample buffer. Samples were separated on a large 12 % SDS gel and proteins were visualised by silver staining.

trypsin. Peptides were identified by MALDI-TOF using a Voyager DE-PRO mass spectrometer. Table 5.1 shows the list of proteins that were identified to associate with ASC. The list includes a variety of interesting proteins such as PSTPIP1, the TRIM family member PML, LRR-containing proteins and many other uncharacterised proteins.

5.2.1.3 PSTPIP1 does not co-immunoprecipitate with ASC

One of the proteins identified in the mass spectrometry screen was PSTPIP1, a protein that has been implicated in inflammasomopathies such as Familial Mediterranean Fever and pyogenic arthritis, pyoderma gangrenosum and acne syndrome. PSTPIP1 had a MOWSE score of 453 and 16 % peptide coverage. The trypsin digest peaks are shown in Figure 5.4.

It was therefore investigated whether the PSTPIP1 and ASC interaction could be confirmed in an over-expression system. Plasmids encoding Myc-PSTPIP1 and ASC were transiently transfected into HEK293T cells, immunoprecipitated with Myc antibody (or Caspase-1 antibody or IgG as controls) and immunoblotted with an ASC specific antibody. The results are shown in Figure 5.5. There is no band in lane 4 of the upper blot, indicating that no interaction took place between ASC and PSTPIP1. The positive control is shown in lane 5 of the upper blot. This shows an interaction between ASC and its known binding partner caspase-1. The lower blots (probing for MYC and caspase-1 respectively) confirm that all transfected proteins were expressed at similar levels between the samples. Therefore, these co-immunoprecipitation results show that the direct interaction between PSTPIP1 and ASC could not be established. This means

that the interaction seen in the mass spectrometry was probably indirect. Therefore, no further investigation was carried out on the association between PSTPIP1 and ASC.

5.2.2 Isolation of inflammasome complexes

A different approach was now taken to investigate the inflammasome. Fernandes-Alnemri *et al.* devised a biochemical procedure to isolate ASC complexes from THP-1 macrophages after LPS stimulation (Fernandes-Alnemri *et al.*, 2007). The ASC complex can be separated by a combination of membrane filtration and centrifugation. The aim of this section was to adopt this technique to isolate inflammasomes and to use a variety of activators and inhibitors to further understand inflammasome signalling.

This procedure was adapted and carried out on immortalised BMDMs. The results are shown in Figure 5.6. Cells were treated for 3 hours with increasing doses of LPS and ATP and it can be seen that ASC complexes form in a dose dependent manner (upper blot, lanes 1 - 4). The amount of ASC in the cell lysates (lower blot: lanes 1 - 4) remained constant indicating that no de-novo synthesis of ASC was required and ASC was becoming incorporated into complexes. Otherwise, cells were treated for 3 hours with increasing doses of Malp2 and ATP and it can be seen that ASC complexes form in a dose dependent manner (lanes 5 -8). The amount of ASC in the cell lysates (lower blot, lanes 5 - 8) again remained constant indicating that no de-novo synthesis of ASC was required and ASC was becoming incorporated into complexes.

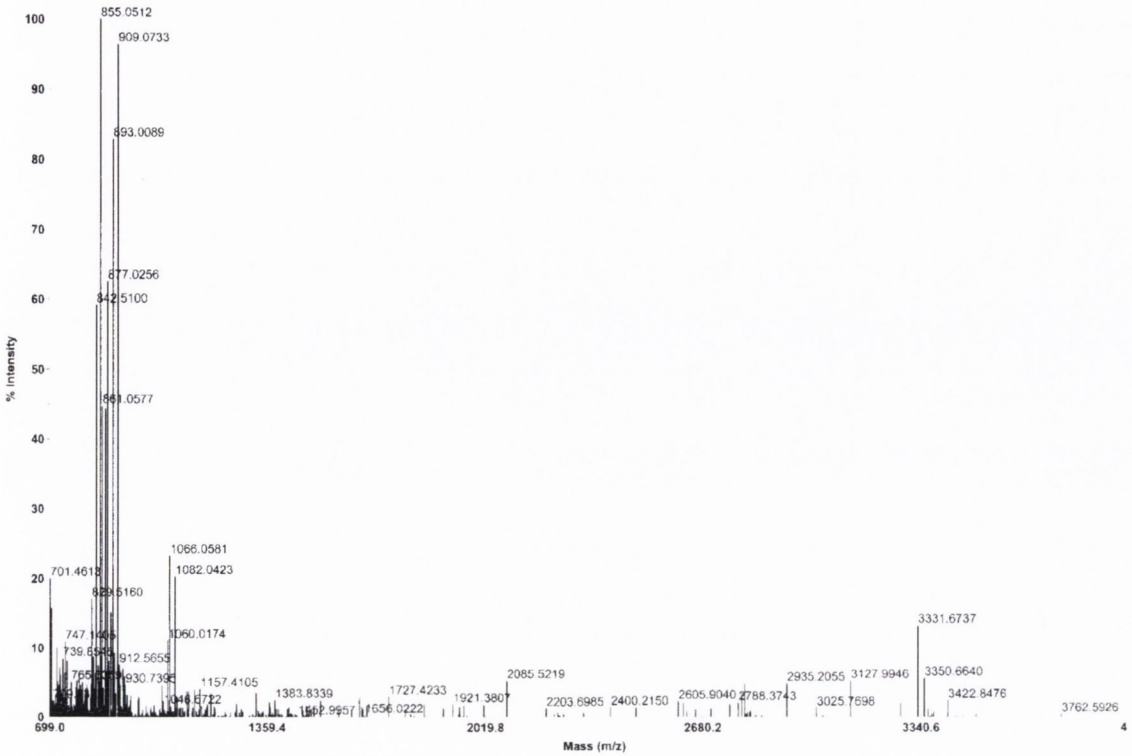
To establish whether TLRs were necessary for this process, it was repeated in Myd88 deficient BMDMs. The results are shown in Figure 5.7. ASC complexes formed in response to LPS and ATP over a 150 minute time course in both WT (upper blot, lanes

Protein		MW	MS FIT MOWSE	Mascot score
Q9NX36	J domain-containg protein C21orf55	45.8	483	
O43586	PSTPIP1	47.5	453	
Q8NB25	Uncharacterised protein C6orf60	119	23080	
P29590	PML	97.5	12915	
O15327	Type II inositol-3,4-bisphosphate 4-phosphate	104.7	5169	
Q9Y2U8	Inner nucleur membrane protein Man 1	99.9	4665	
Q9WJR	HERV-K-19q12 povirus ancestral Pol protein	108	4564	
Q9UPN4	5-azactidine-induced protein 1	122	4533	
Q8NEN0	Armadillo repeat-containing protein 2	96	3817	
O00159	Myosin	118	3814	
P40189	IL-6 receptor subunit beta precursor	103	3361	
P33991	DNA replication licensing factor MCM4	96	3345	
Q9NRE2	Teashirt homolog 2	115	2263	
P57740	Nucleur pore complex protein Nup107	106	2172	
Q8N475	Follistatin-related protein 5 precursor	95	2171	
Q9BXJ9	NMDA receptor-regulated protein 1	101	1711	
Q8IY82	Coiled-coil domain-containing protein 135	103	1663	
P49916	DNA ligase 3	102	1583	
Q13873	Bone morphogenetic protein receptor type-2 precursor	115	1435	
P98073	Enteropeptidase precursor	112	1381	
P67936	Tropomyosin alpha-4 chain	28.5	1115	
IPI00477649	TPM3 isoform 5	28.8		48
IPI00479185	TPM isoform 4	29		38
IPI00218320	TPM isoform 3 of tropomyosin alpha-3 chain	29		38
IPI00854807	TPM3 pututive uncharacterised protein	27		34
IPI00010779	TMP4 isoform 1 of tropomyosin a	28		30

IPI00218319	TPM3 isoform 2 of tropomyosin alha-3 chain	29		29
IPI00178083	TPM3 29kDa protein	29		28
IPI00642042	TPM3	27		27
Q5T655	LRR-containing protein C10orf80	33	106	
Q96MO2	Uncharacterised protein C10orf90	33	76.1	
IPI00152154	Mucin-7 precursor	39		21
IPI00386388	Olfactory receptor 6 K2	37		18
Q8N9R8	Uncharacterised protein C9orf126	32	138	
IPI00791210	HOM-Tes-103	28		28
IPI00785012	DAGLB isoform 3 of Sn1-specific diacylglycerol lipase beta	29		21
IPI00445166	TGOLN2 isoform 6 of trans golgi network integral membrane protein	29		20
IPI00003367	NFE2 transcription factor	41		29
IPI00169353	MAFA v-maf musculoaponeurotic fibrosarcoma oncogene homolog	37		23
IPI00303622	ORIN2 Olafactory receptor OR9-23	37		21
IPI00643947	PALM2	46		21
Q9UIK5	Tomoregulin-2 precursor	41	272	
Q9NR46	SH domain GRB2-like protein B2	44	260	
IPI00166222	Isoform 3 of KASH domain-containing protein C19orf46	38		28
Q9NYBO	Telomeric repeat-binding factor 3-inreacting protein 1	44	817	
Q96IZ6	Methyltransferase-like protein 2	43	706	
Q6IB77	Glycine N-acyltransferase	34	1276	
Q8N4F7	RING finger protein 175	38	979	
O00300	TNF receptor superfamily member 11B precursor	46	485	
IPI00445312	C5orf25	35		27
IPI00470614	OR6C65 uncharacterised protein	35		25
IPI00165237	WDR74 Isoform 2 of WD repeat-containing protein 74	41		24
IPI00031641	TMEM38A Transmemrane protein 38A	34		22
IPI00658190	LENG8	32		22

P68032	Actin	42	22468	
Q5JVX7	Uncharacterised protein C1orf141	46	4394	

Table 5.1 Proteins associating with ASC identified by Mass Spectrometry. A cell free extract preparation was made from THP1 cells. This was incubated at 37 ˚C or kept at 4 ˚C for 2 hours. ASC (or an IgG control) was immunoprecipitated from the CFE an samples were separated on a large 12 % gels. Proteins were visualised by silver staining. Proteins which immunoprecipitated with ASC, but not the IgG control were extracted from the gel and digested with trypsin. Peptides were identified by MALDI-TOF using a Voyager DE-PRO mass spectrometer.



Mowse Score	% Coverage	Protein MW	Protein name
453	16.0	47.5	PSTPIP1 Acc # O43586

Figure 5.4 PSTPIP1 is identified as a potential binding partner of ASC. Trypsin peaks of a sample from ASC immunoprecipitation. Peaks were transferred into the Mascot database and peptides were matched to PSTPIP1.

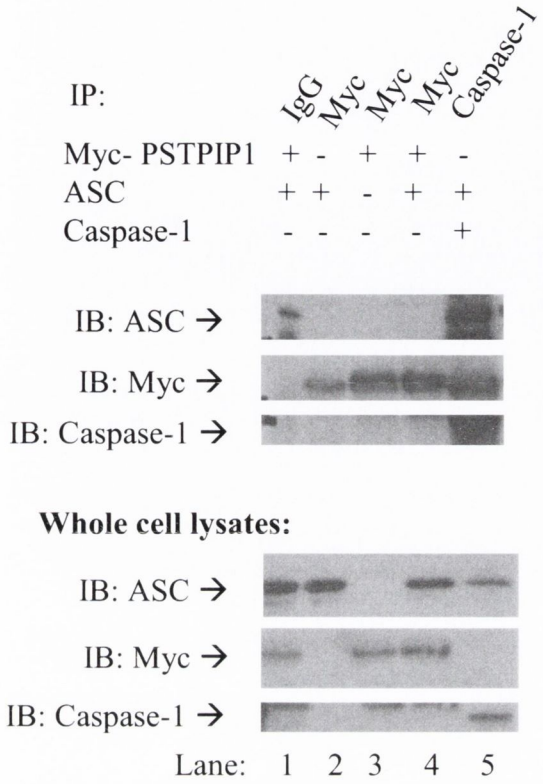


Figure 5.5 ASC and PSTPIP1 do not co-immunoprecipitate. Hek293T cells were set up at 2 x 10^5 cells per ml in 10 cm dishes. After 24 hours they were transfected with plasmids containing Myc-PSTPIP1, ASC or Caspase-1 as indicated such that the total amount of DNA was kept constant at 8 µg. After 36 hours, cells were harvested in low astringency lysis buffer. A 50 µl sample of lysate was removed so that protein expression could be analysed in lysates. The remaining lysate was pre-cleared twice with 15 µl protein A/G beads for 30 minutes. Lysates were incubated with 20 µl of beads and 5 µg of Myc antibody, caspase-1 antibody or IgG control for 4 hours at 4 °C with gentle rolling. Lysates were washed 3 times in 1 ml of lysis buffer and 35 µl of sample buffer was added. IP samples and cell lysates were separated on 12 % gels, analysed by Western blotting and immuno-blotted for ASC, Myc and caspase-1 as indicated. This result represents 3 independent experiments.

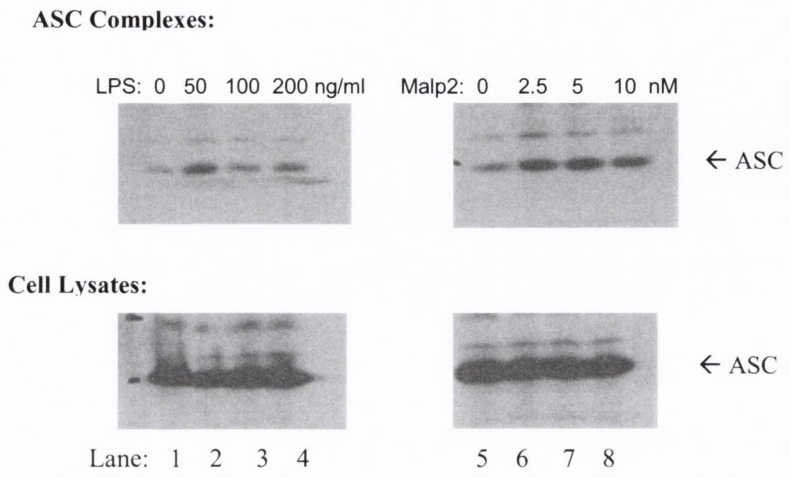


Figure 5.6 ASC complexes can be isolated from BMDM cells. 4 x 10^7 I-BMDM cells per point were prepared and seeded on 10 cm plates at a density of 1 x 10^6 per ml. Cells were treated with the indicated doses of LPS and 5mM ATP or the indicated doses of Malp2 and 5mM ATP. To isolate ASC complexes - cells were centrifuged at 200 rpm for 5 minutes, medium removed, and resuspended in 1 ml PBS. Cells were pelleted at 1500 rpm. Cells were resuspended in 0.5 ml of Buffer A. Cells were lysed on ice by syringing 30 times with a 1 ml syringe with 21-gauge needle. Lysates were centrifuge at 1800 rpm for 8 minutes. Supernatants were transferred to a fresh eppendorf, taking care not to disturb the nuclear pellet. A 30 µl sample was removed and saved for Western blot analysis. The remaining supernatants were diluted with two volumes of buffer A and then filtered with 5 µm Centrifugal Filters at 2000 g. Filtered lysates were collected and diluted with one volume of CHAPS buffer and then centrifuged at 5000 rpm for 8 minutes. Pellets were resuspended in 1 ml CHAPS buffer and then centrifuged at 5000 rpm for 8 minutes. This was repeated twice to wash the ASC complexes. Pellets were resuspended in 30-40 µl CHAPS buffer. For Western blot analysis, equal amounts of the resuspended pellets and 2X SDS sample buffer, were mixed, boiled and then separated on 12 % SDS gels. Proteins were immunoblotted with an anti-ASC antibody. This result represents 2 independent experiments.

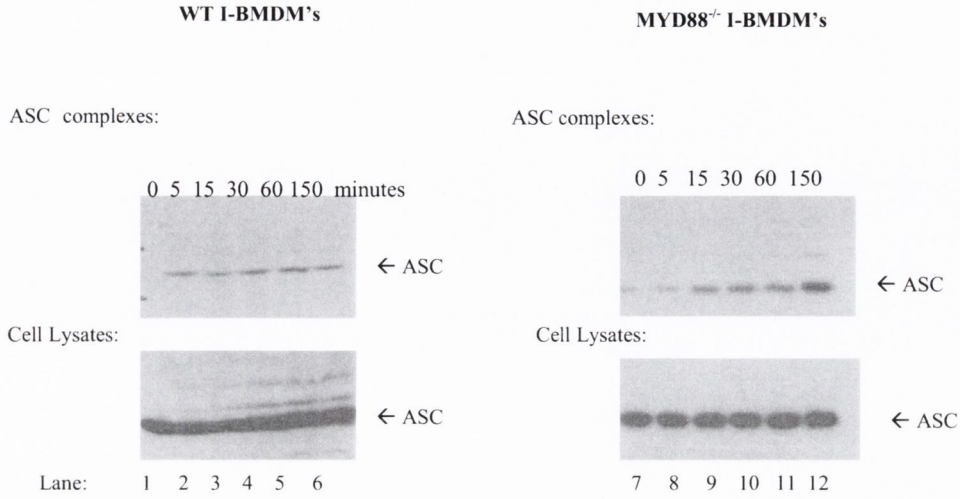


Figure 5.7 ASC complex formation is Myd88 independent. 4 x 10^7 Wt BMDMs or Myd88$^{-/-}$ BMDMS per point were prepared and seeded on 10 cm plates at a density of 1 x 10^6 per ml. Cells were treated with 100 ng/ml LPS or 5 nM Malp2 for the indicated times hours and then treated with 5 mM ATP for 1 hour. To isolate ASC complexes, cells were centrifuged at 200 rpm for 5 minutes, medium removed, and resuspended in 1 ml PBS. Cells were pelleted at 1500 rpm. Cells were resuspended in 0.5 ml of Buffer A. Cells were lysed on ice by syringing 30 times with a 1 ml syringe with 21-gauge needle. Lysates were centrifuge at 1800 rpm for 8 minutes. Supernatants were transferred to a fresh eppendorf, taking care not to disturb the nuclear pellet. A 30 µl sample was removed and saved for Western blot analysis. The remaining supernatants were diluted with two volumes of buffer A and then filtered with 5 µm Centrifugal Filters at 2000 g. Filtered lysates were collected and diluted with one volume of CHAPS buffer and then centrifuged at 5000 rpm for 8 minutes. Pellets were resuspended in 1 ml CHAPS buffer and then centrifuged at 5000 rpm for 8 minutes. This was repeated twice to wash the ASC complexes. Pellets were resuspended in 30-40 µl CHAPS buffer. For Western blot analysis, equal amounts of the resuspended pellets and 2X SDS sample buffer, were mixed, boiled and then separated on 12 % SDS-polyacrylamide gel. Proteins were immunoblotted with an anti-ASC antibody. This result represents 2 independent experiments.

1 - 6) and Myd88$^{-/-}$ deficient cells (upper blot, lanes 7 - 12). The amount of ASC in the cell lysates (lower blots, lanes 1 - 6 and lanes 7 – 12) remained constant indicating that no de-novo synthesis of ASC was required and ASC was becoming incorporated into complexes. This result indicated that ASC complexes could be formed in a MyD88 independent manner as they could be formed in Myd88 deficient cells when treated with Malp2 and ATP.

There were many technical difficulties associated with this isolation procedure and despite considerable optimisation it proved challenging to obtain consistent results.

5.2.3 Analysis of signalling events needed for inflammasome formation

Because of the technical difficulty associated with isolating the inflammasome using the above technique, a new approach was taken to investigate inflammasome signalling. Immortalised mouse macrophages stably transfected with ASC-YFP were used. These were kindly provided by Eicke Latz, University of Massachusettes USA. The cells are a very useful tool for studying inflammasome formation; firstly they are macrophages, secondly they are stably transfected so no further transfection is necessary and thirdly they can be readily viewed by live cell imaging.

5.2.3.1 ASC speck formation requires TLR priming

The first step was to look at ASC distribution in the cell. Figure 5.8 (A) shows that resting cells uniformly express ASC throughout the cytoplasm. Next, the effect of TLR and NLR ligands on ASC distribution was examined. Cells treated for 3 hours with a TLR ligand alone such as 10 ng/ml LPS (TLR4 ligand), 5 nM Malp2 (TLR2/6 ligand), or 25 μg/ml Poly I:C (TLR3 ligand), showed a uniformed cytoplasmic distribution of

ASC. This is shown in Figure 5.8 (B)-(D). Cells treated for 1 hour with 5 mM of the NLRP3 ligand ATP also showed a uniformed cytoplasmic distribution of ASC as shown in Figure 5.8 (E). However, when cells were treated with either LPS, MALP2, or Poly I:C for 3 hours and then treated with ATP for 1 hour, ASC dramatically redistributed in the cell and formed a large speck-like object. This is shown in Figure 5.8 (F)-(H). This indicates that TLR priming was required for NLRP3 activation of the ASC speck. Each cell contained just one ASC aggregate measuring ~2 μM in diameter.

5.2.3.2 Timecourse analysis of ASC speck formation

The next question to address was the length of time needed for each signal. Cells were treated with 10 ng/ml LPS for 3 hours and then 5 mM ATP was added for 0-55 minutes. Figure 5.9 shows that specks begin to form after 10 minutes of ATP treatment with optimal speck formation at 1 hour.

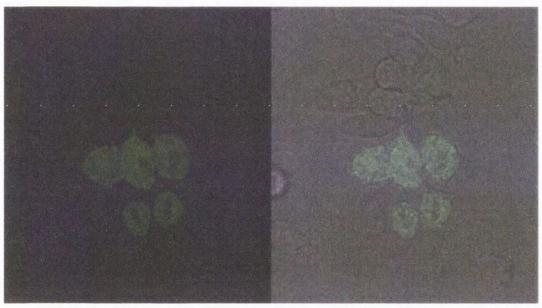
An LPS time-course was next carried out to determine how long the TLR priming signal was needed for. Cells were treated with 10 ng/ml LPS for 0-180 mins followed by 5 mM ATP for 30 minutes. Figure 5.10 demonstrates that specks begin to form after 15 minutes LPS with optimal speck formation after 3 hours.

Together, these results indicate that speck formation is a moderately rapid process which can form after 15 minutes LPS and 15 minutes ATP.

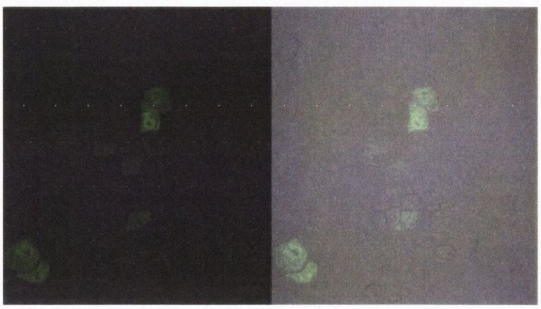
5.2.3.3 ASC speck formation is upstream of caspase-1 activation

The next question addressed was whether caspase-1 activation occurred upstream or downstream of ASC assembly. To address this, cells were pre-treated with 100 μm

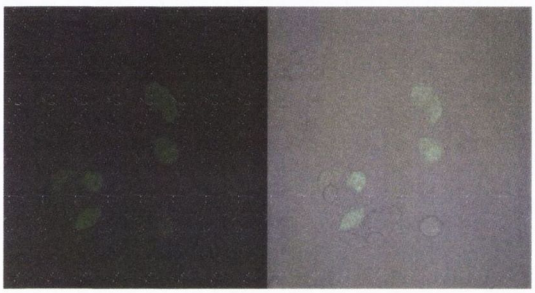
(A)



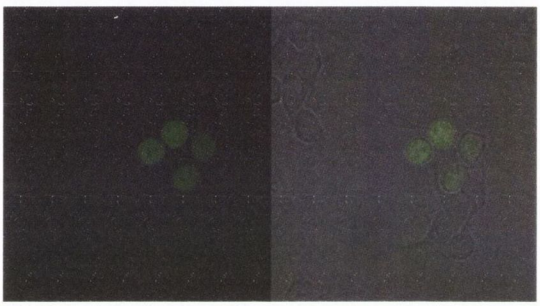
(B)



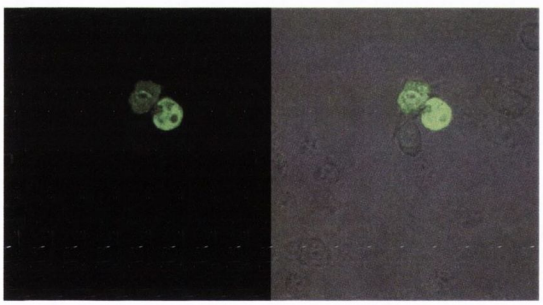
(C)



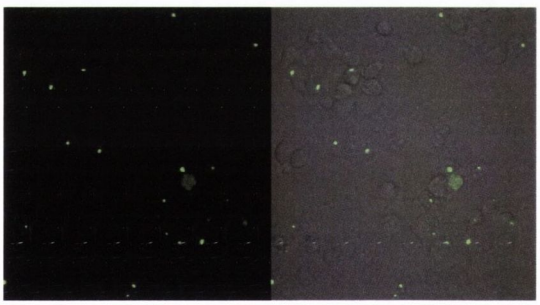
(D)



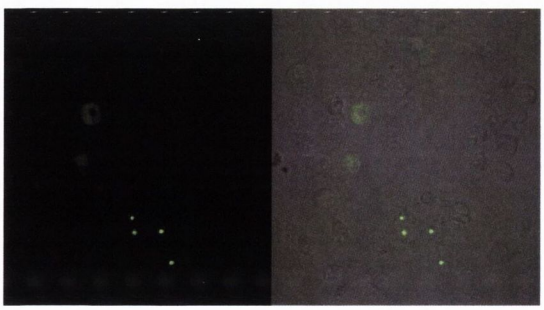
(E)



(F)



(G)



(H)

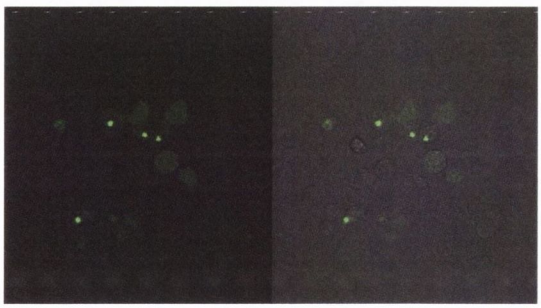


Figure 5.8 ASC speck formation is induced by TLR ligands plus ATP. ASC-FP cells were set up at 2 x 10^5 in glass bottom confocal dishes. 24 hours later cells were stimulated as described below and viewed by live cell imaging using an Olympus FluoViewTM FV1000 Microscope equipped with a temperature and CO_2 controlled chamber. Images on the left show ASC-FP only, whilst images on the right show ASC-FP and phase-contrast. **(A)** Untreated **(B)**10 ng/ml LPS for 3 hours **(C)** 5 nM Malp2 for 3 hours **(D)** 1 μg/ml Poly I:C for 3 hours **(E)** 5 mM ATP for 1 hour **(F)** 10 ng/ml LPS for 3 hours and 5 mM ATP for 1 hour **(G)** 5 nM Malp2 for 3 hours and 5 mM ATP for 1 hour **(H)** 1 μg/ml Poly IC and 5mM ATP for 1 hour. This result represents three independent experiments.

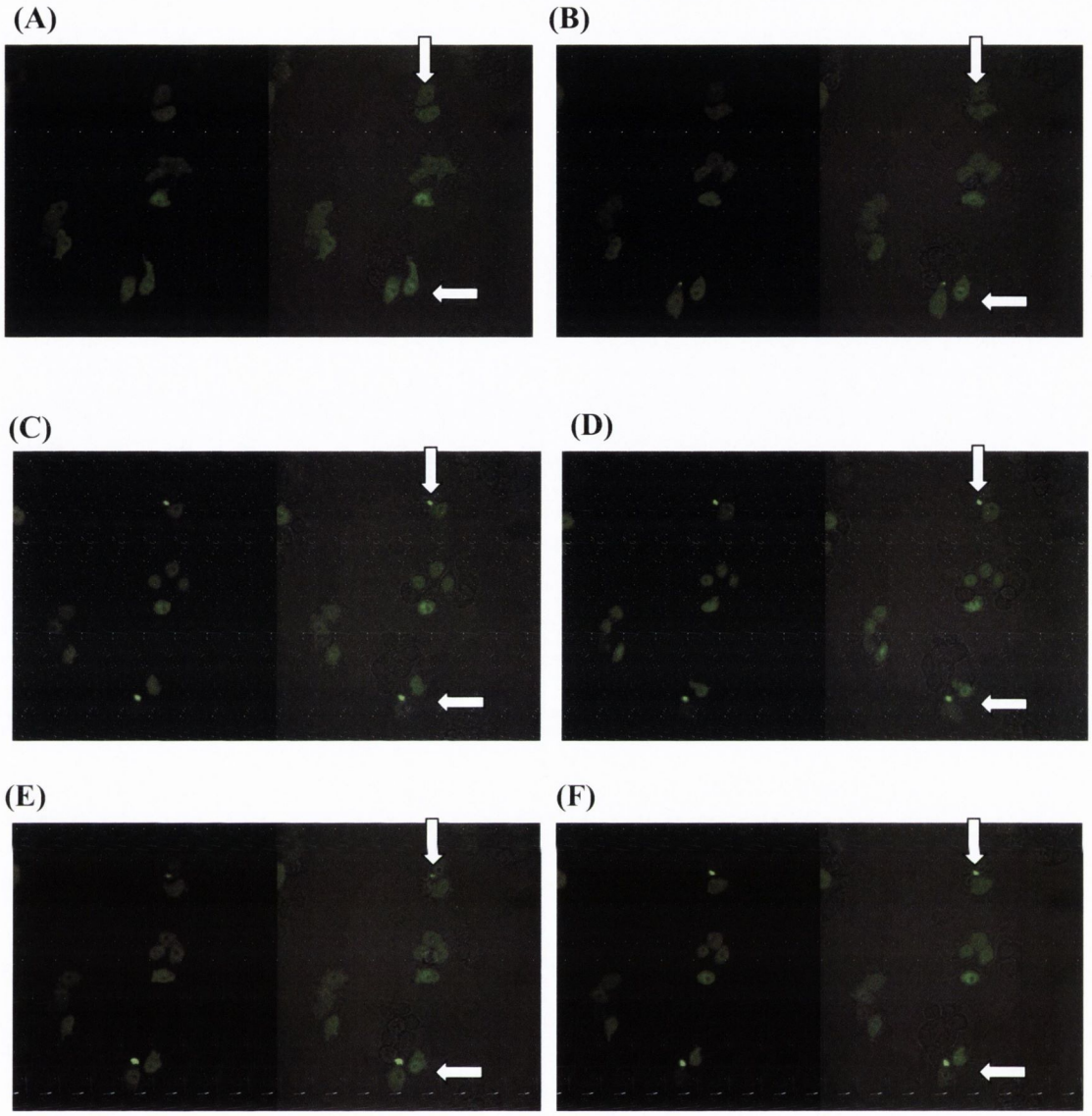
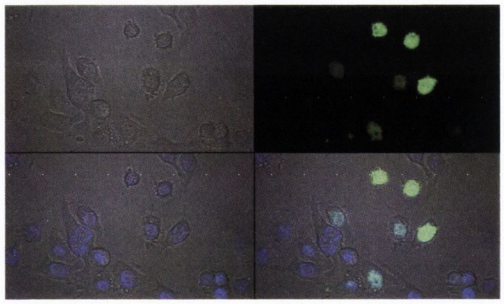
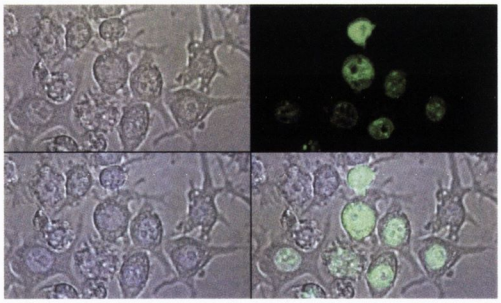


Figure 5.9 ASC specks begin to form after 15 mins of ATP treatment. ASC-FP cells were set up at 2 x 10^5 in glass bottom confocal dishes. 24 hours later cells were stimulated as described below and viewed by live cell imaging using an Olympus FluoViewTM FV1000 Microscope equipped with a temperature and CO_2 controlled chamber. Images on the left show ASC-FP only, whilst images on the right show ASC-FP and phase-contrast. Cells were primed with 10 ng/ml LPS for 3 hours and stimulated with 5 mM ATP for **(A)** 2 minutes, **(B)** 10 minutes, **(C)** 15 minutes **(D)** 30 minutes **(E)** 40 minutes **(F)** 55 minutes. The white arrows indicate cells were specks are forming. This result represents two independent experiments.

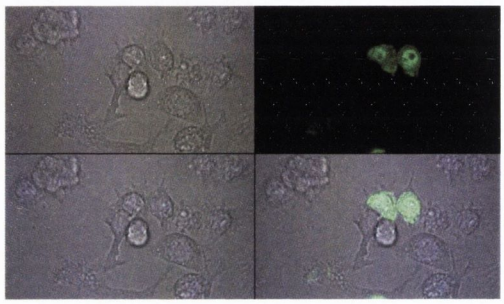
(A)



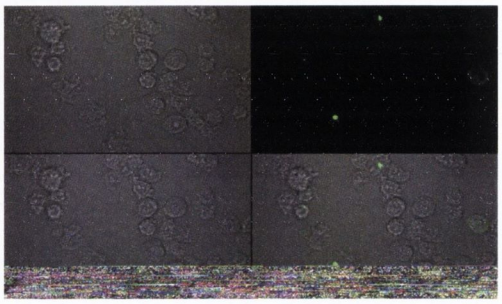
(B)



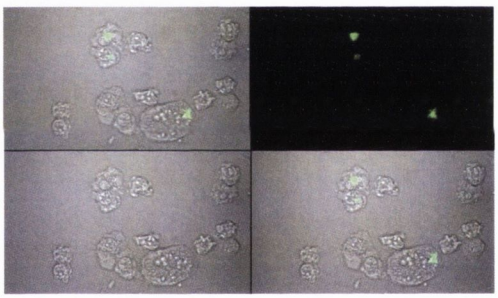
(C)



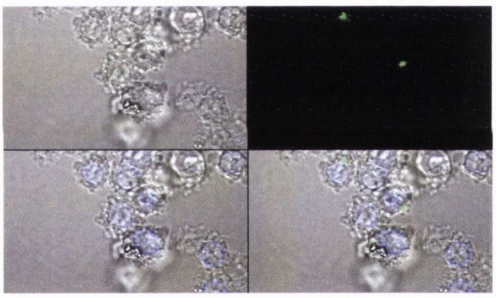
(D)



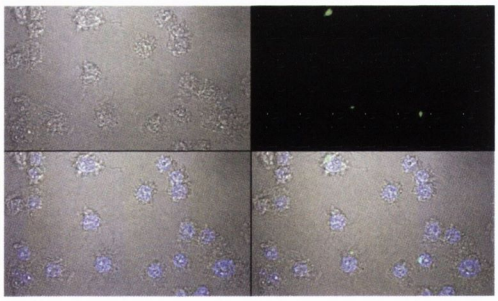
(E)



(F)



(G)



(H)

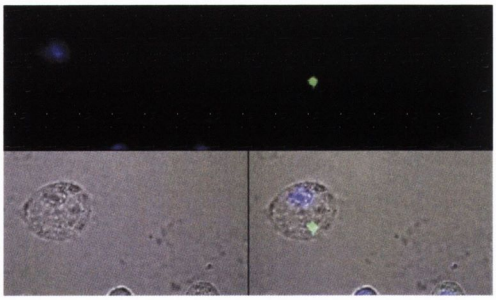


Figure 5.10 ASC specks begin to form after 15 minutes LPS. ASC-FP cells were set up at 2 x 10^5 in glass bottom confocal dishes. 24 hours later cells were stimulated as described below and viewed by live cell imaging using an Olympus FluoViewTM FV1000 Microscope equipped with a temperature and CO_2 controlled chamber. Images in the top left panel show phase contrast, the top right panel shows ASC-FP, the bottom left panel shows phase contrast and the nuclear stain Hoechst and the bottom right panel shows phase contrast, ASC-FP and the nuclear stain Hoechst. Cells were stimulated with 10 ng/ml LPS only **(A)** or 5 mM ATP only **(B)**. Cells were stimulated with 10 ng/ml LPS for 5 minutes **(C)**, 15 minutes **(D)**, 30 minutes **(E)**, 60 minutes **(F)**, 120 minutes **(G)**, 180 minutes **(H)** and 5 mM ATP. This result represents two independent experiments.

caspase-1 inhibitor YVAD for 1 hour prior to stimulating with 10 ng/ml LPS and 5 mM ATP. As shown in Figure 5.11, YVAD treatment did not affect the ability of ASC to form specks indicating that the ASC complex forms prior to caspase-1 activation.

5.2.3.4 ASC speck formation requires new protein synthesis

To determine if new protein synthesis was required for ASC speck formation, cells were pre-treated with the protein syntheisis inhibitor cyclohexamide. Pre-treatment of cells with 20 μg/ml cyclohexamide led to a reduction in the amount of ASC specks, shown in Figure 5.12, indicating that *de novo* protein syntheses was required for ASC speck formation. Earlier, Figure 5.1 showed that *de novo* synthesis of ASC is not needed, so this result therefore implies that synthesis of other proteins is needed.

5.2.3.5 ASC complex formation is inhibited in the presence of MG132

It has previously been suggested that the proteasome may play a role in inflammasome activation (Wickliffe *et al.*, 2008). Therefore, it was tested whether pre-treatment with the proteosome inhibitor MG132 was able to block speck formation. As shown in Figure 5.13 pre-treatment of cells with 5 μm of MG132 followed by LPS and ATP resulted in a reduced number of ASC specks forming indicating that the proteosome may play a role in inflammasome formation.

5.2.3.5.1 ASC contains many possible sites of ubiquitination

Proteins that are targeted for proteosomal degradation are ubiquitinated. It was therefore hypothesized that ASC may undergo ubiquitination. The ASC protein was analysed using bioinformatics to see if it contained any potential ubiquitination sites. Predicted

sites of ubiquitination were found using BDM-PUB (http://bdmpub.biocuckoo.org/). Figure 5.14 shows the possible sites of ubiquitination in the ASC protein.

5.2.3.5.2 ASC is not ubiquitinated

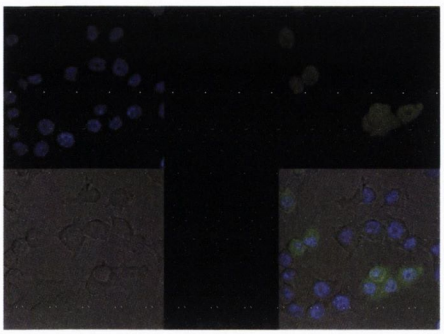
It was therefore investigated whether ASC could undergo ubiquitination. Several approaches were used, but I was unable to show that ASC could be ubiquitinated. Results are shown in Figure 5.15. HA-Ubiquitin and ASC were transfected into TLR4-MD2-CD14 HEK293 cells. After 24 hours, HA was immunoprecipitated from cells and samples were immunoblotted with ASC. There was no evidence of any ubiquitination of ASC in untreated cells (A) or in cells treated with LPS (B).

5.2.3.6 ASC speck formation is dependent on kinase signalling events

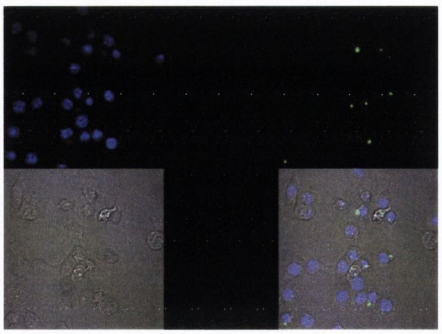
As speck formation appears to be a rapid process the involvement of protein kinases was addressed. Since little is known about the specific signalling events involved in ASC speck formation a variety of kinase inhibitors were tested to see if any had an effect on ASC speck formation. Firstly, cells were analysed to ensure they were responsive. Figure 5.16 (A) shows that resting cells have a cytoplasmic distribution of ASC and Figure 5.16 (B) shows that when cells are treated with 10 ng/ml LPS for 3 hours and 5 mM ATP for 1 hour, ASC redistributes into a speck. To analyse the effects of kinase inhibitors on ASC speck formation, cells were pre-treated for 1 hour with the inhibitor and then LPS and ATP were added as normal.

PD98059 is an inhibitor of the MAP kinase pathway. Specifically, it inhibits MEK-1, by binding to inactive MEK-1 and thereby preventing downstream activation. Pre-treatment with 25 μM of PD98059 prior to LPS and ATP stimulation resulted in a

(A)



(B)



(C)

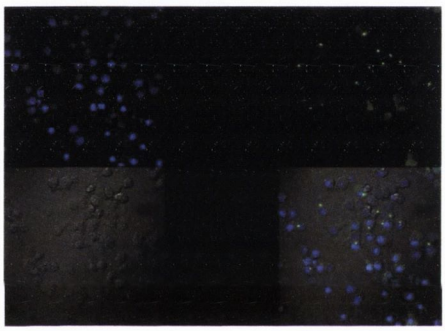


Figure 5.11 ASC speck formation is upstream of caspase-1 activation. ASC-FP cells were set up at 2 x 10^5 in glass bottom confocal dishes. 24 hours later cells were stimulated as described below and viewed by live cell imaging using an Olympus FluoViewTM FV1000 Microscope equipped with a temperature and CO_2 controlled chamber. Images in the top left panel show the nuclear stain Hoechst, the top right panel shows ASC-FP, the bottom left panel shows phase contrast and the bottom right panel shows phase contrast, ASC-FP and the nuclear stain Hoechst. Cells were **(A)** unstimulated, **(B)** stimulated with 10 ng/ml LPS for 3 hours and 5 mM ATP for 1 hour or **(C)** pre-treated with 100 μM YVAD for 1 hour and then stimulated with 10 ng/ml LPS for 3 hours and 5 mM ATP for 1 hour. The number of cells containing ASC specks or cytoplasmic ASC were counted in 5 separate fields and used to determine if YVAD treatment was affecting ASC speck formation. The result shown represents two independent experiments.

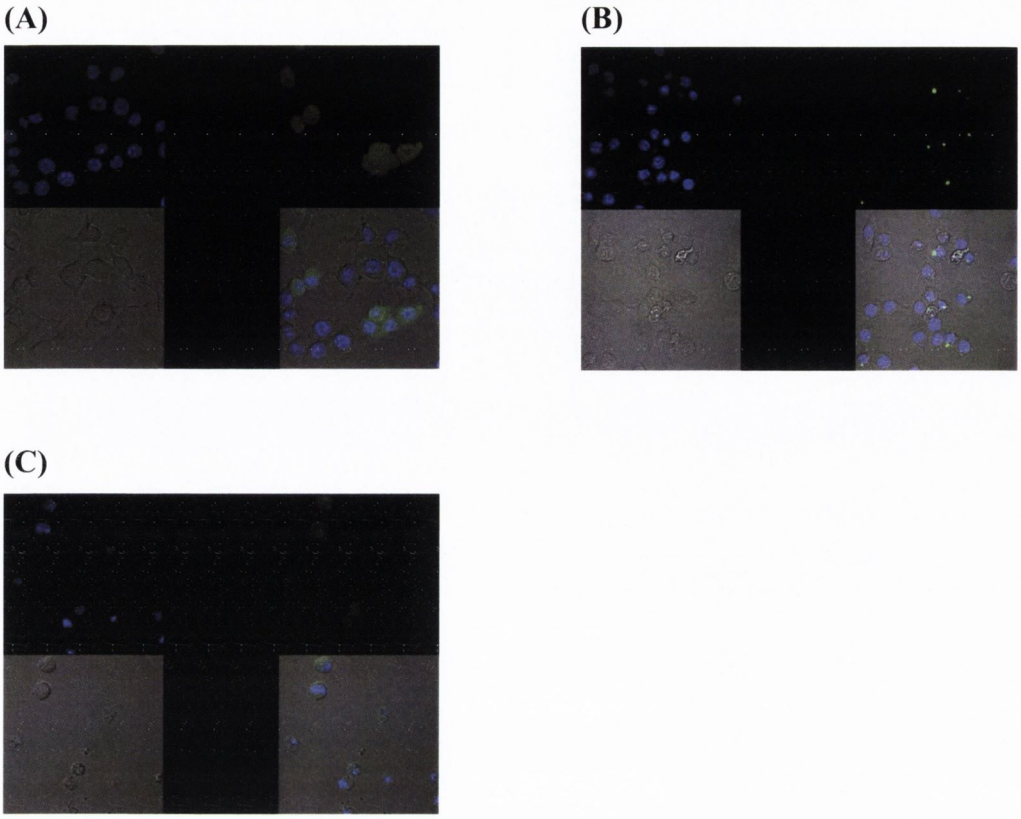


Figure 5.12 ASC speck formation requires de novo protein synthesis. ASC-FP cells were set up at 2 x 10^5 in glass bottom confocal dishes. 24 hours later cells were stimulated as described below and viewed by live cell imaging using an Olympus FluoViewTM FV1000 Microscope equipped with a temperature and CO_2 controlled chamber. Images in the top left panel show the nuclear stain Hoechst, the top right panel shows ASC-FP, the bottom left panel shows phase contrast and the bottom right panel shows phase contrast, ASC-FP and the nuclear stain Hoechst. Cells were **(A)** unstimulated, **(B)** stimulated with 10 ng/ml LPS for 3 hours and 5 mM ATP for 1 hour or **(C)** pre-treated with 20 μg/ml Cyclohexamide for 1 hour and then stimulated with 10 ng/ml LPS for 3 hours and 5 mM ATP for 1 hour. The number of cells containing ASC specks or cytoplasmic ASC were counted in 5 separate fields and used to determine if cyclohexamide treatment was affecting ASC speck formation. The result shown represents two independent experiments.

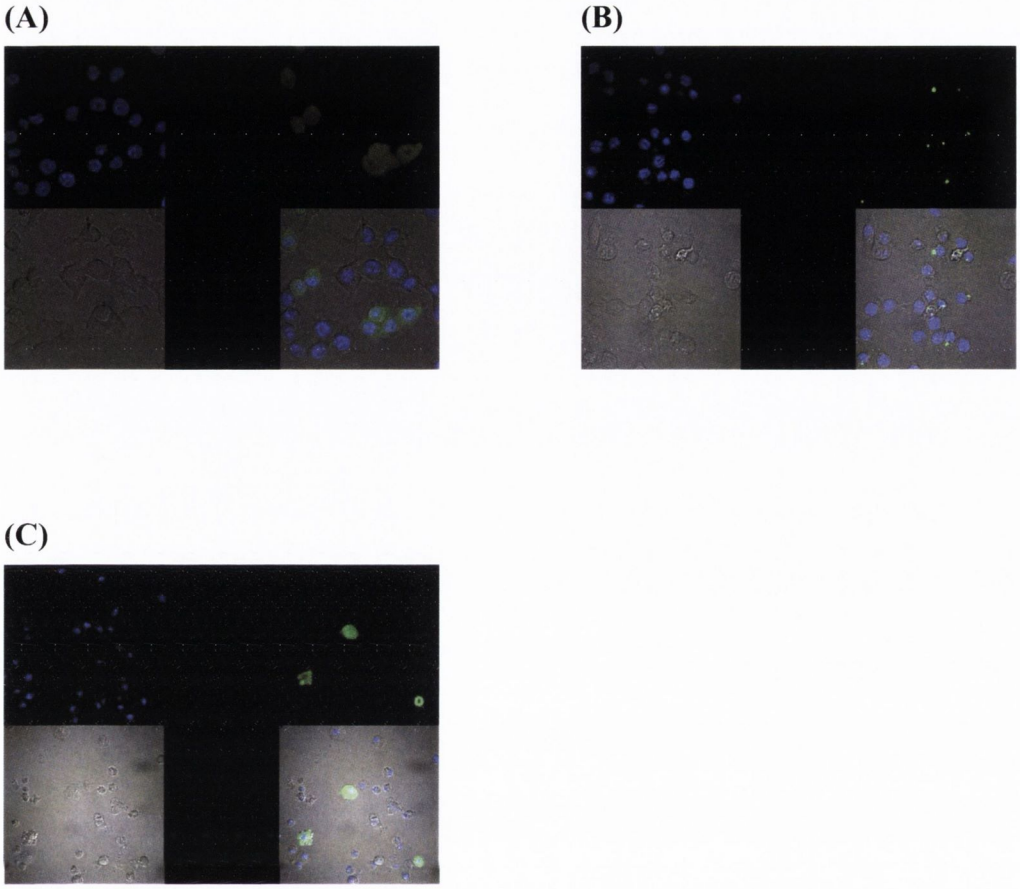


Figure 5.13 ASC speck formation is inhibited in the presence of MG132. ASC-FP cells were set up at 2 x 10^5 in glass bottom confocal dishes. 24 hours later cells were stimulated as described below and viewed by live cell imaging using an Olympus FluoViewTM FV1000 Microscope equipped with a temperature and CO_2 controlled chamber. Images in the top left panel show the nuclear stain Hoechst, the top right panel shows ASC-FP, the bottom left panel shows phase contrast and the bottom right panel shows phase contrast, ASC-FP and the nuclear stain Hoechst. Cells were **(A)** unstimulated, **(B)** stimulated with 10 ng/ml LPS for 3 hours and 5 mM ATP for 1 hour or **(C)** pre-treated with 5 μM MG132 for 1 hour and then stimulated with 10 ng/ml LPS for 3 hours and 5 mM ATP for 1 hour. The number of cells containing ASC specks or cytoplasmic ASC were counted in 5 separate fields and used to determine if MG132 treatment was affecting ASC speck formation. The result shown represents two independent experiments.

MGRARDAILDALENLTAEELKKFKLKLLSVPLREGYGRIPRGALLSMDAL

DLTDKLVSFYLETYGAELTANVLRDMGLQEMAGQLQAATHQGSGAAPA

GIQAPPQSAAKPGLHFIDQHRAALIARVTNVEWLLDALYGKVLTDEQYQ

AVRAEPTNPSKMRKLFSFTPAWNWTCKDLLLQALRESQSYLVEDLERS

Peptide	Position	Score	Threshold
NLTAEELKKFKLKLL	21	1.85	0.30
LTAEELKKFKLKLLS	22	0.66	0.30
AEELKKFKLKLLSVP	24	1.88	0.30
ELKKFKLKLLSVPLR	26	1.95	0.30
DALDLTDKLVSFYLE	55	0.38	0.30
APPQSAAKPGLHFID	109	1.74	0.30
LLDALYGKVLTDEQY	139	0.63	0.30
AEPTNPSKMRKLFSF	158	1.34	0.30
TNPSKMRKLFSFTPA	161	1.15	0.30

Figure 5.14 ASC contains numerous potential ubiquitination sites. Predicted ubiquitination sites of ASC were obtained using the BDM-PUB database (http://bdmpub.biocuckoo.org).

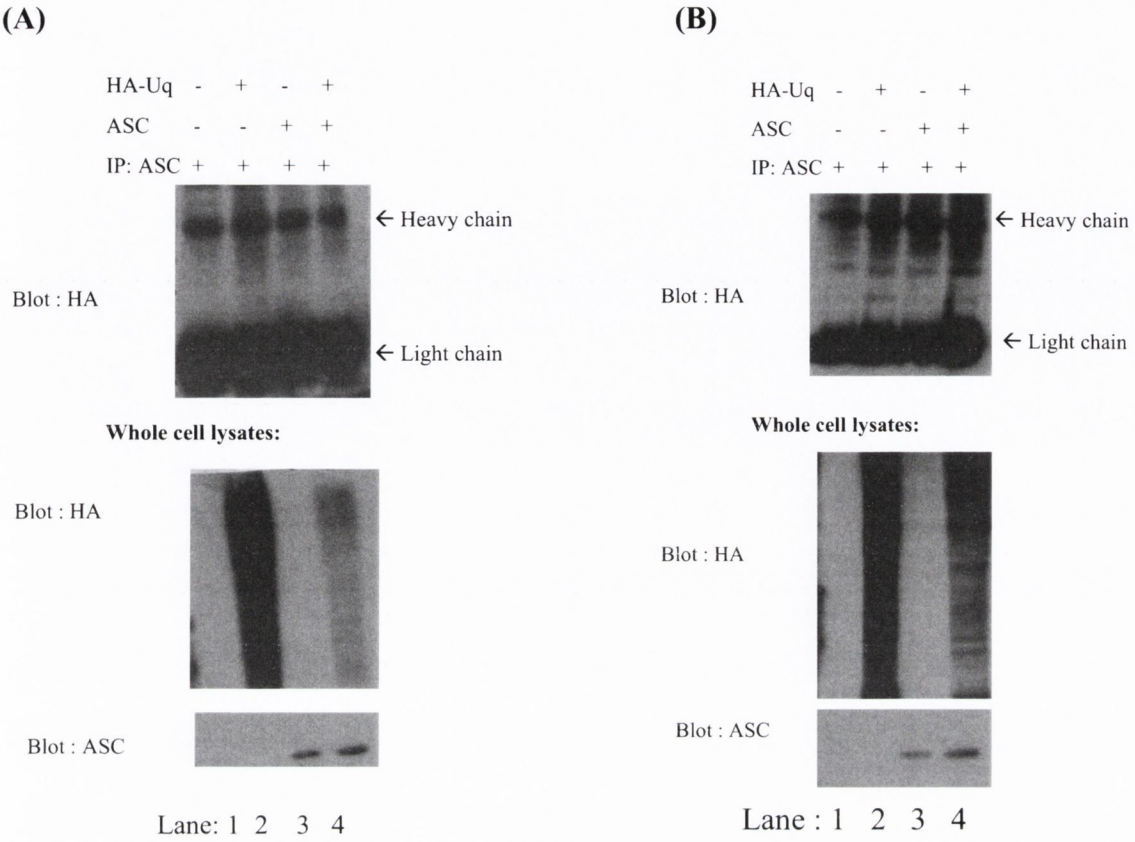


Figure 5.15 ASC does not get ubiquitinated. TLR4-MD2-CD14 HEK293cells were set up at 2 x 10^5 per ml in 6-well plates. 24 hours later cell were transfected with 1 µg of HA-ubiquitin or ASC for 48 hours. Cells were left untreated **(A)** or treated with 100 ng/ml LPS overnight **(B)**. Cells were harvested in low astringency lysis buffer. A 50 µl sample of lysate was removed so that protein expression could be analysed in lysates. The remaining lysate was pre-cleared twice with 10 µl protein A/G beads for 30 minutes. Lysates were incubated with 20 µl of beads and 1 µg of ASC antibody for 4 hours at 4 ˚C with gentle rolling. Lysates were washed 3 times in 1 ml of lysis buffer and 35 µl of sample buffer was added. IP samples and cell lysates were separated on 12 % gels, analysed by Western blotting and immuno-blotted for HA and ASC as indicated. This result represents 2 independent experiments.

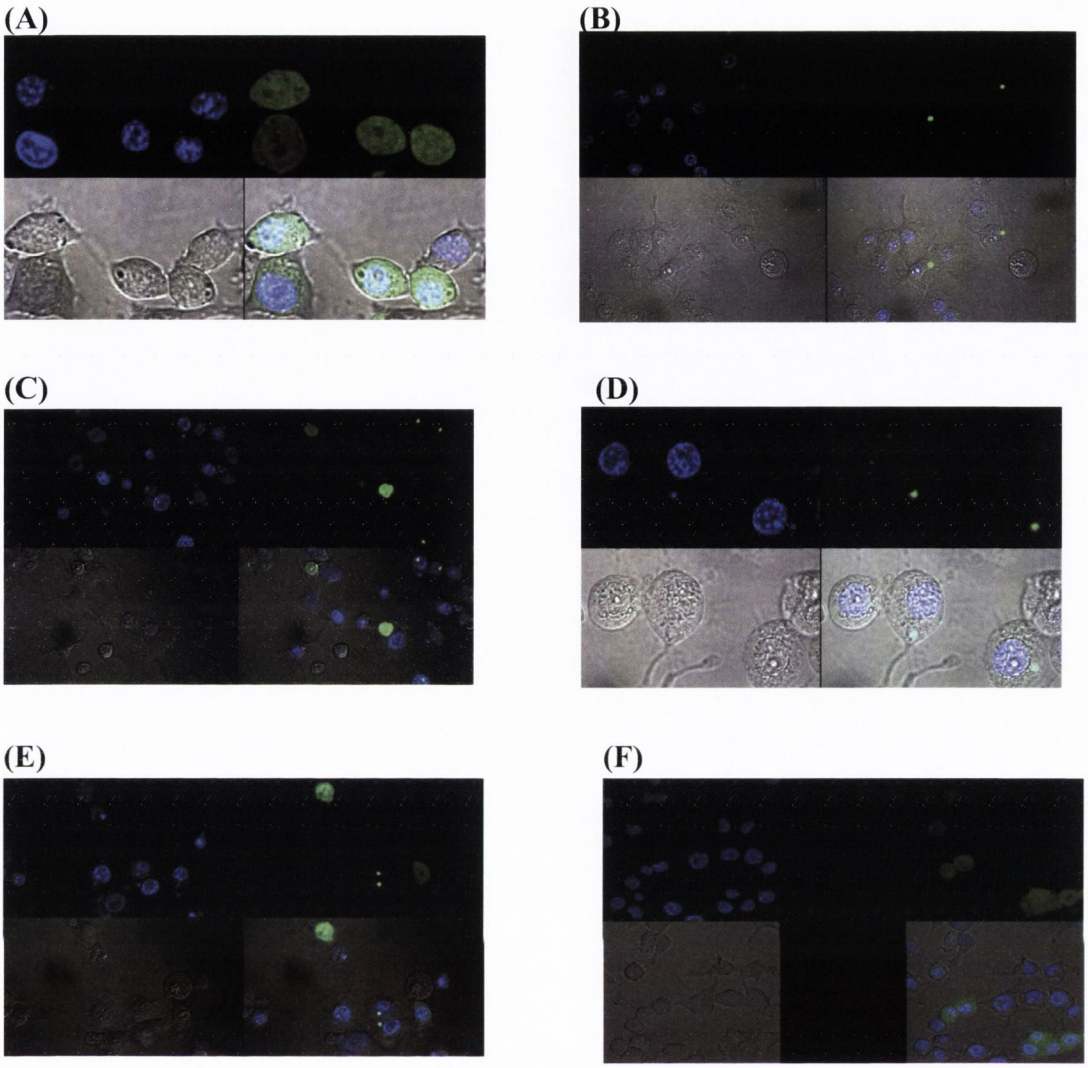


Figure 5.16 ASC speck formation is dependent on kinase signalling events. ASC-FP cells set up at 2 x 10^5 in glass bottom confocal dishes. 24 hours later cells were stimulated as described below and viewed by live cell imaging using an Olympus FluoViewTM FV1000 Microscope equipped with a temperature and CO_2 controlled chamber. Images in the top left panel show the nuclear stain Hoechst, the top right panel shows ASC-FP, the bottom left panel shows phase contrast and the bottom right panel shows phase contrast, ASC-FP and the nuclear stain Hoechst. Cells were **(A)** unstimulated or **(B)** stimulated with 10 ng/ml LPS for 3 hours and 5 mM ATP for 1 hour. Cells were pretreated with 25 μM of the MEK1 inhibitor PD 98059 **(C)**, or 10 μM of Akt inhibitor **(D)**, or the PKC-δ inhibitor Rotlerin **(E)** or 1.6 μM of the PTK inhibitor SU6656 **(F)** for 1 hour and then stimulated with 10 ng/ml LPS for 3 hours and 5 mM ATP for 1 hour. The number of cells containing ASC specks or cytoplasmic ASC were counted in 5 separate fields and used to determine if inhibitor treatment was affecting ASC speck formation. The result shown represents three independent experiments.

50 % reduction of ASC speck formation in cells (Figure 5.16 (C)). This result means that the MAP kinase pathway is important for inflammasome signalling.

AKT is an important kinase on the phospho-inositide (PI) - 3 kinase pathway. The AKT inhibitor is a phospatidylinositol ether analog that potently and selectively inhibits AKT. Pre-treatment with 10 μM AKT inhibitor, led to a slight reduction (10 %) in ASC speck formation (Figure 5.16 (D)). This result indicates that AKT and perhaps the entire PI 3-kinase pathway is not essential for inflammasome formation.

To determine if protein kinase C (PKC) had a role in ASC speck formation, cells were pre-treated with Bisindolylmaleimide (Bis) 1, which is a general inhibitor of PKC. However, this inhibitor was found to auto-fluoresce and could not be used to look at ASC speck formation. An alternative PKC inhibitor was used called Rottlerin which is a specific inhibitor of PKC-δ. Pre-treatment with this inhibitor showed a 50 % reduction in ASC speck formation (Figure 5.16 (E)). This result indicates that PKC- δ plays a role in inflammasome formation.

Tyrosine kinases are important in many signalling pathways. SU6656 is an inhibitor of Src, Fyn, Yes and Lyn tyrosine kinases. Pre-treatment with 1.6 μM of SU6656 showed a 100 % reduction in ASC speck formation (Figure 5.16 (F)). This result indicates that tyrosine kinase signalling is essential for inflammasome formation.

Together, these results highlight that many important signalling events are necessary for inflammasome. The tyrosine kinase inhibitor, SU6656, had the most dramatic effect on

ASC speck formation. Therefore, it was decided to further investigate the role of tyrosine kinase signalling in inflammasome formation.

5.2.3.6.1 ASC contains many potential phosphorylation sites

Since it was clear that tyrosine kinase signalling events were needed for ASC speck formation to happen, it was next assessed whether ASC itself could be phosphorylated. The protein sequence of ASC was analysed to see if it contained any potential phosphorylation sites. The NetPhos 2.0 database was used to predict potential phosphorylation sites. Both the mouse and human sequences of ASC were analysed. In the mouse sequence, there were 14 sites above the required threshold. In the human sequence, there were 4 sites above the required threshold. These are listed in Figure 5.17 (A). Those sites which are conserved between the two species are highlighted in grey. The sequences of mouse and human ASC were aligned and those sites which are conserved are highlighted in grey as shown in Figure 5.17 (B). The conserved sites are Y36, T127 and Y146. The fact that these sites have high prediction scores (0.627, 0.798 and 0.906 respectively) and are conserved substantiates the idea that ASC may be phosphorylated.

5.2.3.6.2 ASC is phosphorylated

Earlier results had shown that a tyrosine kinase inhibitor could prevent ASC speck formation, and now it was evident that ASC contained two conserved putative tyrosine phosphorylation sites. The next step therefore was to examine if ASC could be phosphorylated. Cells that were stably transfected with ASC were pre-treated with 1.6 μM of the protein tyrosine kinase inhibitor SU6656 for 1 hour and then stimulated with 10 ng/ml LPS for 3 hours and 5 mM ATP for 1 hour. Cells were lysed and ASC was

(A)

Phosphorylation sites in mouse ASC

Position	Context	Score	Site
16	LENLSGDEL	0.959	*S*
36	LREGYGRIP	0.627	*Y*
58	DKLVSYYLE	0.852	*S*
87	EQLQTTKEE	0.979	*T*
88	QLQTTKEES	0.694	*T*
92	TKEESGAVA	0.758	*S*
105	VPAQSTART	0.878	*S*
106	PAQSTARTG	0.682	*T*
125	IARVTEVDG	0.912	*T*
144	TEGQYQAVR	0.880	*Y*
151	VRAETTSQD	0.893	*T*
152	RAETTSQDK	0.952	*T*
153	AETTSQDKM	0.852	*S*
170	SWNLTCKDS	0.735	*T*

Phosphorylation sites in human ASC

Position	Context	Score	Site
36	LREGYGRIP	0.627	*Y*
127	IARVTNVEW	0.798	*T*
146	TDEQYQAVR	0.906	*Y*
184	ALRESQSYL	0.783	*S*

(B)

```
mouse          MGRARDAILDALENLSGDELKKFKMKLLTVQLREGYGRIPRGALLQMDAIDLTDKLVSYY 60
human          MGRARDAILDALENLTAEELKKFKLKLLSVPLREGYGRIPRGALLSMDALDLTDKLVSFY 60
               ***************:.:******:***:* ****.*********.***:********:*

mouse          LESYGLELTMTVLRDMGLQELAEQLQTTKEE-SGAVAAAASVPAQSTARTG-HFVDQHRQ 118
human          LETYGAELTANVLRDMGLQEMAGQLQAATHQGSGAAPAGIQAPPQSAAKPGLHFIDQHRA 120
               **:** *** .*********:* ***::.:: ***..*. ..*.**:*:.* **:****

mouse          ALIARVTEVDGVLDALHGSVLTEGQYQAVRAETTSQDKMRKLFSFVPSWNLTCKDSLLQA 178
human          ALIARVTNVEWLLDALYGKVLTDEQYQAVRAEPTNPSKMRKLFSFTPAWNWTCKDLLLQA 180
               *******:*: :****:*.***: ********.*. .********.*:** **** ****

mouse          LKEIHPYLVMDLEQS 193
human          LRESQSYLVEDLERS 195
               *:* :.*** ***:*
```

Figure 5.17 Predicted phosphorylation sites of ASC. (A) Potential sites of phosphorylation in both mouse and human ASC were predicted using NetPhos 2.0 (www.cbs.dtu.dk/services/NetPhos/). Those sites above the 0.5 threshold score are listed. The scores of each predicted site are also given. Sites that are conserved between the mouse and human sequences are listed. **(B)** The human and mouse ASC sequences were aligned using Clustal W2 (www.ebi.ac.uk/Tools/clustalw2) and conserved phosphorylation sites are highlighted in boxes.

immuoprecipitated from the cells using the ASC antibody or an IgG control. Samples were run on a 12 % gel and immunoblotted with 4G10, a phosphotyrosine specific antibody. The results are shown in Figure 5.18. When ASC was immunoprecipitated from the cells it could be detected by the phospho-tyrosine antibody (lanes 3 and 4). This did not occur when cells were pre-treated with the tyrosine kinase inhibitor (lanes 5 and 6). There was no band in the IgG control (lanes 1 and 2) confirming that no non-specific proteins were immuno-precipitated by the ASC antibody. The middle blot shows that equal amounts of ASC were immunoprecipitated (lanes 3 -6). The lower band in this blot is the light chain of the antibody. Cell lysates (lower blot) were taken prior to the immunoprecipitation, analysed by Western blotting and probed for ASC to confirm that equal amounts of ASC were present in each of the samples.

Together, these results suggest that ASC is phosphorylated on a tyrosine residue. Y146 is the most promising candidate site for phosphorylation and results suggest that ASC phosphorylation is necessary for inflammasome formation.

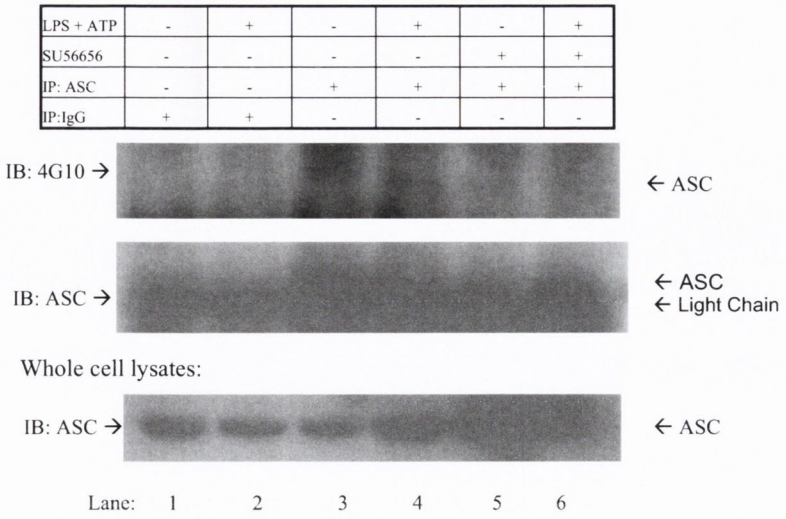


Figure 5.18 ASC is phosphorylated on a tyrosine residue. Immortalised macrophages stably transfected with ASC were set up at 2 x 10^5 per ml in 6-well plates. 24 hours later cells were stimulated with 1.6 μM of the PTK inhibitor SU56656 (lanes 5 and 6) for 1 hour, followed by 3 hours stimulation with 10 ng/ml LPS and 1 hour of 5 mM ATP. Cells were lysed in 400 μl of low astringency lysis buffer. 50 μl of lysate was removed for whole cell lysate analysis. The remaining lysate was pre-cleared with 15 μl Protein A/G beads for 1 hour. 1 μg of ASC antibody (or 1 μg of rabbit IgG control) and 25 μl Protein A/G beads were added to the lysates and cells were incubated at 4 °C for 3 hours with gentle rolling. Beads were washed 3 times in 1 ml of lysis buffer and 35 μl sample buffer was added. Samples were separated on 12 % gels and analysed by Western blotting. The anti-phosphotyrosine antibody 4G10 was used to detect tyrosine phosphorylated products. Samples were also immunoblotted with ASC. Whole cell lysates were immunoblotted with ASC. This result represents 3 independent experiments.

5.3 Discussion

The aim of this chapter was to investigate the protein ASC and to further understand its role in inflammasome signalling. Although a vast amount of knowledge has been acquired with regard to the ligands that activate the inflammasome and the downstream signalling events, little has been published on the upstream signalling events.

As an initial method to discover more about ASC and its role in inflammasome signalling a mass spec screen was carried out to identify novel binding partners of ASC. A variety of putative binding partners of ASC were uncovered. One of these proteins, PSTPIP1, was further investigated but could not be confirmed by Co-IP to bind to ASC. In light of recent evidence it is clear that another protein Pyrin is needed to bridge the gap between ASC and PSTPIP1 (Yu *et al.*, 2007, Waite *et al.*, 2009) and the interaction seen in the mass spectrometry screen was most likely an indirect association.

Other potentially interesting proteins were uncovered. For example, a peptide matching PML was identified. PML is a tumour suppressor essential for the induction of diverse apoptotic stimuli and exists in multiprotein complexes in the nucleus called PODs (PML oncogenic domains). Interestingly, PML is a member of the tripartite motif (TRIM) family, a family of proteins with roles in various cellular processes, including cell proliferation, differentiation, development, oncogenesis and apoptosis (Nisole *et al.*, 2005). Pyrin is also a member of the TRIM family and is a known interactor of ASC (Richards *et al.*, 2001). PML has been implicated in the defence against several viruses, including herpes simplex type 1, vesicular stomatitis virus, influenza A, and human cytomegalovirus (Tavalai *et al.*, 2006, Everett *et al.*, 1994, Doucas *et al.*, 1996). Cells deficient in PML also show reduced caspase-1 activity (Wang *et al.*, 1998). It is

tempting to speculate that PML may function with ASC in the inflammasome in viral defence.

Other proteins of interest found in the mass spectrometry screen include Q5T655 a LRR-domain containing protein; Q8N4F7 a RING-domain containing protein and a host of uncharacterised proteins with unknown functions.

The next approach to further understand ASC and its role in inflammasome signalling was to isolate ASC complexes from THP1 cells and BMDM cells that had been treated with various pro-inflammatory stimuli. Using this approach it was established that ASC complexes could be isolated from the cells. The complexes formed in a dose and time dependent manner to stimulation with LPS and ATP or Malp2 and ATP. Levels of ASC in the lysate remain constant, indicating that no new ASC is formed, but that it may redistribute into these complexes upon stimulation. ASC complex formation was seen in MyD88 deficient macrophages indicating that ASC complex formation was not MyD88 dependent. However, Bauernfeind *et al.* have shown that MyD88$^{-/-}$ or Trif $^{-/-}$ macrophages respond normally to LPS and ATP with processing of caspase-1 (Bauernfeind *et al.*, 2009). Cells that are both MyD88- and Trif- deficient fail to respond, indicating that the MyD88 and Trif pathways can compensate for each other in their ability to prime the inflammasome. Therefore, although results indicate that ASC speck formation is MyD88 independent, it is likely that Trif is compensating during LPS stimulation and Mal may be compensating during Malp2 stimulation.

Because of the technical difficulty isolating these complexes, a different approach was taken to look at ASC complex formation. Immortalised macrophages stably expressing fluorescently labelled ASC were used as an alternative tool to study ASC signalling.

Firstly, the results showed that ASC speck formation needed 2 signals; a TLR signal (LPS/Malp2/Poly IC) and an inflammasome signal (ATP). Time-course analysis showed that specks began to form after 15 minutes of LPS and 15 minutes of ATP treatment, but optimal speck formation occurs after 3 hours treatment with the first signal and 1 hour LPS. This is in agreement with recent results seen by another group (Bauernfeind *et al.*, 2009).

It is clear that this ASC assembly is upstream of caspase-1, as YVAD a caspase-1 inhibitor does not affect speck formation. This was in agreement with other published data (Fernandes-Alnemri *et al.*, 2007).

ASC speck formation was inhibited in the presence of cyclohexamide, a protein synthesis inhibitor indicating that de novo protein synthesis was required upstream of ASC. ASC itself is not induced but it has recently been revealed that NLRP3 must be induced and this occurs through NF-κB activation (Bauernfeind *et al.*, 2009).

MG132 is a proteosome inhibitor and is shown to inhibit ASC speck formation. Proteins targeted for the proteosome are ubiquitinated. Protein ubiquitination has emerged as a key mechanism that regulates immune responses. It has previously been suggested that components of the inflammasome undergo ubiquitination (Martinon *et al.*, 2002, Wickliffe *et al.*, 2008). ASC contains many possible ubiquitination sites and therefore it

seemed plausible that ASC could be ubiquitinated. However, it could not be shown that ASC was ubiquitnated. Several approaches were attempted, using different cells types and conditions. A recent publication explains why treatment with MG132 may have led to the inhibition of ASC speck formation. It is well publicised that NF-κB signalling is tightly regulated by ubiquitination and treatment with MG132 inhibits NF-κB activation by preventing IκB degradation. Since NF-κB signalling has been shown to be required for NLRP3 induction (Bauernfeind *et al.*, 2009), and NLRP3 induction is needed for ASC speck formation in response to ATP stimulation, ASC speck formation is inhibited in the presence of MG132.

ASC speck formation was inhibited in the presence of the PTK inhibitor, indicating that a tyrosine kinase signalling event was needed for ASC speck formation. Members of the PTK family include kinases belonging to the Src, Tec, JAK, Fes, Abl, FAK, Csk, and Syk families. The PTK inhibitor used, SU6656, is a specific inhibitor of the Src tyrosine kinases specifically Src, Fyl, Yes and Lyn.

Very recently, Syk kinase signalling, which is downstream of Src signalling, has been implicated in inflammasome activation. Gross *et al.* demonstrated that *C. albicans* activates the NALP3 inflammasome and using Syk deficient mice showed that that Syk signalling is essential for both pro-IL-1β synthesis and inflammasome activation (Gross *et al.*, 2009). Simultaneously, Shio *et al.*, revealed a pathway involving the Lyn (a Src kinase family member), Syk and Syk-downstream kinases such as PI3K and ERK that collectively are involved in the regulation of malarial Hz inflammasome activation. They were also able to show by Co-IP that ASC binds to Syk (Shio *et al.*, 2009). This

pathway involving Src and Syk signalling is clearly of importance to inflammasome assembly and activation.

Confirming that ASC itself undergoes phosphorylation, results show that ASC can be immunoprecipitated and probed with a phospho-tyrosine specific antibody and this interaction is inhibited in the presence of the PTK inhibitor SU6656. ASC contains several potential tyrosine phosphorylation sites, in particular Y146 has a very high score and this may be the most promising phosporylation site to investigate in the future.

Post-translational modification of ASC by tyrosine phosphorylation could be a way of altering the structural confirmation of the protein. It has previously been suggested that phosphorylation of ASC could alter the structure of ASC such that it dissociates from its inhibitor POP1 (Srimathi *et al.*, 2008). Removing of the POP1 inhibitor could allow ASC to interact with other inflammasome components thereby facilitating caspase-1 recruitment and activation.

As well as being part of the inflammasome, ASC is also reported to be a part of another complex involved in caspase-1 dependent cell death termed the pyroptosome (Fernandes-Alnemri *et al.*, 2007). It has been proposed by a few groups that ASC can form different complexes that facilitate either effective IL-1β secretion (inflammasomes) or cell death (pyroptosomes, pyronecrosomes), (Bryan *et al.*, 2009, Saleh *et al.*, 2007) and that this may be due to levels of caspase-1 activation within the cell. For example, a low level of caspase-1 activation would result in the processing and secretion of pro-inflammatory stimuli. As caspase-1 has been shown to be released from the cell, this may be a mechanism by the cell to remove the cell death machinery from

the cell. On the other hand, increased caspase-1 activation inside the cell could result in caspase-1 dependent cell death. The precise mechanisms of inflammasome versus pyroptosome formation remain to be discovered.

To summarise, this chapter has looked at ASC, a central component of the inflammasome. Mass spectrometry analysis has unveiled a host of potential novel binding partners of ASC. Investigation into YFP-ASC complex formation has revealed a range of signalling events needed for inflammasome formation in particular the role of tyrosine kinase signalling and phosphorylation of ASC.

The molecular mechanisms involved in the signalling events needed for formation of the inflammasome are unfolding and future work in this fast-moving field will undoubtedly reveal the precise mechanisms of inflammasome regulation.

Chapter 6

Final Discussion and Future Perspectives

The innate immune system relies on a variety of PRRs such as TLRs and NLRs to sense microbial structures that are present in pathogens (Creagh *et al.*, 2006). The inflammasome requires input from both of these pathways to elicit an immune response. Pathogen recognition by TLRs is needed for upregulation of inflammasome components and pro-IL-1β, and further signalling through NLRs or AIM2 results in aggregation of inflammasome components and caspase-1 activation. Ultimately, caspase-1 activation results in the processing of pro-IL-1β to its active form which is then secreted from the cell. IL-1β then carries out a variety of functions within the body to help in the fight against invading pathogens.

Results gathered in the course of this thesis focus on various parts of this pathway. Firstly, the GTPase protein Rab39a was found to bind to caspase-1 through mass spectrometry. This binding was confirmed by co-immunoprecipitation and co-localisation experiments. The significance of this interaction was investigated and Rab39a was discovered to have a role in IL-1β secretion. Secondly, a plethora of proteins associated with ASC were uncovered by mass spectrometry. ASC complex formation was investigated and some of the signalling pathways involved in inflammasome formation were highlighted. Figure 6.1 highlights the main aspects of these results which were found in the course of this work.

Several questions remain to be answered to further understand these novel discoveries. In relation to Rab39a and its role in caspase-1-dependent IL-1β secretion the significance of Rab39a cleavage, the importance of the GTPase function of Rab39a and the precise role of Rab39a in exosomes are three key issues which need to be examined.

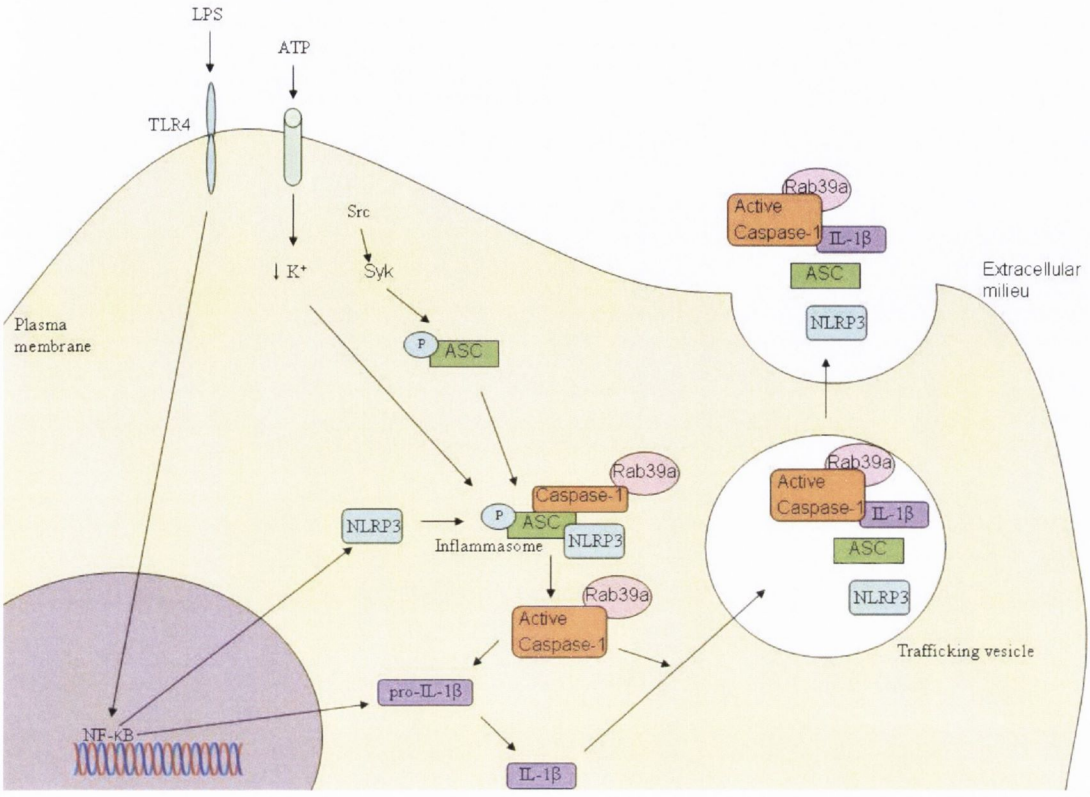


Figure 6.1 Model of signalling mechanisms associated with inflammasome formation and IL-1β release Signalling through TLRs results in the activation of NF-κB. This leads to the induction of NLRP3 and pro-IL-1β. A second signal from ATP leads to the assembly of the inflammasome, consisting of pro-caspase-1, ASC and NLRP3. Tyrosine phosphorylation signalling events are needed and tyrosine phosphorylation of ASC itself may be necessary for inflammasome formation. Assembly of the inflammasome leads to the activation of caspase-1 which leads to the processing and secretion of IL-1β. Rab39a binds to caspase-1 and is needed for the secretion most likely through trafficking vesicles such as exosomes. IL-1β and components of the inflammasome are secreted from the cell into the extracellular milieu.

Several ideas about why caspase-1 cleaves Rab39a were proposed in section 4.3. Future work in this area will elucidate the reasoning behind this highly conserved and specific processing of Rab39a. Rab4a, Rab14 and Rab25 also contain a caspase-1 cleavage site; however they do not undergo caspase-1 dependent processing. Several other Rab proteins contain the site so it will be interesting to test these in the future to determine if Rab39a is the only Rab protein that is processed by caspase-1 or if other Rab proteins possess this feature.

The relevance of the GTPase activity of Rab39a also needs to be clarified. Constitutively active and dominant negative forms of Rab39a still get cleaved by caspase-1 indicating that GTPase activity does not affect the cleavage. This could mean that cleavage is needed for Rab39a to be activated. Interestingly, it has been suggested that not all Rabs have the same requirement for GTP hydrolysis. Ypt1p, a Rab protein found in yeast, and the extensively studied Rab5, lack a requirement for GTPase activity (Richardson *et al.*, 1998, Rybin *et al.*, 1996). It will be interesting to assess the GTP requirement of Rab39a for its functions.

Results indicate that Rab39a is involved in the process of IL-1β secretion through exosome release, which is in agreement with the latest published work in the field (Qu *et al.*, 2007, Qu *et al.*, 2009). Future work needs to further investigate these exosomes and their role in IL-1β secretion. Exosomes are emerging as exciting conveyors of intercellular communication. Exosomes have been reported to carry antigenic material and peptide-MHC complexes, thereby acting as a source for antigen presenting cells. Recently it has been shown that exosomes carry mRNAs and microRNAs, highlighting a novel method of genetic exchange between cells (Valadi *et al.*, 2007). However, the

study of exosomes presents a challenge as it is difficult to either isolate or visualise these vesicles and novel methods are needed to manipulate vesicle secretion *in vivo*. Nevertheless, growing knowledge of the importance of exosomes in IL-1β release and in the immune response in general is an exciting new area of research providing potential lines of investigation for the future.

Results in chapter 4 suggested that as well as having a role in IL-1β secretion, Rab39a may also play a role in phagocytosis. Cytokine secretion and phagocytosis are two critical events in innate immunity that require significant membrane trafficking. This raises some interesting points about the role of Rab39a in these two events. Firstly, it is possible that the function of Rab39a in these two trafficking situations is separate. This is likely as most individual Rab proteins studied to date have each been shown to have a variety of different functions. Secondly, and more intriguingly it is plausible that these events are connected and Rab39a plays a regulatory role in their joint processes. Previously, Murray *et al.* (2005) found a joint trafficking pathway linking phagocytosis and cytokine secretion. They found that TNFα is trafficked from the Golgi to the recycling endosome, where vesicle-associated membrane protein 3 (VAMP3) mediates its delivery to the cell surface at the site of phagocytic cup formation. Fusion of the recycyling endosome at the cup simultaneously allows rapid release of TNFα and expands the membrane for phagocytosis. Perhaps Rab39a is important for mediating the secretion of IL-1β through a similar phagocytic process.

Autophagy is an area of much interest recently and the role of Rab39a in this process could prove worthy of investigation. Autophagy is a mechanism for the catabolism of cytosolic constituents (which are packaged into autophagosomes) during times of stress

and nutrient deprivation. Many other Rab proteins, such as Rab5, Rab7, Rab11, Rab24 and Rab33, have roles in autophagy (Longatti and Tooze, 2009). Autophagy is linked to innate and adaptive immune responses to numerous infectious microorganisms (Harris *et al.* 2009) and interestingly the processes of autophagy and inflammasome activation appear to be linked. For example, deficiency of Atg16L1, a core component of the autophagosome, leads to enhanced IL-1β production upon LPS stimulation (Saitoh *et al.* 2008). The mechanism underlying the regulation of inflammatory responses by autophagy is poorly understood, however these results suggest that autophagy may regulate inflammasome activation. As results in chapter 4 have shown, Rab39a is located on phagosomes and it would be interesting to see if it localised to autophagosomes and also plays a role in autphagy.

The results found in Chapter 5 also raise some concepts requiring further investigation. In particular investigation into some of the proteins found to associate with ASC in the inflammasome complex, the kinase signalling pathways involved in inflammasome signalling, and the relevance of tyrosine phosphorylation of ASC.

Inflammasomes are large complexes and it is likely that there are many proteins in inflammasomes which remain unidentified. Further investigation into some of the proteins found to associate with ASC could prove to be novel inflammasome components or indeed proteins involved in upstream or downstream pathways associated with the inflammasome.

Although rapid progress has been made in identifying inflammasome components, the mechanisms upstream of inflammasome activation are not well understood. Kinase

signalling events were deemed necessary for ASC complex formation and unravelling of these pathways will provide clues as to how inflammasomes are formed.

Tyrosine phosphorylation of ASC could prove to be a key mechanism of regulation. Future work could identify the precise amino acids which are needed for phosphorylation and then the significance of the phosphorylation event could be investigated.

Many hurdles remain to be overcome to further understand the inflammasome. For instance the function of other NLRPs in the inflammasome, the confirmation of novel substrates of caspase-1, and the mechanisms that control inflammasome assembly. Many activators of the NLRP3 inflammasome have been proposed and it remains to be seen what the common downstream pathway of these activators is. Luckily, the area of inflammasome research is expanding rapidly and the growth of knowledge in this area is opening up new areas of therapeutics and treatments of inflammatory diseases.

Elevated IL-1β levels have been shown in a multitude of auto-inflammatory diseases. A further understanding of how the inflammasome assembles to activate caspase-1 and process and release IL-1β is needed. How secretion of this cytokine occurs and how it is regulated may provide us with the tools to develop strategies to control aberrant inflammation due to increased IL-1β production.

Intracellular bacterial pathogens have evolved highly specialized mechanisms to invade and survive within their host. As described earlier, several pathogens exploit the functions of Rab proteins during their invasion process. Further investigations will

elucidate whether pathogens are also able to manipulate the localisation or functioning of Rab39a.

In conclusion, this work has identified that the small GTPase protein Rab39a is a novel binding partner of caspase-1 as identified by mass spectrometry and confirmed by co-immunoprecipitation and co-localisation experiments. The lack of a signal peptide indicates that IL-1β is secreted by a mechanism differing from that used for other secretory proteins and has previously been shown to be secreted in a caspase-1 dependent manner. Results shown here provide an extra link in this pathway and show that Rab39a is required for caspase-1 dependent IL-1β secretion from the cell. This work has also provided novel insights into proteins associated with the inflammasome and the signalling mechanisms involved in inflammasome assembly.

Continued research into these novel mechanisms, and in inflammasome research in general, will provide us with a further understanding of how the inflammasome functions in the innate defence system. A more complete understanding will then provide us with the tools necessary to target and hopefully treat inflammasome-mediated diseases.

Chapter 7

References

Akira, S. (2006). TLR signaling. *Curr Top Microbiol Immunol* **311,** 1-16.

Akira, S., Uematsu, S. and Takeuchi, O. (2006). Pathogen recognition and innate immunity. *Cell* **124,** 783-801.

Akita, K., Ohtsuki, T., Nukada, Y., Tanimoto, T., Namba, M., Okura, T., *et al.* (1997). Involvement of caspase-1 and caspase-3 in the production and processing of mature human interleukin 18 in monocytic THP.1 cells. *J Biol Chem* **272,** 26595-26603.

Aksentijevich, I., Masters, S.L., Ferguson, P.J., Dancey, P., Frenkel, J., van Royen-Kerkhoff, A., *et al.* (2009). An autoinflammatory disease with deficiency of the interleukin-1-receptor antagonist. *N Engl J Med* **360,** 2426-2437.

Allen, I.C., Scull, M.A., Moore, C.B., Holl, E.K., McElvania-TeKippe, E., Taxman, D.J., *et al.* (2009). The NLRP3 inflammasome mediates in vivo innate immunity to influenza A virus through recognition of viral RNA. *Immunity* **30,** 556-565.

Andrei, C., Dazzi, C., Lotti, L., Torrisi, M.R., Chimini, G. and Rubartelli, A. (1999). The secretory route of the leaderless protein interleukin 1beta involves exocytosis of endolysosome-related vesicles. *Mol Biol Cell* **10,** 1463-1475.

Andrei, C., Margiocco, P., Poggi, A., Lotti, L.V., Torrisi, M.R. and Rubartelli, A. (2004). Phospholipases C and A2 control lysosome-mediated IL-1 beta secretion: Implications for inflammatory processes. *Proc Natl Acad Sci U S A* **101,** 9745-9750.

Arend, W.P., Palmer, G. and Gabay, C. (2008). IL-1, IL-18, and IL-33 families of cytokines. *Immunol Rev* **223,** 20-38.

Arimoto, K., Takahashi, H., Hishiki, T., Konishi, H., Fujita, T. and Shimotohno, K. (2007). Negative regulation of the RIG-I signaling by the ubiquitin ligase RNF125. *Proc Natl Acad Sci U S A* **104,** 7500-7505.

Armstrong, J.A. and Hart, P.D. (1971). Response of cultured macrophages to Mycobacterium tuberculosis, with observations on fusion of lysosomes with phagosomes. *J Exp Med* **134,** 713-740.

Auron, P.E., Webb, A.C., Rosenwasser, L.J., Mucci, S.F., Rich, A., Wolff, S.M. and Dinarello, C.A. (1984). Nucleotide sequence of human monocyte interleukin 1 precursor cDNA. *Proc Natl Acad Sci U S A* **81,** 7907-7911.

Bailly, E., McCaffrey, M., Touchot, N., Zahraoui, A., Goud, B. and Bornens, M. (1991). Phosphorylation of two small GTP-binding proteins of the Rab family by p34cdc2. *Nature* **350,** 715-718.

Bakouche, O., Brown, D.C. and Lachman, L.B. (1987). Subcellular localization of human monocyte interleukin 1: evidence for an inactive precursor molecule and a possible mechanism for IL 1 release. *J Immunol* **138,** 4249-4255.

Balachandran, S., Thomas, E. and Barber, G.N. (2004). A FADD-dependent innate immune mechanism in mammalian cells. *Nature* **432,** 401-405.

Bauernfeind, F.G., Horvath, G., Stutz, A., Alnemri, E.S., MacDonald, K., Speert, D., *et al.* (2009). Cutting edge: NF-kappaB activating pattern recognition and cytokine receptors license NLRP3 inflammasome activation by regulating NLRP3 expression. *J Immunol* **183,** 787-791.

Bedoya, F., Sandler, L.L. and Harton, J.A. (2007). Pyrin-only protein 2 modulates NF-kappaB and disrupts ASC:CLR interactions. *J Immunol* **178,** 3837-3845.

Bergsbaken, T. and Cookson, B.T. (2007). Macrophage activation redirects yersinia-infected host cell death from apoptosis to caspase-1-dependent pyroptosis. *PLoS Pathog* **3,** e161.

Bernards, A. and Settleman J. (2004). GAP control: regulating the regulators of small GTPases. Trends Cell Biol 14, 377-85.

Beyaert, R., Kidd, V.J., Cornelis, S., Van de Craen, M., Denecker, G., Lahti, J.M., *et al.* (1997). Cleavage of PITSLRE kinases by ICE/CASP-1 and CPP32/CASP-3 during apoptosis induced by tumor necrosis factor. *J Biol Chem* **272,** 11694-11697.

Blom, N., Gammeltoft, S. and Brunak, S. (1999). Sequence and structure-based prediction of eukaryotic protein phosphorylation sites. *J Mol Biol* **294,** 1351-1362.

Boatright, K.M., Deis, C., Denault, J.B., Sutherlin, D.P. and Salvesen, G.S. (2004). Activation of caspases-8 and -10 by FLIP(L). *Biochem J* **382,** 651-657.

Bottger, G., Nagelkerken, B. and van der Sluijs, P. (1996). Rab4 and Rab7 define distinct nonoverlapping endosomal compartments. *J Biol Chem* **271,** 29191-29197.

Bourne, H.R., Sanders, D.A. and McCormick, F. (1991). The GTPase superfamily: conserved structure and molecular mechanism. *Nature* **349,** 117-127.

Boyden, E.D. and Dietrich, W.F. (2006). Nalp1b controls mouse macrophage susceptibility to anthrax lethal toxin. *Nat Genet* **38,** 240-244.

Brennan, M.A. and Cookson, B.T. (2000). Salmonella induces macrophage death by caspase-1-dependent necrosis. *Mol Microbiol* **38,** 31-40.

Brough, D. and Rothwell, N.J. (2007). Caspase-1-dependent processing of pro-interleukin-1beta is cytosolic and precedes cell death. *J Cell Sci* **120,** 772-781.

Bruey, J.M., Bruey-Sedano, N., Luciano, F., Zhai, D., Balpai, R., Xu, C., *et al.* (2007). Bcl-2 and Bcl-XL regulate proinflammatory caspase-1 activation by interaction with NALP1. *Cell* **129,** 45-56.

Brumell, J.H. and Scidmore, M.A. (2007). Manipulation of rab GTPase function by intracellular bacterial pathogens. *Microbiol Mol Biol Rev* **71,** 636-652.

Bryan, N.B., Dorfleutner, A., Rojanasakul, Y. and Stehlik, C. (2009). Activation of inflammasomes requires intracellular redistribution of the apoptotic speck-like protein containing a caspase recruitment domain. *J Immunol* **182,** 3173-3182.

Burckstummer, T., Baumann, C., Bluml, S., Dixit, E., Durnberger, G., Jahn, H., *et al.* (2009). An orthogonal proteomic-genomic screen identifies AIM2 as a cytoplasmic DNA sensor for the inflammasome. *Nat Immunol* **10,** 266-272.

Butler M., Hanly J., Moynagh P. (2007). Kinase-active interleukin-1 receptor-associated kinases promote polyubiquitination and degradation of the Pellino family: direct evidence for PELLINO proteins being ubiquitin-protein isopeptide ligases. J Biol Chem. **41**, 29729-29737.

Cao, W., Zhang, L., Rosen, D.B., Bover, L., Watanabe, G., Bao, M., *et al.* (2007). BDCA2/Fc epsilon RI gamma complex signals through a novel BCR-like pathway in human plasmacytoid dendritic cells. *PLoS Biol* **5,** e248.

Carta, S., Tassi, S., Semino, C., Fossati, G., Mascagni, P., Dinarello, C.A. and Rubartelli, A. (2006). Histone deacetylase inhibitors prevent exocytosis of interleukin-1beta-containing secretory lysosomes: role of microtubules. *Blood* **108,** 1618-1626.

Carty, M., Goodbody, R., Schroder, M., Stack, J., Moynagh, P.N. and Bowie, A.G. (2006). The human adaptor SARM negatively regulates adaptor protein TRIF-dependent Toll-like receptor signaling. *Nat Immunol* **7,** 1074-1081.

Cassel, S.L., Eisenbarth, S.C., Iyer, S.S., Sadler, J.J., Colegio, O.R., Tephly, L.A., *et al.* (2008). The Nalp3 inflammasome is essential for the development of silicosis. *Proc Natl Acad Sci U S A* **105,** 9035-9040.

Cayrol, C. and Girard, J.P. (2009). The IL-1-like cytokine IL-33 is inactivated after maturation by caspase-1. *Proc Natl Acad Sci U S A* **106,** 9021-9026.

Cervantes, J., Nagata, T., Uchijima, M., Shibata, K. and Koide, Y. (2008). Intracytosolic Listeria monocytogenes induces cell death through caspase-1 activation in murine macrophages. *Cell Microbiol* **10,** 41-52.

Chae, J.J., Komarow, H.D., Cheng, J., Wood, G., Raben, N., Liu, P.P. and Kastner, D.L. (2003). Targeted disruption of pyrin, the FMF protein, causes heightened sensitivity to endotoxin and a defect in macrophage apoptosis. *Mol Cell* **11,** 591-604.

Chae, J.J., Wood, G., Masters, S.L., Richard, K., Park, G., Smith, B.J. and Kastner, D.L. (2006). The B30.2 domain of pyrin, the familial Mediterranean fever protein, interacts directly with caspase-1 to modulate IL-1beta production. *Proc Natl Acad Sci U S A* **103,** 9982-9987.

Chae, J.J., Wood, G., Richard, K., Jaffe, H., Colburn, N.T., Masters, S.L., *et al.* (2008). The familial Mediterranean fever protein, pyrin, is cleaved by caspase-1 and activates NF-kappaB through its N-terminal fragment. *Blood* **112,** 1794-1803.

Chen, W. and Wandinger-Ness, A. (2001). Expression and functional analyses of Rab8 and Rab11a in exocytic transport from trans-Golgi network. *Methods Enzymol* **329,** 165-175.

Chen, Y., Smith, M.R., Thirumalai, K. and Zychlinsky, A. (1996). A bacterial invasin induces macrophage apoptosis by binding directly to ICE. *EMBO J* **15,** 3853-3860.

Cheng, H., Ma, Y., Ni, X., Jiang, M., Guo, L., Ying, K., *et al.* (2002). Isolation and characterization of a human novel RAB (RAB39B) gene. *Cytogenet Genome Res* **97,** 72-75.

Coban C., Ishii K.J., Kawai T., Hemmi H., Sato S., Uematsu S., Yamamoto M., Takeuchi O., Itagaki S., Kumar N., Horii T., Akira S. (2005). Toll-like receptor 9 mediates innate immune activation by the malaria pigment hemozoin. *J Exp Med.* **1**, 19-25.

Conway, K.E., McConnell, B.B., Bowring, C.E., Donald, C.D., Warren, S.T. and Vertino, P.M. (2000). TMS1, a novel proapoptotic caspase recruitment domain

protein, is a target of methylation-induced gene silencing in human breast cancers. *Cancer Res* **60,** 6236-6242.

Creagh, E.M. and O'Neill, L.A. (2006). TLRs, NLRs and RLRs: a trinity of pathogen sensors that co-operate in innate immunity. *Trends Immunol* **27,** 352-357.

Crowle, A.J., Dahl, R., Ross, E. and May, M.H. (1991). Evidence that vesicles containing living, virulent Mycobacterium tuberculosis or Mycobacterium avium in cultured human macrophages are not acidic. *Infect Immun* **59,** 1823-1831.

Cui, S., Eisenacher, K., Kirchhofer, A., Brzozka, K., Lammens, A., Lammens, K., *et al.* (2008). The C-terminal regulatory domain is the RNA 5'-triphosphate sensor of RIG-I. *Mol Cell* **29,** 169-179.

Delaloye, J., Roger, T., Steiner-Tardivel, Q.G., Le Roy, D., Knaup Reymond, M., Akira, S., *et al.* (2009). Innate immune sensing of modified vaccinia virus Ankara (MVA) is mediated by TLR2-TLR6, MDA-5 and the NALP3 inflammasome. *PLoS Pathog* **5,** e1000480.

Dinarello, C.A. (2009). Immunological and inflammatory functions of the interleukin-1 family. *Annu Rev Immunol* **27,** 519-550.

Dix, M.M., Simon, G.M. and Cravatt, B.F. (2008). Global mapping of the topography and magnitude of proteolytic events in apoptosis. *Cell* **134,** 679-691.

Dorfleutner, A., Bryan, N.B., Talbott, S.J., Funya, K.N., Rellick, S.L., Reed, J.C., *et al.* (2007). Cellular pyrin domain-only protein 2 is a candidate regulator of inflammasome activation. *Infect Immun* **75,** 1484-1492.

Dostert, C., Petrilli, V., Van Bruggen, R., Steele, C., Mossman, B.T. and Tschopp, J. (2008). Innate immune activation through Nalp3 inflammasome sensing of asbestos and silica. *Science* **320,** 674-677.

Doucas, V., Ishov, A.M., Romo, A., Juguilon, H., Weitzman, M.D., Evans, R.M. and Maul, G.G. (1996). Adenovirus replication is coupled with the dynamic properties of the PML nuclear structure. *Genes Dev* **10,** 196-207.

Dowds, T.A., Masumoto, J., Chen, F.F., Ogura, Y., Inohara, N. and Nunez, G. (2003). Regulation of cryopyrin/Pypaf1 signaling by pyrin, the familial Mediterranean fever gene product. *Biochem Biophys Res Commun* **302,** 575-580.

Eisenbarth, S.C., Colegio, O.R., O'Connor, W., Sutterwala, F.S. and Flavell, R.A. (2008). Crucial role for the Nalp3 inflammasome in the immunostimulatory properties of aluminium adjuvants. *Nature* **453,** 1122-1126.

Everett, R.D. and Maul, G.G. (1994). HSV-1 IE protein Vmw110 causes redistribution of PML. *EMBO J* **13,** 5062-5069.

Fairbrother, W.J., Gordon, N.C., Humke, E.W., O'Rourke, K.M., Starovasnik, M.A., Yin, J.P. and Dixit, V.M. (2001). The PYRIN domain: a member of the death domain-fold superfamily. *Protein Sci* **10,** 1911-1918.

Faustin, B., Lartigue, L., Bruey, J.M., Luciano, F., Sergienko, E., Bailly-Maitre, B., *et al.* (2007). Reconstituted NALP1 inflammasome reveals two-step mechanism of caspase-1 activation. *Mol Cell* **25,** 713-724.

Feldmeyer L., Keller M., Niklaus G., Hohl D., Werner S., Beer H.D. (2007). The inflammasome mediates UVB-induced activation and secretion of interleukin-1beta by keratinocytes. *Curr Biol.* **13**, 1140-5.

Fernandes-Alnemri, T., Wu, J., Yu, J.W., Datta, P., Miller, B., Jankowski, W., *et al.* (2007). The pyroptosome: a supramolecular assembly of ASC dimers mediating inflammatory cell death via caspase-1 activation. *Cell Death Differ* **14,** 1590-1604.

Fernandes-Alnemri, T., Yu, J.W., Datta, P., Wu, J. and Alnemri, E.S. (2009). AIM2 activates the inflammasome and cell death in response to cytoplasmic DNA. *Nature* **458,** 509-513.

Fitzgerald, M.L. and Reed, G.L. (1999). Rab6 is phosphorylated in thrombin-activated platelets by a protein kinase C-dependent mechanism: effects on GTP/GDP binding and cellular distribution. *Biochem J* **342,** 353-360.

Fukuda, M. (2008). Regulation of secretory vesicle traffic by Rab small GTPases. *Cell Mol Life Sci* **65,** 2801-2813.

Gack, M.U., Kirchhofer, A., Shin, Y.C., Inn, K.S., Liang, C., Cui, S., *et al.* (2008). Roles of RIG-I N-terminal tandem CARD and splice variant in TRIM25-mediated antiviral signal transduction. *Proc Natl Acad Sci USA* **105,** 16743-16748.

Geijtenbeek, T.B. and Gringhuis, S.I. (2009). Signalling through C-type lectin receptors: shaping immune responses. *Nat Rev Immunol* **9,** 465-479.

Gorvel, J.P., Chavrier, P., Zerial, M. and Gruenberg, J. (1991). rab5 controls early endosome fusion in vitro. *Cell* **64,** 915-925.

Goud, B., Salminen, A., Walworth, N.C. and Novick, P.J. (1988). A GTP-binding protein required for secretion rapidly associates with secretory vesicles and the plasma membrane in yeast. *Cell* **53,** 753-768.

Gringhuis, S.I., den Dunnen, J., Litjens, M., van Het Hof, B., van Kooyk, Y. and Geijtenbeek, T.B. (2007). C-type lectin DC-SIGN modulates Toll-like receptor signaling via Raf-1 kinase-dependent acetylation of transcription factor NF-kappaB. *Immunity* **26,** 605-616.

Gross, O., Gewies, A., Finger, K., Schafer, M., Sparwasser, T., Peschel, C., *et al.* (2006). Card9 controls a non-TLR signalling pathway for innate anti-fungal immunity. *Nature* **442,** 651-656.

Gross, O., Poeck, H., Bscheider, M., Dostert, C., Hannesschlager, N., Endres, S., *et al.* (2009). Syk kinase signalling couples to the Nlrp3 inflammasome for anti-fungal host defence. *Nature* **459,** 433-436.

Guan, X., Sagara, J., Yokoyama, T., Koganehira, Y., Oguchi, M., Saida, T. and Taniguchi, S. (2003). ASC/TMS1, a caspase-1 activating adaptor, is downregulated by aberrant methylation in human melanoma. *Int J Cancer* **107,** 202-208.

Gurcel, L., Abrami, L., Girardin, S., Tschopp, J. and van der Goot, F.G. (2006). Caspase-1 activation of lipid metabolic pathways in response to bacterial pore-forming toxins promotes cell survival. *Cell* **126,** 1135-1145.

Hacker, H., Redecke, V., Blagoev, B., Kratchmarova, I., Hsu, L.C., Wang, G.G., *et al.* (2006). Specificity in Toll-like receptor signalling through distinct effector functions of TRAF3 and TRAF6. *Nature* **439,** 204-207.

Halle, A., Hornung, V., Petzold, G.C., Stewart, C.R., Monks, B.G., Reinheckel, T., *et al.* (2008). The NALP3 inflammasome is involved in the innate immune response to amyloid-beta. *Nat Immunol* **9,** 857-865.

Harris J., Hope J., Lavelle E. (2009). Autophagy and the immune response to TB. *Transbound Emerg Dis* **6-7**, 248-54.

Hattula, K., Furuhjelm, J., Tikkanen, J., Tanhuanpaa, K., Laakkonen, P. and Peranen, J. (2006). Characterization of the Rab8-specific membrane traffic route linked to protrusion formation. *J Cell Sci* **119,** 4866-4877.

Hawes, C.R., Brandizzi, F. and Andreeva, A.V. (1999). Endomembranes and vesicle trafficking. *Curr Opin Plant Biol* **2,** 454-461.

Hemmi H., Takeuchi O., Kawai T., Kaisho T., Sato S., Sanjo H., Matsumoto M., Hoshino K., Wagner H., Takeda K., Akira S. (2000) A Toll-like receptor recognizes bacterial DNA. *Nature* **6813**, 740-5.

Hersh, D., Monack, D.M., Smith, M.R., Ghori, N., Falkow, S. and Zychlinsky, A. (1999). The Salmonella invasin SipB induces macrophage apoptosis by binding to caspase-1. *Proc Natl Acad Sci USA* **96,** 2396-2401.

Higgins, J.B. and Casey, P.J. (1996). The role of prenylation in G-protein assembly and function. *Cell Signal* **8,** 433-437.

Hilbi, H., Moss, J.E., Hersh, D., Chen, Y., Arondel, J., Banerjee, S., *et al.* (1998). Shigella-induced apoptosis is dependent on caspase-1 which binds to IpaB. *J Biol Chem* **273,** 32895-32900.

Hogquist, K.A., Unanue, E.R. and Chaplin, D.D. (1991). Release of IL-1 from mononuclear phagocytes. *J Immunol* **147,** 2181-2186.

Hornung V., Ellegast J., Kim S., Brzózka K., Jung A., Kato H., Poeck H., Akira S., Conzelmann K., Schlee M., Endres S., Hartmann G. (2006) 5'-Triphosphate RNA is the ligand for RIG-I. *Science* **5801**, 994-997.

Hornung, V., Bauernfeind, F., Halle, A., Samstad, E.O., Kono, H., Rock, K.L., *et al.* (2008). Silica crystals and aluminum salts activate the NALP3 inflammasome through phagosomal destabilization. *Nat Immunol* **9,** 847-856.

Hornung, V., Ablasser, A., Charrel-Dennis, M., Bauernfeind, F., Horvath, G., Caffrey, D.R., *et al.* (2009). AIM2 recognizes cytosolic dsDNA and forms a caspase-1-activating inflammasome with ASC. *Nature* **458,** 514-518.

Humke, E.W., Shriver, S.K., Starovasnik, M.A., Fairbrother, W.J. and Dixit, V.M. (2000). ICEBERG: a novel inhibitor of interleukin-1beta generation. *Cell* **103,** 99-111.

Ichinohe, T., Lee, H.K., Ogura, Y., Flavell, R. and Iwasaki, A. (2009). Inflammasome recognition of influenza virus is essential for adaptive immune responses. *J Exp Med* **206,** 79-87.

Ingmundson, A., Delprato, A., Lambright, D.G. and Roy, C.R. (2007). Legionella pneumophila proteins that regulate Rab1 membrane cycling. *Nature* **450,** 365-369.

Ishikawa, H. and Barber, G.N. (2008). STING is an endoplasmic reticulum adaptor that facilitates innate immune signalling. *Nature* **455,** 674-678.

Janeway, C.A., Jr. (1992). The immune system evolved to discriminate infectious nonself from noninfectious self. *Immunol Today* **13,** 11-16.

Jin, M.S., Kim, S.E., Heo, J.Y., Lee, M.E., Kim, H.M., Paik, S.G., *et al.* (2007). Crystal structure of the TLR1-TLR2 heterodimer induced by binding of a tri-acylated lipopeptide. *Cell* **130,** 1071-1082.

Junutula, J.R., De Maziere, A.M., Peden, A.A., Ervin, K.E., Advani, R.J., van Dijk, S.M., *et al.* (2004). Rab14 is involved in membrane trafficking between the Golgi complex and endosomes. *Mol Biol Cell* **15,** 2218-2229.

Kahns, S., Kalai, M., Jakobsen, L.D., Clark, B.F., Vandenabeele, P. and Jensen, P.H. (2003). Caspase-1 and caspase-8 cleave and inactivate cellular parkin. *J Biol Chem* **278,** 23376-23380.

Kamal, A. and Goldstein, L.S. (2000). Connecting vesicle transport to the cytoskeleton. *Curr Opin Cell Biol* **12,** 503-508.

Kanneganti, T.D., Body-Malapel, M., Amer, A., Park, J.H., Whitfield, J., Franchi, L., *et al.* (2006). Critical role for Cryopyrin/Nalp3 in activation of caspase-1 in response to viral infection and double-stranded RNA. *J Biol Chem* **281,** 36560-36568.

Kato, H., Sato, S., Yoneyama, M., Yamamoto, M., Uematsu, S., Matsui, K., *et al.* (2005). Cell type-specific involvement of RIG-I in antiviral response. *Immunity* **23,** 19-28.

Kato, H., Takeuchi, O., Sato, S., Yoneyama, M., Yamamoto, M., Matsui, K., *et al.* (2006). Differential roles of MDA5 and RIG-I helicases in the recognition of RNA viruses. *Nature* **441,** 101-105.

Kato H., Takeuchi O., Mikamo-Satoh E., Hirai R., Kawai T., Matsushita K., Hiiragi A., Dermody T., Fujita T., Akira S. (2008). Length-dependent recognition of double-stranded ribonucleic acids by retinoic acid-inducible gene-I and melanoma differentiation-associated gene 5. *J Exp Med* **7**, 1601-1610.

Kawai, T. and Akira, S. (2007). TLR signaling. *Semin Immunol* **19,** 24-32.

Kawai, T., Takahashi, K., Sato, S., Coban, C., Kumar, H., Kato, H., *et al.* (2005). IPS-1, an adaptor triggering RIG-I- and Mda5-mediated type I interferon induction. *Nat Immunol* **6,** 981-988.

Kayagaki, N., Phung, Q., Chan, S., Chaudhari, R., Quan, C., O'Rourke, K.M., *et al.* (2007). DUBA: a deubiquitinase that regulates type I interferon production. *Science* **318,** 1628-1632.

Keating S., Maloney G., Moran E., Bowie A. (2007). IRAK-2 participates in multiple toll-like receptor signaling pathways to NFkappaB via activation of TRAF6 ubiquitination. *J Biol Chem* **46**, 33435-33443.

Keller, M., Ruegg, A., Werner, S. and Beer, H.D. (2008). Active caspase-1 is a regulator of unconventional protein secretion. *Cell* **132,** 818-831.

Kenny, E.F., Talbot, S., Gong, M., Golenbock, D.T., Bryant, C.E. and O'Neill, L.A. (2009). MyD88 adaptor-like is not essential for TLR2 signaling and inhibits signaling by TLR3. *J Immunol* **183,** 3642-3651.

Kim, M.J. and Yoo, J.Y. (2008). Active caspase-1-mediated secretion of retinoic acid inducible gene-I. *J Immunol* **181,** 7324-7331.

Kinchen, J.M. and Ravichandran, K.S. (2008). Phagosome maturation: going through the acid test. *Nat Rev Mol Cell Biol* **9,** 781-795.

Kinoshita, T., Wang, Y., Hasegawa, M., Imamura, R. and Suda, T. (2005). PYPAF3, a PYRIN-containing APAF-1-like protein, is a feedback regulator of caspase-1-dependent interleukin-1beta secretion. *J Biol Chem* **280,** 21720-21725.

Kong, L., Sun, L., Zhang, H., Liu, Q., Liu, Y., Qin, L., *et al.* (2009). An essential role for RIG-I in toll-like receptor-stimulated phagocytosis. *Cell Host Microbe* **6,** 150-161.

Kyei, G.B., Vergne, I., Chua, J., Roberts, E., Harris, J., Junutula, J.R. and Deretic, V. (2006). Rab14 is critical for maintenance of Mycobacterium tuberculosis phagosome maturation arrest. *EMBO J* **25,** 5250-5259.

Lamkanfi, M., Denecker, G., Kalai, M., D'Hondt, K., Meeus, A., Declercq, W., *et al.* (2004). INCA, a novel human caspase recruitment domain protein that inhibits interleukin-1beta generation. *J Biol Chem* **279,** 51729-51738.

Lamkanfi, M. and Dixit, V.M. (2009). IL-33 raises alarm. *Immunity* **31,** 5-7.

Lamkanfi, M., Kanneganti, T.D., Van Damme, P., Vanden Berghe, T., Vanoverberghe, I., Vandekerckhove, J., *et al.* (2008). Targeted peptidecentric proteomics reveals caspase-7 as a substrate of the caspase-1 inflammasomes. *Mol Cell Proteomics* **7,** 2350-2363.

Lara-Tejero, M., Sutterwala, F.S., Ogura, Y., Grant, E.P., Bertin, J., Coyle, A.J., *et al.* (2006). Role of the caspase-1 inflammasome in Salmonella typhimurium pathogenesis. *J Exp Med* **203,** 1407-1412.

Larsen, C.M., Faulenbach, M., Vaag, A., Volund, A., Ehses, J.A., Seifert, B., *et al.* (2007). Interleukin-1-receptor antagonist in type 2 diabetes mellitus. *N Engl J Med* **356,** 1517-1526.

Lee, S.H., Stehlik, C. and Reed, J.C. (2001). Cop, a caspase recruitment domain-containing protein and inhibitor of caspase-1 activation processing. *J Biol Chem* **276,** 34495-34500.

Leung, K.F., Baron, R. and Seabra, M.C. (2006). Thematic review series: lipid posttranslational modifications. geranylgeranylation of Rab GTPases. *J Lipid Res* **47,** 467-475.

Linder, M.D., Uronen, R.L., Holtta-Vuori, M., van der Sluijs, P., Peranen, J. and Ikonen, E. (2007). Rab8-dependent recycling promotes endosomal cholesterol removal in normal and sphingolipidosis cells. *Mol Biol Cell* **18,** 47-56.

Liu, L., Botos, I., Wang, Y., Leonard, J.N., Shiloach, J., Segal, D.M. and Davies, D.R. (2008). Structural basis of toll-like receptor 3 signaling with double-stranded RNA. *Science* **320,** 379-381.

Longatti A., Tooze S., Vesicular trafficking and autophagosome formation (2009). *Cell Death and Differentiation* **16**, 956–965.

Loo, Y.M., Fornek, J., Crochet, N., Bajwa, G., Perwitasari, O., Martinez-Sobrido, L., *et al.* (2008). Distinct RIG-I and MDA5 signaling by RNA viruses in innate immunity. *J Virol* **82,** 335-345.

Luschen, S., Ussat, S., Kronke, M. and Adam-Klages, S. (1998). Cleavage of human cytosolic phospholipase A2 by caspase-1 (ICE) and caspase-8 (FLICE). *Biochem Biophys Res Commun* **253,** 92-98.

Luthi, A.U., Cullen, S.P., McNeela, E.A., Duriez, P.J., Afonina, I.S., Sheridan, C., *et al.* (2009). Suppression of interleukin-33 bioactivity through proteolysis by apoptotic caspases. *Immunity* **31,** 84-98.

Machida, E.O., Brock, M.V., Hooker, C.M., Nakayama, J., Ishida, A., Amano, J., *et al.* (2006). Hypermethylation of ASC/TMS1 is a sputum marker for late-stage lung cancer. *Cancer Res* **66,** 6210-6218.

Machner, M.P. and Isberg, R.R. (2007). A bifunctional bacterial protein links GDI displacement to Rab1 activation. *Science* **318,** 974-977.

MacKenzie, A., Wilson, H.L., Kiss-Toth, E., Dower, S.K., North, R.A. and Surprenant, A. (2001). Rapid secretion of interleukin-1beta by microvesicle shedding. *Immunity* **15,** 825-835.

March, C.J., Mosley, B., Larsen, A., Cerretti, D.P., Braedt, G., Price, V., *et al.* (1985). Cloning, sequence and expression of two distinct human interleukin-1 complementary DNAs. *Nature* **315,** 641-647.

Mariathasan, S., Newton, K., Monack, D.M., Vucic, D., French, D.M., Lee, W.P., *et al.* (2004). Differential activation of the inflammasome by caspase-1 adaptors ASC and Ipaf. *Nature* **430,** 213-218.

Mariathasan, S., Weiss, D.S., Dixit, V.M. and Monack, D.M. (2005). Innate immunity against Francisella tularensis is dependent on the ASC/caspase-1 axis. *J Exp Med* **202,** 1043-1049.

Mariathasan S., Weiss D.S., Newton K., McBride J., O'Rourke K., Roose-Girma M., Lee W.P., Weinrauch Y., Monack D.M., Dixit V.M. (2006). Cryopyrin activates the inflammasome in response to toxins and ATP. *Nature* **7081**, 228-32.

Marshall, A.S., Willment, J.A., Lin, H.H., Williams, D.L., Gordon, S. and Brown, G.D. (2004). Identification and characterization of a novel human myeloid inhibitory C-type lectin-like receptor (MICL) that is predominantly expressed on granulocytes and monocytes. *J Biol Chem* **279,** 14792-14802.

Martinon, F., Burns, K. and Tschopp, J. (2002). The inflammasome: a molecular platform triggering activation of inflammatory caspases and processing of proIL-beta. *Mol Cell* **10,** 417-426.

Marzesco, A.M., Dunia, I., Pandjaitan, R., Recouvreur, M., Dauzonne, D., Benedetti, E.L., *et al.* (2002). The small GTPase Rab13 regulates assembly of functional tight junctions in epithelial cells. *Mol Biol Cell* **13,** 1819-1831.

Masters, S.L., Simon, A., Aksentijevich, I. and Kastner, D.L. (2009). Horror autoinflammaticus: the molecular pathophysiology of autoinflammatory disease. *Annu Rev Immunol* **27,** 621-668.

Masumoto, J., Taniguchi, S., Ayukawa, K., Sarvotham, H., Kishino, T., Niikawa, N., *et al.* (1999). ASC, a novel 22-kDa protein, aggregates during apoptosis of human promyelocytic leukemia HL-60 cells. *J Biol Chem* **274,** 33835-33838.

Matsushima, K., Taguchi, M., Kovacs, E.J., Young, H.A. and Oppenheim, J.J. (1986). Intracellular localization of human monocyte associated interleukin 1 (IL 1) activity and release of biologically active IL 1 from monocytes by trypsin and plasmin. *J Immunol* **136,** 2883-2891.

Meylan, E., Curran, J., Hofmann, K., Moradpour, D., Binder, M., Bartenschlager, R. and Tschopp, J. (2005). Cardif is an adaptor protein in the RIG-I antiviral pathway and is targeted by hepatitis C virus. *Nature* **437,** 1167-1172.

Michallet, M.C., Meylan, E., Ermolaeva, M.A., Vazquez, J., Rebsamen, M., Curran, J., *et al.* (2008). TRADD protein is an essential component of the RIG-like helicase antiviral pathway. *Immunity* **28,** 651-661.

Miggin, S.M., Palsson-McDermott, E., Dunne, A., Jefferies, C., Pinteaux, E., Banahan, K., *et al.* (2007). NF-kappaB activation by the Toll-IL-1 receptor domain protein MyD88 adapter-like is regulated by caspase-1. *Proc Natl Acad Sci USA* **104,** 3372-3377.

Molofsky, A.B., Byrne, B.G., Whitfield, N.N., Madigan, C.A., Fuse, E.T., Tateda, K. and Swanson, M.S. (2006). Cytosolic recognition of flagellin by mouse macrophages restricts Legionella pneumophila infection. *J Exp Med* **203,** 1093-1104.

Moore, I., Schell, J. and Palme, K. (1995). Subclass-specific sequence motifs identified in Rab GTPases. *Trends Biochem Sci* **20,** 10-12.

Mukherjee, A., Morosky, S.A., Shen, L., Weber, C.R., Turner, J.R., Kim, K.S., *et al.* (2009). Retinoic acid-induced gene-1 (RIG-I) associates with the actin cytoskeleton via caspase activation and recruitment domain-dependent interactions. *J Biol Chem* **284,** 6486-6494.

Murray R., Kay J., Sangermani D., Stow J. (2005) A Role for the Phagosome in Cytokine Secretion. *Science* **310**, 1492-1495.

Nachury, M.V., Loktev, A.V., Zhang, Q., Westlake, C.J., Peranen, J., Merdes, A., *et al.* (2007). A core complex of BBS proteins cooperates with the GTPase Rab8 to promote ciliary membrane biogenesis. *Cell* **129,** 1201-1213.

Nisole, S., Stoye, J.P. and Saib, A. (2005). TRIM family proteins: retroviral restriction and antiviral defence. *Nat Rev Microbiol* **3,** 799-808.

O'Neill, L.A. (2006). How Toll-like receptors signal: what we know and what we don't know. *Curr Opin Immunol* **18,** 3-9.

Oganesyan, G., Saha, S.K., Guo, B., He, J.Q., Shahangian, A., Zarnegar, B., *et al.* (2006). Critical role of TRAF3 in the Toll-like receptor-dependent and -independent antiviral response. *Nature* **439,** 208-211.

Palsson-McDermott, E.M., Doyle, S.L., McGettrick, A.F., Hardy, M., Husebye, H., Banahan, K., *et al.* (2009). TAG, a splice variant of the adaptor TRAM, negatively regulates the adaptor MyD88-independent TLR4 pathway. *Nat Immunol* **10,** 579-586.

Palsson-McDermott, E.M. and O'Neill, L.A. (2007). Building an immune system from nine domains. *Biochem Soc Trans* **35,** 1437-1444.

Papin, S., Cuenin, S., Agostini, L., Martinon, F., Werner, S., Beer, H.D., *et al.* (2007). The SPRY domain of Pyrin, mutated in familial Mediterranean fever patients, interacts with inflammasome components and inhibits proIL-1beta processing. *Cell Death Differ* **14,** 1457-1466.

Park, B.S., Song, D.H., Kim, H.M., Choi, B.S., Lee, H. and Lee, J.O. (2009). The structural basis of lipopolysaccharide recognition by the TLR4-MD-2 complex. *Nature* **458,** 1191-1195.

Pelegrin, P., Barroso-Gutierrez, C. and Surprenant, A. (2008). P2X7 receptor differentially couples to distinct release pathways for IL-1beta in mouse macrophage. *J Immunol* **180,** 7147-7157.

Pereira-Leal, J.B. and Seabra, M.C. (2000). The mammalian Rab family of small GTPases: definition of family and subfamily sequence motifs suggests a mechanism for functional specificity in the Ras superfamily. *J Mol Biol* **301,** 1077-1087.

Pichlmair A., Schulz O., Tan C., Näslund T., Liljeström P., Weber F., Reis e Sousa C. (2006). RIG-I-mediated antiviral responses to single-stranded RNA bearing 5'-phosphates. *Science* **5801**, 997-1001.

Pichlmair A., Schulz O., Tan C., Rehwinkel J., Kato H., Takeuchi O., Akira S., Way M., Schiavo G., Reis e Sousa C. (2009). Activation of MDA5 requires higher-order RNA structures generated during virus infection. *J Virol* **20**, 10761-10769.

Pisitkun, T., Shen, R.F. and Knepper, M.A. (2004). Identification and proteomic profiling of exosomes in human urine. *Proc Natl Acad Sci USA* **101,** 13368-13373.

Pop, C. and Salvesen, G.S. (2009). Human caspases: activation, specificity, and regulation. *J Biol Chem* **284,** 21777-21781.

Proikas-Cezanne, T., Gaugel, A., Frickey, T. and Nordheim, A. (2006). Rab14 is part of the early endosomal clathrin-coated TGN microdomain. *FEBS Lett* **580,** 5241-5246.

Qu, Y., Franchi, L., Nunez, G. and Dubyak, G.R. (2007). Nonclassical IL-1 beta secretion stimulated by P2X7 receptors is dependent on inflammasome activation and correlated with exosome release in murine macrophages. *J Immunol* **179,** 1913-1925.

Qu, Y., Ramachandra, L., Mohr, S., Franchi, L., Harding, C.V., Nunez, G. and Dubyak, G.R. (2009). P2X7 receptor-stimulated secretion of MHC class II-containing exosomes requires the ASC/NLRP3 inflammasome but is independent of caspase-1. *J Immunol* **182,** 5052-5062.

Razmara, M., Srinivasula, S.M., Wang, L., Poyet, J.L., Geddes, B.J., DiStefano, P.S., *et al.* (2002). CARD-8 protein, a new CARD family member that regulates caspase-1 activation and apoptosis. *J Biol Chem* **277,** 13952-13958.

Richards, N., Schaner, P., Diaz, A., Stuckey, J., Shelden, E., Wadhwa, A. and Gumucio, D.L. (2001). Interaction between pyrin and the apoptotic speck protein (ASC) modulates ASC-induced apoptosis. *J Biol Chem* **276,** 39320-39329.

Richardson, C.J., Jones, S., Litt, R.J. and Segev, N. (1998). GTP hydrolysis is not important for Ypt1 GTPase function in vesicular transport. *Mol Cell Biol* **18,** 827-838.

Rink, J., Ghigo, E., Kalaidzidis, Y. and Zerial, M. (2005). Rab conversion as a mechanism of progression from early to late endosomes. *Cell* **122,** 735-749.

Roberts, E.A., Chua, J., Kyei, G.B. and Deretic, V. (2006). Higher order Rab programming in phagolysosome biogenesis. *J Cell Biol* **174,** 923-929.

Roberts, T.L., Idris, A., Dunn, J.A., Kelly, G.M., Burnton, C.M., Hodgson, S., *et al.* (2009). HIN-200 proteins regulate caspase activation in response to foreign cytoplasmic DNA. *Science* **323,** 1057-1060.

Rogers, N.C., Slack, E.C., Edwards, A.D., Nolte, M.A., Schulz, O., Schweighoffer, E., *et al.* (2005). Syk-dependent cytokine induction by Dectin-1 reveals a novel pattern recognition pathway for C type lectins. *Immunity* **22,** 507-517.

Rosenstiel, P., Huse, K., Till, A., Hampe, J., Hellmig, S., Sina, C., *et al.* (2006). A short isoform of NOD2/CARD15, NOD2-S, is an endogenous inhibitor of NOD2/receptor-interacting protein kinase 2-induced signaling pathways. *Proc Natl Acad Sci USA* **103,** 3280-3285.

Rothfuchs, A.G., Bafica, A., Feng, C.G., Egen, J.G., Williams, D.L., Brown, G.D. and Sher, A. (2007). Dectin-1 interaction with Mycobacterium tuberculosis leads to enhanced IL-12p40 production by splenic dendritic cells. *J Immunol* **179,** 3463-3471.

Rubartelli, A., Cozzolino, F., Talio, M. and Sitia, R. (1990). A novel secretory pathway for interleukin-1 beta, a protein lacking a signal sequence. *EMBO J* **9,** 1503-1510.

Rybin, V., Ullrich, O., Rubino, M., Alexandrov, K., Simon, I., Seabra, M.C., *et al.* (1996). GTPase activity of Rab5 acts as a timer for endocytic membrane fusion. *Nature* **383,** 266-269.

Saha, S.K., Pietras, E.M., He, J.Q., Kang, J.R., Liu, S.Y., Oganesyan, G., *et al.* (2006). Regulation of antiviral responses by a direct and specific interaction between TRAF3 and Cardif. *EMBO J* **25,** 3257-3263.

Saito, T., Owen, D.M., Jiang, F., Marcotrigiano, J. and Gale, M., Jr. (2008). Innate immunity induced by composition-dependent RIG-I recognition of hepatitis C virus RNA. *Nature* **454,** 523-527.

Saitoh T., Fujita N., Jang M., Uematsu S., Yang B., Satoh T., Omori H., Noda T., Yamamoto N., Komatsu M., Tanaka K., Kawai T., Tsujimura T., Takeuchi O., Yoshimori T. (2008) Loss of the autophagy protein Atg16L1 enhances endotoxin-induced IL-1beta production. *Nature* **7219**, 264-268.

Saleh, M. and Green, D.R. (2007). Caspase-1 inflammasomes: choosing between death and taxis. *Cell Death Differ* **14,** 1559-1560.

Saleh, M., Mathison, J.C., Wolinski, M.K., Bensinger, S.J., Fitzgerald, P., Droin, N., *et al.* (2006). Enhanced bacterial clearance and sepsis resistance in caspase-12-deficient mice. *Nature* **440,** 1064-1068.

Saleh, M., Vaillancourt, J.P., Graham, R.K., Huyck, M., Srinivasula, S.M., Alnemri, E.S., *et al.* (2004). Differential modulation of endotoxin responsiveness by human caspase-12 polymorphisms. *Nature* **429,** 75-79.

Salminen, A. and Novick, P.J. (1987). A ras-like protein is required for a post-Golgi event in yeast secretion. *Cell* **49,** 527-538.

Sato, K., Yang, X.L., Yudate, T., Chung, J.S., Wu, J., Luby-Phelps, K., *et al.* (2006). Dectin-2 is a pattern recognition receptor for fungi that couples with the Fc receptor gamma chain to induce innate immune responses. *J Biol Chem* **281,** 38854-38866.

Schilders, G., Raijmakers, R., Malmegrim, K.C., Vande Walle, L., Saelens, X., Vree Egberts, W., *et al.* (2007). Caspase-mediated cleavage of the exosome subunit PM/Scl-75 during apoptosis. *Arthritis Res Ther* **9,** R12.

Schlee M., Roth A., Hornung V., Hagmann C., Wimmenauer V., Barchet W., Coch C., Janke M., Mihailovic A., Wardle G., Juranek S., Kato H., Kawai T., Poeck H., Fitzgerald K., Takeuchi O., Akira S., Tuschl T., Latz E., Ludwig J., Hartmann G. Recognition of 5' triphosphate by RIG-I helicase requires short blunt double-stranded RNA as contained in panhandle of negative-strand virus. *Immunity* **1,** 25-34.

Schmidt, A. and Hall, A. (2002). Guanine nucleotide exchange factors for Rho GTPases: turning on the switch. *Genes Dev* **16,** 1587-1609.

Schmidt A., Schwerd T., Hamm W., Hellmuth J., Cui S., Wenzel M., Hoffmann F., Michallet M., Besch R., Hopfner K., Endres S., Rothenfusser S. (2009) 5'-

triphosphate RNA requires base-paired structures to activate antiviral signaling via RIG-I. *Proc Natl Acad Sci USA* **29**, 12067-12072.

Schroder, K., Muruve, D.A. and Tschopp, J. (2009). Innate immunity: cytoplasmic DNA sensing by the AIM2 inflammasome. *Curr Biol* **19,** R262-265.

Schröder, M., Baran, M. and Bowie, A.G. (2008). Viral targeting of DEAD box protein 3 reveals its role in TBK1/IKKepsilon-mediated IRF activation. *EMBO J* **27,** 2147-2157.

Schröder, M. (2010). Human DEAD-box protein 3 has multiple functions in gene regulation and cell cycle control and is a prime target for viral manipulation. *Biochem Pharmacol* **3**, 297-306.

Schwartz, S.L., Cao, C., Pylypenko, O., Rak, A. and Wandinger-Ness, A. (2007). Rab GTPases at a glance. *J Cell Sci* **120,** 3905-3910.

Seshadri, S., Duncan, M.D., Hart, J.M., Gavrilin, M.A. and Wewers, M.D. (2007). Pyrin levels in human monocytes and monocyte-derived macrophages regulate IL-1beta processing and release. *J Immunol* **179,** 1274-1281.

Seth, R.B., Sun, L. and Chen, Z.J. (2006). Antiviral innate immunity pathways. *Cell Res* **16,** 141-147.

Shao, W., Yeretssian, G., Doiron, K., Hussain, S.N. and Saleh, M. (2007). The caspase-1 digestome identifies the glycolysis pathway as a target during infection and septic shock. *J Biol Chem* **282,** 36321-36329.

Shio, M.T., Eisenbarth, S.C., Savaria, M., Vinet, A.F., Bellemare, M.J., Harder, K.W., *et al.* (2009). Malarial Hemozoin Activates the NLRP3 Inflammasome through Lyn and Syk Kinases. *PLoS Pathog* **8** e1000559.

Singer, II, Scott, S., Chin, J., Bayne, E.K., Limjuco, G., Weidner, J., *et al.* (1995). The interleukin-1 beta-converting enzyme (ICE) is localized on the external cell surface membranes and in the cytoplasmic ground substance of human monocytes by immuno-electron microscopy. *J Exp Med* **182,** 1447-1459.

Singer, II, Scott, S., Hall, G.L., Limjuco, G., Chin, J. and Schmidt, J.A. (1988). Interleukin 1 beta is localized in the cytoplasmic ground substance but is largely absent from the Golgi apparatus and plasma membranes of stimulated human monocytes. *J Exp Med* **167,** 389-407.

Soulat, D., Burckstummer, T., Westermayer, S., Goncalves, A., Bauch, A., Stefanovic, A., *et al.* (2008). The DEAD-box helicase DDX3X is a critical component of the TANK-binding kinase 1-dependent innate immune response. *EMBO J* **27,** 2135-2146.

Srimathi, T., Robbins, S.L., Dubas, R.L., Chang, H., Cheng, H., Roder, H. and Park, Y.C. (2008). Mapping of POP1-binding Site on Pyrin Domain of ASC. *J Biol Chem* **283,** 15390-15398.

Stankovic, T., Byrd, P.J., Cooper, P.R., McConville, C.M., Munroe, D.J., Riley, J.H., *et al.* (1997). Construction of a transcription map around the gene for ataxia telangiectasia: identification of at least four novel genes. *Genomics* **40,** 267-276.

Stehlik, C. and Dorfleutner, A. (2007). COPs and POPs: modulators of inflammasome activity. *J Immunol* **179,** 7993-7998.

Stehlik, C., Krajewska, M., Welsh, K., Krajewski, S., Godzik, A. and Reed, J.C. (2003). The PAAD/PYRIN-only protein POP1/ASC2 is a modulator of ASC-mediated nuclear-factor-kappa B and pro-caspase-1 regulation. *Biochem J* **373,** 101-113.

Stenmark, H. (2009). Rab GTPases as coordinators of vesicle traffic. *Nat Rev Mol Cell Biol* **10,** 513-525.

Stuart, L.M., Boulais, J., Charriere, G.M., Hennessy, E.J., Brunet, S., Jutras, I., *et al.* (2007). A systems biology analysis of the Drosophila phagosome. *Nature* **445,** 95-101.

Sun, G.W., Lu, J., Pervaiz, S., Cao, W.P. and Gan, Y.H. (2005). Caspase-1 dependent macrophage death induced by Burkholderia pseudomallei. *Cell Microbiol* **7,** 1447-1458.

Sutterwala, F.S., Mijares, L.A., Li, L., Ogura, Y., Kazmierczak, B.I. and Flavell, R.A. (2007). Immune recognition of Pseudomonas aeruginosa mediated by the IPAF/NLRC4 inflammasome. *J Exp Med* **204,** 3235-3245.

Takahashi, K., Kawai, T., Kumar, H., Sato, S., Yonehara, S. and Akira, S. (2006). Roles of caspase-8 and caspase-10 in innate immune responses to double-stranded RNA. *J Immunol* **176,** 4520-4524.

Takahasi, K., Yoneyama, M., Nishihori, T., Hirai, R., Kumeta, H., Narita, R., *et al.* (2008). Nonself RNA-sensing mechanism of RIG-I helicase and activation of antiviral immune responses. *Mol Cell* **29,** 428-440.

Talabot-Ayer, D., Lamacchia, C., Gabay, C. and Palmer, G. (2009). Interleukin-33 is biologically active independently of caspase-1 cleavage. *J Biol Chem* **284,** 19420-19426.

Taniguchi, H. (1999). Protein myristoylation in protein-lipid and protein-protein interactions. *Biophys Chem* **82,** 129-137.

Tavalai, N., Papior, P., Rechter, S., Leis, M. and Stamminger, T. (2006). Evidence for a role of the cellular ND10 protein PML in mediating intrinsic immunity against human cytomegalovirus infections. *J Virol* **80,** 8006-8018.

Thery, C., Ostrowski, M. and Segura, E. (2009). Membrane vesicles as conveyors of immune responses. *Nat Rev Immunol* **9,** 581-593.

Thomas, P.G., Dash, P., Aldridge, J.R., Jr., Ellebedy, A.H., Reynolds, C., Funk, A.J., *et al.* (2009). The intracellular sensor NLRP3 mediates key innate and healing responses to influenza A virus via the regulation of caspase-1. *Immunity* **30,** 566-575.

Thornberry, N.A., Bull, H.G., Calaycay, J.R., Chapman, K.T., Howard, A.D., Kostura, M.J., *et al.* (1992). A novel heterodimeric cysteine protease is required for interleukin-1 beta processing in monocytes. *Nature* **356,** 768-774.

Ting, J.P., Lovering, R.C., Alnemri, E.S., Bertin, J., Boss, J.M., Davis, B.K., *et al.* (2008). The NLR gene family: a standard nomenclature. *Immunity* **28,** 285-287.

Tisdale, E.J., Bourne, J.R., Khosravi-Far, R., Der, C.J. and Balch, W.E. (1992). GTP-binding mutants of rab1 and rab2 are potent inhibitors of vesicular transport from the endoplasmic reticulum to the Golgi complex. *J Cell Biol* **119,** 749-761.

Touchot, N., Chardin, P. and Tavitian, A. (1987). Four additional members of the ras gene superfamily isolated by an oligonucleotide strategy: molecular cloning of YPT-related cDNAs from a rat brain library. *Proc Natl Acad Sci USA* **84,** 8210-8214.

Uno, T., Nakao, A. and Katsurauma, C. (2004). Phosphorylation of Rab proteins from the brain of Bombyx mori. *Arch Insect Biochem Physiol* **57,** 68-77.

Valadi, H., Ekstrom, K., Bossios, A., Sjostrand, M., Lee, J.J. and Lotvall, J.O. (2007). Exosome-mediated transfer of mRNAs and microRNAs is a novel mechanism of genetic exchange between cells. *Nat Cell Biol* **9,** 654-659.

van der Sluijs, P., Hull, M., Webster, P., Male, P., Goud, B. and Mellman, I. (1992). The small GTP-binding protein rab4 controls an early sorting event on the endocytic pathway. *Cell* **70,** 729-740.

van der Velden, A.W., Velasquez, M. and Starnbach, M.N. (2003). Salmonella rapidly kill dendritic cells via a caspase-1-dependent mechanism. *J Immunol* **171,** 6742-6749.

van Kooyk, Y. and Rabinovich, G.A. (2008). Protein-glycan interactions in the control of innate and adaptive immune responses. *Nat Immunol* **9,** 593-601.

Vieira, O.V., Botelho, R.J. and Grinstein, S. (2002). Phagosome maturation: aging gracefully. *Biochem J* **366,** 689-704.

Voronov, E., Shouval, D.S., Krelin, Y., Cagnano, E., Benharroch, D., Iwakura, Y., *et al.* (2003). IL-1 is required for tumor invasiveness and angiogenesis. *Proc Natl Acad Sci USA* **100,** 2645-2650.

Waite, A.L., Schaner, P., Hu, C., Richards, N., Balci-Peynircioglu, B., Hong, A., *et al.* (2009). Pyrin and ASC co-localize to cellular sites that are rich in polymerizing actin. *Exp Biol Med* **234,** 40-52.

Wang, Y., Hasegawa, M., Imamura, R., Kinoshita, T., Kondo, C., Konaka, K. and Suda, T. (2004). PYNOD, a novel Apaf-1/CED4-like protein is an inhibitor of ASC and caspase-1. *Int Immunol* **16,** 777-786.

Wang, Z.G., Ruggero, D., Ronchetti, S., Zhong, S., Gaboli, M., Rivi, R. and Pandolfi, P.P. (1998). PML is essential for multiple apoptotic pathways. *Nat Genet* **20,** 266-272.

Wickliffe, K.E., Leppla, S.H. and Moayeri, M. (2008). Anthrax lethal toxin-induced inflammasome formation and caspase-1 activation are late events dependent on ion fluxes and the proteasome. *Cell Microbiol* **10,** 332-343.

Xu, L.G., Wang, Y.Y., Han, K.J., Li, L.Y., Zhai, Z. and Shu, H.B. (2005). VISA is an adapter protein required for virus-triggered IFN-beta signaling. *Mol Cell* **19,** 727-740.

Yamamoto, M., Sato, S., Hemmi, H., Hoshino, K., Kaisho, T., Sanjo, H., *et al.* (2003). Role of adaptor TRIF in the MyD88-independent toll-like receptor signaling pathway. *Science* **301,** 640-643.

Yamasaki, S., Ishikawa, E., Sakuma, M., Hara, H., Ogata, K. and Saito, T. (2008). Mincle is an ITAM-coupled activating receptor that senses damaged cells. *Nat Immunol* **9,** 1179-1188.

Ye H., Arron J., Lamothe B., Cirilli M., Kobayashi T., Shevde N., Segal D., Dzivenu O., Vologodskaia M., Yim M., Du K., Singh S., Pike J., Darnay B., Choi Y., Wu H. (2002). Distinct molecular mechanism for initiating TRAF6 signalling. *Nature* **6896**, 443-447.

Yoneyama, M. and Fujita, T. (2008). Structural mechanism of RNA recognition by the RIG-I-like receptors. *Immunity* **29,** 178-181.

Yu, J.W., Fernandes-Alnemri, T., Datta, P., Wu, J., Juliana, C., Solorzano, L., *et al.* (2007). Pyrin activates the ASC pyroptosome in response to engagement by autoinflammatory PSTPIP1 mutants. *Mol Cell* **28,** 214-227.

Yu, J.W., Wu, J., Zhang, Z., Datta, P., Ibrahimi, I., Taniguchi, S., *et al.* (2006). Cryopyrin and pyrin activate caspase-1, but not NF-kappaB, via ASC oligomerization. *Cell Death Differ* **13,** 236-249.

Zamboni, D.S., Kobayashi, K.S., Kohlsdorf, T., Ogura, Y., Long, E.M., Vance, R.E., *et al.* (2006). The Birc1e cytosolic pattern-recognition receptor contributes to the detection and control of Legionella pneumophila infection. *Nat Immunol* **7,** 318-325.

Zelensky, A.N. and Gready, J.E. (2005). The C-type lectin-like domain superfamily. *FEBS J* **272,** 6179-6217.

Zerial, M. and McBride, H. (2001). Rab proteins as membrane organizers. *Nat Rev Mol Cell Biol* **2,** 107-117.

Zhong, B., Yang, Y., Li, S., Wang, Y.Y., Li, Y., Diao, F., *et al.* (2008). The adaptor protein MITA links virus-sensing receptors to IRF3 transcription factor activation. *Immunity* **29,** 538-550.

Zychlinsky, A., Prevost, M.C. and Sansonetti, P.J. (1992). Shigella flexneri induces apoptosis in infected macrophages. *Nature* **358,** 167-169.

Chapter 8

Record of Publication

Record of publication

Christine Becker and Luke O'Neill. (2007). Inflammasomes in Inflammatory disorders: The Role of TLRs and their interaction with NLRs. *Semin Immunopathol* **3**, 239-248.

Christine Becker, Emma Creagh, Luke O'Neill (2009). A Role for Rab39a in Caspase-1 Dependent IL-1β Secretion. *Keystone Symposia- Immune Pattern Recognition, Banff, Canada.*

Christine Becker, Emma Creagh, Luke O'Neill. (2009). Rab39a Binds Caspase-1 and is Required for Caspase-1 Dependent IL-1β Secretion. *Journal of Biological Chemistry.* **50**, 34531-34537.

A role for Rab39a in caspase-1 dependent IL-1β secretion

Christine Becker, Emma Creagh, Luke O'Neill. School of Biochemistry and Immunology, Trinity College Dublin, Dublin 2, Ireland.

Caspase-1 plays a pivotal role in the innate immune system and occurs in a multi-protein complex termed the inflammasome which is assembled in response to a diverse set of pro-inflammatory stimuli. Active caspase-1 is responsible for the production of the pro-inflammatory cytokine IL-1β. Using a one-step immunoprecipitation approach we isolated active caspase-1, and identified binding partners of caspase-1 using mass spectrometry. One of these proteins was Rab39a, an uncharacterised member of the Rab family. This interaction was confirmed by co-immunoprecipitation. Rab39a contains a putative caspase-1 cleavage site and can be cleaved by recombinant caspase-1. This cleavage is inhibited in the presence of a caspase-1 inhibitor. Using site directed mutagenesis the cleavage site was determined as D148. IL-1β is known to undergo caspase-1 dependent unconventional secretion. Knockdown of Rab39a by siRNA results in a decrease in IL-1β secretion. Rab proteins have roles in protein trafficking and secretion so it is likely that Rab39a is required to interact with caspase-1 in order for IL-1β to be secreted.

RIP2 is involved in NOD1 and NOD2 signaling, and initial reports suggested that RIP2 deficient macrophages displayed defective TLR signaling in response to LPS (TLR4 ligand), LTA (TLR2 ligand), and poly (IC) (TLR3 ligand) [50–52], indicating that RIP2 is involved in both TLR and NOD signaling. However, many preparations of bacterial components contain NOD1 and NOD2 stimulating molecules, which could explain the reduced TLR signaling observed in these macrophages [29]. Most recently, Park et al. used LPS preparations (that were devoid of any NOD1 and NOD2 activators) on RIP2 deficient macrophages, to show that RIP2 did not have a direct role in TLR signaling. Yet, they found that RIP2 is essential for the cooperation of NOD2 and TLR signaling in the production of cytokines when the amounts of their specific bacterial activators are limiting. So, although the pathways are independent, they do cooperate for optimal immune responses [29].

TLRs and NALPs

The most documented example of crosstalk between TLRs and NLRs is their joint involvement in the inflammasome pathway that leads to the secretion of mature IL-1β during microbial infection [53]. As described above, activation of TLRs by various ligands leads to NF-κB activation via the MyD88 adaptor, which is needed to induce the expression of the 31-kDa inactive precursor, pro IL-1β, in the cytosol. This is referred to as 'priming' the system [54]. A 17-kDa biologically active form of IL-1β is generated by cleavage of the proform by caspase-1. Caspase-1 also cleaves pro-IL-18, which, unlike pro-IL-1β, is constitutively expressed. Caspase-1 itself is synthesized as an inactive 45-kDa zymogen that undergoes autocatalytic processing in response to an appropriate stimulus. The active form of the enzyme comprises the p20 and p10 subunits, which assemble into a heterotetramer. Tschopp et al. discovered that caspase-1 forms the central component of the inflammasome, and the inflammasome acts as a platform for its activation [11].

The inflammasome activating stimulus is thought to be an agent that causes ionic perturbations, specifically potassium efflux. Loss of intracellular potassium results in the activation of calcium-independent phospholipase A2 ($iPLA_2$), and the inhibition of $iPLA_2$ prevents IL-1β processing (Fig. 2). The activation of the purinergic receptor $P2X_7$, for which ATP is the main endogenous ligand, leads to the rapid opening of a potassium-selective channel, followed by the gradual opening of a larger pore and is mediated by a protein called pannexin-1 [55]. Activation results in potassium efflux along with plasma membrane depolarization, cell swelling, and disaggregation of the cytoskeletal network. $P2X_7$ knockout mice have been shown to have defective IL-1β release in response to ATP [56].

Kanneganti and colleagues investigated the role of pannexin-1 in NALP3 mediated caspase-1 activation [29]. Signaling through pannexin-1 was previously found to be crucial for caspase-1 activation and IL-1β secretion in LPS-stimulated macrophages pulsed with ATP or stimulated with the pore-forming toxins nigericin and maitotoxin [55]. Kanneganti and colleagues found that pannexin-1 is essential for $P2X_7$-mediated activation of the NALP3 inflammasome by heat killed bacteria or LPS while infection with wild-type *Salmonella*, *Franciscella* or *Listeria* induced caspase-1 activation in the absence of ATP and independently of NALP3 and pannexin-1. *Salmonella* induces caspase-1 activation through IPAF and requires a bacterial type III or IV secretion system to deliver flagellin into the host

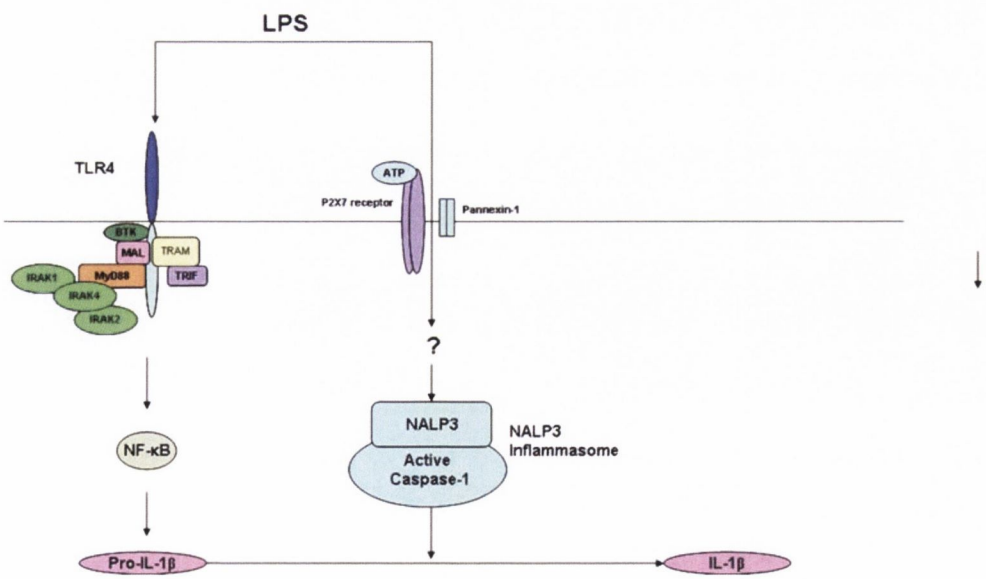


Fig. 2 Crosstalk between TLR4 and NALP3. TLR4 responds to LPS and results in the activation of the NF-κB pathway and the production of pro-IL-1β. LPS stimulated macrophages pulsed with ATP signal through the $P2X_7$ receptor resulting in the activation of the NALP3 inflammasome and the activation of caspase-1. Caspase-1 then cleaves pro-IL-1β to produce active IL-1β

cytosol [57]. *Franciscella* and *Listeria* also use the type III secretion system or pore-forming molecules to gain access to the host cytosol and to activate caspase-1, although the NLRs that they interact with are unknown at present.

Their results demonstrated that intracellular bacteria can induce caspase-1 activation in two ways. In the absence of ATP stimulation, a type III secretion apparatus or a pore-forming protein is required. In the presence of ATP, caspase-1 is activated through pannexin-1 and NALP3 even in the absence of a secretion system or pore-forming toxin [29].

Although TLR signaling is crucial for the upregulation of the IL-1β precursor, there has been some discussion as to whether the TLR pathway is directly involved in caspase-1 activation. An important consideration is the requirement of LPS to allow ATP to activate the inflammasome in priming macrophages. Either stimulus on their own is insufficient, and the mechanism appears to be TLR-independent because it is evident in MyD88 and TRIF knockout cells. PamCys and R848 have similar priming effects. Kanneganti and colleagues [29] found that NALP3-dependent caspase-1 activation induced by LPS is independent of TLR signaling, confirming that TLR signaling is not required for the activation of the NALP3 inflammasome, although it is still necessary for cytokine production (Fig. 2). These TLR-independent effects of LPS will require further analysis, both in the NALP3 inflammasome and in the other inflammasomes identified to date.

We have found what might be an important link between the adaptor protein Mal, used in TLR signaling, and the inflammasome component caspase-1. We showed that Mal is cleaved by caspase-1 and while Mal is not required for caspase-1 signaling, inhibition of caspase-1 activity impaired TLR2 and TLR4 signaling. During infection, bacterial products may be sensed, by TLRs and NLRs, which prime and activate the inflammasome complex. Active caspase-1 may then process Mal into its active form, allowing further signaling through TLR2 and TLR4 [58].

NALP6 and NALP12 have also been shown to activate the NF-κB pathway [59, 60]. However, others have reported that NALP12 dampens NF-κB signals, triggered by TLRs or TNF stimulation [61, 62]. For example, Williams et al. have shown that NALP12 is an antagonist of TLR-induced proinflammatory signals in myeloid cells. NALP12 binds IRAK1, resulting in the downregulation of its (IRAK1) activity in the TLR signaling cascade [62]. NALP3 was also once implicated in NF-κB activation but this was disproved using NALP3 deficient mice [29].

An example of stimulation of both TLRs and NLRs by pathogens is the ability of flagellin to stimulate both TLR5 and IPAF independently of each other, resulting in two different responses. TLR5 activates transcription factor NF-κB, resulting in the expression of pro-IL-1β. IPAF, initiates IL-1β processing through caspase-1 and stimulates the secretion of mature IL-1β. By using two pathways for bacterial flagellin, the innate immune system may be able to modulate the intensity or quality of its response according to the virulence characteristics of the pathogen [57, 63]. Another example is that of R837 and R848, TLR7/8 ligands that have recently been shown to activate NALP3. R837 and R848 are used as immune response modifiers in the clinic and are being considered as vaccine adjuvants. The potent adjuvant, antiviral, and antitumor activities exerted by the imidazoquinoline compounds could be explained by their ability to activate both TLR and cryopyrin signaling [29].

TLRs and diseases

Mutations in genes occur naturally during DNA replication but also as a result of damage to the DNA. Most new alleles are usually eliminated by genetic drift or remain in the population for a period as rare variants. If the DNA variant created by a mutation event becomes common in the population over many generations (found at a frequency of greater than 1%) it becomes known as a polymorphism. The simplest type of polymorphism, a single nucleotide polymorphism (SNP), results from a single base mutation. SNPs occurring in coding regions of genes may cause an alteration in the amino acid sequence and have a direct impact on protein function. However, a SNP located in a noncoding region may also be functionally important, for example, it may influence RNA splicing.

Polymorphisms in TLRs and their signaling molecules have revealed the importance of TLRs in human defense against diseases (Table 1), and many of these are inflammatory disorders, which are highlighted below.

Berdeli et al. found strong evidence for the biological role of TLR2 in acute rheumatic fever. They found that the common TLR2 Arg to Gln polymorphism at position 753 significantly contributes to the pathogenesis of the disease [64]. The R753Q SNP may also predispose people to staphylococcal infections or to tuberculosis [65], although a larger study came to the conclusion that this SNP is not associated with these infections [66]. Another SNP of TLR2—R677W—was found to be associated in Asian people with lepromatous leprosy [67].

Several groups have studied the D299G and T399I polymorphisms in TLR4 and have shown that these polymorphisms increase the risk of gram-negative infections [68]. A further study linked D299Q to an increased risk of systemic inflammatory syndrome [69] and increased susceptibility to late onset Alzheimer's disease [70]. These SNPs occur within the extracellular domain of TLR4, so the decrease in response is most likely mediated by a decrease in recognition of ligands. Inflammation has been implicated

Table 1 SNPs in TLR genes associated with disease

Gene	SNP	Disease association
TLR2	R753Q	Acute rheumatic fever, staphylococcal infections, tuberculosis
	R677W	Lepromatous leprosy
	P631H	Meningitis
	16 934	Asthma
TLR4	D299G	Gram-negative infections, systemic inflammatory syndrome, late-onset Alzheimer's disease
	T399I	Gram-negative infections
	11 381	Prostate cancer
TLR5	392STOP	Legionnaires disease
TLR6	S249P	Asthma
TLR9	−1237	Asthma, Crohn's disease

as an etiological factor in several human cancers, and it is interesting to note that a SNP at position 11,381 in TLR4 was found to be more frequent among people with prostate cancer [71].

An association with a higher susceptibility to Legionnaires disease was shown for a common stop codon polymorphism (R392) in TLR5 [72]. SNPs in TLR6 and TLR10 have also been described and may possibly contribute to asthma susceptibility [73].

SNPs in genes involved in downstream TLR signaling pathways have also been described, e.g., NEMO, IRAK4, and IκBα. For example, anhidrotic ectodermal dysplasia with immune deficiency (EDA-ID) is a rare immunodeficiency characterized with infections by encapsulated pyrogenic bacteria, such as *Haemophilus influenzae*, *Streptoccus pneumoniae* or *Staphyloccus aureus*; viral illnesses caused by herpes simplex virus and cytomegalovirus; and fungal diseases such as *Pneumocystis jiroveci* pneumonitis [74]. Patients carry either X-linked recessive mutations in NF-κB essential modulator (NEMO) or autosomal dominant mutations in IκBα. These mutations result in impaired NF-κB activation and hence impaired TLR signaling [75]. Inherited IRAK4 deficiency is an autosomal recessive disorder mainly due to SNPs that encode stop codons at amino acid positions 287 and 293 of IRAK4 [76, 77]. IRAK4 is a crucial kinase in the TLR signaling pathway, as described earlier, and patients with IRAK4 deficiency are susceptible to invasive bacterial infections. Blood cells from these patients are impaired in their ability to make TNFα in response to activation by TLRs. It is interesting to note that IRAK4 deficient patients seem to improve with age, suggesting that adaptive immune responses compensate for the weakened innate responses. Bruton's tyrosine kinase (BTK) is a member of the Tec family of protein tyrosine kinases and is a component of the TLR signaling pathway. It interacts with the TIR domains of TLRs 4, 6, 8, and 9 and was also found to specifically associate with MyD88, Mal, and IRAK1. Various mutations in the gene have been identified as being responsible for the X-linked agammaglobulinemia (XLA), an immune disorder characterized by a lack of circulating B lymphocytes. These include mutations that affect both the kinase activity of BTK and its ability to translocate to the plasma membrane [78].

However, sometimes SNPs in TLRs can have positive effects. For example, a recent study carried out found a SNP in the adaptor molecule Mal (S180L). This polymorphism is associated with a protective effect against infectious diseases, such as malaria, tuberculosis, and pneumococcal bacteremia [79]. The D299G SNP in TLR4 has also been associated with reduced risk in susceptibility to carotid artery atherosclerosis [80]. This mutation is also correlated with a lower rate of acute allograft rejection after transplantation [81], and a reduced prevalence of diabetic neuropathy in type 2 diabetes [82].

It is interesting to note that many pathogens are capable of exploiting the TLR system to evade the immune system. The α- and ε-Proteobacteria, which include the pathogens *Campylobacter jejuni*, *Helicobacter pylori*, and *Bartonella bacilliformis*, require flagellar motility to efficiently infect mammalian hosts. However, these bacteria possess specific changes in the TLR5 recognition site on flagellin that destroy TLR5 recognition. They have compensatory amino acid changes in their flagellin molecules that preserve their motility [83, 84]. Another bacterium, *M. tuberculosis* survives in host macrophages by inhibiting IFN-γ-mediated signaling in a TLR2- and MyD88-dependent manner [85].

NLRs and diseases

Again reviewed in a separate article in this series, this aspect will only be touched on briefly. Mutations in the gene encoding NOD2 have been associated with a genetic predisposition to Crohn's disease. MDP recognition and subsequent signaling is impaired in monocytes from Crohn's disease patients. Other diseases associated with polymorphisms in NLRs include atopic disease and asthma. Other rare autoinflammatory diseases involving NLRs include Blau syndrome, CINCA, Muckle–Wells syndrome, familial cold urticaria, and early-onset sarcoidosis [86].

IL-1β

An important part of the innate immune system is the secretion of IL-1β. As highlighted in this review, there is abundant evidence to convince us that there is interplay in the TLR and NLR pathways in the production of this cytokine, which is a major mediator of inflammation. IL-1β is a key mediator of the body's response to microbial

invasion and affects a large range of cells and organs; it evokes fever, hypotension, and the production of other cytokines, chemokines, and adhesion molecules. Dysregulated activation and release of IL-1β can lead to various inflammatory disorders [87]. Further understanding the mechanisms by which IL-1β is activated and controlled will involve deciphering the contributions of the TLR and NLR pathways. Ultimately, this will allow the development of therapies to help control chronic inflammatory disorders.

Another important consideration is that TLRs play a crucial role in linking innate and adaptive immune responses, through their actions on dendritic cells (DCs). Upon signaling through TLRs, they undergo a complex maturation process, involving upregulation of MHC molecules and coreceptors that enhance the ability of DCs to activate T cells. Type I IFN production (described above) is also thought to be a central molecule in the adaptive immune response. One of the next challenges will be to establish a better understanding of the complex interplay between TLR and NLRs and how this affects innate responses and the induction of adaptive immunity to a given pathogen.

Conclusions

Recognition of pathogens by the innate immune system relies on specialized receptors to detect them, of which TLRs and NLRs are receiving much attention. Engagement of TLR signaling leads to the production of a variety of inflammatory cytokines. Members of the NLR family are also important in the production of cytokines and in the formation of a multiprotein inflammatory complex, the inflammasome. The view is emerging that the activation of both TLRs and NLRs is important to mount an efficient inflammatory response in the host. The best example of this is in the production of active IL-1β. Future work in this area will involve further delineation of the TLR and NLR signaling pathways and determining the precise mechanism of how they interact.

Continued research is needed to determine further understanding of the roles of TLRs and NLRs in inflammatory diseases. We need to apply this knowledge to further comprehend disease phenotypes and to develop effective therapies to combat these diseases. The association of members of the TLR and NLR families in various human diseases has been described and recent studies have described the genetic association of polymorphisms in genes encoding TLRs and NLRs or their downstream signaling molecules. These polymorphisms have demonstrated that TLR and NLR signaling affects the progression and development of several human diseases [88].

Another important aspect to consider in the future of this field is the involvement of other receptors. The RIG-1-like receptor family (RLR) is a family of PRRs that recognize viral nucleic acids and activate interferon-regulated factor (IRF) family members. They share similarities with the TLRs in relation to their signal activation (NF-κB and IRF3) and the genes they induce (Type 1 IFNs). They also share similarities with NLRs due to the presence of CARD domains. It is likely that RLRs integrate with TLRs and NLRs to provide comprehensive antiviral protection [4]. Other receptors on innate immune cells include the mannose receptors, C-type lectins such as Dectin-1, Fc receptors, and scavenger receptors, which are also involved in the modulation of innate immune responses [89]. Because pathogens have multiple PAMPs and because innate immune cells express multiple PRRs, it can be expected that crosstalk among the signaling pathways occurs. Therefore, it will be important to ascertain the interactions of various PRRs with TLRs and with each other in the understanding of host defense.

References

1. O'Neill LA (2006) How Toll-like receptors signal: what we know and what we don't know. Curr Opin Immunol 18(1):3–9
2. Bowie A, O'Neill LA (2000) The interleukin-1 receptor/Toll-like receptor superfamily: signal generators for pro-inflammatory interleukins and microbial products. J Leukoc Biol 67(4):508–514
3. Kawai T, Akira S (2006) TLR signaling. Cell Death Differ 13 (5):816–825
4. Creagh EM, O'Neill LA (2006) TLRs, NLRs and RLRs: a trinity of pathogen sensors that co-operate in innate immunity. Trends Immunol 27(8):352–357
5. Akira S (2006) TLR signaling. Curr Top Microbiol Immunol 311:1–16
6. Kawai T et al (2004) Interferon-alpha induction through Toll-like receptors involves a direct interaction of IRF7 with MyD88 and TRAF6. Nat Immunol 5(10):1061–1068
7. Honda K et al (2004) Role of a transductional–transcriptional processor complex involving MyD88 and IRF-7 in Toll-like receptor signaling. Proc Natl Acad Sci U S A 101(43):15416–15421
8. Takaoka A et al (2005) Integral role of IRF-5 in the gene induction programme activated by Toll-like receptors. Nature 434 (7030):243–249
9. Yamamoto M et al (2003) Role of adaptor TRIF in the MyD88-independent toll-like receptor signaling pathway. Science 301 (5633):640–643
10. Oshiumi H et al (2003) TIR-containing adapter molecule (TICAM)-2, a bridging adapter recruiting to toll-like receptor 4 TICAM-1 that induces interferon-beta. J Biol Chem 278(50):49751–49762
11. Meylan E et al (2004) RIP1 is an essential mediator of Toll-like receptor 3-induced NF-kappa B activation. Nat Immunol 5 (5):503–507
12. Fitzgerald KA et al (2001) Mal (MyD88-adapter-like) is required for Toll-like receptor-4 signal transduction. Nature 413(6851):78–83
13. Carty M et al (2006) The human adaptor SARM negatively regulates adaptor protein TRIF-dependent Toll-like receptor signaling. Nat Immunol 7(10):1074–1081
14. Liew FY et al (2005) Negative regulation of toll-like receptor-mediated immune responses. Nat Rev Immunol 5(6):446–458

15. Ting JP, Kastner DL, Hoffman HM (2006) CATERPILLERs, pyrin and hereditary immunological disorders. Nat Rev Immunol 6(3):183–195
16. Werts C, Girardin SE, Philpott DJ (2006) TIR, CARD and PYRIN: three domains for an antimicrobial triad. Cell Death Differ 13(5):798–815
17. Barnich N et al (2005) Membrane recruitment of NOD2 in intestinal epithelial cells is essential for nuclear factor-{kappa}B activation in muramyl dipeptide recognition. J Cell Biol 170 (1):21–26
18. Kummer JA et al (2007) Inflammasome components NALP 1 and 3 show distinct but separate expression profiles in human tissues, suggesting a site-specific role in the inflammatory response. J Histochem Cytochem 55(5):443–452
19. LeibundGut-Landmann S et al (2004) Mini-review: specificity and expression of CIITA, the master regulator of MHC class II genes. Eur J Immunol 34(6):1513–1525
20. Chamaillard M, Inohara,N, Nunez G (2004) Battling enteroinvasive bacteria: Nod1 comes to the rescue. Trends Microbiol 12(12):529–532
21. Girardin SE et al (2003) Nod1 detects a unique muropeptide from gram-negative bacterial peptidoglycan. Science 300(5625):1584–1587
22. Inohara N et al (2003) Host recognition of bacterial muramyl dipeptide mediated through NOD2. Implications for Crohn's disease. J Biol Chem 278(8):5509–5512
23. Girardin SE et al (2003) Nod2 is a general sensor of peptidoglycan through muramyl dipeptide (MDP) detection. J Biol Chem 278(11):8869–8872
24. Meylan E, Tschopp J (2005) The RIP kinases: crucial integrators of cellular stress. Trends Biochem Sci 30(3):151–159
25. Kobayashi KS et al (2005) Nod2-dependent regulation of innate and adaptive immunity in the intestinal tract. Science 307(5710):731–734
26. Girardin SE et al (2001) CARD4/Nod1 mediates NF-kappaB and JNK activation by invasive *Shigella flexneri*. EMBO Rep 2 (8):736–742
27. Boyden ED, Dietrich WF (2006) Nalp1b controls mouse macrophage susceptibility to anthrax lethal toxin. Nat Genet 38 (2):240–244
28. Agostini L et al (2004) NALP3 forms an IL-1beta-processing inflammasome with increased activity in Muckle–Wells autoinflammatory disorder. Immunity 20(3):319–325
29. Park JH et al (2007) RICK/RIP2 mediates innate immune responses induced through Nod1 and Nod2 but not TLRs. J Immunol 178(4):2380–2386
30. Mariathasan S et al (2004) Differential activation of the inflammasome by caspase-1 adaptors ASC and Ipaf. Nature 430(6996):213–218
31. Sutterwala FS et al (2006) Critical role for NALP3/CIAS1/cryopyrin in innate and adaptive immunity through its regulation of caspase-1. Immunity 24(3):317–327
32. Watanabe H et al (2007) Activation of the IL-1beta-processing inflammasome is involved in contact hypersensitivity. J Invest Dermatol (in press)
33. O'Neill LA (2000) The interleukin-1 receptor/Toll-like receptor superfamily: signal transduction during inflammation and host defense. Sci STKE 2000(44):RE1
34. Martinon F, Tschopp J (2005) NLRs join TLRs as innate sensors of pathogens. Trends Immunol 26(8):447–454
35. Takeuchi O et al (1999) Differential roles of TLR2 and TLR4 in recognition of gram-negative and gram-positive bacterial cell wall components. Immunity 11(4):443–451
36. Travassos LH et al (2004) Toll-like receptor 2-dependent bacterial sensing does not occur via peptidoglycan recognition. EMBO Rep 5(10):1000–1006
37. Fritz JH et al (2005) Synergistic stimulation of human monocytes and dendritic cells by Toll-like receptor 4 and NOD1- and NOD2-activating agonists. Eur J Immunol 35(8):2459–2470
38. Li J et al (2004) Regulation of IL-8 and IL-1beta expression in Crohn's disease associated NOD2/CARD15 mutations. Hum Mol Genet 13(16):1715–1725
39. van Heel DA et al (2005) Synergistic enhancement of Toll-like receptor responses by NOD1 activation. Eur J Immunol 35 (8):2471–2476
40. van Heel DA et al (2005) Muramyl dipeptide and toll-like receptor sensitivity in NOD2-associated Crohn's disease. Lancet 365 (9473):1794–1796
41. van Heel DA et al (2005) Synergy between TLR9 and NOD2 innate immune responses is lost in genetic Crohn's disease. Gut 54 (11):1553–1557
42. Uehara A et al (2005) Muramyldipeptide and diaminopimelic acid-containing desmuramylpeptides in combination with chemically synthesized Toll-like receptor agonists synergistically induced production of interleukin-8 in a NOD2- and NOD1-dependent manner, respectively, in human monocytic cells in culture. Cell Microbiol 7(1):53–61
43. Tada H et al (2005) Synergistic effect of Nod1 and Nod2 agonists with toll-like receptor agonists on human dendritic cells to generate interleukin-12 and T helper type 1 cells. Infect Immun 73(12):7967–7976
44. Ferwerda G et al (2005) NOD2 and toll-like receptors are nonredundant recognition systems of *Mycobacterium tuberculosis*. PLoS Pathog 1(3):279–285
45. Watanabe H et al (2004) Innate immune response in Th1- and Th2-dominant mouse strains. Shock 22(5):460–466
46. Rosenstiel P et al (2003) TNF-alpha and IFN-gamma regulate the expression of the NOD2 (CARD15) gene in human intestinal epithelial cells. Gastroenterology 124(4):1001–1009
47. Takahashi Y et al (2006) Up-regulation of NOD1 and NOD2 through TLR4 and TNF-alpha in LPS-treated murine macrophages. J Vet Med Sci 68(5):471–478
48. Chen CM et al (2004) Reciprocal cross-talk between Nod2 and TAK1 signaling pathways. J Biol Chem 279(24):25876–25882
49. Kufer TA, Sansonetti PJ (2007) Sensing of bacteria: NOD a lonely job. Curr Opin Microbiol 10(1):62–69
50. Chin AI et al (2002) Involvement of receptor-interacting protein 2 in innate and adaptive immune responses. Nature 416(6877):190–194
51. Kobayashi K et al (2002) RICK/Rip2/CARDIAK mediates signalling for receptors of the innate and adaptive immune systems. Nature 416(6877):194–199
52. Lu C et al (2005) Participation of Rip2 in lipopolysaccharide signaling is independent of its kinase activity. J Biol Chem 280 (16):16278–16283
53. Mariathasan S, Monack DM (2007) Inflammasome adaptors and sensors: intracellular regulators of infection and inflammation. Nat Rev Immunol 7(1):31–40
54. Kahlenberg JM et al (2005) Potentiation of caspase-1 activation by the P2X7 receptor is dependent on TLR signals and requires NF-kappaB-driven protein synthesis. J Immunol 175 (11):7611–7622
55. Pelegrin P, Surprenant A (2006) Pannexin-1 mediates large pore formation and interleukin-1beta release by the ATP-gated P2X7 receptor. EMBO J 25(21):5071–5082
56. Solle M et al (2001) Altered cytokine production in mice lacking P2X(7) receptors. J Biol Chem 276(1):125–132
57. Miao EA et al (2006) Cytoplasmic flagellin activates caspase-1 and secretion of interleukin 1beta via Ipaf. Nat Immunol 7 (6):569–575
58. Miggin SM et al (2007) NF-kappaB activation by the Toll-IL-1 receptor domain protein MyD88 adapter-like is regulated by caspase-1. Proc Natl Acad Sci U S A 104(9):3372–3377
59. Grenier JM et al (2002) Functional screening of five PYPAF family members identifies PYPAF5 as a novel regulator of NF-kappaB and caspase-1. FEBS Lett 530(1–3):73–78

60. Wang L (2002) PYPAF7, a novel PYRIN-containing Apaf1-like protein that regulates activation of NF-kappa B and caspase-1-dependent cytokine processing. J Biol Chem 277(33):29874–29880
61. O'Connor W Jr et al (2003) Cutting edge: CIAS1/cryopyrin/PYPAF1/NALP3/CATERPILLER 1.1 is an inducible inflammatory mediator with NF-kappa B suppressive properties. J Immunol 171(12):6329–6333
62. Williams KL et al (2005) The CATERPILLER protein monarch-1 is an antagonist of toll-like receptor-, tumor necrosis factor alpha-, and *Mycobacterium tuberculosis*-induced pro-inflammatory signals. J Biol Chem 280(48):39914–39924
63. Franchi L et al (2006) Cytosolic flagellin requires Ipaf for activation of caspase-1 and interleukin 1beta in salmonella-infected macrophages. Nat Immunol 7(6):576–582
64. Berdeli A et al (2005) TLR-2 gene Arg753Gln polymorphism is strongly associated with acute rheumatic fever in children. J Mol Med 83(7):535–541
65. Ogus AC et al (2004) The Arg753GLn polymorphism of the human toll-like receptor 2 gene in tuberculosis disease. Eur Respir J 23(2):219–223
66. Moore CE et al (2004) Lack of association between Toll-like receptor 2 polymorphisms and susceptibility to severe disease caused by *Staphylococcus aureus*. Clin Diagn Lab Immunol 11 (6):1194–1197
67. Kang TJ, Chae GT (2001) Detection of Toll-like receptor 2 (TLR2) mutation in the lepromatous leprosy patients. FEMS Immunol Med Microbiol 31(1):53–58
68. Agnese DM et al (2002) Human toll-like receptor 4 mutations but not CD14 polymorphisms are associated with an increased risk of gram-negative infections. J Infect Dis 186(10):1522–1525
69. Child NJ et al (2003) Polymorphisms in Toll-like receptor 4 and the systemic inflammatory response syndrome. Biochem Soc Trans 31(Pt 3):652–653
70. Minoretti P et al (2006) Effect of the functional toll-like receptor 4 Asp299Gly polymorphism on susceptibility to late-onset Alzheimer's disease. Neurosci Lett 391(3):147–149
71. Zheng SL et al (2004) Sequence variants of toll-like receptor 4 are associated with prostate cancer risk: results from the CAncer Prostate in Sweden Study. Cancer Res 64(8):2918–2922
72. Hawn TR et al (2003) A common dominant TLR5 stop codon polymorphism abolishes flagellin signaling and is associated with susceptibility to legionnaires' disease. J Exp Med 198(10):1563–1572
73. Tantisira K et al (2004) Toll-like receptor 6 gene (TLR6): single-nucleotide polymorphism frequencies and preliminary association with the diagnosis of asthma. Genes Immun 5 (5):343–346
74. Abinun M (1995) Ectodermal dysplasia and immunodeficiency. Arch Dis Child 73(2):185
75. Ku CL et al (2005) Inherited disorders of human Toll-like receptor signaling: immunological implications. Immunol Rev 203:10–20
76. Picard C et al (2003) Pyogenic bacterial infections in humans with IRAK-4 deficiency. Science 299(5615):2076–2079
77. Medvedev AE et al (2002) Dysregulation of LPS-induced Toll-like receptor 4-MyD88 complex formation and IL-1 receptor-associated kinase 1 activation in endotoxin-tolerant cells. J Immunol 169(9):5209–5216
78. Jefferies CA, O'Neill LA (2004) Bruton's tyrosine kinase (Btk)-the critical tyrosine kinase in LPS signalling? Immunol Lett 92 (1–2):15–22
79. Khor CC et al (2007) A Mal functional variant is associated with protection against invasive pneumococcal disease, bacteremia, malaria and tuberculosis. Nat Genet 39(4):523–528
80. Kiechl S et al (2002) Toll-like receptor 4 polymorphisms and atherogenesis. N Engl J Med 347(3):185–192
81. Palmer SM et al (2003) The role of innate immunity in acute allograft rejection after lung transplantation. Am J Respir Crit Care Med 168(6):628–632
82. Rudofsky G Jr et al (2004) Asp299Gly and Thr399Ile genotypes of the TLR4 gene are associated with a reduced prevalence of diabetic neuropathy in patients with type 2 diabetes. Diabetes Care 27(1):179–183
83. Andersen-Nissen E et al (2005) Evasion of Toll-like receptor 5 by flagellated bacteria. Proc Natl Acad Sci U S A 102(26):9247–9252
84. Andersen-Nissen E et al (2007) A conserved surface on Toll-like receptor 5 recognizes bacterial flagellin. J Exp Med 204 (2):393–403
85. Fortune SM et al (2004) *Mycobacterium tuberculosis* inhibits macrophage responses to IFN-gamma through myeloid differentiation factor 88-dependent and -independent mechanisms. J Immunol 172(10):6272–6280
86. Rosenstiel P, Till A, Schreiber S (2007) NOD-like receptors and human diseases. Microbes Infect 9(5):648–657
87. Dinarello CA (1996) Biologic basis for interleukin-1 in disease. Blood 87(6):2095–2147
88. Cook DN, Pisetsky DS, Schwartz DA (2004) Toll-like receptors in the pathogenesis of human disease. Nat Immunol 5(10):975–979
89. Trinchieri G, Sher A (2007) Cooperation of Toll-like receptor signals in innate immune defence. Nat Rev Immunol 7(3):179–190

⌘ *Author's Choice*

THE JOURNAL OF BIOLOGICAL CHEMISTRY VOL. 284, NO. 50, pp. 34531–34537, December 11, 2009
© 2009 by The American Society for Biochemistry and Molecular Biology, Inc. Printed in the U.S.A.

Rab39a Binds Caspase-1 and Is Required for Caspase-1-dependent Interleukin-1β Secretion*

Received for publication, July 19, 2009, and in revised form, October 14, 2009 Published, JBC Papers in Press, October 15, 2009, DOI 10.1074/jbc.M109.046102

Christine E. Becker, Emma M. Creagh, and Luke A. J. O'Neill[1]

From the School of Biochemistry and Immunology, Trinity College, Dublin 2, Ireland

Interleukin-1β (IL-1β) is an important pro-inflammatory cytokine that is secreted by unconventional means in a caspase-1-dependent manner. Using a one-step immunoprecipitation approach to isolate endogenous caspase-1 from the monocytic THP1 cell line, we identified previously undescribed binding partners using mass spectrometry. One of the proteins identified was Rab39a, a member of the Rab GTPase family, a group of proteins that have important roles in protein trafficking and secretion. We confirmed by co-immunoprecipitation that Rab39a binds caspase-1. Knock down of Rab39a with small interfering RNA resulted in diminished levels of secreted IL-1β but had no effect on induction of pro-IL-1β mRNA by lipopolysaccharide. Rab39a contains a highly conserved caspase-1 cleavage site and was cleaved in the presence of recombinant caspase-1 or lipopolysaccharide. Finally, overexpression of Rab39a results in an increase in IL-1β secretion, and furthermore, overexpression of a Rab39a construct lacking the caspase-1 cleavage site leads to an additional increase in IL-1β secretion. Altogether, our findings show that Rab39a interacts with caspase-1 and suggest that Rab39a functions as a trafficking adaptor linking caspase-1 to IL-1β secretion.

IL-1β[2] is a potent pro-inflammatory cytokine produced by monocytes, macrophages, and dendritic cells. It is first synthesized as biologically inactive pro-IL-1β and is processed by caspase-1 into mature and biologically active IL-1β. It is subsequently released into the extracellular milieu (1). Most proteins that are secreted from the cell contain signal peptides that direct their transport to the plasma membrane through the endoplasmic reticulum-Golgi pathway. However, certain proteins, including IL-1β, do not contain signal peptides and are secreted by unconventional means, the mechanism of which is not entirely understood. Several models for IL-1β secretion have been described (for review, see ref. 2), including the lysosome-dependent pathway (3, 4), microvesicle shedding (5, 6), and exosome release (7).

Caspase-1 is an important regulatory molecule in the innate immune response that is activated in the inflammasome in response to certain pro-inflammatory stimuli. The inflammasome is a multiprotein complex, which, along with caspase-1, also contains a Nod-like receptor (NLR) protein such as NLRP1, NLRP3, or IPAF and the adaptor protein ASC (8). A diverse range of stimuli can activate inflammasomes such as bacteria, viruses, and in the case of the NLRP3 inflammasome danger signals such as uric acid and ATP and aggregated materials such as silica and asbestos (for review, see ref. 9).

Besides its well documented role in IL-1β processing and in the inflammasome, other roles for caspase-1 are emerging. A recent study describes how caspase-1 is important for the secretion of IL-1β as well as many other unconventionally secreted proteins such as fibroblast growth factor-2 and IL-1α. Using iTRAQ proteomics, 77 leaderless proteins with extracellular functions whose secretion is mediated by caspase-1 were identified. Many of these proteins are involved in inflammation, cytoprotection, or tissue repair (10).

In this study we used an immunoprecipitation approach to isolate caspase-1 from THP1 cells and then identified binding partners using mass spectrometry. One of the proteins identified was Rab39a. The human Rab protein family consists of >60 members. They are associated with specific membranes and are required for vesicle movement in pathways such as secretion and endocytosis (for review, see ref. 11). Rab39a is a relatively uncharacterized member of the Rab GTPase family. It was initially described by Stankovic *et al.* (12) as a novel Rab protein that is widely expressed in a variety of tissues, including spleen and small intestine and in peripheral leukocytes. Rab39a shows 78% identity at the amino acid level to another recently described Rab protein, Rab39b (13).

We have investigated the nature of the interaction between caspase-1 and Rab39a, with particular interest in its role in IL-1β secretion. Our findings suggest that Rab39a functions as a trafficking adaptor linking caspase-1 to IL-1β secretion.

EXPERIMENTAL PROCEDURES

Plasmids and Reagents—PCMV-HA was purchased from Clontech. Rab39a and Rab39b (ATCC) were subcloned into PCMV-HA. AU-1-caspase-1 was a gift from Prof. Seamus Martin, Dept. of Genetics, Trinity College, Dublin, Ireland. Antibodies used were: anti-caspase-1 (A19) (Santa Cruz Biotechnology); anti-β-actin (Sigma), and anti-HA (Covance). Human recombinant caspase-1 and YVAD-Cmk were from Calbiochem. Agonists used were 2-kDa macrophage-activating lipopeptide (Malp-2) from Alexis, LPS from *Escherichia coli*, serotype EH100, from Alexis, Pam_3Cys from Calbiochem, and ATP from Sigma.

* This work was supported by grants from the Health Research Board Science Foundation Ireland and the Wellcome Trust.

⌘ *Author's Choice*—Final version full access.

[1] To whom correspondence should be addressed. E-mail: laoneill@tcd.ie.

[2] The abbreviations used are: IL-1, interleukin-1; CHAPS, 3-[(3-cholamidopropyl)dimethylammonio]-1-propanesulfonic acid; ELISA, enzyme-linked immunosorbent assay; HA, hemagglutinin; LPS, lipopolysaccharide; MALDI-TOF, matrix-assisted laser desorption ionization time-of-flight; NF-κB, nuclear factor κB; NLR, Nod-like receptor; PBMC, peripheral blood mononuclear cell; siRNA, small interfering RNA; TNF-α, tumor necrosis factor-α.

Cell Culture and Transient Transfection—Human peripheral blood mononuclear cells (PBMCs) were isolated from human blood and maintained in RPMI 1640 medium supplemented with 10% fetal calf serum and 1% penicillin/streptomycin solution (v/v). 293T cells were transfected with Genejuice (Novagen). THP1 cells, PBMCs, and Raw 264.7 cells were transfected with the Amaxa system (Lonza) using Nucleofector solution V and Nucleofector program V-001, Y-001, or D-032, respectively.

Mass Spectrometry—Cell-free extracts were prepared from THP1 cells and incubated at 37 °C for 30 min to assemble inflammasomes as described previously (14). Samples were diluted in immunoprecipitation buffer (20 mM HEPES-KOH (pH 7.5), 50 mM NaCl, 0.3% CHAPS, 10 mM KCl, 1.5 mM $MgCl_2$, 1 mM EDTA, 1 mM EGTA, I mM dithiothreitol, 2 μg/ml aprotinin, 1 μg/ml leupeptin, and 250 μM phenylmethylsulfonyl fluoride) and precleared with protein A/G-agarose beads (Santa Cruz Biotechnology) at 4 °C for 1 h. Precleared cell-free extracts were incubated with fresh protein A/G- agarose beads (Santa Cruz Biotechnology) and anti-caspase-1 antibody (Santa Cruz Biotechnology) overnight at 4 °C. Captured complexes were washed three times in immunoprecipitation buffer and eluted into two-dimensional gel sample buffer (8 M urea, 4% CHAPS, 0.05% SDS, 100 mM dithiothreitol, 0.03% bromphenol blue, 0.2% amphylotes). Proteins were separated using two-dimensional gel electrophoresis, silver stained, and in-gel protein digestion and protein identification by MALDI-TOF using a Voyager DE-PRO mass spectrometer were carried out as described previously (14).

Cytokine Analysis—IL-1β and TNF-α were measured by ELISA according to the manufacturer's instructions (R&D Systems). Each experiment was done in triplicate, and data are expressed as picograms/ml (mean ± S.D.) for a representative of at least three independent experiments. For comparison between two groups, Student's t test was used. A p value of < 0.05 was considered significant.

siRNA—Control siRNA and hRab39a siRNA (GGAGCGGUUCAGAUCAAUAtt) were from Ambion. THP1 cells or PBMCs were transfected using Amaxa Nucleofector (Lonza) according to the manufacturer's protocol (Nucleofector solution V, Nucleofector program V-001 or Y-001, respectively) with 1.5 μg of siRNA/10^6 cells. Cells were incubated at 37 °C for 48 h. Cells were stimulated with 100 ng/ml LPS 24 h prior to harvesting.

Real Time PCR—RNA extractions were carried out with RNeasy minikit (Qiagen). cDNA was created using a First Strand Synthesis Kit (Invitrogen). SYBR Green real time PCR (Invitrogen) was then carried out on the cDNA using primers specific for Rab39a or Rab39b and glyceraldehyde-3-phosphate dehydrogenase as a control: Rab39a forward, TCTACCAGTTCCGCCTCATC; Rab39a reverse, ATTGATCTGAACCGCTCCTG; Rab39b forward, TTTTTCCCCATTCTCTGGAA; Rab39b reverse, AGCGGTCCTCCGTTTTTAAT.

Co-immunoprecipitation and Immunoblotting—293T cells were transfected using Genejuice (Novagen) with the indicated plasmids where the total amount of DNA was kept constant. 36 h later, cells were lysed in immunoprecipitation lysis buffer (150 mM NaCl, 50 mM Tris-HCl (pH 8), 1% Nonidet P-40, 1 mM phenylmethylsulfonyl fluoride, 10 μg/ml leupeptin, and 1 μg/ml aprotinin). An aliquot of lysate was removed for whole cell lysate analysis. Lysates were precleared twice with protein A/G beads (Santa Cruz Biotechnology). Precleared cell-free extracts were incubated with fresh protein A/G-agarose beads and anti-caspase-1 antibody (Santa Cruz Biotechnology) for 4 h at 4 °C. The immune complexes were washed three times in immunoprecipitation buffer and eluted by the addition of sample buffer followed by SDS-PAGE and immunoblotting using the indicated antibodies.

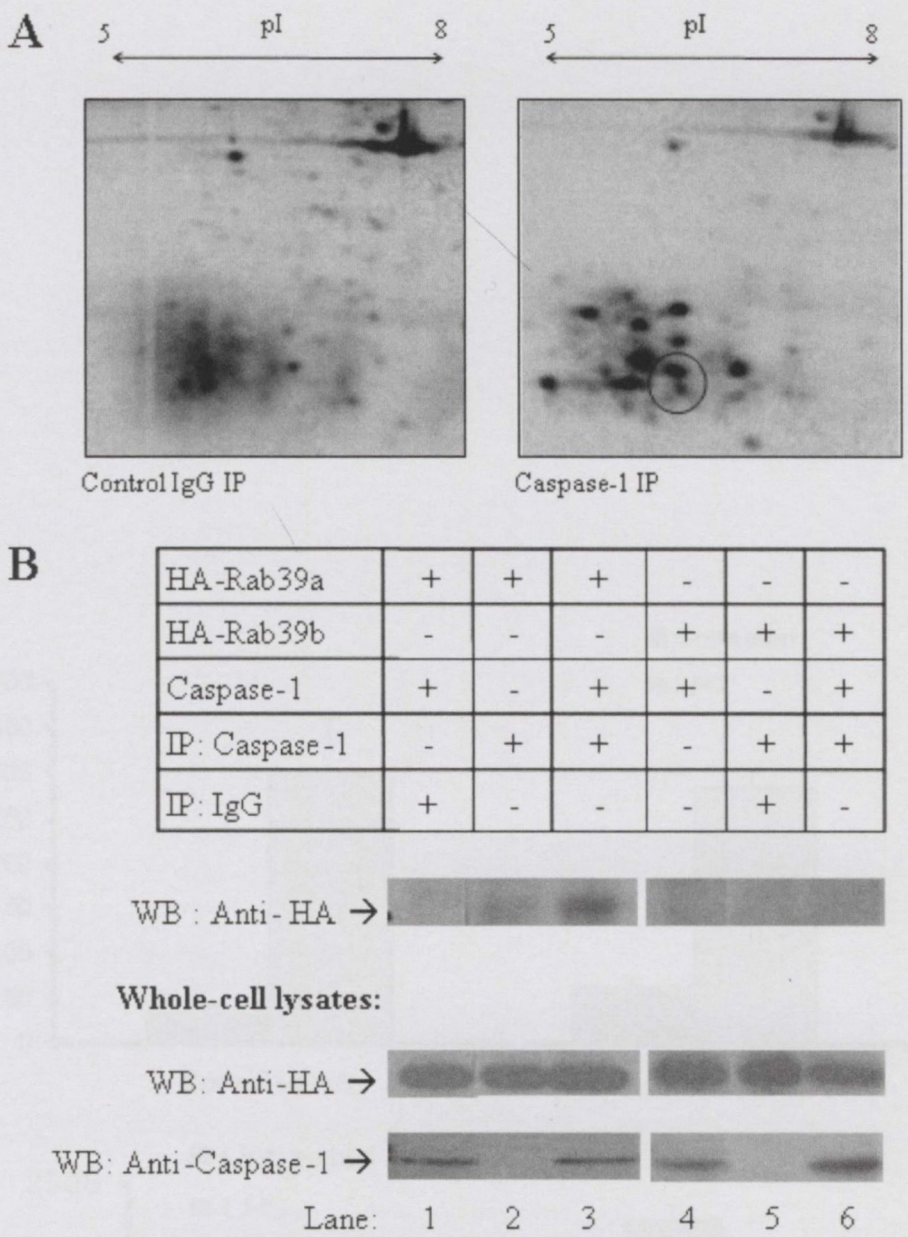


FIGURE 1. **Rab39a is a novel binding partner of caspase-1.** *A*, caspase-1 complexes were isolated from THP1 cell-free extracts. Proteins co-precipitating (*IP*) with caspase-1 were compared with proteins co-precipitating from an IgG control and were analyzed by two-dimensional gel electrophoresis (pI 5–8 first dimension and 12% SDS-PAGE second dimension). Protein spots of interest were identified by mass spectrometry. Rab39a was identified in the indicated area. *B*, 293T cells were transiently transfected with plasmids encoding caspase-1 and HA-Rab39a or HA-Rab39b. Caspase-1 was immunoprecipitated, and samples were probed with HA to show interaction. Whole cell lysates were immunoblotted (*WB*) with anti-HA anti-caspase-1. Results shown are each representative of two to four experiments.

Rab39a Cleavage Assay—293T cells were transfected as indicated, and lysates were used as substrates in a Rab39a cleavage assay, as described for IL-1β (1) and Mal (15) using recombinant caspase-1. Alternatively, Raw 264.7 cells were transfected as indicated and treated with 100 ng/ml LPS for 3 h followed by 5 mM ATP for 1 h.

Site-directed Mutagenesis of Rab39a—Point mutations were introduced into the Rab39a gene sequence using the QuikChange™ site-directed mutagenesis kit (Stratagene) according to the manufacturer's instructions.

Downloaded from www.jbc.org by guest, on February 11, 2010

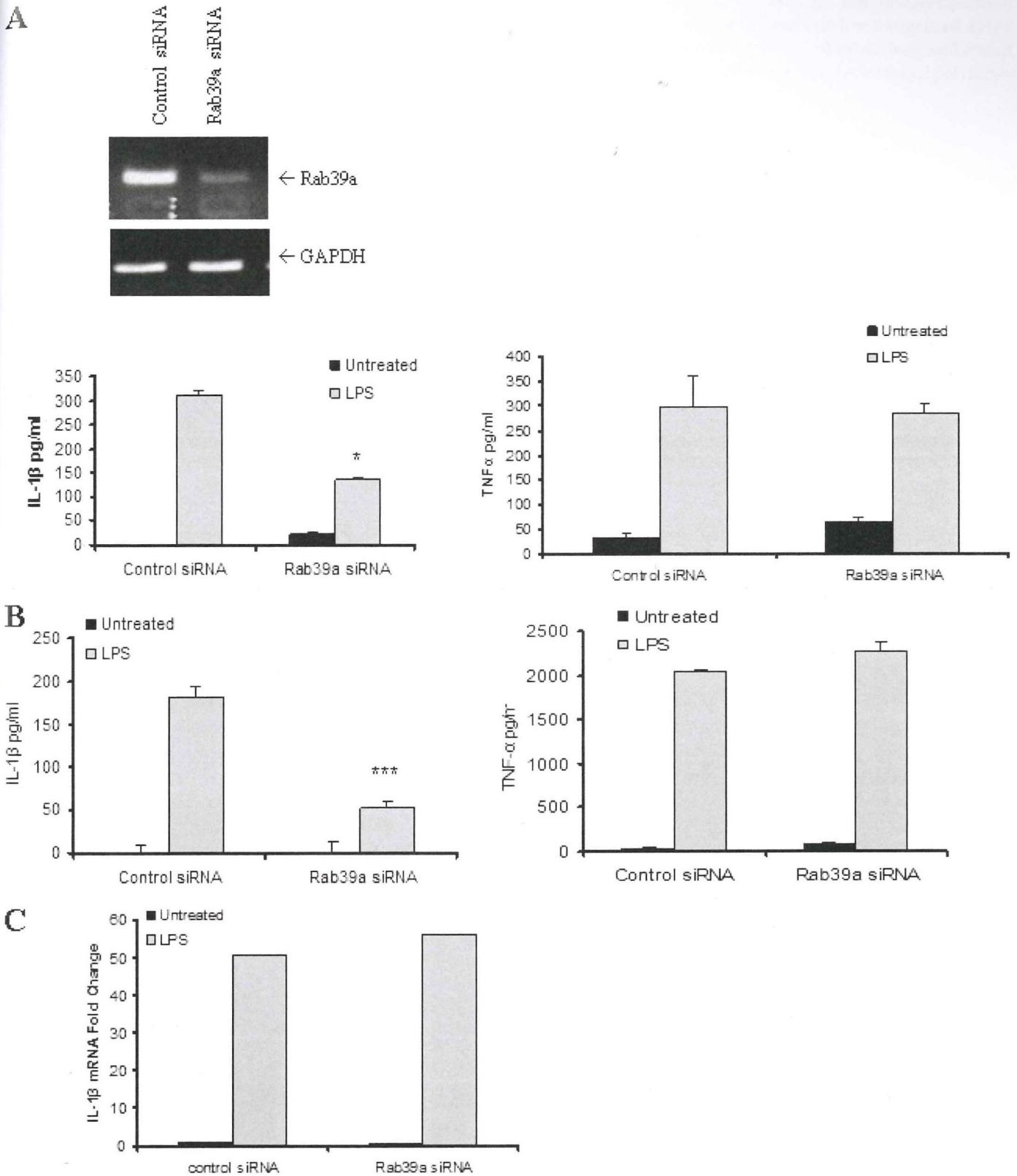
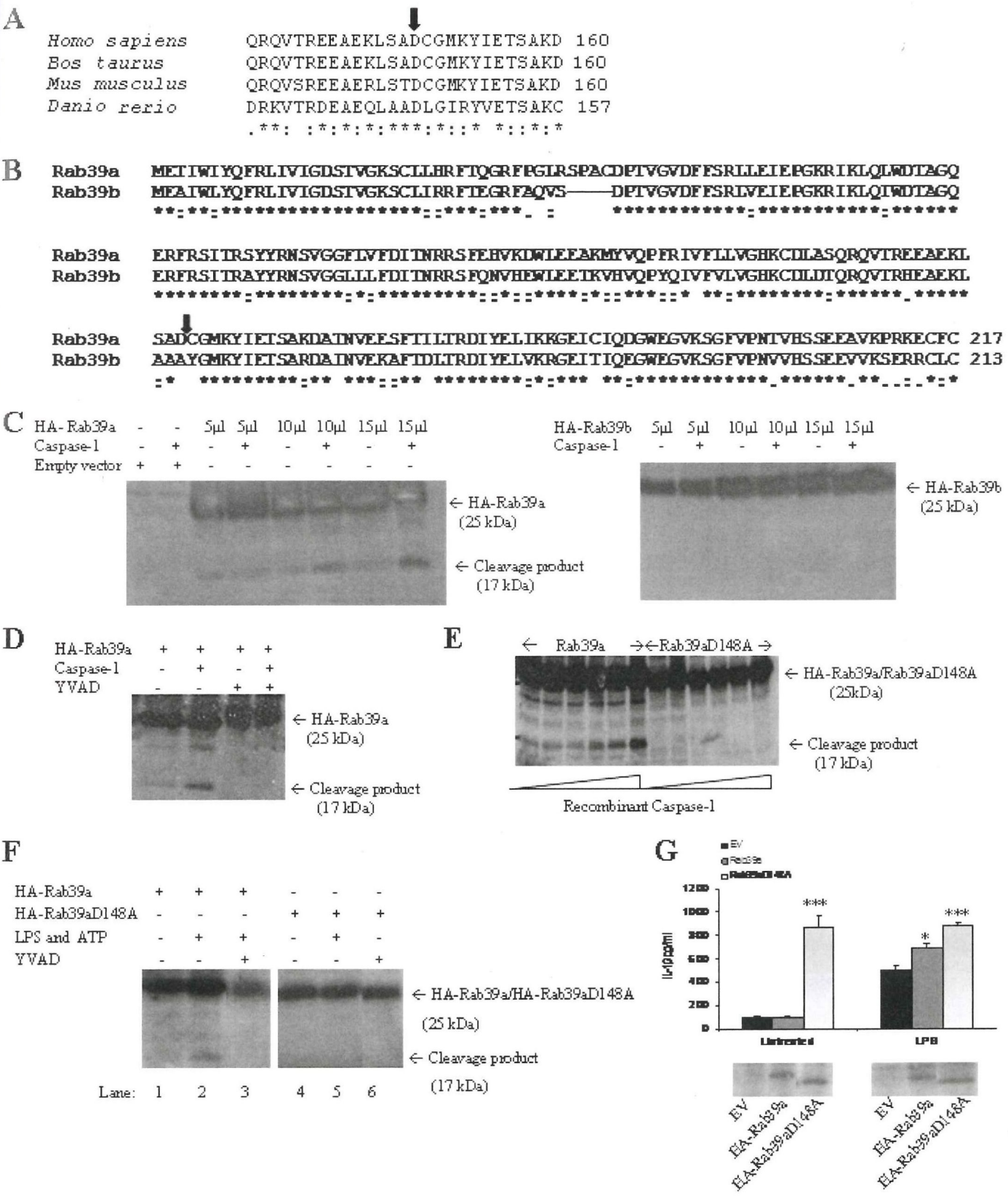


FIGURE 2. **Rab39a is required for IL-1β secretion.** *A*, knock down of Rab39a is shown by PCR (*upper panel*). THP1 cells were transfected with siRNA to Rab39a for 48 h. Cells were stimulated with 100 ng/ml LPS overnight before harvesting. IL-1β and TNF-α levels were measured by ELISA. *B*, PBMCs were transfected with siRNA to Rab39a for 48 h. Cells were stimulated with 100 ng/ml LPS overnight before harvesting. IL-1β and TNF-α levels were measured by ELISA. *A* and *B*, results are expressed as mean ± S.D. for triplicate determinations. ***, $p < 0.005$; *, $p < 0.05$. All results are representative of three separate experiments. *C*, RNA from THP1 cells from siRNA experiments was extracted, and mRNA levels of IL-1β were measured by real time PCR. Expression of IL-1β mRNA was normalized to that of glyceraldehyde-3-phosphate dehydrogenase (*GAPDH*) mRNA. Data were calculated as fold change and are presented relative to that of untreated controls. Results shown are each representative of at least three independent experiments.

RESULTS

Rab39a Is a Previously Undescribed Binding Partner of Caspase-1—At the outset we wished to uncover components of the inflammasome to understand its functions and its regulation further. To do this, we used an immunoprecipitation approach to isolate caspase-1 from cell-free extracts of THP1 cells. Immunoprecipitates were washed extensively and eluted into sample buffer and resolved on two-dimensional polyacryl-



amide gels. Silver staining was used to visualize gels. Protein spots were compared with those from an IgG control immunoprecipitation. Protein spots that were differentially immunoprecipitated with caspase-1 were excised from the gels and were analyzed by MALDI-TOF mass spectrometry. Of these proteins, the Ras-related protein Rab39a (Swiss Protein Database accession no. Q14964) was detected in caspase-1 immunoprecipitates in the area indicated (Fig. 1*A*) with 25% sequence coverage.

To confirm that Rab39a can interact with caspase-1, co-immunoprecipitation experiments were carried out as shown in Fig. 1*B*. Because of the unavailability of an antibody to Rab39a, a HA-tagged version of Rab39a was constructed. HA-Rab39a and caspase-1 were overexpressed in 293T cells. Caspase-1 was immunoprecipitated from cells and probed with HA. Rab39a successfully co-immunoprecipitated with caspase-1 (*top blot, lane 3*) confirming the endogenous interaction identified by mass spectrometry. No interaction was seen in the IgG control (*top blot, lane 1*), confirming that the interaction was specific. Rab39b, which is 78% similar to Rab39a, was unable to co-immunoprecipitate with caspase-1 (*top blot, lane 6*).

Rab39a Is Required for IL-1β Secretion—We hypothesized that Rab39a may play a role in the secretion of IL-1β because many Rab family members are involved in trafficking and secretion of proteins (11). To determine whether Rab39a was necessary for IL-1β secretion, siRNA nucleotides targeting Rab39a were transfected into THP1 cells, and secreted IL-1β was measured by ELISA. As shown in Fig. 2*A* (*upper panel*), the siRNA knocked down the expression of Rab39a. Compared with control siRNA, knock down of Rab39a resulted in a decrease in secreted IL-1β (*left graph*). Levels of TNF-α, which is externalized by the classical secretory pathway, were also measured. TNF-α levels remained constant despite Rab39a knock down, indicating that it is specific for IL-1β secretion (*right graph*).

Knock down of Rab39a in human PBMCs also resulted in a dramatic decrease in IL-1β secretion (Fig. 2*B*, *left graph*) but not TNF-α (*right graph*). Importantly, mRNA levels of IL-1β, induced by LPS, remained constant when Rab39a was knocked down (Fig. 2*C*), indicating that the decrease in IL-1β might be due to a decrease in secretion and not in induction of the mature form of IL-1β.

Rab39a Can Be Cleaved by Recombinant Caspase-1—Rab39a contains a putative caspase-1 cleavage site at amino acid 148. This site in Rab39a is highly conserved and is found across many different species (Fig. 3*A*). Interestingly, Rab39b, which was not found to associate with caspase-1, does not contain this site (Fig. 3*B*).

Thus, the question of whether Rab39a is a substrate of caspase-1 was next addressed. HA-Rab39a was overexpressed in 293T cells, and total cell lysates were incubated with recombinant caspase-1. Western blot analysis revealed the appearance of an additional form of Rab39a at 17 kDa, consistent with cleavage of Rab39a by caspase-1 at the proposed caspase-1 cleavage site. Rab39b, which lacks the cleavage site, showed no additional forms when incubated with recombinant caspase-1 (Fig. 3*C*). Rab39a could not be cleaved in the presence of YVAD-Cmk, a caspase-1 inhibitor (Fig. 3*D*).

To confirm the cleavage site in Rab39a, a mutated form of Rab39a was generated by site-directed mutagenesis in which the putative cleavage site Asp^{148} was replaced by Ala. No cleavage occurred, confirming the cleavage site as Asp^{148} (Fig. 3*E*).

Rab39a processing can also take place in macrophages treated with LPS and ATP. Raw 264.7 cells were transfected with HA-Rab39a, and cells were treated with 100 ng/ml LPS for 3 h and 5 mM ATP for 1 h. Western blot analysis revealed the appearance of the 17-kDa form of Rab39a, consistent with cleavage of Rab39a by caspase-1 at the proposed caspase-1 cleavage site. (Fig. 3*F*, *lane 2*). This effect was blocked by YVAD-Cmk (*lane 3*). Significantly; no cleavage took place with HA-Rab39aD148A (*lane 5*).

Overexpression of HA-Rab39a in THP1 cells resulted in an increase in IL-1β when cells were treated with LPS (Fig. 3*G*). Interestingly, when HA-Rab39aD148 (which lacks the caspase-1 cleavage site) was overexpressed this strongly increased IL-1β secretion on its own. This was not further enhanced by LPS treatment. The caspase-1-resistant form of Rab39a therefore appears to be able to drive IL-1β production.

Rab39a Can Be Induced by Pro-inflammatory Stimuli—To understand further the role that Rab39a was playing in caspase-1-dependent IL-1β secretion, we examined whether Rab39a, like IL-1β, was inducible by pro-inflammatory stimuli. We analyzed the Rab39a promoter and found that it contains many putative transcription factor-binding sites, including NF-κB sites, p53 sites, and SP1 sites (Fig. 4*A*).

We analyzed the expression patterns of Rab39a mRNA by quantitative real time PCR in THP1 cells and tested whether expression was altered by pro-inflammatory stimuli. Our results show that Rab39a mRNA was significantly increased in response to LPS, Malp-2, and Pam_3Cys (Fig. 4*B*).

DISCUSSION

IL-1β is a multifunctional cytokine and plays a major role in host defense (16). Unlike other pro-inflammatory cytokines, IL-1β lacks a signal peptide and is secreted via unconventional methods. The process by which it is secreted from the cell has always been contentious. The role of caspase-1 in inflammasome functions and IL-1β processing has been widely described (17). However, a role

FIGURE 3. **Rab39a contains a putative caspase-1 cleavage site and can be cleaved by recombinant caspase-1.** *A*, caspase-1 cleavage is highly conserved. The *arrow* indicates the conserved putative caspase-1 cleavage site (see expasy peptide cutter site on the web). *B*, ClustalW alignment of the amino acid sequence of Rab39a and Rab39b is shown. The predicted cleavage site is indicated by the *arrow* (see expasy peptide cutter site on the web). *C*, 293T cells were transfected with plasmids encoding HA-Rab39a or HA-Rab39b. Cells were lysed, and increasing volumes of lysate were incubated with recombinant caspase-1 at 30 °C for 90 min. *D*, 293T cells were transfected with HA-Rab39a in the presence or absence of 100 μM caspase-1 inhibitor (YVAD-Cmk) and then incubated with recombinant caspase-1 at 30 °C for 90 min. *E*, 293T cells were transfected with HA-Rab39a or HA-Rab39a D148A. Lysates were incubated at 30 °C for 90 min with increasing concentrations of recombinant caspase-1. *F*, Raw 264.7 cells were transfected with plasmids encoding HA-Rab39a or HA-Rab39aD148A and treated with 100 ng/ml LPS and 5 mM ATP in the presence or absence of 100 μM caspase-1 inhibitor (YVAD-Cmk). Rab39a was detected by immunoblotting for anti-HA. *G*, HA-Rab39a or HA-Rab39aD148 was transfected into THP1 cells for 48 h. Cells were stimulated with 100 ng/ml LPS overnight before harvesting. Results are expressed as mean ± S.D. for triplicate determinations. ***, $p < 0.005$; *, $p < 0.05$. Results are representative of two or three independent experiments. *EV*, empty vector.

Downloaded from www.jbc.org by guest, on February 11, 2010

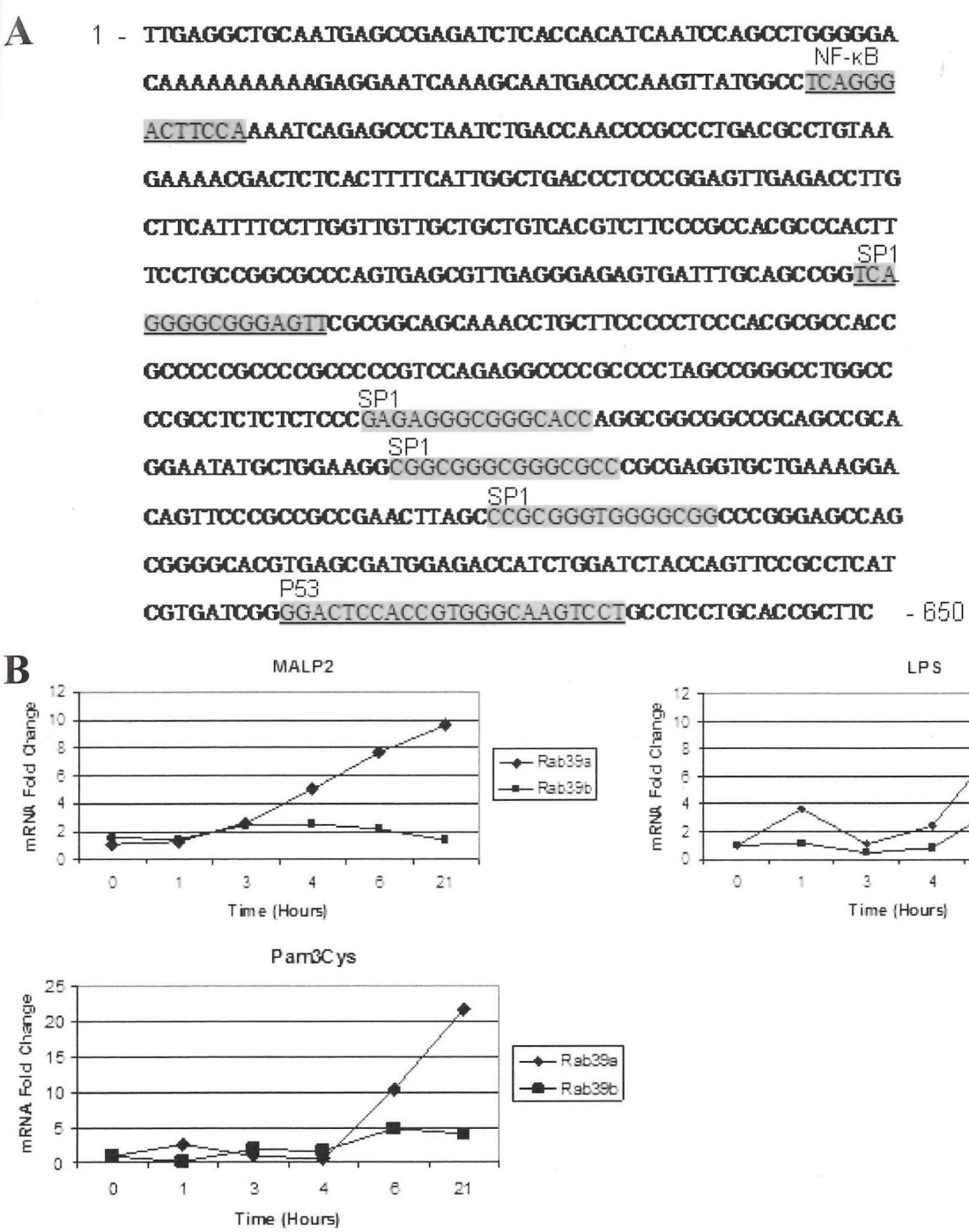


FIGURE 4. **Rab39a can be induced by pro-inflammatory stimuli.** *A*, Rab39a promoter contains numerous putative transcription factor binding sites as indicated (adapted from the Genomatix website). *B*, THP1 cells were stimulated with 100 ng/ml LPS or 5 nM Malp-2 or 1 μg/ml Pam_3Cys for the indicated times. mRNA levels were measured by real time PCR with primers specific for Rab39a and Rab39b; expression is normalized to that of glyceraldehyde-3-phosphate dehydrogenase and is presented relative to that of untreated controls. Results shown are representative of three independent experiments.

for caspase-1 in unconventional protein secretion is emerging. A recent paper describes how IL-1β secretion is mediated by caspase-1. This in turn may be mediated by factors that are substrates of caspase-1, the cleavage products of which might have a direct role in IL-1β secretion (10).

Our results unveil further insight into caspase-1-dependent IL-1β secretion. We have shown that the small GTPase protein Rab39a is a novel binding partner of caspase-1 as identified by mass spectrometry and confirmed by co-immunoprecipitation. We provide evidence that Rab39a is necessary for the secretion of IL-1β but not induction of pro-IL-1β because siRNA targeted to Rab39a results in diminished secretion of IL-1β but does not affect mRNA levels of IL-1β.

Bioinformatic analyses indicated that Rab39a contained a conserved caspase-1 cleavage site, and our results demonstrated that Rab39a was cleaved using an *in vitro* assay. We were also able to show that Rab39a processing could take place in macrophages treated with LPS and ATP. However, this should

be interpreted with caution because cleavage of endogenous Rab39a should be shown. We are currently raising an anti-Rab39a antibody to test this. Interestingly, several other Rab proteins (notably Rab4 and Rab14, which are involved in secretion) contain the putative caspase-1 cleavage site. Cleavage of Rab proteins may represent a general mechanism by which caspase-1 modulates protein trafficking within the cell.

Other recent results have also shown that Rab proteins are important for signaling in the innate immune system. For example, Rab7b can negatively regulate both TLR4 and TLR9 signaling by promoting their translocation to the lysosome for degradation (18, 19). The results presented in this paper further add to this realization of the importance of Rab proteins during innate immunity.

We also found that Rab39a was inducible by pro-inflammatory stimuli, implying that its expression may be coordinated with that of IL-1β to promote secretion.

The precise mechanism of IL-1β secretion remains elusive because many models exist as to how this event may occur. Three of the best described models include the lysosome-dependent pathway (3, 4), microvesicle shedding (5, 6), and exosome release (7). In the lysosome-dependent pathway, pro-IL-1β is translocated into secretory lysosomes together with caspase-1. The mature form of IL-1β is produced within the lysosome by caspase-1 cleavage, after which the lysosomes fuse with the plasma membrane and the contents are released into the extracellular space. In microvesicle shedding, caspase-1 activates IL-1β in the cytoplasm and is exported along with the mature cytokine into the extracellular space. The third mechanism, exosome release, is where caspase-1 and IL-1β are contained in the cytoplasm within endosomal internal vesicles that are released as exosomes.

These models involve many unknown trafficking requirements, and interestingly the last two models require the formation of specific vesicles that exit from the cell. Rab proteins have roles in trafficking and secretion, and Rab39a, although largely uncharacterized is likely to function in this manner.

If Rab39a proves to be a physiological substrate, why it would require such cleavage requires further investigation, but it may be necessary for vesicle formation and secretion. We propose the following mechanism of action in which Rab39a associates with caspase-1 and together they are required for efficient IL-1β secretion. During an inflammatory response, Rab39a is induced and binds to caspase-1. As IL-1β is secreted in a caspase-1-dependent manner, we propose that Rab39a is needed to help traffic IL-1β from the cell in a vesicle-dependent manner. Indeed, caspase-1 itself and other components of the inflammasome that also lack signal peptides are also released from activated macrophages (8, 20–21), and Rab39a may be necessary in helping to secrete the entire inflammasome complex from the cell.

Interestingly, overexpression of a Rab39a construct lacking the caspase-1 cleavage site results in a boosting of IL-1β secretion. This suggests that cleavage of Rab39a by caspase-1 would serve as a mechanism of inactivating Rab39a and therefore act as a mechanism to control levels of IL-1β secretion. Hence, overexpression of a construct that cannot be cleaved results in an excess of IL-1β secretion. We are currently exploring the mechanism here.

The association between Rab39a and caspase-1 is highly specific. Rab39a is 78% similar to another Rab protein, Rab39b, but they have very different profiles with regard to caspase-1. Unlike Rab39a, Rab39b was not found to associate with caspase-1 in our screen, and it does not co-immunoprecipitate with caspase-1. It lacks a caspase-1 cleavage site and cannot be cleaved *in vitro*, and it is not induced by pro-inflammatory stimuli to the same extent as Rab39a. The role of Rab39a in IL-1β secretion is therefore specific.

We have therefore identified Rab39a as a caspase-1-associated protein required for IL-1β secretion. Future studies will aim to understand further precisely how Rab39a participates in this process.

REFERENCES

1. Thornberry, N. A., Bull, H. G., Calaycay, J. R., Chapman, K. T., Howard, A. D., Kostura, M. J., Miller, D. K., Molineaux, S. M., Weidner, J. R., Aunins, J., Elliston, K., Ayala, J., Casano, F., Chin, J., Ding, G., Egger, L., Gaffney, E., Limjuco, W., Palyha, O., Raju, S., Rolando, A., Salley, J., Yamin, T., Lee, T., Shively, J., MacCross, M., Mumford, R., Schmidt, J., and Tocci, M. (1992) *Nature* **356,** 768–774
2. Eder, C. (2009) *Immunobiology* **214,** 543–553
3. Andrei, C., Dazzi, C., Lotti, L., Torrisi, M. R., Chimini, G., and Rubartelli, A. (1999) *Mol. Biol. Cell* **10,** 1463–1475
4. Andrei, C., Margiocco, P., Poggi, A., Lotti, L. V., Torrisi, M. R., and Rubartelli, A. (2004) *Proc. Natl. Acad. Sci. U.S.A.* **101,** 9745–9750
5. MacKenzie, A., Wilson, H. L., Kiss-Toth, E., Dower, S. K., North, R. A., and Surprenant, A. (2001) *Immunity* **15,** 825–835
6. Pelegrin, P., Barroso-Gutierrez, C., and Surprenant, A. (2008) *J. Immunol.* **180,** 7147–7157
7. Qu, Y., Franchi, L., Nunez, G., and Dubyak, G. R. (2007) *J. Immunol.* **179,** 1913–1925
8. Martinon, F., Burns, K., and Tschopp, J. (2002) *Mol. Cell* **10,** 417–426
9. Martinon, F., Mayor, A., and Tschopp, J. (2009) *Annu. Rev. Immunol.* **27,** 229–265
10. Keller, M., Rüegg, A., Werner, S., and Beer, H. D. (2008) *Cell* **132,** 818–831
11. Zerial, M., and McBride, H. (2001) *Nat. Rev. Mol. Cell Biol.* **2,** 107–117
12. Stankovic, T., Byrd, P. J., Cooper, P. R., McConville, C. M., Munroe, D. J., Riley, J. H., Watts, G. D., Ambrose, H., McGuire, G., Smith, A. D., Sutcliffe, A., Mills, T., and Taylor, A. M. (1997) *Genomics* **40,** 267–276
13. Cheng, H., Ma, Y., Ni, X., Jiang, M., Guo, L., Ying, K., Xie, Y., and Mao, Y. (2002) *Cytogenet. Genome Res.* **97,** 72–75
14. Creagh, E. M., Brumatti, G., Sheridan, C., Duriez, P. J., Taylor, R. C., Cullen, S. P., Adrain, C., and Martin, S. J. (2009) *PLoS One* **4,** e5055
15. Miggin, S. M., Pålsson-McDermott, E., Dunne, A., Jefferies, C., Pinteaux, E., Banahan, K., Murphy, C., Moynagh, P., Yamamoto, M., Akira, S., Rothwell, N., Golenbock, D., Fitzgerald, K. A., and O'Neill, L. A. (2007) *Proc. Natl. Acad. Sci. U.S.A.* **104,** 3372–3377
16. Dinarello, C. A. (2009) *Annu. Rev. Immunol.* **27,** 519–550
17. Martinon, F., Agostini, L., Meylan, E., and Tschopp, J. (2004) *Curr. Biol.* **14,** 1929–1934
18. Wang, Y., Chen, T., Han, C., He, D., Liu, H., An, H., Cai, Z., and Cao, X. (2007) *Blood* **110,** 962–971
19. Yao, M., Liu, X., Li, D., Chen, T., Cai, Z., and Cao, X. (2009) *J. Immunol.* **183,** 1751–1758
20. Mariathasan, S., Newton, K., Monack, D. M., Vucic, D., French, D. M., Lee, W. P., Roose-Girma, M., Erickson, S., and Dixit, V. M. (2004) *Nature* **430,** 213–218
21. Feldmeyer, L., Keller, M., Niklaus, G., Hohl, D., Werner, S., and Beer, H. D. (2007) *Curr. Biol.* **17,** 1140–1145